

**Impact of 17 $\beta$ Estradiol on  $\beta$ -cell  
survival of female Munich *Ins2*<sup>C95S</sup>  
mutant mice**

**Marion Susanne Schuster**

**Aus dem Zentrum für Klinische Tiermedizin  
der Ludwig-Maximilians-Universität München**

**Angefertigt unter der Leitung von  
Univ.- Prof. Dr. R. Wanke**

**Impact of 17 $\beta$ Estradiol on  $\beta$ -cell  
survival of female Munich *Ins2*<sup>C95S</sup>  
mutant mice**

Inaugural-Dissertation  
zur Erlangung der tiermedizinischen Doktorwürde  
der Tierärztlichen Fakultät der Ludwig-Maximilians-Universität München

**von  
Marion Susanne Schuster  
aus Kirchheim/Teck**

**München, 2011**

Gedruckt mit Genehmigung der Tierärztlichen Fakultät  
der Ludwig-Maximilians-Universität München

Dekan: Univ.-Prof. Dr. Braun

Berichterstatter: Univ.-Prof. Dr. Wanke

Korreferent/en: Univ.-Prof. Dr. Göbel  
Univ.-Prof. Dr. Aigner  
Prof. Dr. Kaltner  
Univ.-Prof. Dr. Sutter

Tag der Promotion: 12. Februar 2011

*Meiner lieben Mutter  
und meiner Nichte Stefanie*

<b>1</b>	<b>INTRODUCTION</b>	<b>1</b>
<b>2</b>	<b>LITERATURE REVIEW</b>	<b>3</b>
<b>2.1</b>	<b>Diabetes mellitus</b>	<b>3</b>
2.1.1	Definition and description	3
2.1.2	Classification and diagnosis criteria in human beings	4
2.1.2.1	Classification	4
2.1.2.2	Diagnosis criteria	5
2.1.3	Global and economical burden	7
2.1.3.1	Global burden of diabetes mellitus	7
2.1.3.2	Economical burden	8
<b>2.2</b>	<b>Animal models in diabetic research</b>	<b>9</b>
2.2.1	The role of animal models for human diseases	9
2.2.2	Animal models for diabetes mellitus	10
2.2.3	ENU mutagenesis	10
2.2.3.1	Munich ENU Mouse Mutagenesis Project	11
2.2.3.2	ENU-induced hyperglycaemia models	12
<b>2.3</b>	<b>Insulin gene mutations</b>	<b>13</b>
2.3.1	Mutations in humans	13
2.3.2	The Munich <i>Ins2</i> <sup>C95S</sup> mutant mouse	15
2.3.2.1	Heterozygous Munich <i>Ins2</i> <sup>C95S</sup> mutant mice	15
2.3.2.2	Homozygous Munich <i>Ins2</i> <sup>C95S</sup> mutant mice	17
2.3.3	Akita mouse	17
2.3.3.1	Heterozygous Akita mutant mice	18
2.3.3.2	Homozygous Akita mutant mice	20
2.3.3.3	ER-stress in the Akita mouse	20
2.3.4	<i>Ins1</i> and <i>Ins2</i> null mutant mice	23
2.3.4.1	Double homozygous <i>Ins1</i> and <i>Ins2</i> null mutant mice	24
2.3.4.2	Single homozygous <i>Ins1</i> and <i>Ins2</i> null mutant mice	24
2.3.4.3	Single heterozygous <i>Ins1</i> and <i>Ins2</i> null mutant mice	25
<b>2.4</b>	<b>Estrogen</b>	<b>26</b>
2.4.1	Estrogen production and action	26
2.4.2	Estrogen receptors	28
2.4.2.1	Classical genomic estrogen receptors (ER $\alpha$ and ER $\beta$ )	29
2.4.2.2	Rapid estrogen signalling	30
2.4.2.3	Non-classical estrogen receptors	31
2.4.3	Role of estrogen in glucose homeostasis	32
2.4.4	Effects of estrogen on pancreas	33
2.4.4.1	Impact of estrogen on pancreatic insulin content	34

2.4.4.2	Enhancement of insulin secretion by estrogen	36
2.4.5	Effects of estrogen on skeletal muscle, adipose tissue and liver	38
2.4.5.1	Insulin sensitivity and insulin resistance	38
2.4.5.2	Modulation of GLUT4 expression by estrogen	39
2.4.6	Positive effects of estrogen on oxidative stress and apoptosis	39
2.4.7	Role of estrogen in endoplasmic reticulum stress	41
<b>3</b>	<b>RESEARCH DESIGN AND METHODS</b>	<b>43</b>
<b>3.1</b>	<b>Research design</b>	<b>43</b>
<b>3.2</b>	<b>Materials and methods</b>	<b>43</b>
3.2.1	Animals	43
3.2.2	Genotyping	45
3.2.3	Ovariectomy and pellet implantation	49
3.2.4	Body weight	50
3.2.5	Blood glucose concentration	50
3.2.5.1	Randomly fed mice	50
3.2.5.2	Fasted mice	50
3.2.6	Oral glucose tolerance test (OGTT)	50
3.2.7	Intraperitoneal insulin tolerance test	52
3.2.8	Serum insulin concentration	52
3.2.9	Serum estradiol concentration	52
3.2.10	Serum lipid peroxidation	53
3.2.11	Western blot analyses of isolated islets	53
3.2.11.1	Islet isolation	54
3.2.11.2	Islet protein content	57
3.2.11.3	SDS-PAGE	58
3.2.11.4	Western blot	59
3.2.11.5	Silver staining and drying	60
3.2.11.6	Western blot analysis	62
3.2.12	Necropsy and pancreas preparation	64
3.2.13	Immunohistochemistry of the pancreas	65
3.2.13.1	Insulin	65
3.2.13.2	Glucagon, somatostatin and pancreatic polypeptide	66
3.2.14	Quantitative stereological analyses	66
3.2.14.1	Quantification of the total pancreas volume ( $V_{\text{pan}}$ )	66
3.2.14.2	Determination of the relative pancreas weight	67
3.2.14.3	Quantitative stereological parameters	67
3.2.15	Transmission electron microscopy (TEM)	68

<b>4</b>	<b>RESULTS</b>	<b>72</b>
<b>4.1</b>	<b>Clinical investigations</b>	<b>72</b>
4.1.1	Body weight	72
4.1.2	Blood glucose concentration	73
4.1.2.1	Randomly fed mice	73
4.1.2.2	Fourteen-hours fasted mice	74
4.1.3	Oral glucose tolerance test (OGTT)	75
4.1.4	Intraperitoneal insulin tolerance test (ipITT)	79
4.1.5	Serum insulin concentration	80
4.1.6	Serum estradiol concentration	82
<b>4.2</b>	<b>Beta cell function indices</b>	<b>83</b>
4.2.1	HOMA B and HOMA IR	84
4.2.2	Quicki	85
4.2.3	FGIR	86
<b>4.3</b>	<b>Oxidative stress</b>	<b>86</b>
<b>4.4</b>	<b>Isolated pancreatic islets</b>	<b>88</b>
4.4.1	ER-stress	88
4.4.1.1	BiP/ $\beta$ -actin	88
4.4.1.2	PeIF2alpha/ $\beta$ -actin	89
4.4.1.3	CHOP/ $\beta$ -actin	89
4.4.2	Apoptosis	90
4.4.3	Cell proliferation	91
<b>4.5</b>	<b>Qualitative histological evaluations of the endocrine pancreas</b>	<b>92</b>
4.5.1	Insulin	92
4.5.2	Glucagon, somatostatin and pancreatic polypeptide (PP)	94
4.5.3	Isolated $\beta$ -cells	95
<b>4.6</b>	<b>Quantitative stereological analyses of the endocrine pancreas</b>	<b>95</b>
4.6.1	Total pancreas volume	95
4.6.2	Relative pancreas weight	96
4.6.3	Volume density of islets in the pancreas	97
4.6.4	Total islet volume	97
4.6.5	Volume density of $\beta$ -cells in the islets	98
4.6.6	Total $\beta$ -cell volume	98
4.6.7	Volume density of non- $\beta$ -cells in the islets	99
4.6.8	Total volume of non- $\beta$ -cells in the islets	99
4.6.9	B-cell to non- $\beta$ -cell ratio	100

4.6.10	Volume density of isolated $\beta$ -cells in the pancreas	101
4.6.11	Total volume of isolated $\beta$ -cells	101
<b>4.7</b>	<b>Transmission electron microscopy</b>	<b>102</b>
<b>5</b>	<b>DISCUSSION</b>	<b>107</b>
<b>5.1</b>	<b>Glucose homeostasis</b>	<b>107</b>
5.1.1	Blood glucose and insulin secretion	107
5.1.2	Insulin sensitivity	113
<b>5.2</b>	<b>Body weight</b>	<b>114</b>
<b>5.3</b>	<b>Oxidative stress</b>	<b>116</b>
<b>5.4</b>	<b>ER-stress</b>	<b>117</b>
5.4.1	Islet isolation	117
5.4.2	ER-stress markers	118
<b>5.5</b>	<b>Qualitative and quantitative morphological investigations of the endocrine pancreas</b>	<b>120</b>
5.5.1	Qualitative histological analyses	121
5.5.2	Quantitative stereological analyses	121
<b>5.6</b>	<b>Electron microscopic findings in <math>\beta</math>-cells</b>	<b>128</b>
<b>5.7</b>	<b>Conclusion</b>	<b>131</b>
<b>6</b>	<b>PERSPECTIVE</b>	<b>133</b>
<b>7</b>	<b>SUMMARY</b>	<b>134</b>
<b>8</b>	<b>ZUSAMMENFASSUNG</b>	<b>136</b>
<b>9</b>	<b>REFERENCES</b>	<b>139</b>
<b>10</b>	<b>ACKNOWLEDGEMENTS</b>	<b>162</b>

# 1 Introduction

Diabetes mellitus is one of the most common human diseases worldwide with a still increasing prevalence. Today there are more than 300 million people suffering from diabetes and its accompanying diseases. It is expected, that the number of diabetic patients will reach close to 500 million within 20 years, if nothing is done to slow down the epidemic (International Diabetes Federation 2009).

Animal models, particularly mouse models, play an essential role for studying the pathogenesis of diabetes mellitus and its complications. Transgenic and knock-out mouse models used to be a common and powerful tool to explore the pathogenesis of diabetes mellitus. In recent years, more and more mutant mouse models, especially with point mutations in a diabetes relevant gene, have additionally been established. Due to the fact that such mutations are also found in human patients, these mutant mouse models are of great value in prospective diabetes research.

The Munich *Ins2*<sup>C95S</sup> mutant mouse and the Akita mutant mouse are two mouse models, which possess point mutations in the *Ins2* gene. These mutations lead to the loss of the interchain and the intrachain disulfide bond of insulin 2, respectively (Herbach *et al.* 2007, Wang *et al.* 1999). Extensive studies could demonstrate that misfolded (pro-)insulin accumulates in  $\beta$ -cells of Akita mice, what leads to endoplasmic reticulum (ER)-stress and  $\beta$ -cell dysfunction (Izumi *et al.* 2003, Nozaki *et al.* 2004, Zuber *et al.* 2004). Moreover it could be shown that misfolded and accumulated proteins can also induce  $\beta$ -cell apoptosis (Scheuner and Kaufman 2008, Xu *et al.* 2005).

The disease pattern of both *Ins2* mutant models is similar. It is characterized by a progressive diabetic phenotype with severe hyperglycaemia, disturbed insulin secretion, insulin resistance and profound  $\beta$ -cell loss of male mutant mice, and a much milder disease-form with preserved  $\beta$ -cell mass of female mutant mice. This considerable difference is probably based on several protective effects attributed to estrogen, such as antioxidative effects (Katalinic *et al.* 2005, Le May *et al.* 2006), enhancement of insulin sensitivity (Gonzalez *et al.* 2001, Lee *et al.* 1999), insulin secretion (Balhuizen *et al.* 2010, Ropero *et al.* 1999) and diminution of ER-stress (Kozlov *et al.* 2010).

The aim of the present study was to investigate the impact of 17 $\beta$ Estradiol on the survival of  $\beta$ -cells in female Munich *Ins2*<sup>C95S</sup> mutant mice. To exclude effects of other ovarian hormones, one group of ovariectomized female mutant mice was supplemented with 17 $\beta$ Estradiol long-term pellets. Sham-operated placebo-treated mutant and wild-type mice served as controls.

Besides various clinical tests to determine  $\beta$ -cell function and insulin sensitivity, isolated pancreatic islets were analysed with respect to ER-stress, islet-cell apoptosis and cell proliferation, and further oxidative stress was investigated in serum samples. Additionally, the effects of ovariectomy and estradiol supplementation on the endocrine pancreas were determined, using qualitative histological as well as quantitative stereological methods.

## 2 Literature review

### 2.1 Diabetes mellitus

#### 2.1.1 Definition and description

Diabetes mellitus is recognized as a group of metabolic diseases characterized by chronic hyperglycaemia and glucose intolerance resulting from insulin deficiency, impaired effectiveness of insulin or both. Various organs, particularly eyes, nerves, heart, and blood vessels, can be affected by long-term consequences of sustained hyperglycaemia, appearing in organ dysfunction culminating in organ failure (American Diabetes Association 2009).

The development of diabetes is a complex interaction of several pathogenic processes. Three important factors are involved in the pathogenesis of diabetes mellitus: genetic predisposition, peripheral insulin resistance as well as  $\beta$ -cell dysfunction and failure, resulting in inadequate insulin secretion (Lehmann and Spinas 2005). The genetic predispositions comprise monogenetic defects leading to  $\beta$ -cell dysfunction, including mutations in genes encoding for transcription factors or mutations in the glucokinase gene (maturity onset diabetes of the young, MODY 1-6), as well as genetic defects in insulin action which are based on various mutations of the insulin receptor (American Diabetes Association 2009).

Additionally, a cellular mediated autoimmune destruction of the  $\beta$ -cells within the pancreas can occur, leading to complete insulin deficiency (Type 1 diabetes). Key contributors to the susceptibility of Type 1 diabetes include genetic but also environmental factors like virus infections or chemicals that can lead to an induction of the disease (Kukreja and Maclaren 1999).

The most common symptoms of diabetic patients are polyuria and polydipsia, blurred vision and sometimes weight loss combined with polyphagia, retarded growth of children and susceptibility to distinct infections (American Diabetes Association 2009).

Chronic elevation of blood glucose levels along with the impact of increased blood pressure, abnormal lipid levels and abnormalities of small blood vessels can lead to long-term complications such as cardiovascular disease (CVD), nephropathy,

retinopathy, autonomic neuropathy causing gastrointestinal, genitourinary and cardiovascular symptoms and sexual dysfunction as well as peripheral neuropathy with risk of foot ulcers, amputations and Charcot joints. Moreover, the incidence of atherosclerotic cardiovascular, peripheral arterial and cerebrovascular disease is increased (American Diabetes Association 2009).

Uncontrolled hyperglycaemia can lead to the two most serious acute and life-threatening complications, diabetic ketoacidosis (DKA) and the hyperglycaemic hyperosmolar syndrome (HHS), which are both still associated with excess mortality (American Diabetes Association 2009, Chiasson *et al.* 2003).

## **2.1.2 Classification and diagnosis criteria in human beings**

### **2.1.2.1 Classification**

In the last decades, the classification for diabetes mellitus was revised several times, due to the considerable new knowledge about the aetiology of different forms of diabetes and better information about the validity of blood glucose concentrations with regard to diabetic complications (Alberti and Zimmet 1998). The first systematic classification was published in 1979 by the National Diabetes Data Group (NDDG) and was mainly based on the pharmacological treatment. This classification differentiated between insulin-dependent (IDDM, type 1 diabetes), non-insulin-dependent (NIDDM, type 2 diabetes), gestational diabetes and a fourth group named diabetes associated with other conditions and syndromes (Harris 1988). Expert groups of the World Health Organisation (WHO) revised this classification in 1980 and 1985, defining 5 classification groups which also considered pathogenic aspects and were named IDDM, NIDDM, gestational diabetes, malnutrition-related diabetes and other types.

In May 1995, an International Expert Committee, working under the sponsorship of the American Diabetes Association (ADA), was established to review scientific literature since 1979 and to decide if changes to the classification and diagnosis of diabetes were warranted. They revised the NDDG/WHO classification in 1997 in order to establish a classification, reflecting the aetiology and pathogenesis of diabetes mellitus. The main features of the changes were deletion of the terms IDDM, NIDDM and malnutrition-dependent diabetes, while the terms type 1 and type 2 as well as gestational diabetes, were retained. Type 2 diabetes includes all forms

of diabetes which result from insulin resistance with an insulin secretory defect (American Diabetes Association 2003). According to the recommendations of the ADA and the WHO, human diabetes mellitus is classified into four main groups:

#### **I. Type 1 diabetes**

Immune mediated or idiopathic  $\beta$ -cell destruction with usually total insulin deficiency

#### **II. Type 2 diabetes**

May range from predominantly insulin resistance with relative insulin deficiency to a predominantly secretory defect with insulin resistance

#### **III. Other specific types**

- Genetic defects resulting in  $\beta$ -cell dysfunction or disturbed insulin action
- Diseases of the endocrine pancreas
- Endocrinopathies
- Drug- or chemical-induced
- Infections
- Uncommon forms of immune-mediated diabetes
- Other genetic syndromes sometimes associated with diabetes

#### **IV. Gestational diabetes mellitus (GDM)**

Defined as any degree of glucose intolerance with onset or first recognition during pregnancy, regardless of whether insulin is used for treatment or the condition persists after pregnancy (Metzger *et al.* 2007).

##### 2.1.2.2 Diagnosis criteria

The diagnosis of diabetes mellitus and the assignment to one type of diabetes is sometimes difficult due to the particular circumstances present at the time of diagnosis and the lack of an identified unique qualitative biological marker that separates diabetic from non-diabetic people (American Diabetes Association 2009, Genuth *et al.* 2003). In 1997, the Expert Committee on the Diagnosis and Classification of Diabetes Mellitus re-examined the till then generally accepted diagnosis criteria, which relied on distributions of glucose levels, rather than on the relationship of glucose levels with complications. The committee made two seminal contributions: First they refocused attention on the relationship between glucose

levels and the presence of long-term complications. Second, they recommend that the fasting plasma glucose (FPG) level, rather than the plasma glucose 2 hours after oral glucose challenge (2HPG), be the preferred test for diagnosis, based on the fact that it is more convenient for the patients and less costly as well as less time consuming and, moreover, the reproducibility of the repeat-test is superior (American Diabetes Association 2003). The WHO adopted most of these recommendations in a consultation. However, for the WHO the 2HPG remained the “gold standard” for diagnosis of diabetes mellitus, especially for individuals with impaired fasting glucose (IFG) (Gillett 2009). According to the Expert Committee, three possibilities for the diagnosis of diabetes exist. Prerequisite for the diagnosis is the presence of at least one point listed in Table 2.1. If no explicit hyperglycaemia is detectable, each test has to be confirmed on a subsequent day by any of the three methods (American Diabetes Association 2009). This requirement is necessary particularly for people without diabetic symptoms, because several impacts like severe infections, trauma or even stress can lead to transient hyperglycaemia in non-diabetic individuals (Lehmann and Spinass 2005).

---

**Table 2.1 Criteria for the diagnosis of diabetes**

---

- 1) Fasting plasma glucose (FPG)  $\geq 126$  mg/dl (7.0 mmol/l). Fasting is defined as no caloric intake for at least 8 hours\*
- 2) Symptoms of hyperglycaemia and a casual plasma glucose  $\geq 200$  mg/dl (11.1 mmol/l). Casual is defined as any time of day without regard to time since last meal. The classic symptoms of hyperglycaemia include polyuria, polydipsia, and unexplained weight loss.
- 3) 2-h plasma glucose (2HPG)  $\geq 200$  mg/dl (11.1 mmol/l) during an oral glucose tolerance test (OGTT). The test should be performed as described by the WHO, using a glucose load containing the equivalent of 75 g anhydrous glucose dissolved in water.\*

---

\*In the absence of unequivocal hyperglycaemia, these criteria should be confirmed by repeat testing on a different day.

Some individuals feature slightly elevated plasma glucose levels, which are too low to meet criteria for diabetes. The Committee therefore introduced the term “impaired fasting glucose” (IFG) to differentiate the intermediate metabolic state from a

physiologic state (FPG < 100 mg/dl or 5.6 mmol/dl) and diabetes (FPG  $\geq$  126 mg/dl or  $\geq$  7.0 mmol/l) by using the FPG test. If an OGTT is used for the diagnosis, the intermediate glycaemic state (2HPG between 140 and 200 mg/dl or between 7.8 and 11.1 mg/dl) is called “impaired glucose tolerance” (IGT) as in the NDDG report from 1979 (Genuth *et al.* 2003).

Due to the perception that chronic hyperglycaemia, which is sufficient to cause diabetic long-term complications, is the hallmark of diabetes, laboratory measures which capture long-term glycaemic exposure are better markers for the presence and severity of the disease than single measures of glucose concentration (Nathan 2009). The glycated haemoglobin A<sub>1c</sub> (HbA<sub>1c</sub>) assay (A1C-test) captures the degree of glucose exposure over the previous 8-12 weeks and correlates well with the risk of diabetic complications. The concentration of HbA<sub>1c</sub>, which is formed through non-enzymatic attachment of glucose to haemoglobin, is commonly considered to reflect the integrated mean glucose level (Nathan *et al.* 2007). The HbA<sub>1c</sub> assay is the test of choice for the management of chronic diabetes and therefore is recommended since July 2010 by the International Expert Committee for the diagnosis of diabetes. Therefore diabetes should be diagnosed when the HbA<sub>1c</sub> level is  $\geq$  6.5%, and the result should be confirmed with a repeat A1C-test. Confirmation is not necessary in persons with plasma glucose levels > 200mg/dl (>11.1 mmol/l). Individuals with an A1C level  $\geq$  6% but < 6.5% are likely at the highest risk for progression to diabetes, but this range should not be considered an absolute threshold at which preventative measures are initiated. People with HbA<sub>1c</sub> levels below 6.0% may still be at risk and, particularly when other diabetic risk factors are present, they should also benefit from prevention efforts (Nathan 2009). If it is not possible to obtain a standardised or an affordable A1C-test, the previously recommended diagnostic methods (fasting and post-challenge glucose) remain acceptable (American Diabetes Association 2009, Fonseca *et al.* 2009).

### **2.1.3 Global and economical burden**

#### **2.1.3.1 Global burden of diabetes mellitus**

The International Diabetes Federation (IDF) reports 2009, that the prevalence of diabetes mellitus has reached globally epidemic levels. It is estimated that 285 million adults are suffering from diabetes in the seven regions of the IDF 2010, implying an

increase by 39 million compared to 2007 and by 255 million in the last 35 years. Moreover, the IDF expects an ongoing increase to almost 439 million people in the next 20 years which relates to an annual growth of 2.2%, nearly twice the annual growth of the total world adult population (Egede and Ellis 2010, International Diabetes Federation 2009). From this anticipated absolute global increase by 154 million people, 36% is projected to occur in India and China alone. The main reason for this huge increase is likely population growth, ageing of populations, and urbanization with associated lifestyle change, resulting in reduced physical activity and increased obesity. There are marked differences between developed and developing countries: In developing countries, numbers of diabetic adults are likely to increase by 69% from 2010 to 2030, compared to 20% for developed countries, whereas total adult populations are expected to increase by 36% and 2%, respectively (Shaw *et al.* 2010). One reason for the great increase of (mainly type 2) diabetes prevalence in developing countries could be the growing urbanization that is associated with a more sedentary lifestyle (Ramachandran *et al.* 1999). Specific lifestyle intervention programs have been shown to be efficacious in reducing diabetes incidence (Pan *et al.* 1997). Currently, the greatest number of people worldwide suffering from diabetes is in the 40- to 59-year-old age-group, but a tendency to older age-groups during the next 20 years is expected. The highest regional prevalence for 2010 can be stated for North America (10.2%), followed by the EMME (Eastern Mediterranean and Middle-East) (9.3%) and South Asia (7.6%). The African region is expected to have the largest proportional increase of the number of diabetic adults by 2030 (98.1%), followed by the EMME (93.9%), but North America will continue to have the world's highest prevalence (12.1%) (Shaw *et al.* 2010).

#### 2.1.3.2 Economical burden

The treatment and prevention of diabetes mellitus and its accompanying diseases requires huge amounts of money every year. It is expected to reach 11.6% of the total healthcare expenditure in the world for the year 2010 (at least 376 billion US Dollar). Due to the increasing prevalence of the disease, the projections for the year 2030 are expecting 490 billion US Dollar for global healthcare expenditure to treat and prevent diabetes mellitus. In the year 2010, approximately 75% of the global expenditure on care for diabetic patients will be spent for individuals between 50 and

80 years of age. The disparity between regions and countries is also alarming. In regions where 70% of people with diabetes live, namely low- and middle-income countries, less than 20% of the estimated global expenditures are spent, whereas the remaining 80% are spent in the world's economically richest countries, first of all the United States of America, with an expected 52.7% of global expenditure in 2010. Additionally, indirect costs of diabetes based on loss of production caused by disability as well as mortality are estimated to be even higher than the direct healthcare costs (International Diabetes Federation 2009).

## **2.2 Animal models in diabetic research**

### **2.2.1 The role of animal models for human diseases**

Animal models are used for studying the genetics and pathogenesis of diabetes and its accompanying complications, to develop new treatment strategies, including islet cell transplantation, and to find preventative strategies (Rees and Alcolado 2005).

Animal models, especially rodents like rats and mice play an essential role in the investigation of human diseases. Due to their small size, short generation time of about 10 weeks, easy availability, possibility of breeding under standardised conditions as well as economic considerations, rodents are mostly preferred to other animal models like pigs or dogs (Silver 1995, Srinivasan and Ramarao 2007). Moreover, large regions of synteny between the mouse and human genome exist, thus linkages can be easily translated between the two genomes (Waterston *et al.* 2002).

Mainly two conceptually different approaches exist for the generation of animal models for human diseases. The disease-driven directed genetic approach is based on identifying human disease genes and the characterization of the nature of the underlying mutation. Afterwards, the aim is to detect the corresponding gene in the murine genome and to create either the exact copy of the mutation observed in humans or to alter the genome, creating a physiologically similar situation. The second possibility is the mutagenesis-driven, non directed approach with the idea to create a mutation by radiation or chemical substances (e.g. N-ethyl-N-nitrosourea, ENU) and then identify the disease caused by the mutation as well as the underlying mutation. This random mutagenesis-driven approach has become a feasible way to

identify disease genes and is a rich source of novel disease genes and new animal models (Hardouin and Nagy 2000).

### **2.2.2 Animal models for diabetes mellitus**

Various diabetic animal models have been created in recent years and it is a still ongoing process. Most experiments are carried out on rodents, although some studies are performed on larger animals. Several methods are available to induce diabetes in animal models (Rees and Alcolado 2005, Srinivasan and Ramarao 2007):

- Toxins like streptozotocin and alloxan induce hyperglycaemia by toxic  $\beta$ -cell destruction
- Diabetogenic diets (e.g. high fat diet)
- Surgical manipulations (e.g. partial pancreatectomy)
- Selective inbreeding has already produced several diabetic strains that are useful models for Type 1 and Type 2 diabetes as well as related phenotypes such as obesity and insulin resistance.
- Gene targeting for the generation of e.g. transgenic animals, constitutive or conditional knock-out mice

Furthermore, genetic polymorphisms linked to different plasma glucose phenotypes of already existing mouse strains are examined in a genome-wide search for causative loci. The mapping of these so called quantitative trait loci (QTL) was carried out in independent as well as combined crosses of inbred mouse strains (Aigner *et al.* 2008, Clee and Attie 2007).

### **2.2.3 ENU mutagenesis**

The alkylating agent *N*-ethyl-*N*-nitrosourea (ENU) is a chemical compound which is known for a long time to be one of the most effective mutagens for the induction of specific-locus-mutations in murine premeiotic spermatogonial stem cells (Russell *et al.* 1979). Its great advantage over other mutagens is the potential of creating primarily point mutations. Therefore, most of the observed abnormal phenotypes are based on a single gene effect (Nolan *et al.* 2002). Moreover, ENU mutagenesis creates not only recessively acting null alleles but also dominant hypermorphic, hypomorphic and antimorphic alleles. This is a very important aspect in view of the fact that approximately 51% of human disease alleles do not act in a recessive way. In addition, the potential of ENU to create an allelic series for any

gene may provide useful informations for mapping of functional domains (Barbaric and Dear 2007).

Due to the fact that ENU not only possesses mutagenic but also toxic potential, the optimal dose must be found out, so that the highest mutation rate can be induced without rendering the animal infertile. It was determined that a repeated dosing regimen can achieve a higher mutation frequency (Hitotsumachi *et al.* 1985). Optimised treatment protocols can reach mutation frequencies of one mutation in 0.1-2.5 Mb (Beier 2000, Concepcion *et al.* 2004, Sakuraba *et al.* 2005). Numerous phenotype-driven ENU mouse mutagenesis projects were established world-wide during the last 12 years and provide the opportunity for the systematic, genome-wide, large-scale production and analysis of mouse mutants which can serve as models for inherited human diseases. The projects facilitate the identification as well as the functional characterization of genes that are relevant for the prevention, diagnosis and therapy of diseases (Aigner *et al.* 2008).

#### 2.2.3.1 Munich ENU Mouse Mutagenesis Project

In the Munich ENU mouse mutagenesis project, mutations in single genes and their effects on the animal organism are investigated. Standardised procedures to characterize mutant phenotypes have been developed and include screens for dysmorphological malformations and alterations in clinical chemistry, biochemistry, immunology, allergy and behaviour (Balling 2001, Soewarto *et al.* 2000). The project is carried out on the inbred C3HeB/FeJ (C3H) genetic background, known as a highly glucose-tolerant strain with a robust insulin secretory response (Clee and Attie 2007, Kaku *et al.* 1988). Starting at an age of ten weeks, male C3H mice receive three intraperitoneal ENU injections in weekly intervals. After a period of infertility, these treated male mice are mated to female C3H wild-type mice. The offspring (G1 animals) are screened for dominant mutations. Afterwards, different back- and side-crosses are performed to determine the inheritance of the mutation as well as to reveal recessive mutations (Aigner *et al.* 2008). Backcrossing phenotypic mutant mice for several generations to C3H wild-type mice will reduce the amount of non-causative mutations. Due to the fact that every backcross will decrease the number of mutations on average by 50 %, after 5 backcrosses a mouse will harbour approximately only one mutation and mutations on other chromosomes are eliminated (Aigner *et al.* 2008, Keays *et al.* 2006).

To determine the chromosomal position of the causative mutation, linkage analysis is carried out. For this purpose, heterozygous phenotypic mutant mice on the C3H inbred genetic background are bred to wild-type mice of a second inbred strain (C57Bl/6J). The male hybrid offspring (G1) are screened for the aberrant phenotype. Mice displaying the abnormal phenotype are then backcrossed to wild-type female mice of the second inbred strain (to screen for dominant mutations) or intercrossed (to detect recessive mutations). The resulting progenies (G2) are also screened and then separated into phenotypic mutant and phenotypic wild-type mice. The chromosomal location of the causative mutation is determined by analysing DNA samples of phenotypic G2 mutant mice and wild-type littermates via genome-wide linkage analysis, using a panel of DNA markers (single-nucleotide polymorphisms (SNPs) or microsatellites (Xing *et al.* 2005)) which are polymorphic for the two inbred strains used. Further linkage analysis and candidate gene sequencing are carried out to reveal the exact position of the mutation within the identified chromosomal section (Aigner *et al.* 2008).

#### 2.2.3.2 ENU-induced hyperglycaemia models

Several hyperglycaemic mouse strains with identified dominant causative mutations have already been generated in ENU mouse mutagenesis projects. Most of the identified mutations are related to the glucokinase gene (*Gck*) (Aigner *et al.* 2008). About 600 heterozygous mutations in the human glucokinase gene are already known to cause maturity-onset diabetes of the young type 2 (MODY 2), whereas homozygous mutations are reported to cause permanent neonatal diabetes mellitus (PNDM) (Osbak *et al.* 2009). A total number of 15 ENU-induced glucokinase mutant mouse strains have been generated in various ENU-driven mutagenesis projects (Fenner *et al.* 2009, Inoue *et al.* 2004, Toye *et al.* 2004) (<http://www.informatics.jax.org/>). Five of the identified mutations could also be found in humans with MODY 2 or PNDM (Inoue *et al.* 2004). Recently, a new mouse model for MODY 2 generated in the large-scale Munich ENU mouse mutagenesis project could be identified. The so-called Munich *Gck*<sup>M210R</sup> mutant mouse exhibits a T to G transversion mutation at nt 629 in *Gck* which leads to a reduction of the hepatic glucokinase enzyme activity (van Burck *et al.* 2010).

Another hyperglycaemic strain derived from the Munich ENU mouse mutagenesis screen, the Munich *Ins2*<sup>C95S</sup> mutant mouse, exhibits a missense mutation in the

insulin 2 gene (*Ins2*) (Herbach *et al.* 2007). Insulin gene mutations in human beings are also known to be associated with PNDM (Støy *et al.* 2007) (see below).

## 2.3 Insulin gene mutations

### 2.3.1 Mutations in humans

More than 20 mutations in the insulin gene have recently been described as a new monogenic cause of neonatal diabetes (Colombo *et al.* 2008, Edghill *et al.* 2008, Støy *et al.* 2007). The clinical manifestation of these new mutations is more severe like that of most previously described INS mutations and diabetes-onset already occurs at a mean age of 11 weeks (Støy *et al.* 2007). Mutations reported earlier, primarily affected the biological activity of the altered (pro)insulin molecules but did not impair their biosynthesis significantly, thereby leading to impaired (pro)insulin clearance with hyperinsulinaemia and hyperproinsulinaemia. Therefore, in these patients, diabetes only occurred in the presence of insulin resistance and in adults but most of the carriers were asymptomatic (Nanjo *et al.* 1986, Støy *et al.* 2007). New studies could demonstrate that mutations in the INS gene are the second most common cause of permanent neonatal diabetes mellitus (PNDM). One study demonstrated that out of 141 patients with PNDM which was diagnosed in the first 6 months of life, 33 (23%) exhibited missense mutations in the INS gene. From 86 cases of diabetes diagnosed between 6 and 12 months only 2% were caused by INS gene mutations. From 263 cases of MODY 2 and 463 cases of type 2 diabetes occurring in young patients, only one case each could be attributed to mutations in the insulin gene. Sixteen different heterozygous INS mutations could be determined in the 35 patients with diabetes diagnosed during infancy (the first 12 months of life). The three most common (46%) mutations were A24D, F48C and R89C, representing amino acid exchanges at different positions in the preproinsulin molecule (Edghill *et al.* 2008). Moreover, one mutation (C96Y) was found in three patients and was already identified in the Akita mouse (Støy *et al.* 2007, Wang *et al.* 1999). Most of the observed mutations result in addition or removal of a cysteine, which leads to an odd number of potential disulfide pairing sites, resulting in an imbalance that is thought to cause misfolding and aggregation of mutant (pro)insulin (Weiss 2009). Dominant inheritance was only observed in 20% of the identified INS gene mutations, whereas the majority results from sporadic de novo mutations (Edghill *et al.* 2008).

Recently, studies could also identify some novel INS gene mutations as a cause for MODY (Boesgaard *et al.* 2010, Molven *et al.* 2008). The relatively mild phenotype in most of these cases suggests, that a spectrum of phenotypes may exist in patients with INS mutations, ranging from mild diabetes and hyperinsulinaemia in patients with mutations that cause reduced biological activity of the insulin molecule (i.e., B24Ser, B25Leu, and A3Leu) to MODY in patients with mutations that are predicted to reduce the structural stability of the insulin molecule (i.e., R46Q). Finally, neonatal diabetes can occur in patients with mutations that cause severe defects in the biosynthesis of the insulin molecule (for example B8Ser and B19Gly) with the consequence of presumably unfolded protein response (UPR), ER-stress and  $\beta$ -cell apoptosis (Molven *et al.* 2008, Støy *et al.* 2007). The severity of the phenotype is likely depending on the perturbation grade of disulfide pairing in nascent proinsulin, on the site of the mutation and the properties of the substituted side chain. It is still unclear, why expression of the wild-type allele is not sufficient to maintain glucose homeostasis. It is suggested, that the misfolded protein variant also perturbs synthesis of wild-type insulin (Weiss 2009). In one study on isolated pancreatic islets of *Akita* mice it could be shown, that the mutant C(A7)Y proinsulin forms high-molecular-weight protein complexes, and that the intermolecular protein complexes also include wild-type endogenous proinsulin, involving covalent as well as possible hydrophobic interactions. Liu *et al.* (2007) also suggested that the retention of mutant proinsulin in the ER leads to impaired transport of non-mutant proinsulin and to ER-associated protein degradation of the mutant- and non-mutant proinsulin complexes. This thesis is affirmed by the observation of a decrease in steady-state levels of non-mutant proinsulin and insulin, induced by dominant negative effects of the C(A7)Y mutant (Liu *et al.* 2007).

The misfolding of insulin, and consequently defective trafficking to secretory granules, has been recognized as the likely underlying cause of  $\beta$ -cell dysfunction and death in several rodent models of non-immune diabetes like in the *Akita* mouse and the Munich *Ins2*<sup>C95S</sup> mutant mouse (Meur *et al.* 2010).

Unlike in *Akita* and Munich *Ins2* mutant mice, the phenotype of male and female human patients harbouring INS mutations does not differ, however, the birth weight of male patients in some cases was lower compared to that of newborn female mutation carriers (Edghill *et al.* 2008).

Due to the fact that a spectrum of phenotypes exists in INS mutation carriers, screening for INS mutations was suggested not only in neonatal diabetes, but also in MODY and in selected cases of type 1 diabetes (Molven *et al.* 2008).

### 2.3.2 The Munich *Ins2*<sup>C95S</sup> mutant mouse

The nonobese diabetic mouse model Munich *Ins2*<sup>C95S</sup> was generated in the Munich ENU Mouse Mutagenesis Project on the genetic background of the inbred strain C3HeB/FeJ (C3H). The hyperglycaemic phenotype is caused by an autosomal dominant mutation at nucleotide position 1903 in exon 3 of the *Ins2* gene with the consequence of an amino acid exchange from cysteine to serine at position 95 of preproinsulin (C95S), corresponding to amino acid 6 on the A chain of proinsulin (A6). This in turn, inhibits the formation of the A6 - A11 intrachain disulfide bond (Herbach *et al.* 2007).

#### 2.3.2.1 Heterozygous Munich *Ins2*<sup>C95S</sup> mutant mice

Heterozygous mutant mice showed significantly elevated blood glucose concentrations both 15-hours fasted and 1.5-hours postprandially at 1, 3 and 6 months of age as compared to sex- and age-matched littermate controls. At an age of 3 weeks, blood glucose levels did not differ yet between mutant and wild-type mice.

Blood glucose levels of male mutant mice increased steadily between 1 and 6 months of age, whereas female mutant mice only featured a mild diabetic phenotype with almost stable blood glucose concentrations.

Mutant mice of both genders also showed significantly higher blood glucose concentrations versus wild-type mice during oral glucose tolerance tests (OGTT). Three- and 6-month-old male mutant mice demonstrated significantly elevated blood glucose concentrations during OGTT as compared to female mutant mice at all time points investigated.

Fasting and 1.5-h postprandial serum insulin levels of male and female mutant mice were similar to those of sex-matched controls. The serum insulin levels 10 minutes after glucose stimulation however, were significantly reduced in male and female mutant mice as compared to controls, irrespective of the age at sampling. Serum insulin levels of male and female mutant mice were equal, despite much lower blood glucose levels in female vs. male mutants.

The homeostasis model assessment (HOMA) of  $\beta$ -cell function index of mutant versus wild-type mice was largely reduced in both genders at 1, 3 and 6 months of age. The HOMA of insulin resistance index at an age of 3 and 6 months was significantly higher in male mutant mice as compared to controls, whereas female mutant mice exhibited almost similar insulin sensitivity as the accordant wild-type mice.

At an age of 3 and 6 months, the insulin content in the pancreas was significantly reduced in both male and female mutant mice as compared to sex-matched wild-type mice. In female mutant mice, the insulin content at an age of 6 months was still about half of the amount of wild-type mice, whereas in male mutant mice almost no insulin was detectable.

Immunohistochemical investigations of the endocrine pancreas for insulin and glucagon of 6-month-old mutant mice showed a disturbed islet structure: The amount of insulin positive  $\beta$ -cells was reduced, whereas the amount of glucagon producing  $\alpha$ -cells was increased and  $\alpha$ -cells were distributed all over the islet. In contrast, islets of wild-type mice demonstrated a typical murine islet structure, with a core of insulin-expressing cells, surrounded by a few non- $\beta$ -cells. Moreover, the staining intensity of insulin-positive cells in mutants was much weaker as compared to that of wild-type mice (Herbach *et al.* 2007). All the described alterations were less distinct in female mutant mice compared to male mutants (Herbach *et al.* personal communication).

Quantitative stereological investigations showed no difference concerning total pancreas volume between 6-month-old mutant and wild-type mice.

The total islet volume, the total  $\beta$ -cell volume as well as the volume density of  $\beta$ -cells in the islets were significantly reduced in male but not in female mutant mice compared to sex-matched wild-type mice.

Both, male and female mutant mice demonstrated a significantly increased volume density of  $\alpha$ -cells in the islets compared to wild-type mice, whereas the total volume of  $\alpha$ -cells was only significantly increased in female mutants compared to wild-type mice.

Only male mutant mice exhibited a significantly higher volume density and total volume of somatostatin producing  $\delta$ -cells as well as of pancreatic polypeptide producing PP-cells as compared to male wild-type mice.

Electron microscopically, the  $\beta$ -cells of 6-month-old male mutant mice featured a variety of ultrastructural alterations compared to male wild-type mice, such as prominent disorganization of the rough endoplasmic reticulum (rER) with dilated cisternae, mitochondrial swelling with largely destroyed crests and apparent myelin figures. Moreover, in male mutant mice only few small immature insulin granules were found, in contrast to the high numbers of granules apparent in male wild-type mice (Herbach *et al.* 2007). In female mutants, these ultrastructural alterations were less distinct compared to male mutants, however, female mutant mice also demonstrated less secretory granules than female wild-type mice (Herbach *et al.* personal communication).

No signs of apoptosis, including chromatin condensation or apoptotic bodies could be found in islets of male mutants (Herbach *et al.* 2007).

These results demonstrate that male and female heterozygous Munich *Ins2*<sup>C95S</sup> mutant mice both develop diabetes mellitus. Male mutants show a progressive diabetic phenotype with massive hyperglycaemia, insulin resistance and profound decrease of  $\beta$ -cell mass. In contrast, female mutant mice demonstrate a much milder and stable diabetic phenotype with no signs of insulin resistance and an almost unaltered  $\beta$ -cell mass (Herbach *et al.* 2007).

#### 2.3.2.2 Homozygous Munich *Ins2*<sup>C95S</sup> mutant mice

Homozygous mutant mice demonstrated no diabetic phenotype until 18 days postnatally. At 21 days of life, mutant mice of both genders already showed severe hyperglycaemia, reaching blood glucose levels of almost 400 mg/dl. At an age of 28 days, the body weight of both male and female mutant mice was reduced compared to wild-type mice and further decreased until time of death. Homozygous male and female mutants died at a mean age of 46 and 52 days, respectively (Herbach *et al.* 2007).

### 2.3.3 Akita mouse

The Akita mouse is a nonobese diabetic mouse model that arose from a female C57BL/6 mouse harbouring a spontaneous point mutation in *Ins2*. A stable mouse line was established by breeding male heterozygous mutant mice with female C57BL/6 (B6) wild-type mice (Yoshioka *et al.* 1997). The mutation is characterized by

a G→A transversion at nucleotide position 1907 in exon 3 of *Ins2*, leading to a substitution of cysteine on position 96 of the A chain of preproinsulin 2 by tyrosine (C96Y). As a consequence, the mutation prevents formation of the A7-B7 interchain disulfide bond of insulin 2, resulting in a reduced processing of proinsulin and a severe reduction of mature insulin. The mutation is inherited in an autosomal dominant way (Clee and Attie 2007, Wang *et al.* 1999).

The identical mutation (C96Y) in the *Ins2* gene could be identified in humans with PNDM (2.3.1 Mutations in humans).

#### 2.3.3.1 Heterozygous Akita mutant mice

Soon after weaning, heterozygous Akita mutant mice exhibit a diabetic phenotype, including symptoms like hyperglycaemia, polydipsia and polyuria. Male mice develop a progressive diabetic phenotype, whereas female mutant mice only show mild diabetic symptoms.

From the age of 18 weeks, male mutant mice did not gain further weight and moreover, weight loss was apparent by 30 weeks of age, whereas female mutant mice demonstrated growth rates comparable to female wild-type mice up to an age of 43 weeks. The 50% survival rate of male mutant mice was less than half that of male wild-type mice, whereas female mutant mice showed a similar life expectancy as the accordant controls.

From an age of 4 weeks onwards, randomly fed blood glucose concentrations of both male and female Akita mutant mice were significantly higher as compared to sex- and age-matched wild-type mice. Male mutants showed a constant increase of blood glucose levels up to an age of 9 weeks, afterwards blood glucose remained relatively stable (approximately 550-600mg/dl). In contrast, female mutant mice demonstrated blood glucose concentrations below 330mg/dl. At 7 weeks of age, randomly fed plasma insulin levels were significantly lower in mutant mice of both genders as compared to sex- and age-matched wild-type mice (Yoshioka *et al.* 1997).

The insulin content in the pancreas of pooled male and female mutant Akita mice at an age of 2 weeks was about half that of wild-type mice (Kayo and Koizumi 1998). At an age of 8 weeks, the pancreatic insulin content of male and female mutant mice was approximately 25 and 50% that of wild-type mice, respectively (Oyadomari *et al.* 2002). The loss of only mutant insulin 2 cannot explain such a drastic reduction of proinsulin and insulin protein levels (Izumi *et al.* 2003).

Heterozygous Akita mutant mice should also have native insulin molecules derived from 3 wild-type alleles (two *Ins1* and one *Ins2*). *Ins1* transcripts represent approximately 25% of the total insulin transcripts in mutant as well as in wild-type mice and transcripts of *Ins2* were also similar in mutants and wild-type mice, representing 75% of the total insulin transcripts. Mutant and the wild-type *Ins2* alleles in heterozygous mutant mice were also transcribed in similar amounts (Wang *et al.* 1999). If the native insulin molecules were secreted efficiently, severe glucose intolerance and insulin deficiency should not occur in Akita mice (Izumi *et al.* 2003).

Morphologic studies of islets on pancreas sections immunostained for insulin and glucagon of 4-, 10-, 20- and 30-week-old-mice revealed that irrespective of sex and age, the relative areas (%) of islets in diabetic mice were not significantly different from those of wild-type mice. At the age of 4 weeks, mutant mice of both genders demonstrated a significantly lower proportion of insulin-positive cells in the islets than sex-matched wild-type mice. At the age of 30 weeks, the proportion of insulin positive islet cells decreased further in male mutant mice, whereas the proportion in female mutant and wild-type mice remained stable (Yoshioka *et al.* 1997).

The staining intensity for insulin in age-matched 8-12 week-old male mutant mice was weaker as compared to sex-and age-matched wild-type mice. Since the insulin-autoantibody only detects the wild-type and not the mutated insulin, the weak staining intensity indicates a dramatic decrease in wild-type insulin. The immunoreactivity of C-peptide was also much weaker in  $\beta$ -cells of mutant mice as compared to wild-type mice, strongly suggesting that the amount of proinsulin from both mutant and wild-type alleles was decreased (Wang *et al.* 1999).

Electron microscopic analysis of  $\beta$ -cells from 4- to 18-week-old male Akita mutant mice revealed that the lumina of ER-like organelles were markedly enlarged and had a more electron-dense appearance, suggesting that misfolded proinsulin 2 is trapped and accumulated. Mitochondria of older mice were markedly swollen and denatured without distinct cristae (Izumi *et al.* 2003). The average volume and the volume density of secretory granules of 8- to 12-week-old mutant mice were severely reduced versus age-matched wild-type mice, however the number of secretory granules (numerical density per unit volume) was not altered from that of control mice

Moreover, immunogold labelling suggested, that proinsulin accumulates in the pre-Golgi intermediates of Akita mutant mice (Zuber *et al.* 2004).

In recent studies it could be demonstrated that islets of mutant Akita mice contain more apoptotic cells than islets of wild-type mice. Moreover, disruption of the C/EBP homologous protein (CHOP)/growth arrest and DNA damage (Gadd)153 gene resulted in an ameliorated diabetic phenotype, indicating that apoptosis was induced by ER-stress (Oyadomari *et al.* 2002).

#### 2.3.3.2 Homozygous Akita mutant mice

One-day-old homozygous mutant Akita mice showed reduced body weight but only slightly elevated blood glucose levels as compared to heterozygous mutant and wild-type mice, whereas 14-day-old homozygous mutant mice demonstrated much higher blood glucose levels than the other two genotypes, reaching approximately 450 mg/dl. Gender differences in blood glucose levels or other cytometric parameters could not be observed until 14 days of age. The relative area (%) of islets in pancreas sections of sex-matched homozygous mutant mice at an age of 1 and 14 days was less than half that of the two other genotypes. At the same age, immunohistochemical examinations revealed a markedly lower proportion of insulin positive  $\beta$ -cells as compared to heterozygous mutant as well as wild-type mice, whereas the proportion of glucagon positive  $\alpha$ -cells was largely increased.

Electron microscopy of pancreas sections from 14-day-old homozygous mutant mice showed a decreased density of secretory granules, increased amount of ER and swollen mitochondria (Kayo and Koizumi 1998).

#### 2.3.3.3 ER-stress in the Akita mouse

Proinsulin from mutant Akita mice is more hydrophobic and less stable than wild-type proinsulin. As a result of hydrophobic interactions between the molecules, it is likely that mutant proinsulin aggregates more easily than wild-type proinsulin. Mutant proinsulin is mainly found as a tetramer, wild-type as a dimer, but it is also possible that the wild-type insulin is incorporated into aggregates of the mutant insulin (Yoshinaga *et al.* 2005). Liu *et al.* (2007) could directly show that the intermolecular mutant proinsulin complexes also include wild-type proinsulin, involving covalent as well as possible hydrophobic interactions (Liu *et al.* 2007). Aggregation of hydrophobic mutant proinsulin can lead to ER-stress by mobilizing the ER-stress

chaperone binding Ig protein (BiP), also called glucose regulated protein 78 (GRP78) (Yoshinaga *et al.* 2005). This protein was overexpressed in pancreatic islets of 8- to 12-week-old Akita mutant mice, probably forming complexes with proinsulin (Wang *et al.* 1999). In response to the accumulation of unfolded proteins in the ER, eukaryotic cells activate an intracellular signalling pathway from the ER to the nucleus known as the unfolded protein response (UPR). This response consists mainly of three components that counteract ER-stress: First, up-regulation of genes encoding ER chaperone proteins such as BiP/GRP78 to increase the protein folding capacity in the ER, second, translational attenuation to reduce the load of new protein synthesis and prevent further accumulation of unfolded proteins, and third, transcriptional induction of components of the ER-associated protein degradation system (ERAD) to eliminate misfolded proteins by the ubiquitin-proteasome system (Mori 2000, Oyadomari and Mori 2004) (Figure 2.1).

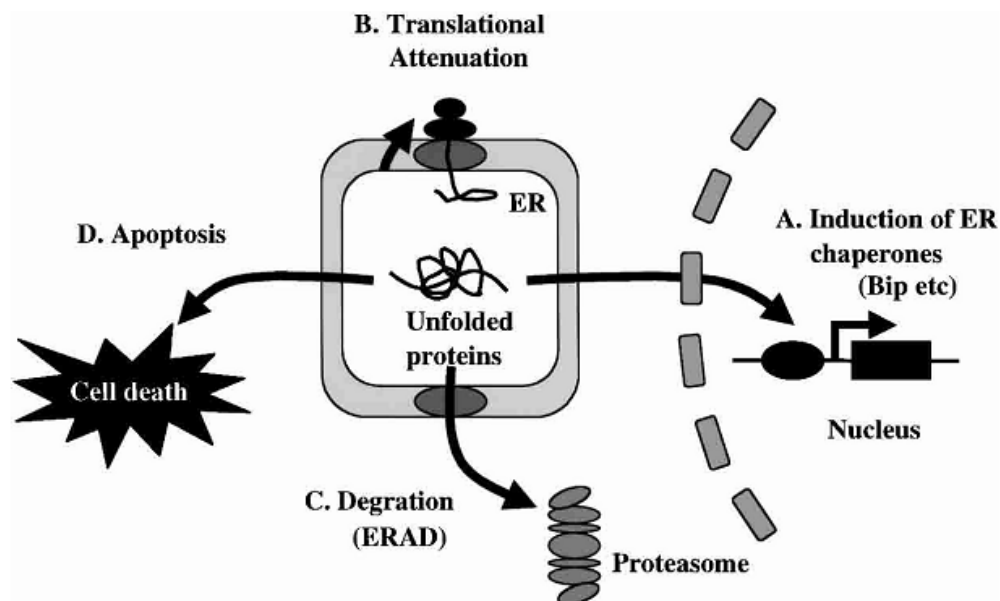


**Figure 2.1: ER-stress response pathway**

Accumulation of unfolded proteins in the ER activates four distinct cellular responses. (A) Transcriptional induction of ER chaperones increases protein folding activity and prevents protein aggregation. (B) Translational attenuation reduces the load of new protein synthesis and prevents further accumulation of unfolded proteins. (C) The ER-associated degradation (ERAD) pathway eliminates misfolded proteins by the ubiquitin-proteasome system (UPS). (D) When functions of the ER are severely impaired, apoptosis is induced to destroy the cell (Araki *et al.* 2003).

Inositol-requiring protein-1 (IRE1), double-stranded RNA-dependent protein kinase-related ER kinase (PERK) and activating transcription factor-6 (ATF6) are the proximal sensors of unfolded protein accumulation in the ER. These sensors control the load of nascent polypeptides entering the ER lumen as well as the concentration of chaperones and catalysts participating in disulfide bond formation and the machinery for degradation of misfolded protein (Scheuner and Kaufman 2008). It could be demonstrated, that BiP as well as the ERAD components HMG-CoA reductase degradation protein 1 (HRD-1) and protein sel-1 homolog 1 (Sel1L) were up-regulated in the islets of mutant Akita mice. Moreover, X-box binding protein 1 (XBP-1) splicing levels were elevated as compared to wild-type mice. Due to these results, it is supposed that misfolded (pro)insulin is degraded by a HRD-1 mediated pathway (Allen *et al.* 2004). When the functions of the ER are severely impaired and cell protective changes mediated by the UPR fail to restore folding capacity, apoptosis can occur as a fourth component of the UPR, to protect the organism by eliminating the damaged cells (Lai *et al.* 2007, Oyadomari and Mori 2004). One of the components of the ER-stress-mediated apoptosis pathway is C/EBP homologous protein (CHOP), also known as growth arrest- and DNA damage-inducible gene 153 (GADD153) (Oyadomari and Mori 2004). It is one of the most highly up-regulated genes during prolonged ER-stress and encodes a transcription factor that promotes programmed cell death (Lai *et al.* 2007, Ron 2002). All three UPR signalling pathways are involved in inducing CHOP transcription, although the PERK pathway is essential (Lai *et al.* 2007) (Figure 2.2).

In 8-week-old heterozygous mutant Akita mice with an additional *Chop* knockout (*Chop*<sup>-/-</sup>), the onset of diabetes began 8 – 10 weeks later as compared to Akita mice without intact *Chop* (*Chop*<sup>+/+</sup>). The pancreatic insulin content of both male and female heterozygous *Chop*<sup>-/-</sup> Akita mutant mice was significantly higher as compared to accordant sex- and age- matched *Chop*<sup>+/+</sup> mice. It was also shown, that pancreatic islets of 4-week-old heterozygous *Chop*<sup>-/-</sup> Akita mutant mice exhibited significantly less apoptotic cells as compared to *Chop*<sup>+/+</sup> Akita mutants (Oyadomari *et al.* 2002). All these findings show that the activation of CHOP in heterozygous Akita mutant mice leads to  $\beta$ -cell apoptosis and therefore enhances the progression of diabetes mellitus.

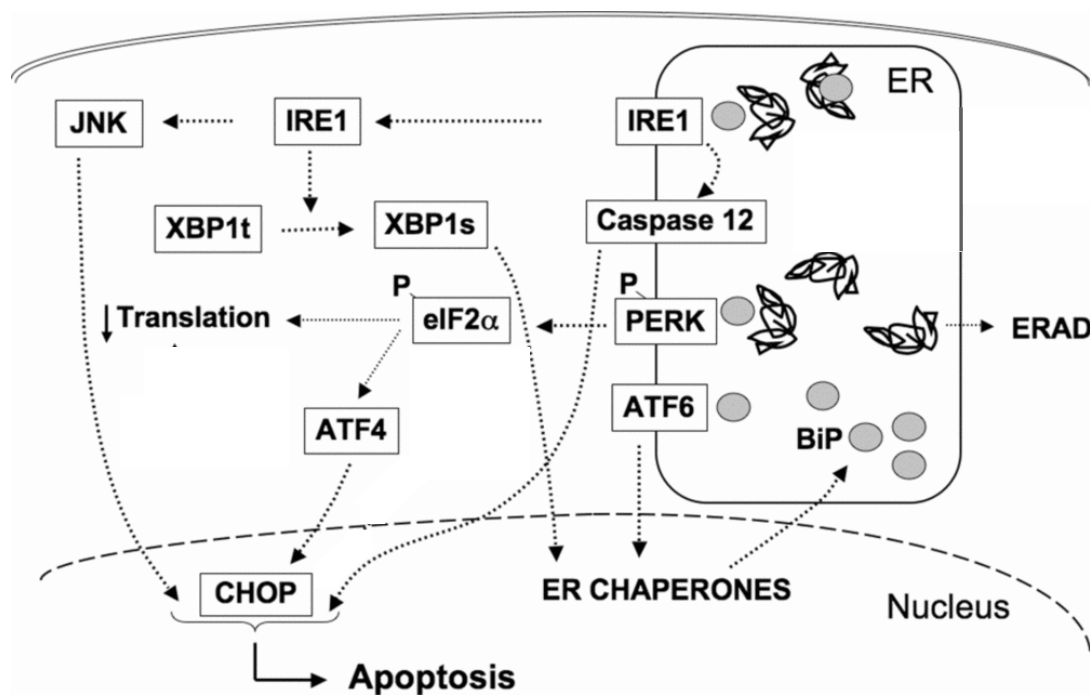


**Figure 2.2: ER-stress signalling**

IRE1, ATF6 and PERK are the three main ER-stress transducers. They are inactive due to binding to the ER chaperone BiP, which is a key regulator of the ER-stress response. When proteins misfold in the ER lumen, BiP dissociates from the ER-stress transducers, leading to their activation. The IRE1 endoribonuclease splices *XBP1* mRNA, allowing its translation. XBP1s is a transcription factor regulating expression of ER genes involved in protein folding and export as well as ERAD (ER-associated protein degradation). IRE1 also activates JNK. ATF6 induces ER chaperones, such as BiP. PERK phosphorylates eIF2 $\alpha$ , thereby inhibiting translation initiation and reducing the arrival of newly synthesized proteins in the ER. Translation of some proteins such as ATF4 is facilitated. ATF4 induces expression of the pro-apoptotic transcription factor CHOP. In the case of prolonged and excessive ER-stress, apoptosis will be triggered. Apoptosis is caused through JNK, CHOP and the ER-specific caspase 12 (modified according to Cnop *et al.* 2008).

### 2.3.4 *Ins1* and *Ins2* null mutant mice

For the creation of insulin deficient double homozygous null mutant mice (*Ins1*<sup>-/-</sup>, *Ins2*<sup>-/-</sup>) as well as single homozygous null mutant mice (*Ins1*<sup>-/-</sup>, *Ins2*<sup>+/+</sup> or *Ins1*<sup>+/+</sup>, *Ins2*<sup>-/-</sup>), the particular insulin genes (*Ins1* and/or *Ins2*) were disrupted by means of gene targeting (Duvillie *et al.* 1997). Further, single heterozygous null mutant mouse models were created harbouring only one single copy of one *Ins* gene (*Ins1*<sup>+/-</sup>, *Ins2*<sup>-/-</sup> or *Ins1*<sup>-/-</sup>, *Ins2*<sup>+/-</sup>) (Babaya *et al.* 2006).

#### 2.3.4.1 Double homozygous *Ins1* and *Ins2* null mutant mice

In double homozygous *Ins* null mutant mice, the absence of embryonic insulin had no impact on embryonic lethality. Intrauterine growth retardation, with a 15 - 20% reduction in body weight as compared to control mice was observed at day 18.5 of fetal life. The relative organ weights of homozygous *Ins* null mutants remained unaltered and no differences in blood glucose concentrations were observed. As soon as the mutant mice started to suckle, glucosuria was detected, followed by ketonuria developing within a day, and homozygous null mutants finally died on average within 48 h (Duvillie *et al.* 1997).

The mean islet area was higher in double homozygous null mutant mice than in wild-type controls as well as in heterozygous single null mutant mice (*Ins1*<sup>-/-</sup>, *Ins2*<sup>+/-</sup>) at embryonic day 18.5 and also in the newborn (Duvillie *et al.* 1997, Duvillie *et al.* 2002). The individual  $\beta$ -cell size in insulin deficient mice was similar to controls, suggesting that islets were enlarged due to a higher replication rate of established endocrine islet-cells within existing islets. Additionally, insulin deficient mutant mice demonstrated a significantly lower incidence of apoptotic islet cells, which may be related to a 2-fold increased vascularisation of the pancreas. Morphometric analysis demonstrated that the area fraction of  $\beta$ -cells in the islets of *Ins1*<sup>-/-</sup>, *Ins2*<sup>-/-</sup> and *Ins1*<sup>-/-</sup>, *Ins2*<sup>+/-</sup> mutant mice at embryonic day 18.5 was about 76 % and that of  $\alpha$ -cells about 17 %. Due to the fact that the proportional contribution of  $\alpha$ - and  $\beta$ -cells in *Ins1*<sup>-/-</sup>, *Ins2*<sup>-/-</sup> mutant mice was similar to that of *Ins1*<sup>-/-</sup>, *Ins2*<sup>+/-</sup> mutant as well as to that of wild-type mice, the increased mean islet area of double homozygous null mutant mice seems to be caused by an increase of both, the total estimated  $\beta$ -cell and  $\alpha$ -cell mass. It was therefore suggested that insulin may act as a negative regulator of islet size *in utero* (Duvillie *et al.* 2002).

#### 2.3.4.2 Single homozygous *Ins1* and *Ins2* null mutant mice

Single homozygous *Ins1*<sup>-/-</sup> as well as *Ins2*<sup>-/-</sup> mutant mice did not show major metabolic disorders and were both viable and fertile. Both mutants as well as wild-type mice exhibited similar plasma insulin levels at an age of 2 – 4 months and the pancreatic insulin content was also comparable to wild-type mice. RT-PCR revealed that *Ins2* transcripts of *Ins1*<sup>-/-</sup> mutant mice were comparable to wild-type mice, whereas in *Ins2*<sup>-/-</sup> mutant mice a dramatic increase of *Ins1* transcripts was observed. This finding led to the conclusion that in *Ins2*<sup>-/-</sup> mutants, the absence of *Ins2*, which represents the

majority of total insulin transcripts in wild-type mice, is being compensated by up-regulation of *Ins1* transcription. This compensation first occurred during late gestation or postnatally and explains the similar pancreatic insulin content of mutant and wild-type mice as well as the prevention from developing diabetes mellitus.

From one week of age onwards, blood glucose concentrations of both *Ins1*<sup>-/-</sup> and *Ins2*<sup>-/-</sup> mutant mice were similar to those of wild-type mice. Moreover, 4- to 6-month-old *Ins2*<sup>-/-</sup> mutants showed similar intraperitoneal glucose tolerance tests as compared to wild-type mice.

Immunocytochemical staining of pancreas sections from 2- to 4-month-old male *Ins1*<sup>-/-</sup> and *Ins2*<sup>-/-</sup> mutant mice indicated normal distribution of  $\beta$ -,  $\alpha$ -,  $\delta$ - and PP-cells in the islets and therefore, the overall islet morphology as well as the distribution of the different endocrine islet cell types were not altered compared to wild-type mice.

Morphometric analyses were accomplished on pancreas sections of 7- to 11-week-old male *Ins1*<sup>-/-</sup> and *Ins2*<sup>-/-</sup> mutant mice immunostained with anti-insulin antibody. These investigations revealed an almost 3-fold increased  $\beta$ -cell mass in *Ins2*<sup>-/-</sup> mutant mice and a less than 2-fold increased  $\beta$ -cell mass in *Ins1*<sup>-/-</sup> mutant mice as compared to wild-type mice, whereas the mean individual  $\beta$ -cell size was similar. It is suggested, that the lack of insulin or low insulin production may lead to  $\beta$ -cell hyperplasia (Leroux *et al.* 2001).

The compensatory increase of *Ins1* transcription in *Ins2* deficient  $\beta$ -cells was confirmed in *in vitro* studies using a  $\beta$ -cell line ( $\beta$ *Ins2*<sup>-/-lacZ</sup>) derived from *Ins2*<sup>-/-</sup> mice that carry the *lacZ* reporter gene under control of the *Ins2* promoter. *Ins1* gene expression was largely increased in  $\beta$ *Ins2*<sup>-/-lacZ</sup> cells, which was interpreted as a compensatory effect due to the absence of *Ins2* transcripts and explains the similar total insulin content compared to other murine  $\beta$ -cell lines, in which both *Ins* genes were functional. When  $\beta$ *Ins2*<sup>-/-lacZ</sup> cells were incubated for 2 hours in glucose supplemented Krebs-Ringer secretion buffer, the amount of insulin released from the  $\beta$ *Ins2*<sup>-/-lacZ</sup> cells increased with increasing glucose concentrations (Leroux *et al.* 2003).

#### 2.3.4.3 Single heterozygous *Ins1* and *Ins2* null mutant mice

Babaya *et al.* (2006) described a novel insulin-deficient mouse model on a nonobese diabetic (NOD) background with a single copy of the gene encoding insulin 1 (*Ins1*) and no gene encoding insulin 2 (*Ins2*) (NOD<sup>*Ins1*<sup>+/-</sup>,*Ins2*<sup>-/-</sup></sup>). In addition they established 3 other lines with different knock-outs (NOD<sup>*Ins1*<sup>-/-</sup>,*Ins2*<sup>+/-</sup></sup>, NOD<sup>*Ins1*<sup>+/+</sup>,*Ins2*<sup>-/-</sup></sup>, NOD<sup>*Ins1*<sup>-/-</sup>,*Ins2*<sup>+/+</sup></sup>).

By 10 weeks of age, all male NOD<sup>Ins1+/-,Ins2-/-</sup> mice developed diabetes, whereas no male mouse with only a single *Ins2* gene (NOD<sup>Ins1-/-,Ins2+/-</sup>) as well as mice with single homozygous knock-outs (NOD<sup>Ins1+/+,Ins2-/-</sup>, NOD<sup>Ins1-/-,Ins2+/+</sup>) developed diabetes by this age and in addition, none of the female knock-outs showed a diabetic phenotype, irrespective of the number of genes encoding for insulin. After 10 weeks of age, female NOD<sup>Ins1+/+,Ins2-/-</sup> and NOD<sup>Ins1+/-,Ins2-/-</sup> mice showed a high prevalence of diabetes and severe insulinitis. Both male and female homozygous *Ins1* knock-out mice (NOD<sup>Ins1-/-,Ins2+/+</sup>) and mice with only a single *Ins2* gene (NOD<sup>Ins1-/-,Ins2+/-</sup>) did not develop diabetes until 36 weeks of age.

The pancreatic insulin content in 4- to 5-week-old male and female NOD<sup>Ins1+/-,Ins2-/-</sup> mice was extremely low compared to all other genotypes including wild-type mice but no difference between male and female NOD<sup>Ins1+/-,Ins2-/-</sup> mice was detected, prefiguring a higher insulin-resistance of male NOD mice. During intraperitoneal insulin tolerance tests (ipITTs) at an age of 10 weeks, male NOD<sup>Ins1+/-,Ins2-/-</sup> mice showed significantly higher fasted blood glucose levels as compared to female NOD<sup>Ins1+/-,Ins2-/-</sup> mice and the blood glucose concentrations 15 and 30 minutes after an intraperitoneally insulin injection also were significantly higher in male mutants as compared to female mutants, substantiating the suspicion of increased insulin-resistance in male mice.

All these results demonstrate that existing sex differences between male and female NOD<sup>Ins1+/-,Ins2-/-</sup> mice lead to a milder diabetic phenotype in female mice and suggested less insulin resistance as compared to male mice (Babaya *et al.* 2006).

## 2.4 Estrogen

### 2.4.1 Estrogen production and action

Estrogens belong to the group of sex steroid hormones (SSH) comprising also progestagens (pregnenolone, progesterone) and androgens (testosterone, dihydrotestosterone, dehydroepiandrosterone, androstenedione) (Bulun and Adashi 2008).

The naturally occurring estrogens estradiol (E2), estrone (E1), and estriol (E3) are C18 steroids derived from cholesterol. Aromatization is the last step in estrogen formation, catalyzed by the P450 aromatase monooxygenase enzyme complex that is present in the smooth endoplasmic reticulum. In three consecutive hydroxylating

reactions, estrone and estradiol are formed from their obligatory precursors androstenedione and testosterone, respectively (Gruber *et al.* 2002). The primary sources of estrogen in premenopausal women are the theca and granulosa cells of the ovaries. According to the “two-cell” theory of estrogen synthesis, the theca cells secrete androgens that diffuse to the granulosa cells to be aromatized to estrogens (Hillier *et al.* 1994). The principal sites of aromatase expression in pregnant women are the placental syncytiotrophoblast, and in the postmenopausal woman the adipose tissue and skin fibroblasts (Simpson *et al.* 1994). Both in men and postmenopausal women, aromatization of C19 steroids in peripheral tissues (adipose tissue and skin) is the primary mechanism for estrogen formation (Grodin *et al.* 1973).

Estradiol (E2) is the predominant form in non pregnant females and is produced in at least 3 major sites (Figure 2.3). Estrone arises primarily from peripheral aromatisation of androstendione and, in part, from ovarian secretion. It is not a potent estrogen, but can be viewed as a precursor that must be converted to estradiol to exert full estrogenic action (Bulun *et al.* 1999). Estriol is the predominant estrogen during pregnancy (Mucci *et al.* 2003).

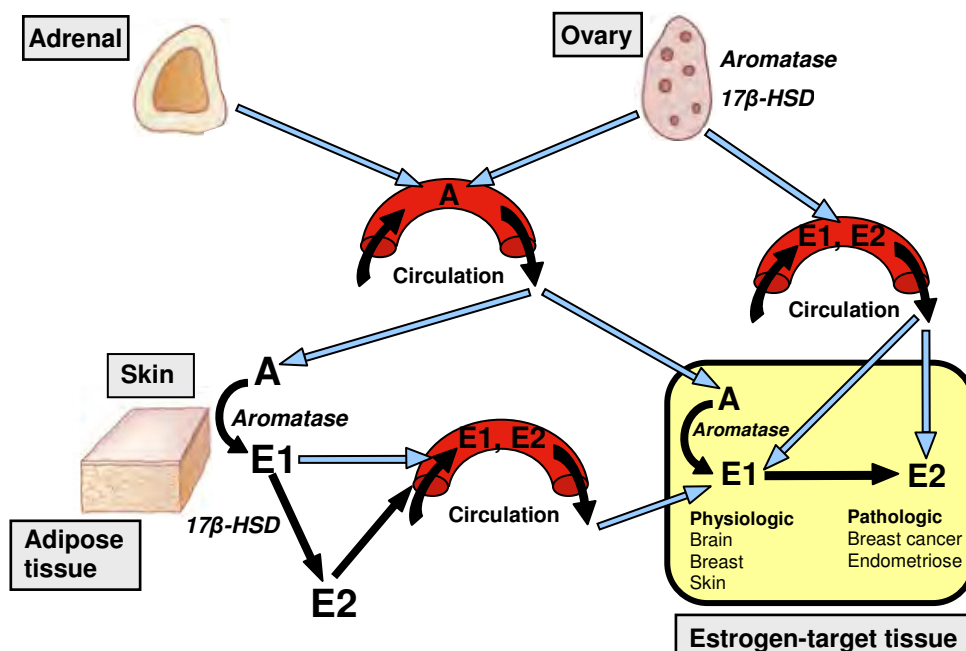


**Figure 2.3: Estrogen biosynthesis in women**

The biologically active estrogen estradiol (E2) is produced in at least three major sites: First by direct secretion from the ovary in reproductive-age women; second by conversion of circulating androstenedione (A) of adrenal or ovarian origins, or both, to estrone (E1) in peripheral tissues; and third by conversion of A to E1 in estrogen target tissues. In the latter two instances, estrogenically weak E1 is further converted to E2 within the same tissue. The presence of the enzyme aromatase and 17β-hydroxysteroid dehydrogenase (17β-HSD) is critical for E2 formation at these sites (modified according to Bulun and Adashi 2008).

While estrogens are present in both men and women, they are usually present at significantly higher levels in women of reproductive age and responsible for the development of secondary sexual characteristics, regulation of gonadotropin secretion for ovulation, preparation of tissues for progesterone response, maintenance of bone mass, regulation of lipoprotein synthesis, prevention of urogenital atrophy, regulation of insulin responsiveness, and maintenance of cognitive function (Nelson and Bulun 2001). Unlike ovulating women, in whom most of the circulating estrogen is derived from the ovaries, in males 85% of circulating estradiol and more than 95% of circulating estron is derived from extragonadal conversion of testosterone and androstendione, mostly in fat and skin (Hemsell *et al.* 1974, Simpson *et al.* 1994). It regulates certain functions of the reproductive system such as the maturation of sperm (Fisher *et al.* 1998) and it is important for the fusion of epiphyses and maintenance of bone mass in young adult men (Carani *et al.* 1997).

#### **2.4.2 Estrogen receptors**

During the last 40 years, several different estrogen receptors (ER) have been identified. The classical genomic estrogen action is known for the longest time and involves the diffusion of estrogen across the plasma membrane and the activation of specific intracellular receptors (Nadal *et al.* 1998). Until 1995, it was assumed that there was only one estrogen receptor responsible for all of the physiological and pharmacological effects of natural and synthetic estrogens as well as antiestrogens, namely the ER $\alpha$ . In 1996, an additional estrogen receptor was cloned from rat prostate. This novel receptor was designated ER $\beta$ . In the following years, several ER subtypes, isoforms and products of mRNA splice variants have been identified (Katzenellenbogen and Katzenellenbogen 1996, Nilsson *et al.* 2001). Both, the concentration of these receptors and the relative ratio of subtypes and isoforms vary in different target tissues and at different stages of development (Katzenellenbogen and Katzenellenbogen 1996). In the last three decades, increasing evidence for rapid, non-classical steroid effects through a membrane-associated ER has been demonstrated for virtually all groups of steroids. In contrast to the delayed genomic steroid actions, non-genomic steroid effects are principally characterized by their insensitivity to inhibitors of transcription and protein synthesis, and by their rapid onset of action (within seconds to minutes)

(Falkenstein *et al.* 2000). In addition, recent studies discovered an orphan G protein-coupled receptor (GPR30) that seems to be involved in several non-genomic rapid estrogen actions (Thomas *et al.* 2005) as well as other non-classical membrane estrogen receptors (ncmER), like the so-called  $\gamma$ -adrenergic receptor (Nadal *et al.* 2000).

#### 2.4.2.1 Classical genomic estrogen receptors (ER $\alpha$ and ER $\beta$ )

Classical estrogen receptors are located in the cytoplasm and act as intracellular transcription factors whose principal target is in the nucleus where they exert positive or negative effects on the expression of target genes (Beato *et al.* 1996, Katzenellenbogen and Katzenellenbogen 1996). The classical ERs belong to the steroid/thyroid hormone superfamily of nuclear receptors, which members share a common structural architecture (Evans 1988, Katzenellenbogen and Katzenellenbogen 1996). These receptors are composed of a ligand binding domain, a DNA-binding domain and several transactivating functions distributed along the molecule (Beato 1989). Ligand binding to the ER regulates gene expression by recognizing palindromic estrogen response elements (ERE) of the DNA after homo- or heterodimerization of the ligand-receptor complex. Together with different coactivators, repressors and transcription regulators, the basal transcription complex binds with high affinity to specific EREs in the regulatory regions of target genes to either activate or repress gene expression. The expression of steroid-induced genes is modulated at the protein level some hours after stimulation with the steroid (Falkenstein *et al.* 2000).

ER $\alpha$  and ER $\beta$  are products of distinct genes on different chromosomes and are widely distributed throughout the body, exhibiting various tissue- and cell-type specific expression patterns. ER $\alpha$  is expressed primarily in the uterus, liver, kidney, and heart, whereas ER $\beta$  basically is expressed in the ovary, prostate, lung, gastrointestinal tract, bladder, as well as the hematopoietic and central nervous system. In studies with mice lacking ER $\alpha$  ( $\alpha$ ERKO) or ER $\beta$  ( $\beta$ ERKO) or both ( $\alpha\beta$ ERKO) it could be demonstrated that both receptor subtypes have overlapping as well as unique roles in estrogen-dependent action (Matthews and Gustafsson 2003). In a number of tissues, including for example the mammary gland, thyroid, adrenal, bone and certain brain regions, the two receptors are coexpressed and form functional heterodimers in which ER $\beta$  can oppose the actions of ER $\alpha$  in many

instances (Liu *et al.* 2002, Matthews and Gustafsson 2003). In addition, the synthetic antiestrogens tamoxifen and raloxifene can exhibit distinctive responses and can be for example partial agonists for ER $\alpha$  whereas they act as pure antagonists for ER $\beta$  (Barkhem *et al.* 1998). Moreover, several isoforms of ER $\alpha$  and ER $\beta$  exist, also altering estrogen-mediated gene expression (Shupnik *et al.* 1998). Specific pharmacologic targeting of ER $\alpha$  or ER $\beta$  would open up novel therapeutic opportunities, stratifying hormonal treatment, thereby reducing undesired side effects (Zhao *et al.* 2008). Moreover it was recognized that 17 $\beta$ Estradiol (E2) actions were mediated by at least two more other “non-classical” ER pathways: first, ligand-independent ER signalling, in which gene activation occurs through second-messenger pathways that alter intracellular kinase and phosphatase activity, resulting in changed phosphorylation of the ER (Weigel and Zhang 1998). Second, genotropic, estrogen response element (ERE)-independent signalling, in which ER regulates genes independent of direct DNA binding via protein-protein interaction with other transcription factors, such as c-Fos/c-Jun B (AP-1), Sp1, and nuclear factor kappa B (NF- $\kappa$ B) (Jakacka *et al.* 2002, Marino *et al.* 2006). This ER-indirect DNA association transcribes roughly 35% of the categorized human primary E2-responsive genes (O’Lone *et al.* 2004).

#### 2.4.2.2 Rapid estrogen signalling

Various studies could demonstrate that classic estrogen receptors may be involved not only in classical steroid action, but also in rapid non-genomic steroid effects. Such a receptor is most often localized to the plasma membrane and is structurally similar to the classic intracellular estrogen receptors mentioned above (Falkenstein *et al.* 2000, Hammes and Levin 2007). The rapid signalling can be inhibited by classic ER antagonists like tamoxifen or ICI-182,780 (Lantin-Hermoso *et al.* 1997).

Clarke *et al.* (2000) could supply evidence for the existence of ER $\alpha$  in close proximity to the plasma membrane in isolated fetal rat hippocampal neurons (Clarke *et al.* 2000). Other studies demonstrated that these receptors can be located in the cell membrane with epitopes exposed on the outer surface (Pappas *et al.* 1995). Whether ERs span the plasma membrane or contain an extracellular ligand binding region is still controversial (Levin 2005). Alternatively,

evidence exists for ER $\beta$  within isolated caveolae vesicles shorn from the plasma membrane of cultured endothelial cells (Chambliss *et al.* 2002).

Binding of 17 $\beta$ Estradiol (E2) activates various rapid signalling pathways which could be classified into four main signalling cascades, presenting numerous interactions with several other pathways (Marino *et al.* 2006):

- 1) Phospholipase C/protein kinase C
- 2) Ras/Raf/MAPK
- 3) Phosphatidyl inositol 3 kinase (PI3K)/AKT
- 4) cAMP/protein kinase A

These signals subsequently mediate the posttranslational modification of many proteins, leading to rapid enzyme induction and modulation of cell functions, mainly by phosphorylation (Levin 2005). The activation of these signalling pathways by E2 is cell type-specific and depends on a number of conditions such as the set of signal transduction molecules and downstream targets in the target cell, thus the responses are likely to be diverse (Marino *et al.* 2006). The fact that estrogen effects are triggered outside the nucleus does not mean that gene expression is not affected. Actually, the rapid activation of signalling cascades such as those involving MAPKinase, as well as the generation of second messengers such as cAMP, cGMP and intracellular Ca<sup>2+</sup>, regulates the activation of transcription factors such as cAMP response element-binding protein (CREB) and nuclear factor of activated T-cells (NFAT), thereby regulating gene expression (Ropero *et al.* 2006). This implies that the regulation of gene expression by estrogen has both genomic and non-genomic inputs, and that the balance of these inputs may vary in a cell- and gene-specific manner (Madak-Erdogan *et al.* 2008). It seems like ER $\alpha$  is the main endogenous mediator of rapid estrogen actions and less is known about the role of ER $\beta$  in rapid non-genomic mechanisms although several studies indicate that ER $\beta$  could also originate cell-specific signal transduction cascade (Geraldes *et al.* 2003, Marino *et al.* 2006).

#### 2.4.2.3 Non-classical estrogen receptors

In the last years, other estrogenic effects have been described through membrane receptors other than ER $\alpha$  and ER $\beta$  and therefore were named “non-classical membrane estrogen receptors” (ncmER). Some of them have been molecularly characterized and defined as new membrane estrogen receptors, such as the orphan

G protein-coupled seven-transmembrane receptor 30 (GPR30) (Ropero *et al.* 2006) which is suggested to work as a cell surface receptor, activating G proteins after stimulation through E2 (Filardo and Thomas 2005). It is assumed that GPR30 is redistributed from the plasma membrane to cathrin-coated vesicles after stimulation with E2 (Filardo *et al.* 2007). Moreover, it is reported that GPR30, additionally to its appearance in the plasma membrane, localizes in both the endoplasmic reticulum and Golgi apparatus (Revankar *et al.* 2005). But this fact needs to be evaluated carefully because expression of exogenous genes often leads to an accumulation in the endoplasmic reticulum. Additionally, the use of insufficiently specific antibodies might be the reason for confusion concerning the localization of GPR30. The biological functions of GPR30 are mainly attributed to the immunological and circulatory system as well as to glucose homeostasis and colon functions (Mizukami 2010). The official new acronym is G-protein coupled estrogen receptor 1 (GPER), due to its action as an estrogen receptor (Maggiolini and Picard 2010). The high concentrations of E2 needed for the activation of GPR30 raise the question, whether these concentrations are physiological in living animals, or whether another physiological ligand is present in cells (Mizukami 2010). The current knowledge about this receptor in terms of its contributions to physiological as well as pathological estrogen responses is yet very little and needs to be further investigated (Maggiolini and Picard 2010).

### **2.4.3 Role of estrogen in glucose homeostasis**

Estrogens were known to be involved in energy balance and glucose metabolism for a long time and several studies have reported on the potential relationship between E2 and glucose metabolism in physiological and pathological states with variability in E2 levels, such as menstrual cycle, gestation, gestational diabetes mellitus and polycystic ovarian syndrome (PCOS) (Barros *et al.* 2006a). In aromatase knock-out mice (ArKO), estrogen cannot be produced and as a consequence, both male and female ArKO mice show reduced glucose oxidation accompanied by obesity and increased insulin levels, eventually leading to diabetes mellitus (Heine *et al.* 2000, Jones *et al.* 2000). Moreover, it could be demonstrated that the lack of estrogen in male ArKO mice after 12 weeks of age, can lead to glucose intolerance and insulin resistance, accompanied by an increase of body weight. These effects can be reversed by estrogen treatment (Takeda *et al.* 2003). In humans, all patients with

aromatase deficiency, based on a point mutation in the aromatase gene, show an impairment of glucose metabolism and insulin resistance (Zirilli *et al.* 2008). On the other hand, high concentrations of E2, such as in oral contraceptives or estrogen replacement therapy, are related to insulin resistance and the development of diabetes mellitus (Godsland 2005).

With the development of ER $\alpha$  ( $\alpha$ ERKO) and ER $\beta$  ( $\beta$ ERKO) knockout mice, it could be demonstrated that ER $\alpha$  and ER $\beta$  both participate in the regulation of many processes related to the control of energy homeostasis. Nevertheless, evidence points to ER $\alpha$  as the main mediator (Ropero *et al.* 2008b). ER $\alpha$  is involved in glucose metabolism in different tissues, including skeletal muscle, adipose tissue, liver, brain and endocrine pancreas (Barros *et al.* 2009). Both female and male  $\alpha$ ERKO mice exhibit profound insulin resistance, impaired glucose tolerance and adipocyte hyperplasia as well as hypertrophy (Bryzgalova *et al.* 2006, Heine *et al.* 2000). To understand the role of ER $\beta$  in glucose homeostasis,  $\alpha$ ERKO mice were ovariectomized to remove the action of E2 on ER $\beta$ . Such mice showed improved glucose and insulin metabolism, indicating that ER $\beta$  activation might have a diabetogenic effect and therefore ER $\beta$  may oppose the action of ER $\alpha$  (Naaz *et al.* 2002).

#### **2.4.4 Effects of estrogen on pancreas**

In pancreatic tissue there exist different expression profiles of receptors for the three different types of sex steroid hormones (estrogens, progestagens and androgens). Moreover, specific enzymes involved in the synthesis of sex steroid hormones are present (Robles-Diaz and Duarte-Rojo 2001).

It could be demonstrated that both ER $\alpha$  and ER $\beta$  are existent in pancreatic  $\beta$ -cells. Long-term exposure to 17 $\beta$ -estradiol (E2) in physiological concentrations can lead to an increase of  $\beta$ -cell insulin content, insulin gene expression and insulin release, yet pancreatic  $\beta$ -cell mass is unaltered. Studies, using synthetic selective estrogen receptor modulators (SERMs) such as propyl-pyrazole-triol (PPT) for ER $\alpha$  and diarylpropionitrile (DPN) for ER $\beta$  as well as studies in  $\alpha$ ERKO and  $\beta$ ERKO mice suggest that ER $\alpha$  is the estrogen receptor responsible for these effects (Alonso-Magdalena *et al.* 2008).

Further, the existence of an estrogen membrane receptor in pancreatic  $\beta$ -cells was demonstrated, which is responsible for the rapid insulinotropic effect of E2 when it is applied in physiological concentrations (Alonso-Magdalena *et al.* 2006,

Nadal *et al.* 1998). This non-classical membrane estrogen receptor (ncmER) has a completely different pharmacological profile as compared to ER $\alpha$  and ER $\beta$ . It does not bind the antiestrogen ICI182,780, but binds catecholamines with a similar profile to the so-called gamma-adrenergic receptor (Nadal *et al.* 2000). By binding to this receptor, estrogen can increase insulin secretion from pancreatic  $\beta$ -cells (Nadal *et al.* 1998).

#### 2.4.4.1 Impact of estrogen on pancreatic insulin content

Estrogen is known to influence  $\beta$ -cell function by an increase of pancreatic insulin production, leading to a release of higher amounts of insulin granules after glucose stimulus (Alonso-Magdalena *et al.* 2006, Marban *et al.* 1989).

Effects of 17 $\beta$ Estradiol on blood glucose homeostasis can be imitated by the widespread environmental contaminant Bisphenol-A (BPA) that acts through both a rapid non-classical pathway and a classical estrogen receptor pathway (Alonso-Magdalena *et al.* 2006). BPA is a plasticizer, mainly used to manufacture polycarbonate plastic and as an additive in other widely used plastics such as polyvinylchlorid (PVC) and polyethylenterephthalat (PET) (Ropero *et al.* 2008a). The exposure of adult mice to a single dose of either E2 or BPA rapidly increases plasma insulin, leading to a decrease of blood glucose concentration through a non-classical pathway. This is unaffected by the antiestrogen ICI and is most likely initiated by the ncmER. Longer exposure to BPA and E2 increases  $\beta$ -cell insulin content, an effect that is completely blocked by ICI and therefore likely involves the classical ER pathway (Alonso-Magdalena *et al.* 2006). It could also be demonstrated that this long-term action is mediated by the estrogen receptor ER $\alpha$ . It is unlikely that ER $\alpha$  operates via estrogen response elements (ERE), because ERE has not been described in the promoters of mouse insulin genes (Alonso-Magdalena *et al.* 2008). E2 can also work via alternative pathways, triggered outside the nucleus, likely through other transcription factors binding to their respective response elements, involving phosphatidylinositol 3-kinase (PI3K) or extracellular-regulated kinases (ERK) activation (Nadal *et al.* 2005, Ropero *et al.* 2006). It is documented that insulin gene transcription is regulated by ERK1/2 which are essential in glucose-stimulated insulin gene transcription by phosphorylating the transcription factors Neuro-D1 and pancreatic and duodenal homeobox 1 (PDX-1), which directly activate the insulin promoter (Khoo *et al.* 2003). ER $\alpha$  rapidly associates with the tyrosine kinase Src in

$\beta$ -cells, then activating ERK1/2. E2-induced insulin expression occurs predominantly at physiological stimulatory glucose concentrations, suggesting that E2 amplifies the glucose signal (Wong *et al.* 2010) (Figure 2.4).

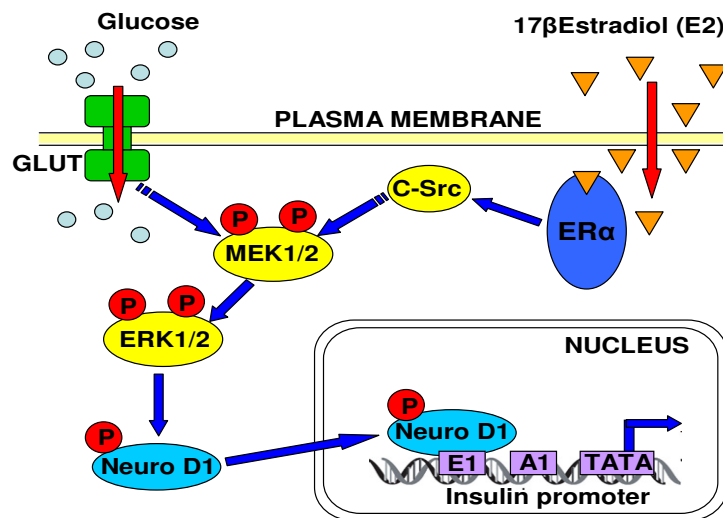


**Figure 2.4: Proposed mechanism of E2 amplification of insulin gene transcription**

ER $\alpha$ -induced insulin transcription involves NeuroD1 binding to the insulin promoter through phosphorylation of ERK1/2 (modified according to Wong *et al.* 2010).

The E2-induced increase in insulin content and secretion would be beneficial when it occurs during an appropriate period of time and at doses within the physiological range like it may happen during pregnancy. However, if this estrogenic action occurs at an inappropriate time, or at doses out of the physiological levels, it may cause adverse effects. Longer E2-exposure can generate chronic hyperinsulinaemia in the fed state and peripheral insulin resistance as indicated by altered glucose and insulin tolerance tests. However, the extent of insulin resistance induced by E2-treatment is not enough to induce hyperglycaemia in the fasted state (Alonso-Magdalena *et al.* 2006). It is also known in humans that the persistence of chronic physiologic euglycaemic hyperinsulinaemia for 3–5 days can induce severe insulin resistance in healthy subjects with normal glucose tolerance (Del Prato *et al.* 1994). Whether insulin resistance precedes hyperinsulinaemia or

hyperinsulinaemia precedes insulin resistance in the development of type 2 diabetes is controversial. The only clear conclusion is that both seem to walk hand in hand (Prentki *et al.* 2002).

Beside this, the direct effect of Bisphenol A on peripheral tissue (e.g. down-regulation of GLUT4 transporters in adipose tissue as well as the favoured conversion of fibroblasts to adipocytes with an enhanced risk for obesity) might also be of importance to developing insulin resistance (Alonso-Magdalena *et al.* 2006).

#### 2.4.4.2 Enhancement of insulin secretion by estrogen

Beta-cells are electrically excitable and electrical activity consists of oscillations in the membrane potential. Glucose metabolism increases the intracellular ATP/ADP ratio, leading to the closure of ATP-regulated  $K^+$  ( $K_{ATP}$ ) channels (Rorsman *et al.* 2000), thereby inducing membrane depolarisation, opening of voltage-operated  $Ca^{2+}$  channels and  $Ca^{2+}$  influx (Valdeolmillos *et al.* 1992). As a consequence, a  $[Ca^{2+}]_i$  oscillatory pattern is originated triggering a pulsatile insulin secretion (Gilon *et al.* 1993, Nadal *et al.* 1999).

By binding to a gamma-adrenergic membrane receptor, E2 can trigger the synthesis of cGMP, which in turn activates protein kinase G (PKG). PKG can induce the closure of ATP-dependent potassium channels ( $K_{ATP}$ ) by a phosphorylation-dependent process, leading to plasma membrane depolarisation (Ropero *et al.* 1999). The maximum effect is reached 3 to 7 minutes after estradiol application and the effect is transient, returning to normal levels 30 minutes later (Alonso-Magdalena *et al.* 2010). Plasma membrane depolarisation increases the frequency of  $[Ca^{2+}]_i$  oscillations and due to this, an enhanced insulin secretion (rapid insulinotropic effect) occurs when estradiol is applied along with a stimulatory glucose concentration. A minor participation of cAMP as a second messenger in addition to cGMP in this process cannot be completely ruled out (Ropero *et al.* 1999). Moreover, latest studies could demonstrate that GPR30-specific ligand G-1 stimulated insulin release and inhibited glucagon and somatostatin release in a manner almost identical to  $17\beta$ Estradiol, inducing an increase of cAMP content in parallel with an amplified insulin release, but the intracellular signalling following the activation of GPR30 in the different islet cells is far from being elucidated (Balhuizen *et al.* 2010) (Figure 2.4).

Worth to mention is the fact that such an ncmER not only exists in pancreatic  $\beta$ -cells, but in  $\alpha$ -cells as well. When E2 acts through this receptor in  $\alpha$ -cells, it inhibits  $[Ca^{2+}]_i$  oscillations induced at low glucose concentrations and therefore abolishes glucagon release (Ropero *et al.* 2002).

An additional rapid effect of BPA and E2 on isolated islet cells is the increased activation of the ubiquitous transcription factor CREB (Quesada *et al.* 2002). This effect may be of great importance for the  $\beta$ -cell physiology, since CREB activation induces insulin gene expression and is implicated in  $\beta$ -cell survival (Jhala *et al.* 2003).

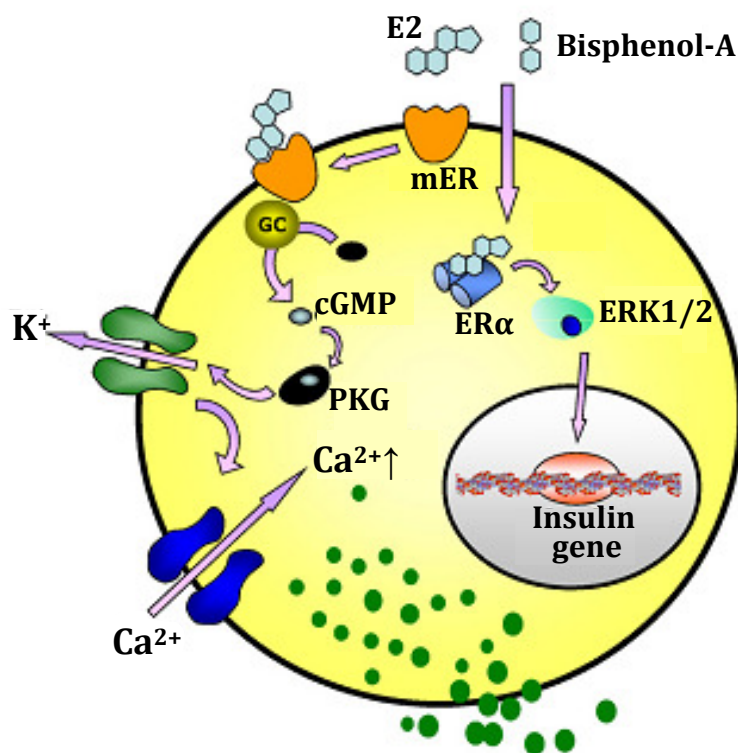


**Figure 2.5: Proposed model for the action of 17 $\beta$ Estradiol and bisphenol-A (BPA) in  $\beta$ -cells**

In synergy with a stimulatory glucose concentration, binding of BPA or 17 $\beta$ Estradiol to a membrane ER activates a guanylyl cyclase (GC) and as a consequence a protein kinase G (PKG), whose action involves the closing of  $K_{ATP}$  channels. The subsequent depolarization opens L-type calcium channels; inducing  $Ca^{2+}$  influx and potentiating insulin release. At the same time the activation of ER $\alpha$  by either E2 or BPA in the presence of stimulatory glucose levels rapidly activates ERK1/2 that regulates insulin gene expression through a still unknown pathway (modified according to Nadal *et al.* 2009).

## 2.4.5 Effects of estrogen on skeletal muscle, adipose tissue and liver

### 2.4.5.1 Insulin sensitivity and insulin resistance

Insulin action in insulin dependent tissues like skeletal muscle, adipose tissue and liver involves the tyrosine phosphorylation of intracellular substrates, thereby transmitting the insulin signal (White and Kahn 1994). Insulin receptor substrate 1 (IRS-1) is considered the major substrate for the insulin receptor (Sun *et al.* 1992). The level of tyrosine kinase activity reflects the serum concentration of insulin and appears to mediate the insulin response (DeFronzo *et al.* 1992). It could be shown that estrogen can induce the expression of the downstream signalling molecules IRS-1 and IRS-2 (Lee *et al.* 1999). Moreover, it is known that IRS-1 promoter does have four consensus half-estrogen response elements (Kato *et al.* 1992).

When plasma concentration of  $17\beta$ Estradiol is low, like it is seen in early pregnancy, IRS-1 is up-regulated by a transcriptional mechanism and insulin sensitivity increases in peripheral tissues. However, when the concentration of E2 is high, like it is found in late pregnancy, the binding of many complexes of ER-estradiol to the IRS-1 promoter could induce a decrease in IRS-1 expression, probably by displacement of other transcription factors linked to the IRS-1, leading to diminished insulin sensitivity in peripheral tissues (Gonzalez *et al.* 2001). IRS-1 knockout mice develop insulin resistance due to impaired insulin signalling in skeletal muscle and adipose tissues, but they do not develop diabetes mellitus due to islet hyperplasia and hyperinsulinaemia. In contrast, IRS-2 knockout mice are unable to increase their  $\beta$ -cell mass sufficiently to fulfill the increased insulin requirement, and they develop severe diabetes mellitus (Withers *et al.* 1998). Further, it is suggested that E2 treatment employs a common mechanism (such as induction of IRS-2 expression through the activation of CREB (Jhala *et al.* 2003)) that improves  $\beta$ -cell function and subsequently reverses insulin resistance. Elevated levels of IRS-2 can potentiate an insulin signalling cascade, leading to increased  $\beta$ -cell proliferation and decreased apoptosis (Choi *et al.* 2005).

Moreover, estrogens have been shown to increase hepatic insulin sensitivity by decreasing gluconeogenesis and glycogenolysis in ovariectomized mice (Ahmed-Sorour and Bailey 1981). It is proposed that hepatic insulin resistance results from the upregulation of lipogenic genes via the suppression of Leptin receptor expression (Bryzgalova *et al.* 2006).

#### 2.4.5.2 Modulation of GLUT4 expression by estrogen

ER $\alpha$  and ER $\beta$  are expressed in all tissues involved in glucose homeostasis but have different roles in its regulation. In skeletal muscle as well as in adipose tissue, insulin stimulates glucose uptake by inducing the expression of GLUT4 (glucose transporter 4) (Gould and Holman 1993). GLUT4 belongs to a family of glucose transporters that include 12 members from which only GLUT4 responds to insulin (Wood and Trayhurn 2003). The uptake of glucose in muscle cells is responsible for 75% of the whole-body glucose uptake (Bjornholm and Zierath 2005). Estrogen receptor  $\alpha$  and  $\beta$  are co-expressed in skeletal muscle where they have opposing effects on modulation of GLUT4 expression. ER $\alpha$  is a positive regulator of GLUT4 expression while ER $\beta$  has a suppressive role. Therefore the effect of estrogen depends on the balance between the two receptor isoforms (Barros *et al.* 2006b). Tamoxifen (Tam) is a non steroidal selective ER modulator (SERM) that binds to both ERs with high affinity, causing agonist or antagonist actions in a tissue-specific way (Jensen *et al.* 2003). In skeletal muscle, ER $\beta$  is predominant and blocking of ER $\beta$  by tamoxifen (Tam) in  $\alpha$ ERKO mice increased GLUT4 expression, whereas blocking of ER $\alpha$  by Tam in  $\beta$ ERKO mice had very small effects on GLUT4 expression. In white adipose tissue, ER $\alpha$  is predominant and may regulate GLUT4 expression through peroxisome proliferator-activated receptor gamma 2 (PPAR $\gamma$ 2). The loss of ER $\alpha$  as well as treatment of  $\beta$ ERKO mice with TAM decreased GLUT4 expression and diminished glucose uptake. In the liver, ER $\alpha$  is predominant and has an important role in the regulation of genes involved in glucose metabolism (Barros *et al.* 2009).

#### 2.4.6 Positive effects of estrogen on oxidative stress and apoptosis

Disregarding the causal events, in type 1 and the late stages of type 2 diabetes, proinflammatory cytokines and/or chronic elevation of blood glucose (glucotoxicity) generate oxidative stress in pancreatic islets, which ultimately provokes  $\beta$ -cell death by apoptosis (Mathis *et al.* 2001, Robertson *et al.* 2003). Estrogen deficient ArKO mice are vulnerable to  $\beta$ -cell apoptosis and prone to insulin-deficient diabetes mellitus after exposure to streptozotocin (STZ), which augments the generation of reactive oxygen species in pancreatic islets, leading to acute oxidative stress (Le May *et al.* 2006). E2 protects  $\beta$ -cells through ER $\alpha$  and ER $\beta$  via ERE-independent, extra-nuclear mechanisms, but ER $\beta$  plays a minor cytoprotective

role compared to ER $\alpha$ . In  $\alpha\beta$ ERKO<sup>-/-</sup> mice and their isolated pancreatic islets, E2 partially prevents apoptosis, suggesting that an alternative pathway compensates for ER $\alpha$ /ER $\beta$  deficiency. This pathway seems to be G-protein coupled estrogen receptor 1 (GPER)-dependent, due to the fact that a selective GPER agonist can improve islet survival, and GPERKO<sup>-/-</sup> mice are susceptible to streptozotocin-induced insulin deficiency. It could also be shown that cytoprotection by E2 is impaired in ER $\alpha$ -deficient islets and can be compensated, only partially, by GPER or ER $\beta$ . Thus, ER $\alpha$  is the major E2 receptor to favour islet survival in mice (Liu *et al.* 2009). Moreover it could be shown that estrogens do have antioxidant effects by both up-regulation of the expression of the superoxide dismutase (SOD) and glutathione peroxidase (GPx) gene. This is mediated by interaction with classical estrogen receptors  $\alpha$  and/or  $\beta$ , located at the plasma membrane, but a direct genomic effect of estradiol is unlikely because neither superoxide dismutase nor glutathione peroxidase have estrogen responsive elements in their promoter region. The action of estradiol is suggested to be mediated via intracellular signalling cascades: After binding of estrogen to its membrane receptor, mitogen activated protein kinases (MAPK) are activated by phosphorylation, which in turn activates nuclear factor kappa B (NF- $\kappa$ B). As a consequence, NF- $\kappa$ B up-regulates the expression of the SOD and GPx genes, whose promoters contain putative NF- $\kappa$ B-binding motifs (Viña *et al.* 2005).

Recent studies could demonstrate, that 17 $\beta$ Estradiol can modulate apoptosis in pancreatic  $\beta$ -cells dependent on expression of sulfonylurea receptor 1 (SUR1), which obviously can act as a “non-classical” estrogen receptor (Ackermann *et al.* 2009). SURs are known to be regulatory subunits of ATP-sensitive potassium channels (K<sub>ATP</sub> channels) (Ashcroft 2007). The isoform SUR1 is the regulatory subunit of pancreatic ATP-sensitive K<sup>+</sup>-channels and E2 treatment can modulate  $\beta$ -cell apoptosis under specific involvement of SUR1. Moreover, an age-dependent difference in apoptotic and anti-apoptotic effects of E2 could be demonstrated. A clear apoptotic effect is likewise found in elderly mice (20-32 week-old), whereas clear anti-apoptotic effects were observed in young mice (5-7 week-old) (Ackermann *et al.* 2009).

Furthermore it is suggested that activation of c-Jun N-terminal kinase (JNK) is the signal transducer for oxidative stress as well as for toxicity of proinflammatory

cytokines (PICs) to  $\beta$ -cells (Ammendrup *et al.* 2000). PICs, such as tumor necrosis factor- $\alpha$  (TNF- $\alpha$ ), interleukin-1 $\beta$  (IL-1 $\beta$ ), and interferon- $\gamma$  (IFN- $\gamma$ ), cause islet dysfunction, apoptosis, and induce the expression of the cytokine inducible NO synthase, which results in intracellular NO synthesis in  $\beta$ -cells (Eizirik and Mandrup-Poulsen 2001). A number of transcription factors regulated by JNK, including c-Jun, c-Fos, c-myc and activating transcription factor 2 (ATF-2), have been implicated with the onset of apoptosis (Eckhoff *et al.* 2003). It could be demonstrated that estrogen reduces the production and effects of PICs by blocking JNK activity and the resulting phosphorylation of c-Jun and JunD. The consequent decrease in the nuclear levels of c-Jun and JunD leads to diminished binding of c-Jun/c-Fos and JunD/c-Fos heterodimers to the activator protein 1 (AP-1) consensus sequence in the TNF promoter and, thus, to decreased transactivation of the TNF gene (Srivastava *et al.* 1999).

#### **2.4.7 Role of estrogen in endoplasmic reticulum stress**

ER-stress triggers the initially protective unfolded protein response (UPR), an adaptive endoplasmic reticulum signalling pathway that allows cells to survive the accumulation of unfolded proteins in the endoplasmic reticulum lumen (Zhang and Kaufman 2006). Although the UPR is initially a compensatory mechanism by which cells can reset normal endoplasmic reticulum function, prolonged UPR will induce cell death (Gomez *et al.* 2007). Induced by cellular stressors, UPR can be initiated by each of three molecular sensors, i.e., insulin-response-element 1 (IRE1), activating transcription factor 6 (ATF6), and PKR-like endoplasmic reticulum kinase (PERK) (Araki *et al.* 2003). Splicing of X-box binding protein 1 (XBP-1) by IRE1 is an obligate component in both IRE1- and ATF6-induced UPR. XBP-1 mRNA has been shown to be unconventionally spliced by IRE1 in response to endoplasmic reticulum stress, resulting in production of a highly active transcription factor (XBP-1(S)) that can activate the mammalian unfolded protein response (Yoshida *et al.* 2001). Trauma-hemorrhage (T-H) and resuscitation have been shown to induce ER-stress (Jian *et al.* 2008). In an experiment with 6- to 8-week-old rats it could be demonstrated that XBP1(S) is increased at the end of the shock phase in trauma-hemorrhage, two hours after removal of 62% of the circulating blood volume. Administration of 17 $\beta$ Estradiol after T-H decreased the level of XBP-1(S) in shock animals. A similar picture was observed for C/EBP homologous

protein (CHOP) expression at mRNA level, showing a significantly elevated expression in the T-H group but not in the T-H + E2 group. It must be mentioned that all of these effects appeared to be liver-specific and were not observed in the kidney (Kozlov *et al.* 2010).

## 3 Research design and methods

### 3.1 Research design

The study consisted of two subsequent parts. The first part (Group 1) was designed to find out, if ovariectomy has any effects on glucose homeostasis, histological as well as quantitative stereological parameters of the pancreas. For this purpose, 11 female Munich *Ins2*<sup>C95S</sup> mutant mice were ovariectomized and 10 mutant and 11 wild-type females were sham-operated.

The second part (Group 2) was accomplished to study the effects of estradiol-replacement therapy in ovariectomized mutant mice. This second test group included placebo-treated ovariectomized, placebo-treated sham-operated and estradiol-treated ovariectomized female Munich *Ins2*<sup>C95S</sup> mutant mice as well as placebo-treated sham-operated wild-type mice (n=9 per group).

For most of the accomplished tests, non-treated (nt) mice of Group 1 and the accordant placebo-treated (p) mice of Group 2 were pooled (nt/p).

### 3.2 Materials and methods

#### 3.2.1 Animals

Munich *Ins2*<sup>C95S</sup> mutant mice were generated within the Munich *N*-ethyl-*N*-nitrosurea (ENU) mouse mutagenesis project. Male heterozygous mutants were bred onto a C3HeB/FeJ genetic background.

Animals received standard rodent diet (Altromin C1324, Germany) and tap water ad libitum. They were housed in a temperature- and light-controlled room (21 - 23°C, 55 ± 3 % relative humidity, 12 hours light : 12 hours dark cycle). At the age of 21 days, mice were weaned, separated depending on sex, and marked by ear perforation. Tail tip biopsies for genotyping were taken, and blood glucose concentrations were measured.

At the age of 30 days 29 female heterozygous mutant mice were ovariectomized (mt-ovx-nt/p), 19 female heterozygous mutant mice (mt-sham-nt/p) and 20 wild-type mice (wt-sham-nt/p) were sham-operated. Nine ovariectomized female mutants (mt-ovx-E2) of Group 2 received 17βEstradiol supplementation by implanting a subcutaneous

$^{17}\beta$ Estradiol long-term pellet subsequent to ovariectomy still under anaesthesia and the remaining 27 mice of Group 2 received a placebo-pellet. Serum was collected at intervals of at least 50 days starting at the age of 65 days to examine serum estradiol levels. Regular clinical examinations were carried out, starting with 20 non-/placebo-treated sham-operated wild-type, 20 non-/placebo-treated ovariectomized mutant, 19 non-/placebo-treated sham-operated mutant and 9 estradiol-supplemented ovariectomized mutant mice. At the age of 25, 50, 90 and 180 days, oral glucose tolerance tests (OGTTs) were carried out and serum insulin levels were determined before and 10 minutes after glucose challenge. Intraperitoneal insulin tolerance tests (ipITTs) were performed at the age of 60, 100 and 187 days. At the age of 190 days, 35 animals (11 wt-sham-nt/p, 10 mt-ovx-nt/p, 10 mt-sham-nt/p and 4 mt-ovx-E2) were exsanguinated under general anaesthesia and finally killed by cervical dislocation for qualitative histological and quantitative stereological analyses of the pancreas. The remaining 31 animals (9 wt-sham-nt/p, 10 mt-ovx-nt/p, 9 mt-sham-nt/p and 3 mt-ovx-E2) were also exsanguinated under general anaesthesia at the age of 210 days and finally killed by cervical dislocation. The islets were isolated and assayed in respect of ER-stress via Western blot analyses. From both groups the collected serum was assayed in order to examine serum estrogen concentrations as well as serum oxidative stress markers (TBARS levels). The number of animals used in the distinct examinations is stated in table 3.1. All experiments were performed under the approval and in accordance with the guidelines of the responsible animal welfare authority (AZ 55.2-1-54-2531-94-07). Further information about companies, from whom chemicals and other materials were purchased, is listed below (Companies and materials).

**Table 3.1: Number of animals investigated in distinct tests**

Investigations after weaning	Group 1			Group 2			
	mt ovx nt	mt sham nt	wt sham nt	mt ovx p	mt sham p	mt ovx E2	wt sham p
<b>genotyping</b>	11	10	11	9	9	9	9
<b>body weight</b>	11	10	11	9	9	9	9
<b>blood glucose</b>	11	10	11	9	9	9	9
<b>OGTT</b>							
50 d	8	7	9	7	7	7	6
90 d	8	7	10	7	7	7	6
180 d	8	7	10	7	7	5	6
<b>Insulin, serum</b>							
50 d	3	3	6	3	2	2	6
90 d	8	6	9	7	6	5	6
180 d	8	7	10	7	7	5	6
<b>ipITT</b>							
50 d	8	7	10				
90 d	8	7	10				
180 d	8	7	10				
<b>Estradiol, serum</b>							
65 d	2	0	6	8	8	9	8
110 d	2	3	4	8	9	9	9
160 d	5	4	6	9	9	7	6
190 d	2	1	4	5	4	4	5
<b>TBARS, serum</b>							
190 d	5	5	5	5	5	4	5
<b>Pancreas (LM, IHC)</b>							
190 d	5	5	6	5	5	4	5
<b>Pancreas (LM and TEM)</b>							
190 d				3	3	2	3
<b>ER-stress, Apoptosis and Cell proliferation, islets</b>							
210 d	6	5	5	4	4	3	4

wt: wild-type mice; mt: mutant mice; ovx: ovariectomized mice; sham: sham-operated mice; nt: non-treated mice; p: placebo-treated mice; E2: 17 $\beta$ Estradiol supplemented mice;

d: days of age; OGTT: oral glucose tolerance test; ipITT: intra peritoneal insulin tolerance test; TBARS: thiobarbituric acid reactive substances; ER: endoplasmic reticulum; LM: light microscopy; IHC: immunohistochemistry; TEM: transmission electron microscopy

### 3.2.2 Genotyping

The genotype of mice was determined by a restriction fragment length polymorphism (RFLP) based method as previously described (Herbach *et al.* 2007). The missense mutation in *Ins2* creates a new *Hpy* 188I restriction site which is used for the allelic differentiation of *Ins2*. After DNA amplification with the primers *Ins2\_5for* and *Ins2\_6rev*, which are specific for *insulin2*, and digestion of the 529 bp PCR amplicates, wild-type mice show a 521 bp fragment, heterozygous Munich *Ins2*<sup>C95S</sup> mutant mice show both the 473 bp and the 521 bp fragment, and homozygous

mutants demonstrate the 473 bp fragment (Fig. 3.1). Tail tip biopsies of approximately 0.3 cm length were taken at weaning and stored at -80°C until assayed. For DNA extraction, the tail tip was incubated in 400 µl master mix over night in a heating block at 55°C over night. Thereafter, undigested components were separated by centrifugation for two minutes at 15,000 rpm. The supernatant was poured into an Eppendorf cup. To precipitate DNA, 400 µl isopropanol (neoLab, Germany) were added. The DNA pellet was washed three times with 400 µl 70% EtOH (Merck, Germany), the liquid phase was discarded and the DNA pellet was dried at room temperature. DNA was suspended in 30 - 150 µl 1\*TE buffer, according to the size of the DNA pellet. To make sure that the DNA was dissolved completely, it was stored at 4°C for at least 24h before proceeding with the PCR. 19 µl of the PCR master mix and 1 µl of the suspended DNA were mixed carefully in PCR analysis cups (Eppendorf, Germany), before starting the PCR-program in a Mastergradient thermocycler (Eppendorf, Germany). PCR-H<sub>2</sub>O served as quality control. If needed, PCR samples were stored at -20°C until further use. Enzymatic digestion took place in a thermocycler (Eppendorf; 37°C, 30 minutes), using 9 µl of the amplified DNA sample, and 11 µl of restriction enzyme master mix. After enzymatic digestion, 4 µl of loading dye was added to each sample before being transferred into the sample wells of a 2 % agarose gel. The gel was positioned in an Easy Cast™ gel chamber (PeqLab, Germany) and filled with 1\*TAE running buffer. At the beginning of the row 12 µl pUC Mix Marker 8 (MBI Fermentas, Germany) was placed in a well in order to allow estimation of amplified fragment size. Electrophoresis was run at 65 volt for the first 15 minutes, afterwards at 110 volt for about 100 minutes (PowerPac 300, Bio-Rad, USA). The gel was stained in an ethidium bromide solution (Roth, Germany) for 20 minutes. The amplified products were visualised (Universal Hood, Bio-Rad, USA) under UV light (306 nm), and a digital picture was taken to document the result.

## Materials

### Master Mix for DNA isolation

Cutting Buffer	375 µl
20% SDS (Roth, Germany)	20 µl
Proteinase K (20 mg/ml)	5 µl

**Cutting buffer**

1 M Tris/HCl, pH 7.5 (Roth, Germany)	2.5 ml
0.5 M EDTA, pH 8.0 (Sigma, Germany)	5.0 ml
5 M NaCl (AppliChem, Germany)	1.0 ml
1 M DTT (Roth, Germany)	250 $\mu$ l
Spermidine (500 mg/ml, Sigma, Germany)	127 $\mu$ l
ad 50 ml aqua bidest; stored at 4 °C	

**TE buffer**

10 mM Tris/HCl, pH 8.0 (Roth, Germany)
1 mM EDTA (Sigma, Germany)

**PCR master mix: Taq PCR Master Mix Kit (Quiagen, Germany)**

10x Buffer:	2 $\mu$ l
MgCl <sub>2</sub> :	1.25 $\mu$ l
Q-solution:	4 $\mu$ l
Taq polymerase:	0.1 $\mu$ l
Redistilled water:	8.65 $\mu$ l
dNTP 1 mM (Eppendorf, Germany):	1 $\mu$ l
Primer sense (Ins2_5for):	1 $\mu$ l
Primer antisense (Ins2_6rev):	1 $\mu$ l
Primer concentration 2 $\mu$ M each (Genzentrum/DNSynthese, Germany; primer sequences: Ins2_5for: 5'-TGA CCT TCA GAC CTT GGC AC-3' Ins2_6rev: 5'-TAG CTG CCA TCA CCC ATG CC-3')	
all reagents stored at -20 °C	

**Restriction enzyme master mix:**

Restriction enzyme <i>Hpy</i> 188I (New England BioLabs, UK):	0.8 $\mu$ l
NEBuffer 4 (New England BioLabs, UK):	2.0 $\mu$ l
Redistilled water:	8.2 $\mu$ l
stored at -20 °C	

**Loading dye 6x:**

Glycerine (Merck, Germany):	3 ml
Bromphenol blue (Merck, Germany):	spatula tip
Redistilled water:	7 ml

**Agarose gel, 2%:**

Agarose (Roth, Germany)	2g
dissolved in boiling TAE buffer:	100 ml

**Marker:**

100 bp DNA Ladder (New England BioLabs, UK):	25 $\mu$ l
Loadind dye x6:	25 $\mu$ l
Redistilled water:	100 $\mu$ l

**Ethidium bromide solution:**

Ethidium bromide 1% (Roth, Germany):	100 $\mu$ l
TAE:	1,000 ml

**EDTA 0.5 M pH 8.0, stock solution:**

EDTA (Roth, Germany):	14.89 g
Distilled water	80 ml
adjust to pH 8.0 with NaOH 5 M (Merck, Germany)	

**TRIS 1M:**

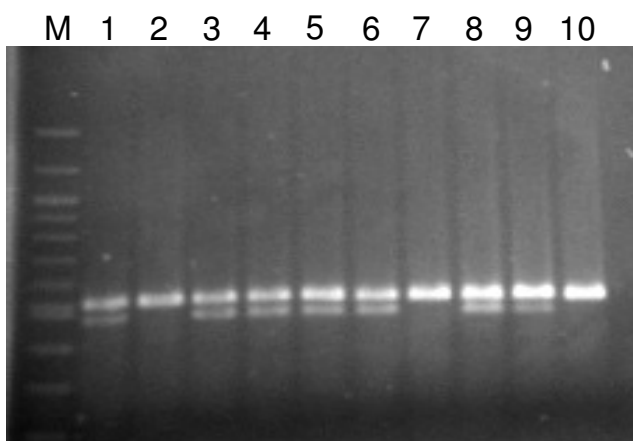
Tris base (Roth, Germany):	6.057 g
ad 50 ml distilled water;	
adjust to pH 8.0 with 37% HCl (Merck, Germany)	

**TAE x 50:**

Tris base (Roth, Germany):	242 g
Glacial acetic acid (Merck, Germany)	57.1 ml
EDTA 0.5 M, pH 8.0:	100 ml
ad 1,000 ml distilled water	

**Program for DNA amplification:**

1. 94 °C, 5 minutes (denaturation, initiation)	
2. 94 °C, 45 seconds (denaturation)	34 cycles
3. 62 °C, 45 seconds (primer annealing)	
4. 72 °C, 90 seconds (elongation)	
5. 72 °C, 10 minutes (final extension)	
hold on 4 °C	

**Figure 3.1: Genotyping via polymerase chain reaction (PCR) and restriction fragment length polymorphism (RFLP)**

After PCR and RFLP analysis, wild-type mice (2, 7, 10) present DNA fragments of 521 base pairs (bp), heterozygous mutant mice (1, 3, 4, 5, 6, 7, 9) exhibit fragments of 473 bp and 521 bp, homozygous mutants (not shown) possess fragments of 473 bp; M: marker

### 3.2.3 Ovariectomy and pellet implantation

One hour before surgical intervention, each mouse received 10 µl of Metacam<sup>®</sup> solution (15 mg/ml Meloxicam, Boehringer, Germany) per os, using a pipette. Analgesia was repeated once a day for at least 5 days. An anaesthetic mixture of Medetomidine (0.5 mg/kg body weight, Domitor<sup>®</sup>, Pfizer, Germany), Midazolam (5 mg/kg body weight, Midazolam-Ratiopharm<sup>®</sup>, Ratiopharm, Germany) and Fentanyl (0.05 mg/kg body weight, Fentanyl DeltaSelect<sup>®</sup>, Delta Select, Germany) was injected intraperitoneally with a 30-gauge needle. A dexpanthenol containing ointment (Bepanthen<sup>®</sup>, Roche, Germany) was applied into both eyes. Approximately 15 minutes after the injection, an area of 2 cm<sup>2</sup> was shaved caudal the costal arch on either lateral sides of the mouse using an electric shaver. Subsequently the mice were placed laterally on a warm base. Once the anaesthesia was in the stage of surgical tolerance, shaved skin was disinfected (Softasept<sup>®</sup>N, Braun, Germany). Approximately 1 cm behind the costal arch a cut of about 1 cm length was made through the skin with a surgical pair of scissors. After that, the peritoneum was held up with a forceps and the abdominal cavity was opened with a cut of about 5 mm length. A forceps was inserted into the abdominal cavity, the forceps was closed and the ovary was gently retracted. After ligation of the vessels (Monosyn<sup>®</sup> metric2, Braun, Germany), the ovary was removed and fixed in 4% neutral buffered formaldehyde solution (SAV LP, Germany). The peritoneum was closed by a continuous monofilament absorbable suture (Syneture metric 1.5, Tyco Healthcare, UK). Finally, the skin was closed, using 2 or 3 suture clips (Heiland, Germany). After moving the mouse to the other side, the other ovary was removed the same way. When the operation was finished, the narcosis was antagonized, by intraperitoneal injection of a mixture of Atipamezol (2.5 mg/kg body weight, Antisedan<sup>®</sup>, Pfizer, Germany), Flumazenil (0.5 mg/kg body weight, Anexate<sup>®</sup>, Roche, Germany) and Naloxon (1.2 mg/kg body weight, Naloxon DeltaSelect<sup>®</sup>, DeltaSelect, Germany). The animals were kept under an infrared lamp until complete recovery. Sham-operation followed the same procedure as described for the ovariectomized mice, with the exception, that the ovaries were retracted, manipulated and placed back into physiological position. Directly after ovariectomy/sham-operation, mice of Group 2 additionally received either a 17βEstradiol longterm pellet (containing 0.18mg E2) or a placebo pellet (Innovative Research of America, USA). Therefore an area of about

1 cm<sup>2</sup> in the mid dorsal region of the mouse was shaved, using an electric shaver and the skin was disinfected (Softasept<sup>®</sup>N, Braun, Germany). A cut of about 0.3cm length was made through the shaved and disinfected skin with a surgical pair of scissors. Afterwards, a 16-gauge trocar containing the pellet was pushed through the skin orifice and the pellet was placed under the skin. Finally skin was closed with one suture clip (Heiland, Germany).

### **3.2.4 Body weight**

Body weights of randomly fed mice were determined at least every 4 weeks during the investigation period to the nearest 0.1 g, using a precision balance (KERN, Germany).

### **3.2.5 Blood glucose concentration**

#### **3.2.5.1 Randomly fed mice**

Starting at the age of weaning (21 days), blood glucose levels were measured in 4-week intervals. Blood samples were taken from the nicked tail tip with a 10 µl open-end capillary (HITADO, Germany) by softly massaging the tail. The capillary was placed into a tube filled with 500 µl haemolysis solution (Glucapil<sup>®</sup>, HITADO, Germany), and blood glucose concentration was determined, using the blood glucose analyser SUPER GL<sup>®</sup> (HITADO, Germany). Blood glucose levels during oral glucose tolerance tests and intraperitoneal insulin tolerance tests were evaluated in an analogue way. Additionally, the glucose concentration in blood collected from the retroorbital plexus of 190- and 210-day-old mice was determined as described above.

#### **3.2.5.2 Fasted mice**

Starting at the age of 50 days, fasting blood glucose levels (fasting from 7 pm until 9 am) were measured at least every 4 weeks as described above.

### **3.2.6 Oral glucose tolerance test (OGTT)**

Glucose tolerance tests were performed at an age of 50, 90 and 180 days. The mice were fasted over night for 14 hours, starting at 7 pm. The next morning at 9 am, each mouse was placed into an individual cage with tap water access ad libitum. The tail tip was nicked, and blood samples were collected to analyse basal blood glucose

and serum insulin concentrations. The mice received 11.1  $\mu\text{l}$  of a 1 M glucose solution per gram body weight ( $\alpha\text{-D-Glucose}$ , Sigma, Germany; diluted in tap water) into the stomach via gavage tube. Ten minutes after glucose administration, further blood samples for determination of blood glucose and serum insulin levels were taken. At 20, 30, 60, 90 and 120 minutes, samples for analysing the blood glucose concentrations were collected. Blood glucose levels were measured immediately as described above (3.2.5). The area under the glucose curve was calculated using the program GraphPad Prism 3.0 (GraphPad Software, USA).

For serum insulin determination, about 100 - 120  $\mu\text{l}$  blood was collected from the tail tip, using a 75  $\mu\text{l}$  capillary tube (Hirschmann, Germany). After centrifugation (1K15, Sigma, Germany; 10 minutes, 10,000 rpm), serum was removed and stored at  $-80^{\circ}\text{C}$  until assayed. The area under the blood glucose curve was calculated, using GraphPad Prism 3.0. (GraphPad Software, USA). The  $\beta$ -cell function indices homeostasis model assessment of baseline insulin secretion (HOMA B) and insulin resistance (HOMA IR), were calculated by means of fasting blood glucose and serum insulin concentrations according to the following equation (Wallace *et al.* 2004):

HOMA B =	$(20 \times \text{FSI}) / (\text{FBG} - 3.5)$
HOMA IR =	$(\text{FSI} \times \text{FBG}) / 22.5$

FSI = Fasting serum insulin (mU/L)

FBG = Fasting blood glucose (mmol/L)

The quantitative insulin-sensitivity check index (Quicki) (Katz *et al.* 2000) and the fasting glucose-to-insulin ratio (FGIR) (Legro *et al.* 1998), both useful methods for assessing insulin sensitivity, were also calculated by means of fasting blood glucose and serum insulin concentrations according to the following equation:

Quicki =	$1 / (\log \text{FSI} + \log \text{FBG})$
FGIR =	$(\text{FBG} / \text{FSI})$

FSI = Fasting serum insulin (mU/L)

FBG = Fasting blood glucose (mg/dl)

### 3.2.7 Intraperitoneal insulin tolerance test

Insulin tolerance tests were performed at an age of 60, 100 and 187 days with mice of Group 1. At 2 pm, each mouse was placed into an individual cage with tap water access ad libitum. Blood samples were collected from the nicked tail tip to determine basal blood glucose levels. Straight after that, 0.75 I.U. insulin per kilogram body weight (40 U/ml, Insuman<sup>®</sup> Rapid, Aventis, Germany; diluted 1:247 in 0.9 % NaCl; 120  $\mu$ l injection volume) were injected intraperitoneally, using a 30G x 1/2" needle. Ten, 20, 30, 60 and 90 minutes after insulin application, further blood samples were taken for determination of blood glucose concentrations as described above (3.2.5 Blood glucose concentration)

### 3.2.8 Serum insulin concentration

The serum insulin concentrations were determined from samples, which were collected during OGTT (3.2.6 Oral glucose tolerance test) at the age of 50, 90 and 180 days. A rat insulin radioimmunoassay kit (Linco Research, USA), which fully cross-reacts with murine insulin, was used for the detection. Due to small sample volumes (55 - 70  $\mu$ l serum), the assay was performed using the half amount of sample and assay reagents as denoted in the instruction sheet. The assay was performed according to the manufacturer's protocol. Additionally, the difference between the insulin levels 10 minutes after glucose application and basal values (0 minutes) was calculated.

### 3.2.9 Serum estradiol concentration

The serum 17 $\beta$ Estradiol concentration of 65-, 105-, 160-, 190- and 210-day-old mice was determined using an Estradiol ELISA KIT (DRG Instruments GmbH, Germany). The assay was performed according to the manufacturer's protocol. Blood samples

were obtained from the nicked tail tip (65-, 110- and 160-day-old) or the retroorbital plexus (190- and 210-day-old) and serum was separated as described above (3.2.6 Oral glucose tolerance test). Additional blood glucose determinations were performed at the same time points (3.2.5 Blood glucose concentration).

### 3.2.10 Serum lipid peroxidation

Lipid peroxidation in the serum of 190- and 210-day-old mice was examined, using a TBARS Assay Kit<sup>®</sup> (Cayman, USA), according to the manufacturer's protocol. Mice were anaesthetised by intraperitoneal injection of 200 µl of a ketamine/xylazine mixture, exsanguinated from the retroorbital plexus and finally killed by cervical dislocation. The serum was separated from cellular components via centrifugation (1K15, Sigma, Germany; 10 minutes, 10,000 rpm) and stored at -80 °C until assayed. Serum samples were diluted 1:2 (mt-sham-nt/p, mt-ovx-E2 and wt-sham-nt/p mice) or 1:4 (mt-ovx-nt/p mice) in HPCL grade water (Applichem, Germany). Blood glucose concentrations were measured at the same time points (see 3.2.5 Blood glucose concentration).

## Materials

### Narcotics:

Ketamine 10% (Selectavet, Germany):	1 ml
Xylazine 2% (Rompun 2%, Bayer, Germany):	0.25 ml
NaCl 0.9%:	5 ml

### 3.2.11 Western blot analyses of isolated islets

For analysis of endoplasmic reticulum stress, islets of 210-day-old mice were isolated and examined with regard to the endoplasmic reticulum stress markers BiP/Grp78 (Binding Ig protein/Glucose regulated protein 78), PeIF2 $\alpha$  (phosphorylated eukaryotic initiation factor 2 $\alpha$ ), GADD153/CHOP-10 (Growth arrest and DNA damage 153/C/EBP-homologous protein 10). For detection of apoptosis and cell proliferation, the isolated islets were investigated with regard to the apoptosis marker caspase-3 and the cell proliferation marker PCNA. Actin was used as loading control. The optical density of BiP, PeIF2 $\alpha$ , CHOP and PCNA was determined, using ImageJ 1.41o and divided by the optical density of actin.

### 3.2.11.1 Islet isolation

Sixteen mice of Group 1 were euthanized by intraperitoneal injection of 200  $\mu$ l ketamine/xylazine mixture and cervical dislocation. After abdominal incision, the bowel was retracted and placed on the right side of the mouse in order to expose the pancreas and the bile duct. The small intestine was clamped 1 cm left and right of the bile duct orifice with two arterial clamps to exclude collagenase solution efflux into the intestine. The bile duct was ligated as close as possible to the liver with a thin string. Using a winged infusion set (Venofix<sup>®</sup>, B.Braun, Germany), the bile duct was cannulated via the small intestine, and 2 ml collagenase solution (Sigma, Germany) was injected into the pancreas. The pancreas was carefully separated from adjacent tissue, and transferred immediately into a 15 ml screw-cap tube, filled with 3.5 ml perfusion solution and 1.5 ml collagenase solution. Fifteen mice of Group 2 were euthanized the same way as mice of Group 1, but were additionally perfused through the left heart ventricle with body warm filtered 0.02% neutral red in 0.9% NaCl at 60 mmHg, using a perfusion device developed by Dr. Andreas Blutke (German utility patent no. DE 202006001542 U1, Figure 3.2). Neutral red selectively stains pancreatic islets, exocrine pancreas remains unstained. After opening the chest by a pair of scissors, the needle was placed into the left heart ventricle. An incision in the inferior vena cava, cranial of the diaphragm provided outflow of the perfusate. After neutral red perfusion, collagenase solution was injected into the pancreas as described above. Pancreatic tissue was digested for at least 20 minutes up to at most one hour in a water bath (GFL, Germany; 37°C) under occasional gently agitation. Digested tissue fragments were transferred into a petri dish filled with ice cold HANK's with 0.3% BSA to stop digestion. All reagents and tissues were kept on ice during the ongoing procedure steps. Islets were hand picked with an Eppendorf pipette under a stereomicroscope (Stemi DV4, Zeiss, Germany; magnification x32) and transferred into a 1.5 ml Eppendorf tube. After centrifugation for 1 minute at 1,000 rpm (1K15, Sigma, Germany), the supernatant was discarded and the islets were resuspended in 20-50  $\mu$ l (1 $\mu$ l/6 islets) of protein extraction buffer. Cell membranes were destroyed by freezing at -80°C, thawing on ice for 30 minutes, followed by sonication (7 strokes <1 s each by a Branson sonifier cell disruptor B15 (Branson Ultrasonic Corporation, USA)), and lysing on ice for another 30 minutes.

After centrifugation (5 minutes, 5,000 rpm), the supernatant was separated, and stored at -80 °C until assayed.

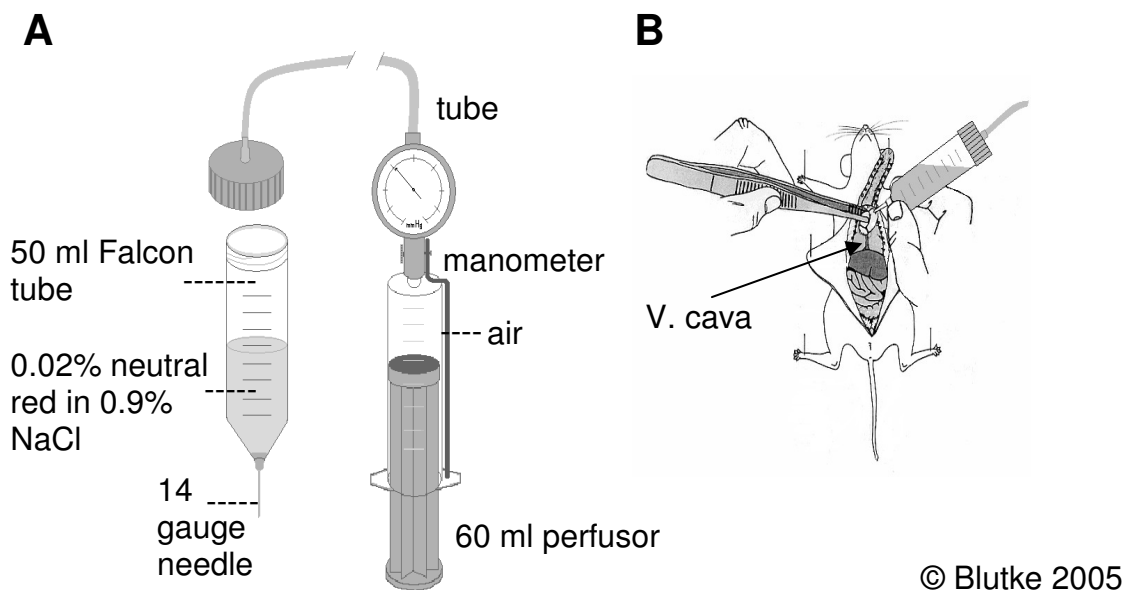


**Figure 3.2: Device used for perfusion (A) and Perfusion technique (B).**

**A:** Perfusion can be performed under adjustable pressure conditions.

**B:** Perfusion was performed at a pressure of 60 mm Hg via the left heart ventricle. An incision in the vena cava caudalis (indicated) provided outflow of the perfusate (Courtesy of A. Blutke).

## Materials

### Anaesthetics

described above (3.2.9)

### 0.02% Neutral red solution

Neutral red	200mg
NaCl 0.9%	1000ml

### 4x Hank's solution

NaCl (AppliChem, Germany)	16.0 g
HEPES (Sigma, Germany)	4.76 g
KCl (Roth, Germany)	0.80 g
NaHCO <sub>3</sub> (Merck, Germany)	0.70 g
KH <sub>2</sub> PO <sub>4</sub> (Roth, Germany)	0.12 g
Na <sub>2</sub> HPO <sub>4</sub> (Merck, Germany)	0.12 g
MgSO <sub>4</sub> (Merck, Germany)	0.40 g
CaCl <sub>2</sub> (Merck, Germany)	0.37 g

distilled water	500 ml
stored at 4 °C	
<b>1x Hank's solution</b>	
Hank's 4x	375 ml
α-D-Glucose (Sigma, Germany)	0.60 g
adjust to pH 7.25 and keep on ice	
<b>1x Hank's with 0.3% BSA</b>	
Hank's 1x	500 ml
BSA (Sigma, Germany)	1.5 g
<b>Perfusion solution</b>	
Hank's 1x	20 ml
CaCl <sub>2</sub> 1 M (Merck, Germany)	47 μl
Hepes 1 M (Sigma, Germany)	500 μl
kept on ice	
<b>Collagenase solution</b>	
Perfusion solution	10 ml
Collagenase type 1 (#C0130, Sigma, Germany)	20 mg
kept on ice	
<b>Protein extraction buffer</b>	
200 mM NaCl/Tris pH 7.6	100 μl
Ipegal CA 630 (ICN Biomedicals GmbH, Germany)	5 μl
300 mM EDTA	10 μl
300 mM EGTA	10 μl
100 mM PMSF	10 μl
200 mM NaOV	10 μl
1M DTT	1 μl
25x Complete	40 μl
Aqua bidest	814 μl
<b>Stock solutions</b>	
<i>200 mM NaCl/Tris pH 7.6:</i>	
Tris base(Roth, Germany)	1.58 g
NaCl (AppliChem, Germany)	7.31 g
dissolved in 30 ml aqua bidest and adjusted to pH 7.6; ad 50 ml aqua bidest	
<i>300 mM EDTA:</i> 1.12 g EDTA (Sigma, Germany); ad 10 ml aqua bidest	
<i>300 mM EGTA:</i> 1.41 g EDTA (Sigma, Germany); ad 10 ml aqua bidest	
<i>100 mM PMSF:</i> 17.4 mg PMSF (Sigma, Germany)	
dissolved in 1 ml isopropanol (Merck, Germany) and stored at -20 °C.	

*200 mM NaOV*: 0.92 g NaOV (ICN Biomedicals GmbH, Germany)

dissolved in 20 ml distilled water and adjusted to pH 10 until the solution turns yellow. Solutions were reiterated boiled and cooled down on ice until remaining clear and of stable pH. After addition of 22.5 ml aqua bidest, the solution was aliquoted and stored at -20°C. Prior to use, solutions were boiled for 10 minutes on a heating block (Biometra TB1 Thermoblock, Whatman, Germany) to remove crystallisation.

*1 M DTT*: 77.0 mg DTT (Roth, Germany); ad 500 µl aqua bidest

*25x Complete*: Complete Protease Inhibitor Cocktail Tablets (Roche, Germany)

dissolved according to manufacturer's instructions

### 3.2.11.2 Islet protein content

To evaluate the protein content of islet samples, the Bradford method was applied. A protein standard was created by dissolving 10 mg of bovine serum albumin (BSA, Sigma, Germany) in 1 ml phosphate buffered saline (PBS). From this initial solution, standard concentrations of 25, 12.5, 6.25, 3.125, 1.56, 0.78, 0.39 and 0.195 µg BSA/ml were produced in duplicate by 1:2 dilution in a NUNC™ 96-well Optical Bottom Plate (Thermo Fisher Scientific (Nunc GmbH & Co. KG), Germany). Two µl sample were added to 198 µl PBS in the first well, and diluted 1:2 in PBS in the adjacent 4 wells ending in a 1:16 dilution. The reaction was initiated by addition of 100 µl 40% Bradford reagent (Bio-Rad, Germany) to each well. After incubation for at least 5 minutes, absorbance was determined spectrophotometrically at a wavelength of 595 nm using a plate reader (SUNRISE, Tecan, Germany) and the corresponding software (Magellan 2, Tecan, Germany).

## Materials

### Phosphate buffered saline (PBS)

NaCl (AppliChem, Germany)	7.95 g
Na <sub>2</sub> HPO <sub>4</sub> (Roth, Germany)	1.15 g
KCl (Merck, Germany)	0.20 g
KH <sub>2</sub> PO <sub>4</sub> (AppliChem, Germany)	0.20 g
ad 1,000 ml distilled water	

### Bradford reagent:

Bio-Rad Protein Assay 100% (Bio-Rad, Germany):	2 ml
Distilled water:	5 ml

protected from light and stored at 4°C

### 3.2.11.3 SDS-PAGE

Islet proteins were separated by SDS-PAGE, using a 10% separating SDS gel (ER-Stress markers and replication-marker) or a 12% separating SDS gel (apoptosis marker). The separating gel solutions were poured into the intercept of 2 glass plates, clamped in a Mini-Protean III<sup>®</sup> gel casting chamber (Bio-Rad, Germany) and were immediately covered with isopropanol. After a polymerization period of about 45 min, the isopropanol was drained and the stacking gel was casted onto the separation gel and a 10-well-comb was inserted into the still fluid stacking gel in order to create sample wells. After polymerization of the stacking gel, the comb was carefully removed, and the gel was placed into an electrophoresis cell (Protean III<sup>®</sup>, Bio-Rad, Germany). The inner cell of the chamber was then filled to the top with running buffer and the outer cell was filled up to about 3 cm from the bottom. The islet sonicates were diluted creating a protein concentration of 20 µg/20 µl, but at least with equal volumes of sample buffer, whereas the maximum final volume did not exceed 25 µl. After denaturation of proteins in a thermoblock (TB1, Biometra, Germany; 10 minutes, 100 °C) samples were loaded into the wells. Furthermore, a molecular weight standard (Precision Plus Protein<sup>™</sup>, Bio-Rad, Germany) was pipetted into the first well of the gel and then electrophoresis was run at 200V (Biorad PowerPac 300, Bio-Rad, USA) for about 50 minutes.

## Materials

### Reducing sample buffer:

Sample buffer, stock solution:	475 µl
β-mercaptoethanol (Sigma, Germany):	25 µl

### Sample buffer, stock solution:

Tris/HCl 0.5 M, pH 6.8:	1.2 ml
SDS 10% (Sigma, Germany):	2 ml
Glycerol (Merck, Germany):	1 ml
Bromphenol blue 0.05% (Merck, Germany):	0.6 ml
Distilled water:	4.8 ml

### 10%-SDS polyacrylamide gel:

Distilled water	2.085 ml
Tris/HCl 1.5 M, pH 8.8:	1.25 ml
SDS 10% (Sigma, Germany):	50 µl
Acrylamide 30% (Roti Phenol <sup>®</sup> , Roth, Germany):	1.665 ml
Ammonium persulfate (APS) 10% (Bio-Rad, Germany):	25 µl
Tetraethylethylenediamine (TEMED) (Roth, Germany):	5 µl

**12%-SDS polyacrylamide gel:**

Distilled water	1.75 ml
Tris/HCl 1.5 M, pH 8.8:	1.25 ml
SDS 10% (Sigma, Germany):	50 µl
Acrylamide 30% (Roti Phenol <sup>®</sup> , Roth, Germany):	2 ml
Ammonium persulfate (APS) 10% (Bio-Rad, Germany):	25 µl
Tetraethylethylenediamine (TEMED) (Roth, Germany):	5 µl

**Stacking gel (5%-SDS polyacrylamid gel):**

Distilled water	1.525 ml
Tris/HCl 0.5 M, pH 6.8:	0.625 ml
SDS 10%, (Sigma, Germany):	25 µl
Acrylamide 30% (Roti Phenol <sup>®</sup> , Roth, Germany)	0.325 ml
Ammonium Persulfate (APS) 10% (Bio-Rad, Germany)	25 µl
Tetraethylethylenediamine (TEMED) (Roth, Germany)	5 µl

**Tris/HCl 0.5 M, pH 6.8:**

Tris base (Roth, Germany):	6.057 g
ad 100 ml distilled water	
adjust to pH 6.8 with HCl 37% (Merck, Germany)	

**Tris/HCl 1.5 M, pH 8.8:**

Tris base (Roth, Germany):	18.5 g
ad 100 ml distilled water	
adjust to pH 8.8 with HCl 37% (Merck, Germany)	

**Running buffer, ready to use:**

Stock solution:	40 ml
SDS 10% (Sigma, Germany):	4 ml
ad 400 ml distilled water	

**Running buffer, stock solution:**

Tris base (Roth, Germany):	30.3 g
Glycine (Merck, Germany):	144 g
ad 1,000 ml distilled water	

**3.2.11.4 Western blot**

Following electrophoresis, the gels were covered with a nitrocellulose membrane (Schleicher & Schuell, Germany), which had been moistened in Towbin buffer and placed between 3 layers of absorbent paper and a fibre pad (both humidified with Towbin buffer) each side in a gel holder cassette. Two cassettes were inserted into the electrode module which was positioned in the buffer tank (Mini Trans-Blot Cell, Biorad, Germany) filled with ice cold Towbin buffer, and contained a frozen cooling

unit, and a magnetic stir bar. The whole tank was additionally cooled in a box with crushed ice while running the transfer for 90 minutes at 100 volt on a magnetic stirrer (IKA, Germany). Subsequently, the membrane was washed in Tris buffered saline-Tween (TBS-T) for 10 minutes. Finally, silver staining of the gel was done to demonstrate blotting success (3.2.11.5 Silver staining and drying).

## Materials

### Towbin buffer

Tris base (Roth, Germany)	3.03 g
Glycine (Merck, Germany)	14.4 g
Methanol (neoLab, Germany)	200 ml
Distilled water	800 ml
stored at 4 °C	

### Tris buffered saline (TBS), ready to use:

TBS, stock solution:	500 ml
Distilled water:	4,500ml

### Tris buffered saline (TBS), stock solution x10:

Tris base (Roth, Germany):	60.6 g
NaCl (AppliChem, Germany):	87.6 g
ad 1,000 ml distilled water	
adjust to pH 7.4 with HCl 37% (Merck, Germany)	

### TBS-T:

TBS, stock solution x10:	50 ml
Distilled water:	450 ml
Tween 20 (Merck, Germany):	250 µl

#### 3.2.11.5 Silver staining and drying

The SDS gel was incubated for at least 30 minutes in fixation solution and afterwards washed 3 times for 20 minutes with 50% ethanol (Merck, Germany). Then it was pretreated in sodium thiosulfate solution for one minute before being rinsed with distilled water (3 x 20 seconds). Thereafter, it was impregnated for 20 minutes and washed (2 x 20 seconds) with distilled water. The gel then was developed under visual control until bands appeared. Afterwards it was rinsed for 20 seconds in distilled water and then the reaction was stopped with EDTA solution. After 3 times washing for 2 minutes in distilled water, the gel was incubated over night (4 °C) in drying solution on a tumbling shaker. The next day, the first part of the DryEase gel

drying frame, (Novex, Germany) was brought into position on a dryer base (DryEaseMini-Gel Drying Base, Novex, Germany) and covered with a cellophane sheet (DryEase Mini Cellophane, Novex, Germany) which was moistened in drying solution for 30 seconds. Then the gel was placed in the centre of the film and another moistened cellophane sheet was used to cover the gel. Air blisters and wrinkles were carefully removed before closing the gel/cellophane sandwich with the second part of the frame with 5 plastic clips. The gel was dried in an upright position for 36 hours in a draft-protected place, removed from the frame and placed under a heavy book for straightening.

## Materials

### Fixation solution:

Ethanol 100% (Merck, Germany):	500 ml
Glacial acetic acid (Merck, Germany):	120 ml
Formaldehyde 37% (SAV-LP, Germany):	0.5 ml
ad 1,000 ml distilled water	

### Pre-treating solution:

(Na <sub>2</sub> S <sub>2</sub> O <sub>3</sub> ) x 5 H <sub>2</sub> O (Merck, Germany)	50 mg
Distilled water:	50 ml

### Impregnation solution:

AgNO <sub>3</sub> (AppliChem, Germany):	50 mg
Distilled water:	50 ml
Formaldehyde 37% (SAV-LP, Germany):	35 µl

### Development solution:

Na <sub>2</sub> CO <sub>3</sub> (Merck, Germany):	1.5 g
(Na <sub>2</sub> S <sub>2</sub> O <sub>3</sub> ) x 5 H <sub>2</sub> O (Merck, Germany):	0.1 g
Distilled water:	100 ml
Formaldehyde 37% (SAV-LP, Germany):	50 µl

### Stop solution:

EDTA 0.1 M, pH 8.0 (Sigma, Germany):	14.8 g
Distilled water:	400 ml

### Drying solution:

Methanol 15%	
Glycerol 3%	
diluted in distilled water	

### 3.2.11.6 Western blot analysis

Detection of specific antigens was performed by Western blot analysis. Washing and incubation procedures were accomplished under consequent agitation of the membranes on a tumbling shaker (Heidolph, Germany) to allow consistent moistening of the membranes. Washing was carried out 3 times for 10 minutes with TBS-Tween (TBS-T) if not stated differently. All reaction steps were carried out at room temperature unless stated otherwise.

#### **ER-stress markers**

The membrane was blocked in 1% bovine serum albumin (BSA) in TBS for one hour at room temperature to avoid non-specific binding of the antibodies used. Antibodies were diluted in 10 ml of 1% BSA in TBS. After washing, the membrane was simultaneously incubated in polyclonal rabbit anti-Grp78 (Stressgen, Canada; 1:10,000), monoclonal rabbit anti-PeIF2 $\alpha$  (Cell Signalling, USA; 1:1,000), and polyclonal rabbit anti-GADD153 (Santa Cruz Biotechnology, USA; 1:500) antibodies over night at 4°C. The next day, the membrane was washed and then incubated for one hour with a horseradish peroxidase conjugated anti-rabbit antibody (Cell signalling, USA; 1:10,000), followed by another washing step. Afterwards, the membrane was covered with Luminol Reagent (Santa Cruz Biotechnology, USA) for 1 minute, before being placed into a film cassette (Ortho Fine, AGFA, Germany). To avoid dehydration, the membrane was covered with a plastic transparency. An Amersham Hyperfilm ECL (GE Healthcare, Germany) was laid upon the covered membrane in a dark room. After an exposition time of about 2 minutes, the film was developed (Kodak professional developer, Kodak, USA), shortly rinsed in a 12% acetic acid solution, fixed (Kodak professional fixer, Kodak, USA), rinsed thoroughly with tap water, and dried. Afterwards, the membrane was removed from the cassette, washed for 5 minutes in TBS-T, incubated for 10 minutes in stripping buffer, washed for 2 x 10 minutes in PBS and for 2 x 5 minutes in TBS-T (mild stripping protocol according to Abcam, UK). Subsequently the membrane was blocked for one hour in 1% BSA in TBS, washed and then incubated with a monoclonal mouse anti-actin antibody (Chemicon international, Germany; 1:10,000, over night, 4°C). After another washing step, a horseradish peroxidase rabbit anti-

mouse antibody was added (DAKO, Germany; 1:10,000) and detection of immunoreactivity was performed as described.

### **Apoptosis markers**

The membrane was blocked for 1 hour at room temperature in Blotto A (5% non fat dry milk (Roth, Germany) in 0.05% TBS-T) to avoid non-specific binding of the antibody used. After washing, the membrane was incubated over night at 4°C with polyclonal rabbit anti-Caspase-3 antibody (Cell Signalling, USA; 1:1,000), which was diluted in 10ml Blotto A. The next day, the membrane was washed and then incubated for one hour at room temperature with a horseradish peroxidase conjugated anti-rabbit antibody (Cell Signalling, USA; 1:2,000) diluted in 10 ml Blotto A, followed by another washing step. Detection of immunoreactivity then was performed as described above, but exposing the film for 12 minutes.

### **Cell proliferation markers**

After blocking in 3% BSA in TBS for one hour at room temperature to avoid non specific binding of the antibody used, the membrane was washed and then incubated with a mouse monoclonal anti-PCNA antibody (Abcam, USA; 1:2,500) diluted in 10 ml 1% BSA in TBS at 4°C over night. The next day, the membrane was first washed and then incubated for one hour at room temperature with a horseradish peroxidase conjugated rabbit anti-mouse antibody (DAKO<sup>®</sup>, Germany; 1:10,000), followed by another washing step. Detection of immunoreactivity then was performed as described above, exposing the film for 2 minutes.

## **Materials**

**TBS and TBS-T:** described above (3.2.11.4)

### **Luminol Reagent (Santa Cruz Biotechnology, USA):**

Solution A	5 ml
Solution B	5 ml

### **Developer:**

Kodak professional developer (Kodak, USA):	7.8 g
Distilled water	50 ml

### **Fixer:**

Kodak professional fixer (Kodak, USA):	9.2 g
--	-------

Distilled water	50 ml
<b>Stripping buffer:</b>	
Glycine (neoLab, Germany):	15 g
SDS 10% (Sigma, Germany):	1 g
Tween 20 (Merck, Germany):	10 ml
ad 1,000 ml distilled water	
adjust to pH 2.2 with 37% HCl (Merck, Germany)	

### 3.2.12 Necropsy and pancreas preparation

At the age of 190 days, 35 mice were exsanguinated by puncture of the retroorbital plexus under general anaesthesia (ketamine/xylazine mixture; refer to chapter 3.2.9) and finally killed by cervical dislocation. Pancreata were obtained for qualitative histological and quantitative stereological analyses as well as for transmission electron microscopy. The pancreas was separated from adjacent tissues and weighed to the nearest 0.1 g (Mettler AE200 Electronic Analytical Balance; Mettler-Toledo Intl. Inc., Germany). The specific weight of the pancreas ( $1.10 \text{ mg/mm}^3$ ) was determined by the submersion method (Scherle 1970). A piece of  $2 \text{ mm}^3$  was cut from the splenic end of the pancreas and was fixed by immersion in 1 ml of 3% glutaraldehyde in Sørensen's phosphate buffer for transmission electron microscopy. The remaining pancreas was laid on a biopsy pad (Bio-optica, Italy) placed in a plastic tissue capsule (Engelbrecht, Germany) and fixed in 4% neutral buffered formaldehyde solution (SAV LP, Germany) overnight at room temperature. After fixation, the pancreas was embedded in agar (Bacto™ Agar, Becton&Dickinson, USA) to alleviate its later slicing, put into a tissue capsule, routinely processed and embedded in paraffin (Histomaster, Bavimed, Germany). The length of the embedded pancreas was determined and the whole pancreas was sectioned perpendicular to its longitudinal axis into parallel slices of approximately 1 mm thickness with the first cut positioned randomly within an interval of 1 mm length at the splenic end of the pancreas. The slices were then positioned with the right cut surface facing downwards, and paraffin embedding was finished. Approximately 5  $\mu\text{m}$  thick serial sections for histology were cut with a HM 315 microtome (Micom GmbH, Germany), mounted on 3-aminopropyltriethoxy-silane-treated glass slides (Starfrost® microscope slides, Engelbrecht, Germany), and dried in a heating cabinet (Wagner & Munz GmbH, Germany) at 37 °C for at least 12 hours.

### 3.2.13 Immunohistochemistry of the pancreas

Immunohistochemical staining for insulin, glucagon, somatostatin, and pancreatic polypeptide producing cells were performed, using the indirect immunoperoxidase method. All incubations were carried out at room temperature in a humidity chamber. Normal serum and antibodies were diluted in Tris buffered saline (TBS, pH 7.4). TBS was used for washing if not stated differently.

#### 3.2.13.1 Insulin

For qualitative histological investigations and for the determination of the volume density and the total volume of isolated  $\beta$ -cells in the pancreas, immunohistochemical staining for insulin was performed (see 3.2.14.2). Pancreas sections were dewaxed in xylene (SAV, Germany) for 20 minutes, rehydrated in a descending alcohol series (2 x 100%, 2 x 96%, 1 x 70% ethanol), and rinsed in distilled water. Endogenous peroxidase activity of tissue sections was blocked by incubation in 1% hydrogen peroxide (neoLab, Germany) solution for 15 minutes. After washing for 10 minutes, sections were pre-treated with normal rabbit serum (MP Biomedicals, USA; dilution 1:10, 30 minutes) to reduce non-specific binding. Afterwards, a polyclonal guinea pig anti-swine insulin (DAKO<sup>®</sup>, Germany) antibody, diluted 1:500 in TBS, was applied for 1 hour. After rinsing for 10 minutes in TBS, the secondary horseradish peroxidase conjugated rabbit anti-guinea pig IgG (DAKO<sup>®</sup>, Germany; diluted 1:50 in TBS, containing 5% mouse serum) was applied for 1 hour. The sections were washed for 10 minutes in TBS before adding the chromogen substrate 3,3'-diaminobenzidine tetrahydrochloride dihydrate (DAB, KEM-EN-TEC, Denmark) containing 0.1% H<sub>2</sub>O<sub>2</sub> to visualise immunoreactivity. Slides were rinsed in tap water for 5 minutes, counterstained with Mayer's Haemalaun (Applichem, Germany) and washed under running tap water (5 minutes). Subsequently, the sections were dehydrated in an ascending alcohol series, cleared in xylene (SAV, Germany), and mounted under glass coverslips, using Roti<sup>®</sup> Histokitt II (Roth, Germany).

## Materials

**TBS:**described above (see 3.2.11.4)

### Hydrogen peroxide 1%

30% H<sub>2</sub>O<sub>2</sub> (neoLab, Germany)  
Aqua bidest

6 ml  
194 ml

**DAB solution**

DAB pellets (KEM-EN-TEC, Denmark)	1 piece
Aqua bidest	10 ml

dissolved for 1 hour (protected from light), filtered, aliquoted and stored at  $-20^{\circ}\text{C}$  ad  $1\ \mu\text{l}$  30%  $\text{H}_2\text{O}_2$  (neoLab, Germany) per 1 ml DAB solution directly before use.

**3.2.13.2 Glucagon, somatostatin and pancreatic polypeptide**

The immunostaining procedure was similar to the staining of insulin (see 3.2.13.1 Insulin). To reduce non-specific binding, normal swine serum (MP Biomedicals, USA; dilution 1:10, 30 minutes) was used. Sections were incubated with an antibody cocktail containing polyclonal rabbit anti-human glucagon (dilution 1:50), polyclonal rabbit anti-human somatostatin (dilution 1:100), and polyclonal rabbit anti-human pancreatic polypeptide (dilution: 1:500) for 75 minutes. Horseradish peroxidase conjugated porcine anti-rabbit IgG (1:50, containing 5% mouse serum, 1 hour) served as secondary antibody. All antibodies used were purchased from DAKO<sup>®</sup> (Germany).

**3.2.14 Quantitative stereological analyses**

Pancreata of 190-day-old mice were analysed, using state-of-the-art quantitative stereological methods as previously described (Herbach *et al.* 2007, Wanke *et al.* 1994).

**3.2.14.1 Quantification of the total pancreas volume ( $V_{\text{pan}}$ )**

The pancreas volume, including non-pancreatic tissue ( $V_{\text{Pan}0}$ ) was calculated by dividing the pancreas weight by its specific weight ( $1.10\text{mg}/\text{mm}^3$ ). To determine the pancreas volume corrected for non-pancreatic tissue ( $V_{\text{pan}}$ ), it is necessary to subtract non-pancreatic tissue from the observed volume. Therefore the complete cut surface of HE-stained pancreas sections was photographed (Leica DFC 320 Digital Camera System, Leica, Germany) at a 16-times final magnification (M 400 photomicroscope, Wild, Switzerland). For calibration, an object micrometer (Zeiss-Kontron, Germany) was photographed at the same magnification. All photographs were printed under equal conditions. Point counting was performed with a point counting grid photocopied onto an overhead transparency. The sum of points ( $\Sigma P$ ) hitting pancreatic tissue (endocrine and exocrine pancreas, including connective

tissue of the pancreas;  $\sum P_{\text{pan}}$ ), and the sum of points hitting the whole section ( $\sum P_{\text{section}}$ , including extra pancreatic tissue) were determined separately. To calculate the volume fraction of pancreatic tissue in the section ( $Vv_{(\text{pan/section})}$ ),  $\sum P_{\text{pan}}$  was divided by  $\sum P_{\text{section}}$ . The mean area corresponding to one point was determined using the Videoplan<sup>®</sup> image analysis system (Zeiss-Kontron, Germany) after calibration with the printed photograph of the object micrometer. The sum of cross-sectional areas of the pancreas ( $\sum A_{\text{pan}}$ ) was obtained by multiplying  $\sum P_{\text{pan}}$  with the calculated mean area, corresponding to 1 point on the point-counting grid. To calculate the total pancreas volume ( $V_{\text{pan}}$ ),  $V_{\text{pan}0}$  was multiplied with the volume fraction of pancreatic tissue ( $Vv_{(\text{pan/section})}$ ), in order to correct for non-pancreatic tissue.

#### 3.2.14.2 Determination of the relative pancreas weight

The relative weight of the pancreas (%) was calculated by dividing the pancreas weight by the body weight.

#### 3.2.14.3 Quantitative stereological parameters

Quantitative stereological analyses were carried out on sections immunostained for insulin as well as on sections simultaneously immunostained for glucagon, somatostatin and pancreatic polypeptide, using a Videoplan<sup>®</sup> image analysis system (Zeiss-Kontron, Germany) coupled to a light microscope (Orhoplan; Leitz, Germany) via a colour video camera (CCTV WVCD132E; Matsushita, Japan). Images were displayed on a colour monitor at a final magnification of x250. The sum of cross-sectional areas of islets,  $\beta$ -cells and non- $\beta$ -cells ( $\sum A_{\text{islets}}$ ,  $\sum A_{\beta\text{-cells}}$ ,  $\sum A_{\text{non-}\beta\text{-cells}}$ , respectively) were measured planimetrically by circling their outlines with a cursor on the digitising tablet of the image analysis system after calibration with an object micrometer (Zeiss, Germany). Volume fractions of the structures of interest (islets,  $\beta$ -cells, non- $\beta$ -cells) in the reference compartments (pancreas, islets) were calculated according to the principle of Delesse:

$$A_A = V_V$$

$A_A$ = Area fraction of a target structure in a reference compartment

$V_V$ = Estimated volume fraction of a target structure in a reference compartment

The volume density of islets in the pancreas ( $Vv_{(islets/pan)}$ ) was calculated by dividing  $\sum A_{islets}$  by  $\sum A_{pan}$ .

The total volume of islets in the pancreas ( $V_{(islets,pan)}$ ) was attained by multiplying  $Vv_{(islets/pan)}$  with  $V_{pan}$ .

$\sum A_{\beta-cells}$  was calculated from  $\sum A_{islet} - \sum A_{non-\beta-cells}$ . The volume density of  $\beta$ -cells ( $Vv_{(\beta-cells/islet)}$ ) and non- $\beta$ -cells ( $Vv_{(non-\beta-cells/islet)}$ ) in the islets was calculated by dividing  $\sum A_{\beta-cells}$  and  $\sum A_{non-\beta-cells}$ , respectively, by  $\sum A_{islet}$ . Moreover, the volume density of insulin positive cells in the islets ( $Vv_{(ins-cells/islet)}$ ) was established by dividing  $\sum A_{ins-cells}$  by  $\sum A_{islet}$ .

The total  $\beta$ -cell volume ( $V_{(\beta-cells, islet)}$ ) and the total non- $\beta$ -cell volume ( $V_{(non-\beta-cells, islet)}$ ) in the islets was obtained by multiplying  $Vv_{(\beta-cells/islet)}$  and  $Vv_{(non-\beta-cells/islet)}$ , respectively, with  $V_{(islets, pan)}$ .

The  $\beta$ -cell/non- $\beta$ -cell ratio was calculated by dividing  $V_{(\beta-cells, islet)}$  by  $V_{(non-\beta-cells, islet)}$ .

The volume density ( $Vv_{(isol.\beta-cells/pan)}$ ) and total volume ( $V_{(isol.\beta-cells, pan)}$ ) of isolated  $\beta$ -cells in the pancreas was determined using sections immunostained for insulin. Isolated  $\beta$ -cells were defined as single  $\beta$ -cells or small clusters of  $\beta$ -cells that were not contained within established islets (up to four  $\beta$ -cell nuclear profiles) (Bonner-Weir *et al.* 2008). The area of isolated  $\beta$ -cell profiles was determined planimetrically using an image analysing system, consistent of a light microscope (BX41, Olympus, Germany), a colour video camera (DP72, Olympus, Germany) and the software new CAST<sup>TM</sup> (computer assisted stereological toolbox, Visiopharm<sup>®</sup>, Denmark). The sum of cross-sectional areas of isolated  $\beta$ -cell profiles ( $\sum A_{isol.\beta-cells}$ ) was quantified by circling their outlines with the cursor of the image analysis system.

The volume density of isolated  $\beta$ -cells in the pancreas ( $Vv_{(isol.\beta-cells/pan)}$ ) was calculated by dividing  $\sum A_{isol.\beta-cells}$  by  $\sum A_{pan}$ . The total volume of isolated  $\beta$ -cells ( $V_{(isol.\beta-cells, pan)}$ ) was generated by multiplying ( $Vv_{(isol.\beta-cells/pan)}$ ) by  $V_{pan}$ .

### 3.2.15 Transmission electron microscopy (TEM)

Pancreatic islets of 190-day-old mice were investigated electron microscopically. A piece of 2 mm<sup>3</sup> from the splenic end of the pancreas (see 3.2.12) was fixed by immersion in 3% glutaraldehyde in Sørensen's phosphate buffer. After fixation for about 2 hours, tissue samples were washed at least 3 times in washing solution (0.2 M buffered saccharose solution) until no glutaraldehyde could be smelled

anymore. Subsequently, the pancreas was fixed for two hours at 4°C in a fixative solution for Epon embedding, containing 2% osmium tetroxide. After washing 3 times in washing solution, pancreas samples were dehydrated by an ascending acetone series (Roth, Germany). Pancreatic tissue was incubated in a solution containing equal amounts of 100% acetone and glycid ether 100 (Serva, Germany) for 1 hour at room temperature, followed by incubation in glycid ether 100 (2 x 30 minutes, room temperature). Samples were embedded in glycid ether-embedding mixture in dried gelatine capsules (Plano, Germany). Polymerization was carried out at 60°C for 48 hours.

Epon blocks were trimmed, using a Reichert-Jung TM60 milling machine (Leica, Germany). Semi-thin sections (0.5 µm) were produced with a Reichert-Jung Ultracut E microtome (Leica, Germany), and stained with toluidine blue and Safranin O. After identifying the islets within the semi-thin sections via light microscopy, and marking their positions in a drawing, the areas of the Epon blocks containing islets were trimmed, and ultra-thin sections (70 - 80 nm) were prepared (Reichert-Jung Ultracut E, Leica, Germany). The sections were mounted on coated copper rings, contrasted with uranyl acetate and lead citrate (Reynolds 1963), and examined using an EM 10 transmission electron microscope (Zeiss, Germany).

## Materials

### Sorensen's phosphate buffer

Solution A:	192ml
Solution B:	808ml

#### Solution A:

Potassium dihydrogen phosphate (KH <sub>2</sub> PO <sub>4</sub> ; Neolab, Germany)	4.539g
Distilled water	500ml

#### Solution B:

Sodium phosphate dibasic dihydrate (Na <sub>2</sub> HPO <sub>4</sub> ·2H <sub>2</sub> O; Neolab, Germany)	11.876g
Distilled water	1000ml

### Washing solution

D(+)Saccharose (Neolab, Germany)	6.84g
Sorensen's phosphate buffer	100ml
1% Merthiolat solution	0.1ml

Merthiolat solution	
Ethylmercury thiosalicylic acid Na-salt (SERVA, Germany)	1g
Distilled water	100ml
<b>Fixative solution for Epon embedding</b>	
D(+)-Saccharose (?)	0.45g
0.1m HCl (Merck, Germany)	2ml
Veronalacetate buffer	2ml
2% Osmium tetroxide solution	5ml
Distilled water	1ml
Veronal-acetate buffer:	
5.5-Diethylbarbituric acid Na-salt (Merck, Germany)	1.47g
Sodium acetate (C <sub>2</sub> H <sub>3</sub> NaO <sub>2</sub> ; Merck, Germany)	0.97g
Distilled water	50ml
adjust to pH 10.3	
2% Osmium tetroxide solution	
Osmium tetroxide (OsO <sub>4</sub> ; Chempur®, Germany)	1g
Distilled water	50ml
<b>Ascending acetone series (Roth, Germany):</b>	
Acetone 50%: 3 x 2 minutes, 4 °C	
Acetone 70%: 2 x 10 minutes, 4 °C	
Acetone 90%: 2 x 10 minutes, 4 °C	
Acetone 100%: 2 x 20 min, 4 °C	
Acetone 100%: 1 x 20 min, room temperature)	
<b>Osmium tetroxide 2%</b>	
Osmium tetroxide (OsO <sub>4</sub> , Merck, Germany):	1 g
Distilled water:	50 ml
<b>Glycid ether embedding mixture</b>	
Solution A:	70 ml
Solution B:	130 ml
2,4,6-tris-(dimethylaminomethyl) phenol (Serva, Germany):	3 ml
Solution A:	
glycid ether 100 (Serva, Germany):	62 ml
2-dodecenyl succinic acid anhydride (Serva, Germany):	100 ml
Solution B:	
glycid ether 100 (Serva, Germany):	100 ml
methyl nadic anhydride (Serva, Germany):	89 ml

**Staining protocol:** semi-thin sections: Toluidine blue and Safranin O

## Toluidin blue:

Di-sodiumtetraborate (Borax, Merck, Germany):	1 g
Toluidin blue (Roth, Germany):	1 g
Distilled water:	100 ml

Dissolve Borax in distilled water, add Toluidin blue and stir for approximately 2 hours. Filter before use. Stain sections for 45 - 60 seconds on a heating plate (Meditel, Germany; 55°C), rinse with distilled water and let dry.

## Safranin O:

Di-sodium tetraborate (Borax, Merck, Germany):	1 g
Safranin O (Chroma, Germany):	1 g
Saccharose (Merck, Germany):	40 g
Formaldehyde 37% ( Roth, Germany):	2-3 drops
Distilled water:	100ml

Dissolve Borax in distilled water, add Safranin O and saccharose and stir for approximately 2 hours. The next day, add formaldehyde. Filter before use.

Stain sections for 15 seconds on a heating plate (Meditel, Germany, 55°C), rinse with distilled water and let dry. Cover the sections with coverslips (Menzel GmbH & Co KG, Germany) using Histofluid (Superior<sup>®</sup>, Germany).

**Contrasting ultra-thin sections with uranyl acetate and lead citrate**  
(Reynolds 1963)

## Uranyl acetate (Reynolds):

Uranyl acetate (Merck, Germany):	1 g
Redistilled water:	50 ml

Swing carefully, don't stir. Filter before use.

Stain sections for 30 minutes at room temperature.

## Lead acetate (Reynolds):

Sodium citrate 1M (Merck, Germany):	6 ml
Lead nitrate solution 1 M (Merck, Germany):	4 ml
Sodium hydrate solution 1 M (Merck, Germany):	8 ml
Redistilled water:	32 ml

Mix sodium citrate with redistilled water while gently stirring. Add lead nitrate drop by drop, the solution gets milky (precipitation). Use sodium hydrate to clear the solution. Filter before use. Stain sections for 10 minutes at room temperature.

## 4 Results

### 4.1 Clinical investigations

#### 4.1.1 Body weight

From the age of 21 days onwards, the body weight of randomly fed mice was determined in regular intervals. At the age of 21 days (data not shown) and 30 days, there were no significant differences between the four groups. From 30 days after ovariectomy/pellet implantation (arrow) onwards, estradiol-treated ovariectomized mutant mice (mt-ovx-E2) weighed significantly less than mice of the three other groups. Non-/placebo-treated ovariectomized mutant mice (mt-ovx-nt/p) were significantly heavier than mice of all other groups at the age of 60 days (Figure 4.1).

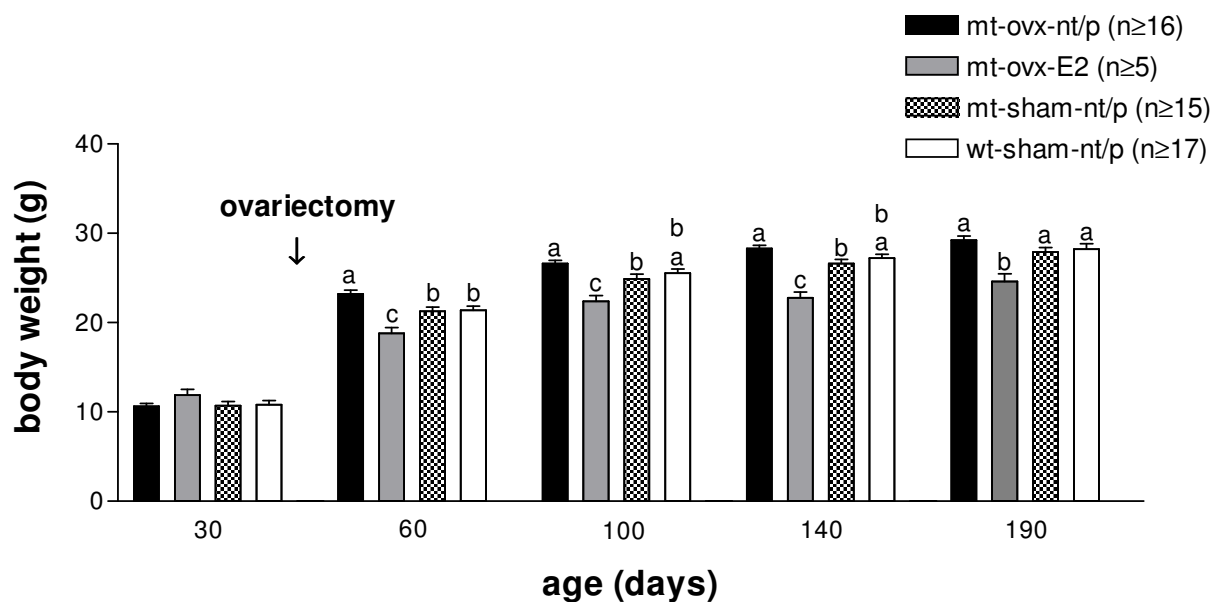


**Figure 4.1: Randomly fed body weights**

Figure shows body weights of randomly fed non-/placebo-treated ovariectomized mutant mice (mt-ovx-nt/p), non-/placebo-treated sham-operated mutant mice (mt-sham-nt/p), estradiol-treated ovariectomized mutant mice (mt-ovx-E2) as well as non-/placebo-treated sham-operated wild-type mice (wt-sham-nt/p). At the age 30 days, the 4 groups were just different in genotype (mutant and wild-type mice) because ovariectomy/pellet implantation was accomplished at the age of 30 days (arrow).

Data are means  $\pm$  SEM; a-c: different superscripts show significant differences ( $p < 0.05$ ); (n): number of animals investigated

## 4.1.2 Blood glucose concentration

### 4.1.2.1 Randomly fed mice

Randomly fed blood glucose concentrations were measured in approximately 4-week intervals, starting with weaning at an age of 21 days. At weaning, there were no significant differences between the four groups. Five days after ovariectomy/pellet implantation mt-ovx-nt/p mice exhibited a progressive diabetic phenotype with increasing blood glucose levels, reaching  $359 \pm 126$  mg/dl at 160 days of age. Moreover, mt-ovx-nt/p mice showed significantly higher blood glucose concentrations than mt-ovx-E2 as well as wild-type mice at all investigated time-points and from the age of 60 days onwards, also as compared to mt-sham-nt/p mice. Mt-ovx-E2 mice showed significantly lower blood glucose concentrations at each time point after ovariectomy as compared to mt-ovx-nt/p and mt-sham-nt/p mice, and almost similar blood glucose concentrations as wild-type mice. The blood glucose levels of mt-ovx-E2 and wild-type mice remained stable during the investigation period, ranging from approximately 110 to 140mg/dl. Mt-sham-nt/p mice featured significantly higher blood glucose concentrations than wild-type mice from day 35 up to day 190 (Figure 4.2).

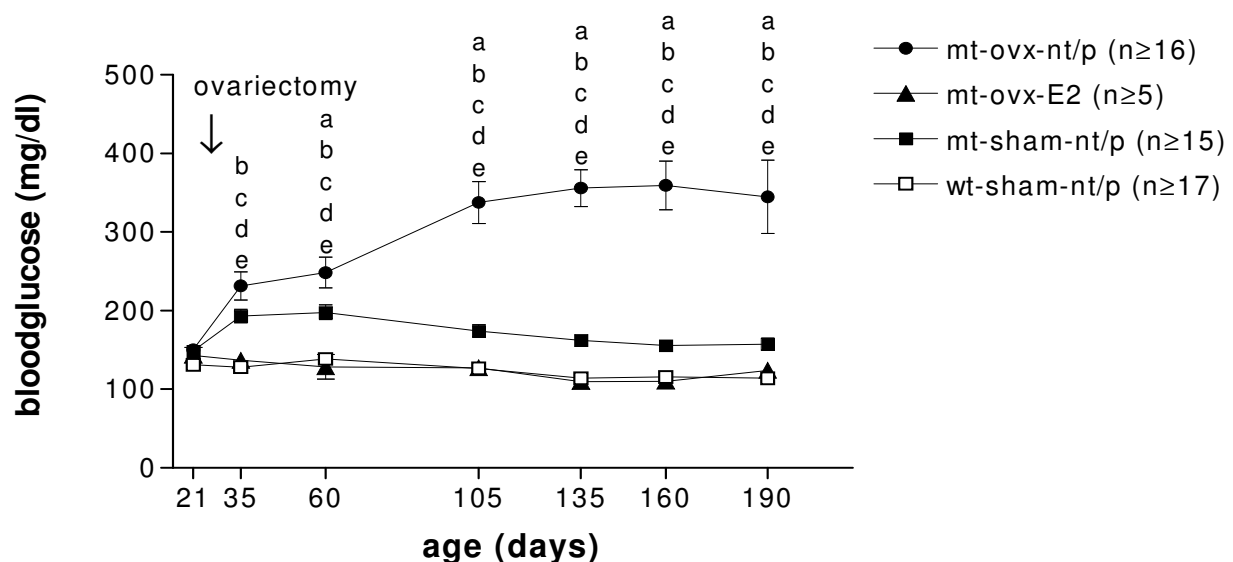


**Figure 4.2: Randomly fed blood glucose levels between 21 and 190 days**

Non-/placebo-treated ovariectomized mutant mice (mt-ovx-nt/p) show a progressive diabetic phenotype. Blood glucose concentrations of E2-treated ovariectomized mutant mice (mt-ovx-E2) remain stable and there is no significant difference as compared to wild-type mice (wt-sham-nt/p).

Data are means  $\pm$  SEM; a, b, c, d, e:  $p < 0.05$ : a) mt-ovx-nt/p vs. mt-sham-nt/p; b) mt-ovx-nt/p vs. wt-sham-nt/p; c) mt-sham-nt/p vs. wt-sham-nt/p; d) mt-ovx-E2 vs. mt-ovx-nt/p; e) mt-ovx-E2 vs. mt-sham-nt/p;  $\downarrow$  ovariectomy/pellet implantation (30 days of age); (n): number of animals investigated

#### 4.1.2.2 Fourteen-hours fasted mice

Fasting blood glucose concentrations were examined approximately every 4 weeks, starting at the age of 50 days. Non-/placebo-treated ovariectomized mutant mice (mt-ovx-nt/p) exhibited a clinical manifest diabetic phenotype with increasing fasting blood glucose concentrations, reaching  $200 \pm 76$  mg/dl at an age of 120 days and exhibited significantly higher blood glucose concentrations than all other groups during the complete investigation period. Non-/placebo-treated sham-operated mutant mice (mt-sham-nt/p) also exhibited significantly higher blood glucose concentrations as compared to E2-treated ovariectomized mutant (mt-ovx-E2) and wild-type mice (wt-sham-nt/p) from an age of 50 days up to 155 days. Mt-ovx-E2 mice showed significantly lower blood glucose concentrations from 50 to 155 days of age, as compared to mt-ovx-nt/p and mt-sham-nt/p mice. From an age of 70 to 155 days, the fasting blood glucose of E2-treated mutants was even significantly lower as compared to wild-type mice (Figure 4.3).

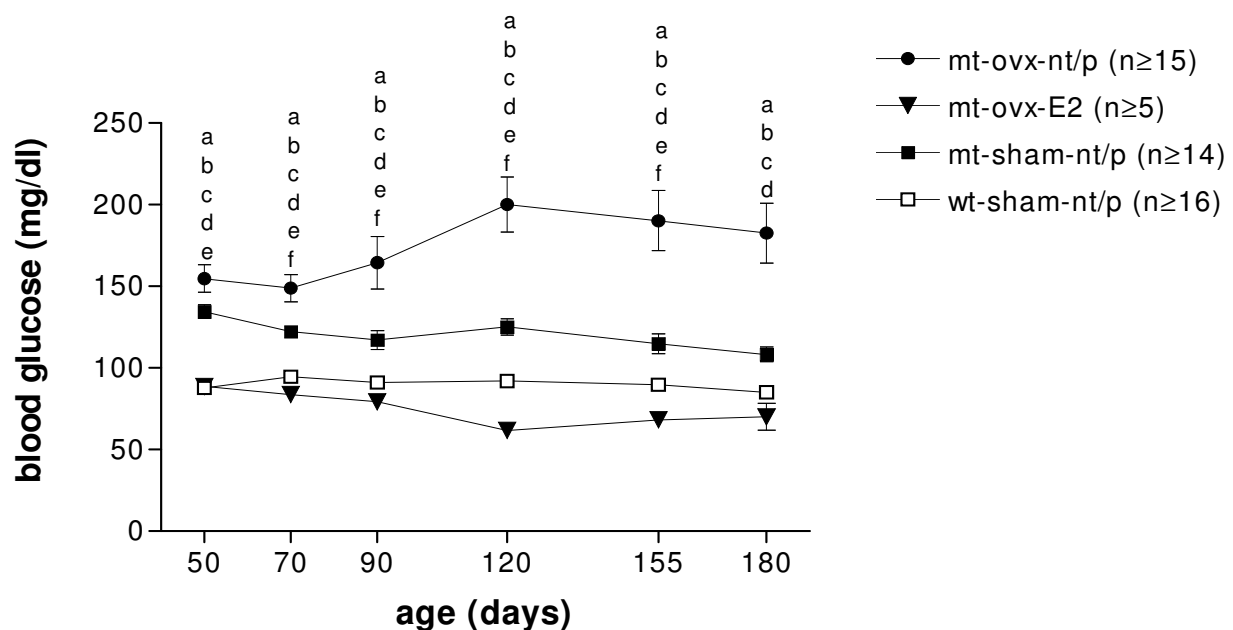


**Figure 4.3: 14 hours fasted blood glucose levels between 50 and 180 days of age**

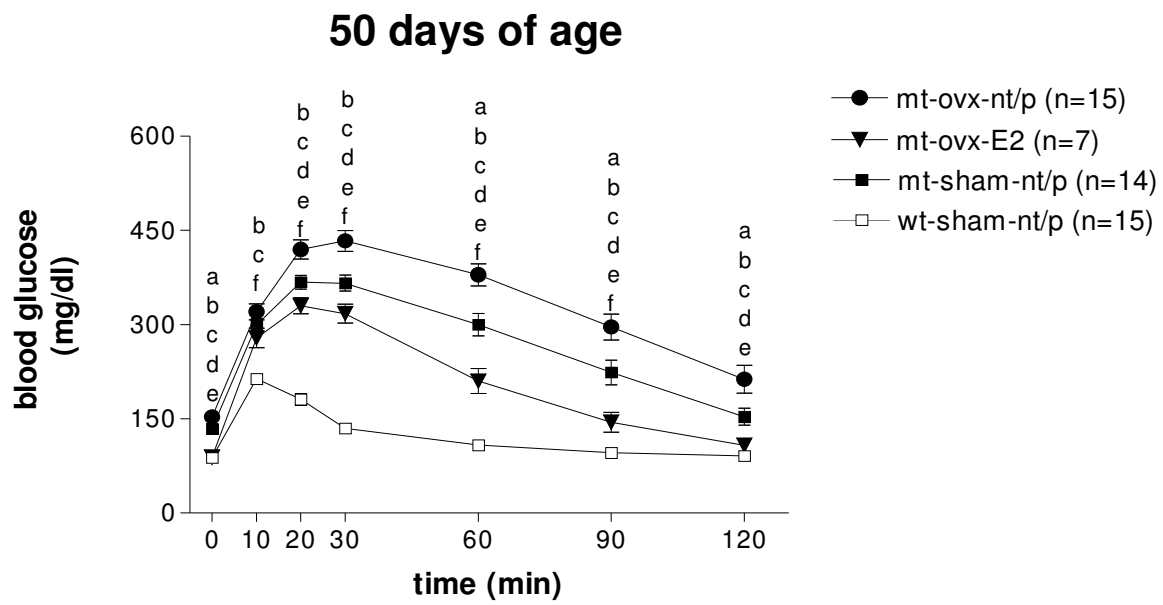
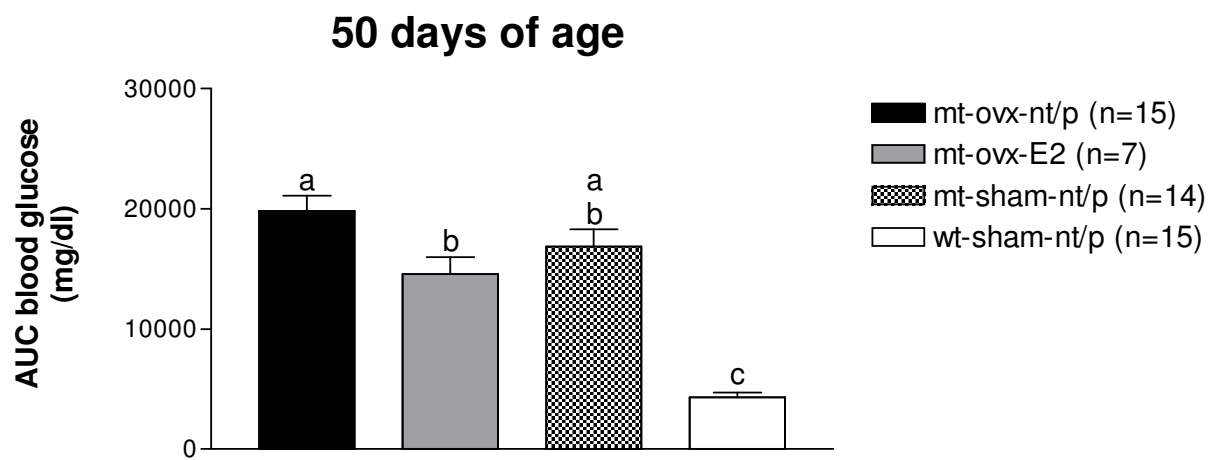
Non-/placebo-treated ovariectomized mutant mice (mt-ovx-nt/p) show higher blood glucose levels than the three other groups. Blood glucose concentrations of estradiol-treated ovariectomized mutant mice (mt-ovx-E2) are lower than those of the two other mutant groups (mt-ovx-nt/p and mt-sham-nt/p) and even lower than those of wild-type mice (wt-sham-nt/p).

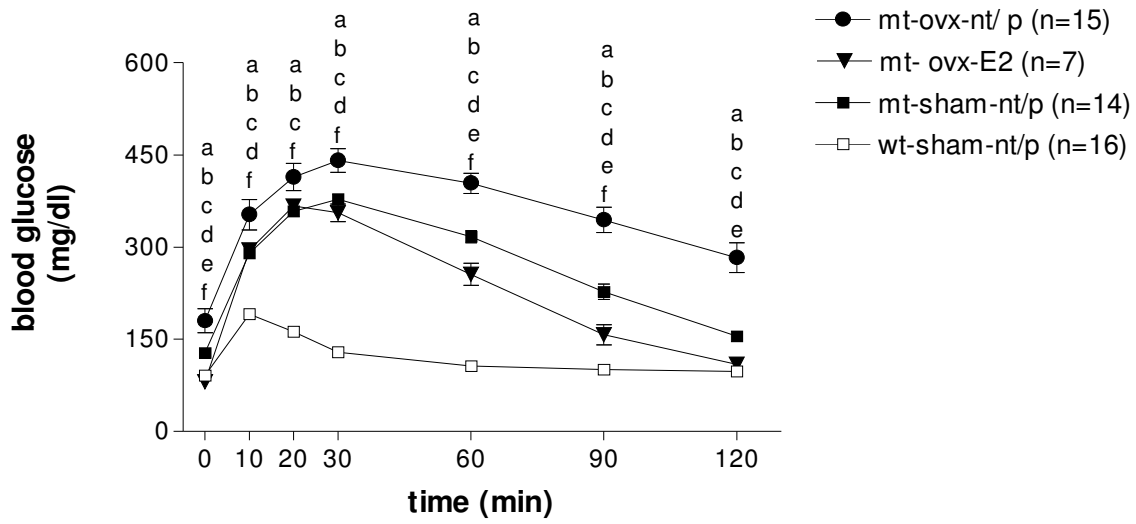
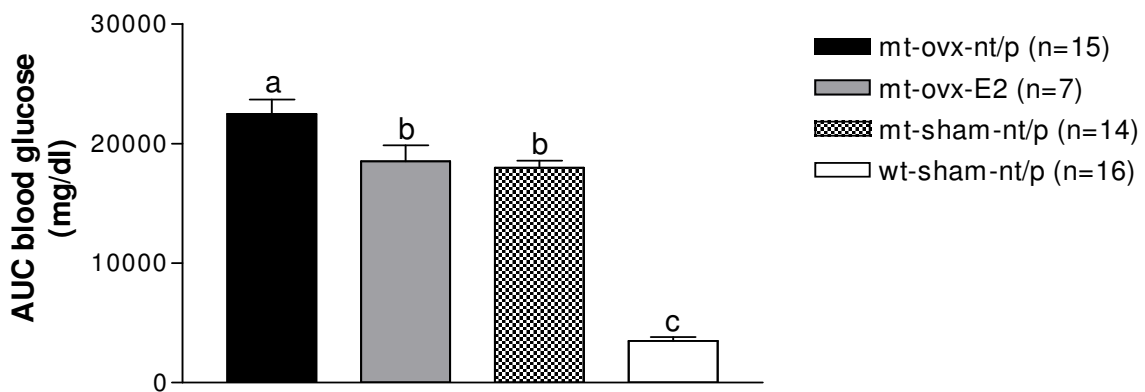
Data are means  $\pm$  SEM; a, b, c, d, e, f:  $p < 0.05$ : a) mt-ovx-nt/p vs. mt-sham-nt/p; b) mt-ovx-nt/p vs. wt-sham-nt/p; c) mt-sham-nt/p vs. wt-sham-nt/p; d) mt-ovx-E2 vs. mt-ovx-nt/p; e) mt-ovx-E2 vs. mt-sham-nt/p; f) mt-ovx-E2 vs. wt-sham-nt/p; (n): number of animals investigated

### 4.1.3 Oral glucose tolerance test (OGTT)

Oral glucose tolerance tests were performed at an age of 50, 90 and 180 days of life (Figure 4.4, A1 – C1). Non-/placebo-treated ovariectomized mutant mice (mt-ovx-nt/p) featured significantly higher blood glucose concentrations as compared to wild-type mice (wt-sham-nt/p) as well as to E2-treated ovariectomized mutant mice (mt-ovx-E2) during all OGTTs (Figure 4.4, A1 – C1).

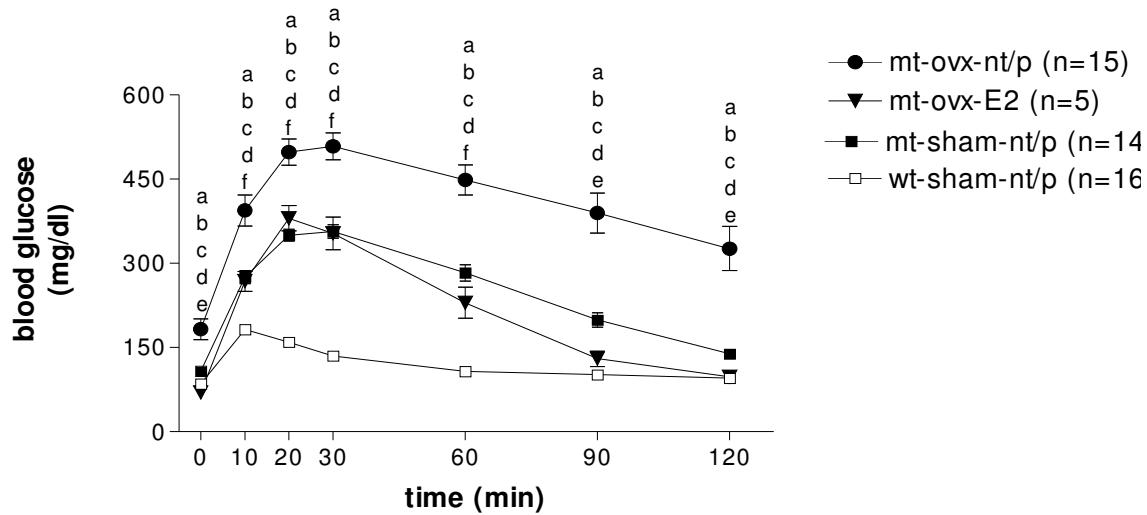
At the age of 90 and 180 days (Figure 4.4, B1 and C1), mt-ovx-nt/p mice also showed significantly higher blood glucose concentrations as compared to mt-sham-nt/p mice. Therefore, the corresponding areas under the blood glucose curves ( $AUC_{\text{blood glucose}}$ ) of mt-ovx-nt/p mice were also significantly higher as compared to the other groups (Figure 4.4, A2 – C2). Mt-ovx-E2 mice showed lower blood glucose concentrations as compared to mt-sham-nt/p mice, in the second part of the test (starting at 20 min with 50 days, 60 min with 90 days and 90 min with 180 days), however, the corresponding area under the glucose curve showed no significant difference between the two groups. In wild-type mice, blood glucose values already declined between 10 and 20 minutes after glucose challenge, in estradiol-treated mice between 20 and 30 minutes, and in the mice of the two other mutant groups primal between 30 and 60 minutes (90 and 180 days of life). The results show that ovariectomy diminishes glucose tolerance in female mutant mice and that estrogen-replacement therapy can restore glucose tolerance at least to the levels of sham-operated mutant mice (Figure 4.4).

**A1****A2**

**B1****90 days of age****B2****90 days of age**

## C1

## 180 days of age



## C2

## 180 days of age

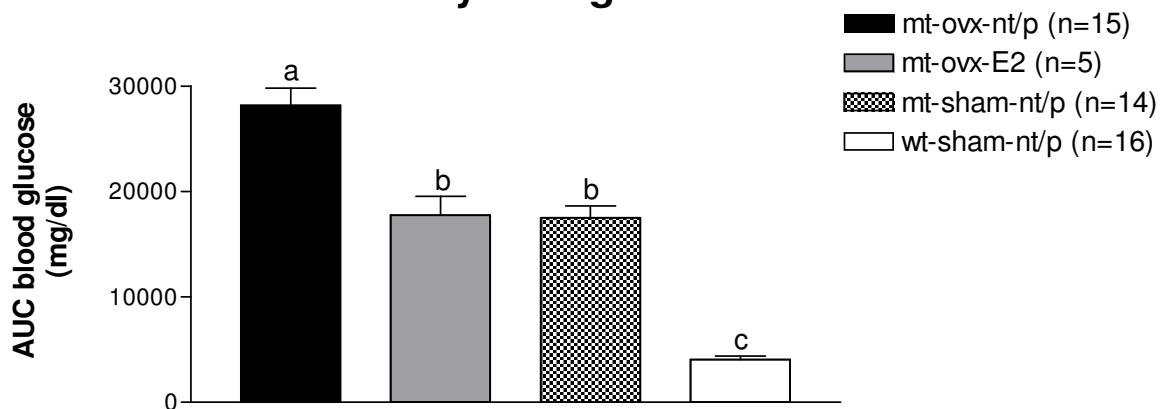


**Figure 4.4 (A-C): Oral glucose tolerance tests (OGTT) at 50, 90 and 180 days of age (A1) – (C1): Blood glucose levels during OGTT**

Non-/placebo-treated ovariectomized mutant mice (mt-ovx-nt/p) present significantly higher blood glucose levels as compared to E2-treated mice (mt-ovx-E2) at almost every time point of the test, irrespective of age and sampling. Blood glucose concentrations of mt-ovx-E2 mice decline later than those of wild-type mice (wt-sham-nt/p), but earlier than those of mt-ovx-nt/p and mt-sham-nt/p mice. a, b, c, d, e, f: a) mt-ovx-nt/p vs. mt-sham-nt/p; b) mt-ovx-nt/p vs. wt-sham-nt/p; c) mt-sham-nt/p vs. wt-sham-nt/p; d) mt-ovx-E2 vs. mt-ovx-nt/p; e) mt-ovx-E2 vs. mt-sham-nt/p; f) mt-ovx-E2 vs. wt-sham-nt/p;  $p < 0.05$

**(A2) – (C2): Area under blood glucose curve (AUC<sub>blood glucose</sub>)**

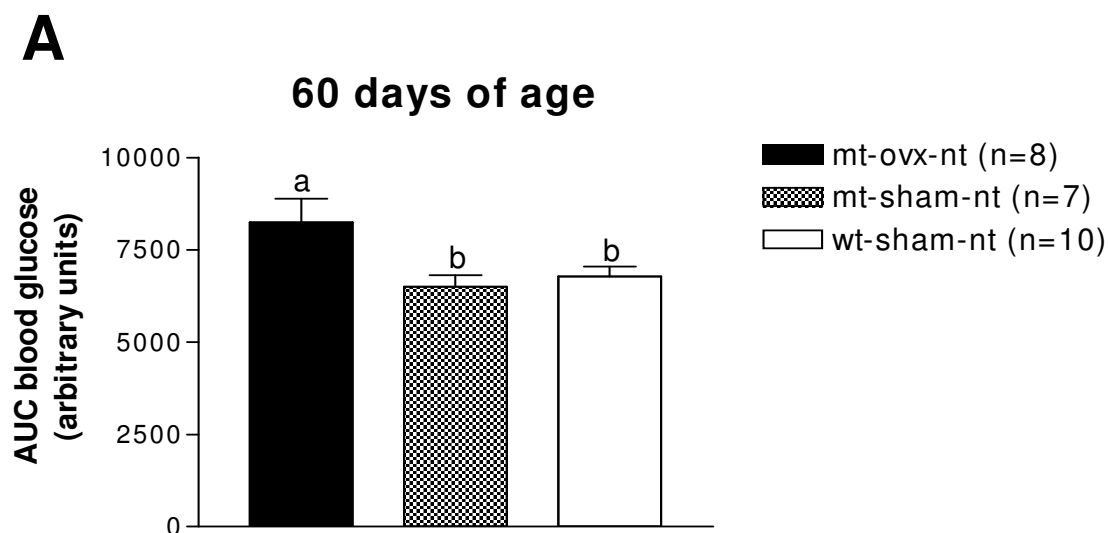
The area under blood glucose curve is significantly increased in mt-ovx-nt/p mice as compared to all three other groups at an age of 90 (B2) and 180 days (C2). There is no significant difference between the AUC<sub>blood glucose</sub> of mt-ovx-E2 and mt-sham-nt/p mice. Wild-type mice (wt-sham-nt/p) exhibit a significantly smaller area under their glucose curve than all three other groups, irrespective of age.

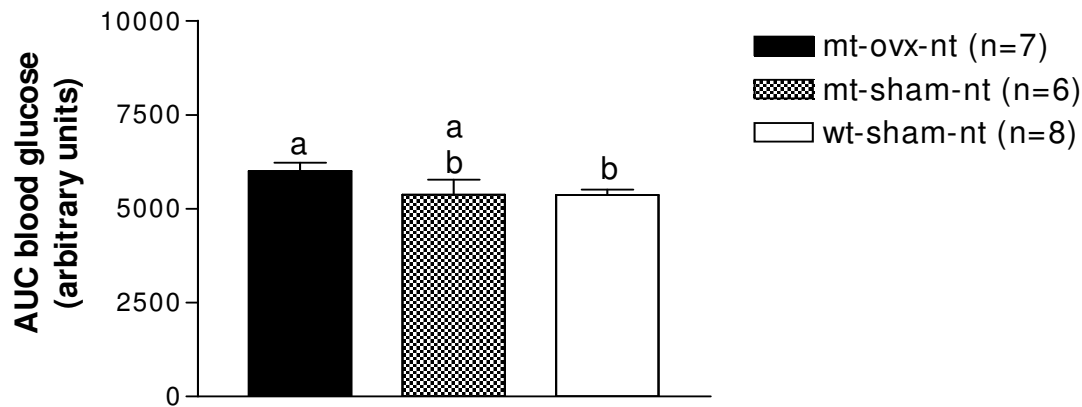
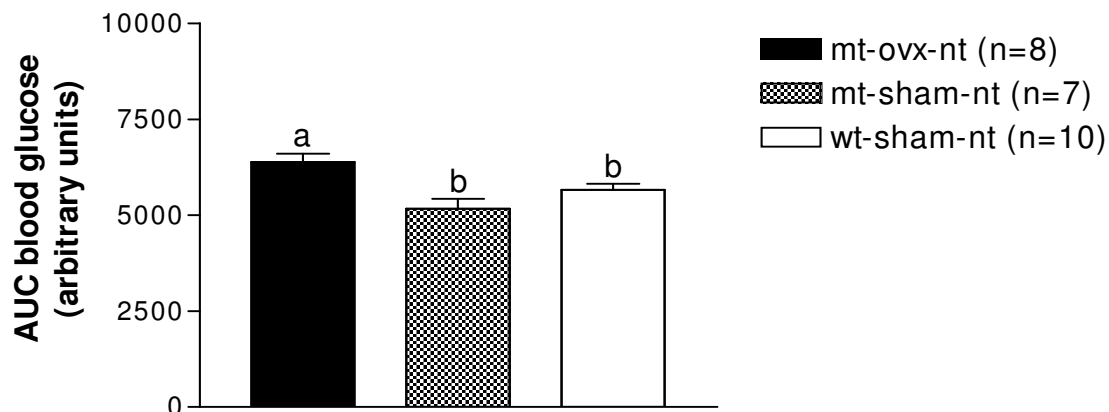
a-c: different letters show significant differences ( $p < 0.05$ );

Data are means  $\pm$  SEM; (n): number of animals investigated

#### 4.1.4 Intraperitoneal insulin tolerance test (ipITT)

ipITTs were performed at an age of 60 (A), 100 (B) and 187 (C) days of life to investigate insulin sensitivity of ovariectomized or sham-operated mutant and wild-type mice that were not supplied with E2 or placebo pellets. Ten, 20, 30, 60 and 90 minutes after intraperitoneal insulin injection, blood glucose concentration was determined. The percentage decrease from basal value ( $T_0=100\%$ ) after insulin injection was calculated (data not shown). The corresponding areas under these curves are shown in Figure 4.5. At an age of 60 and 187 days, ovariectomized mutant mice (mt-ovx-nt) exhibited a significantly higher  $AUC_{\text{blood glucose}}$  than sham-operated mutant mice (mt-sham-nt) and wild-type mice (wt-sham-nt). At an age of 100 days, ovariectomized mutant mice showed a significantly higher area under blood glucose curve than wild-type mice. There existed no significant differences between sham-operated mutant mice and wild-type mice at all time points investigated. These results indicate that ovariectomy worsens insulin sensitivity in female mutant mice, whereas sham-operated mutant mice show similar insulin sensitivity as wild-type mice (Figure 4.5).



**B****100 days of age****C****187 days of age**

**Figure 4.5 (A-C): Area under the curve of the percentage blood glucose decrease from basal value ( $AUC_{\text{blood glucose}}$ ) of the ipITT at the age of 60 (A), 100 (B) and 187 (C) days**

Data are means  $\pm$  SEM; a-b: different letters show significant differences ( $p < 0.05$ ); (n): number of animals investigated

#### 4.1.5 Serum insulin concentration

To examine basal and glucose induced insulin secretion, serum insulin concentrations were measured before and ten minutes after oral glucose application during oral glucose tolerance tests at an age of 90 and 180 days (see 4.3). At an age of 90 days, basal serum insulin concentrations of 14-hours fasted mice (T0) showed no significant differences between the 4 groups. At an age of 180 days, the basal

serum insulin concentrations of mt-ovx-E2 mice were significantly lower than those of mt-ovx-nt/p mice and mt-ovx-nt/p mice showed higher insulin levels than mt-sham-nt/p mice. Ten minutes after glucose application (T10), all mutant mice showed significantly lower serum insulin concentrations as compared to wild-type mice, irrespective of the age at sampling (Figure 4.6).

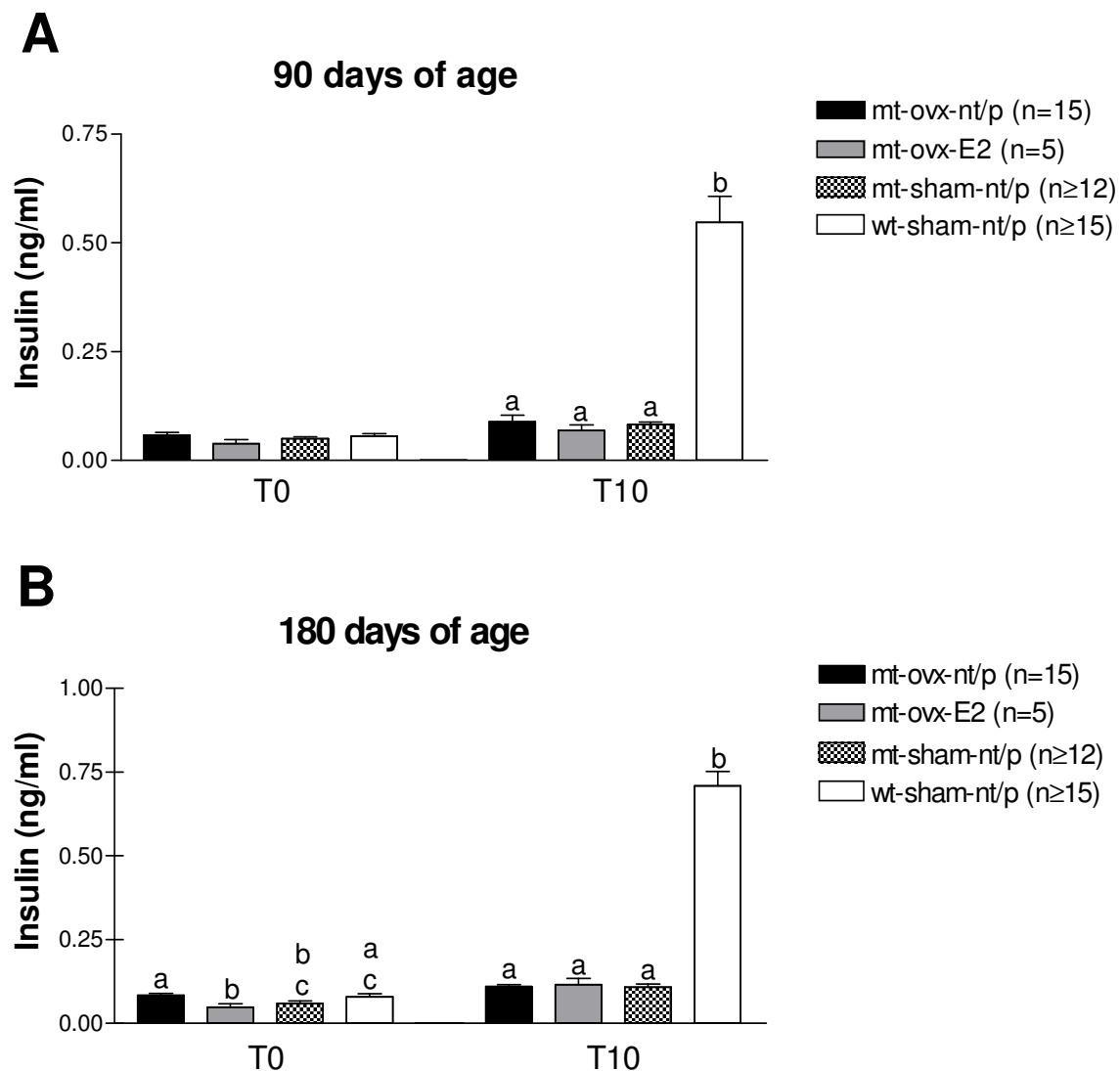


**Figure 4.6: Serum insulin concentrations 14 hours-fasted (T0) and 10 minutes after oral glucose challenge (T10) of 90 (A)- and 180 (B)-day-old mice**

The serum insulin concentrations 10 minutes after glucose challenge of the three mutant groups are significantly lower compared to wild-type mice at both time points investigated.

Data are means  $\pm$  SEM; a-c: different letters show significant differences ( $p < 0.05$ ); (n): number of animals investigated

Figure 4.7 shows the increase of serum insulin concentrations as x-fold increase from basal concentrations (T0). At 90 days of life, wild-type mice showed a more than 10-fold increase whereas all three mutant groups only demonstrated a 2- to 3-fold increase in insulin levels. Ninety days later, wild-type mice showed again an increase of about 10-fold as compared to basal values. Mt-ovx-nt/p mice showed the lowest increase (1.4-fold) as compared to the other groups, whereas mt-ovx-E2 mice demonstrated the highest increase (2.5-fold) of insulin secretion among the three mutant groups (Figure 4.7).

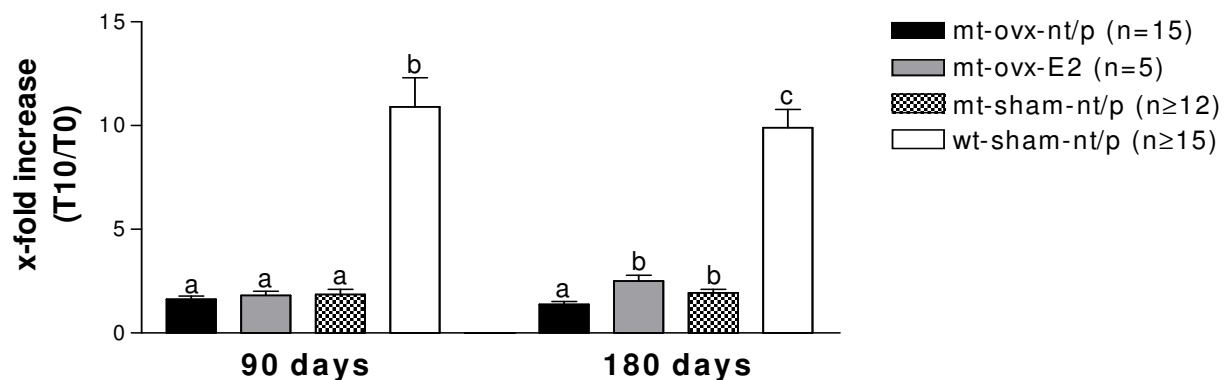


**Figure 4.7: Increase of serum insulin concentrations 10 minutes after oral glucose challenge of 90- and 180-day-old mice**

The serum insulin concentrations 10 minutes after glucose challenge (T10) were divided by the insulin concentrations of fasted mice (T0). Wild-type mice show a significantly higher increase of insulin levels than mice of the three other groups at both time points. Mt-ovx-nt/p mice both times demonstrate the lowest increase of insulin levels.

Data are means  $\pm$  SEM; a-c: different letters show significant differences ( $p < 0.05$ ); (n): number of animals investigated

#### 4.1.6 Serum estradiol concentration

Serum estradiol concentrations have been measured at 65, 105, and 160 days of life. The sensitivity of the ELISA-Kit often was not high enough to detect the low estradiol concentrations of ovariectomized mutant mice as well as of sham-operated mutant mice and wild-type mice (also depending on sexual cycles of the intact sham-operated mice) and estradiol levels ranged from 0 to 10 pg/ml (data not shown). Therefore, the test was used as a control for estradiol treatment. Figure 4.8 shows the  $17\beta$ Estradiol concentration of 60-, 105- and 160-day-old estradiol-treated ovariectomized mutant mice. The first pellet was applied at an age of 30 days and

pellets were replaced at an age of 115 days (as recommended by the manufacturer). Thirty days after the implantation of the first estradiol pellet (60 days of life), serum estradiol concentrations were the highest. At an age of 105 days, 10 days before changing the pellets, serum estradiol levels had declined by 75 % as compared to those of 60-day-old E2-treated mice. Forty-five days after replacing the pellets, estradiol levels lie between the latter to values (Figure 4.8). The results show that, although the amount of  $17\beta$ Estradiol released from the pellets decreased with time, serum estradiol levels were at least 10-times higher in E2-treated as compared to non-/placebo-treated mice.

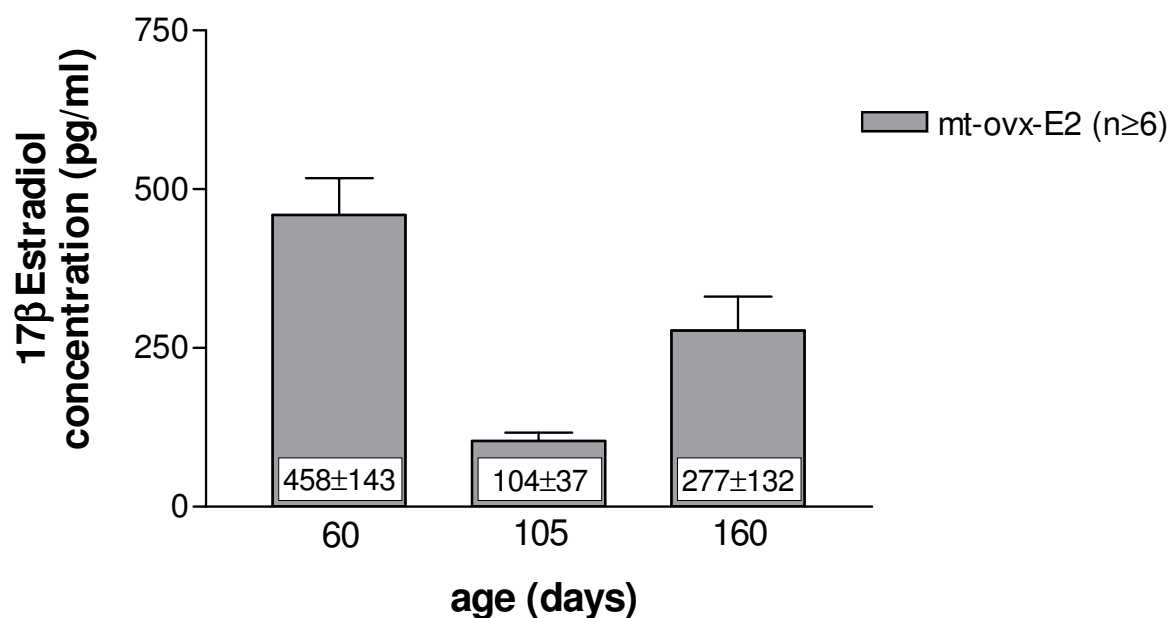


**Figure 4.8: Serum  $17\beta$ Estradiol levels of estradiol-treated ovariectomized mutant mice (mt-ovx-E2) at an age of 60, 105 and 160 days of life**

The serum  $17\beta$ Estradiol levels are the highest at 60 days of life (30 days after first pellet implantation) and decrease until 85 days after first implantation (105 days of age). (n): number of animals investigated

## 4.2 Beta cell function indices

The homeostasis model assessments of baseline insulin secretion (HOMA B) and of insulin resistance (HOMA IR) were calculated by means of fasting blood glucose and serum insulin levels obtained in the course of OGTTs at 50, 90 and 180 days of age. Moreover, Quicki (quantitative insulin-sensitivity check index) and FGIR (fasting glucose-to-insulin ratio) were calculated with the obtained data.

#### 4.2.1 HOMA B and HOMA IR

The HOMA B was significantly reduced in non-/placebo-treated ovariectomized (mt-ovx-nt/p) and sham-operated mutant mice (mt-sham-nt/p), as compared to wild-type mice (wt-sham-nt/p) at the age of 50, 90 and 180 days. Estradiol-treated ovariectomized mutant mice (mt-ovx-E2) showed a higher HOMA B as compared to the two non-/placebo-treated mutant mice groups (mt-ovx-nt/p and mt-sham-nt/p) at all examined time points, but only at the age of 90 days, the difference reached statistical significance (Figure 4.9).

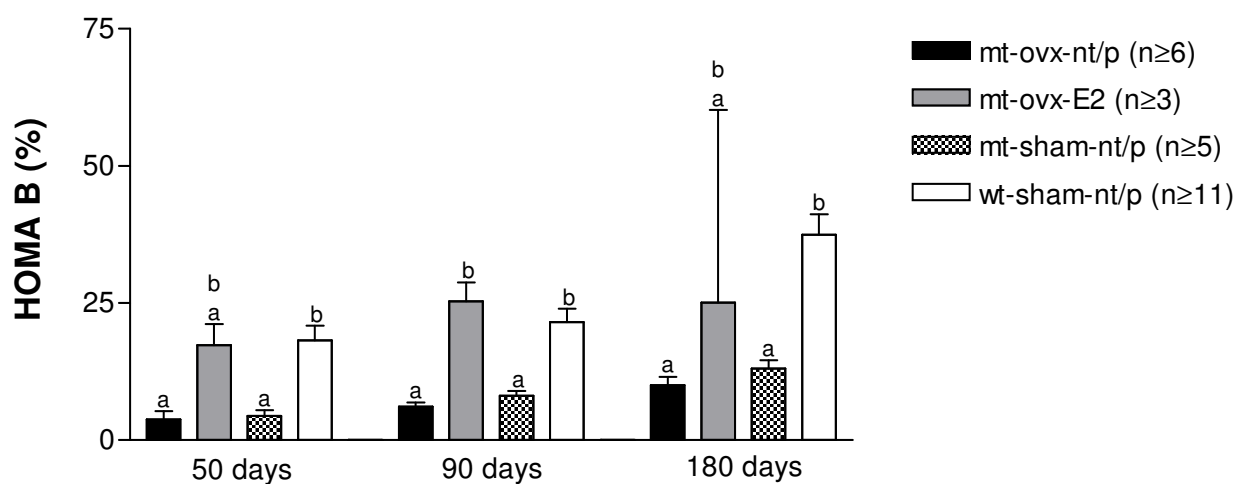


**Figure 4.9: Homeostasis model assessments of baseline insulin secretion (HOMA B) of 50-, 90- and 180-day-old mice**

Non-/placebo-treated ovariectomized (mt-ovx-nt/p) and sham-operated (mt-sham-nt/p) mutant mice demonstrate a lower baseline insulin secretion than estradiol-treated ovariectomized mutant mice (mt-ovx-E2) and wild-type mice (wt-sham-nt/p) at all time points investigated.

Data are means  $\pm$  SEM; a-b: different letters show significant differences ( $p < 0.05$ ); (n): number of animals investigated

At the age of 50 days, the insulin resistance index (HOMA IR) was not significantly different in mice of the 4 groups. At the age of 90 and 180 days, mt-ovx-nt/p mice showed a higher HOMA IR as compared to mice of the 3 other groups. This difference was significant as compared to mt-ovx-E2 mice (3.4 fold higher) and wild-type mice (2.4 fold higher) at the age of 90 days. Moreover, mt-ovx-E2 mice exhibited a significantly lower HOMA IR than mt-sham-nt/p mice (1.9 fold lower) (Figure 4.10).

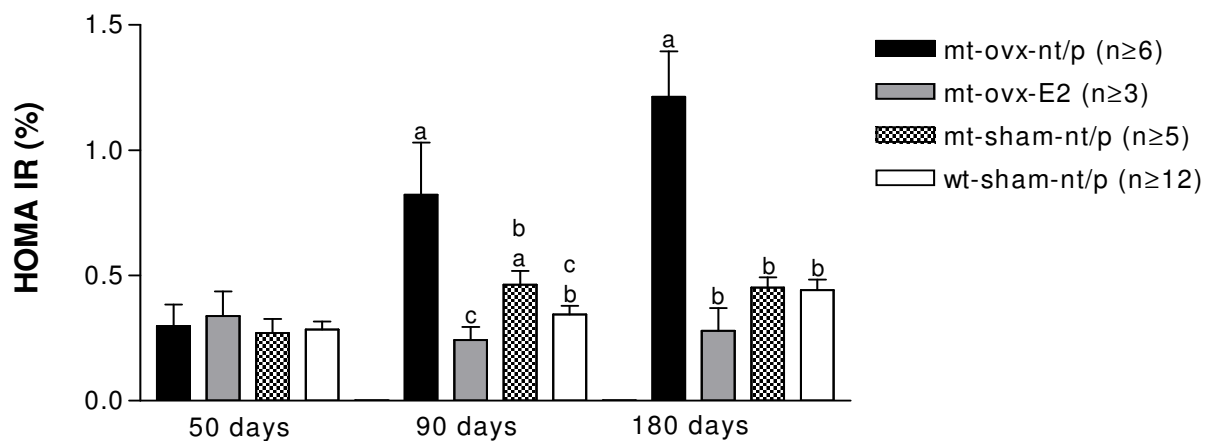


**Figure 4.10: Homeostasis model assessments of insulin resistance (HOMA IR) of 50-, 90- and 180-day-old mice**

The HOMA IR, as an index of insulin resistance, is not different at an age of 50 days. Ninety-day-old non-/placebo-treated ovariectomized mutant mice (mt-ovx-nt/p) already show a significantly increased HOMA IR as compared to the two sham-operated groups (mt-sham-nt/p and wt-sham-nt/p) and at the age of 180 days, the difference is significant as compared to all the other groups, including wild-type mice.

Data are means  $\pm$  SEM; a-c: different letters show significant differences ( $p < 0.05$ ); (n): number of animals investigated

#### 4.2.2 Quicki

The quantitative insulin-sensitivity check index (Quicki) showed no significant difference between the four groups at an age of 50 days. At 90 and 180 days of age, mt-ovx-nt/p mice demonstrated a lower Quicki as compared to the three other groups (Figure 4.11).

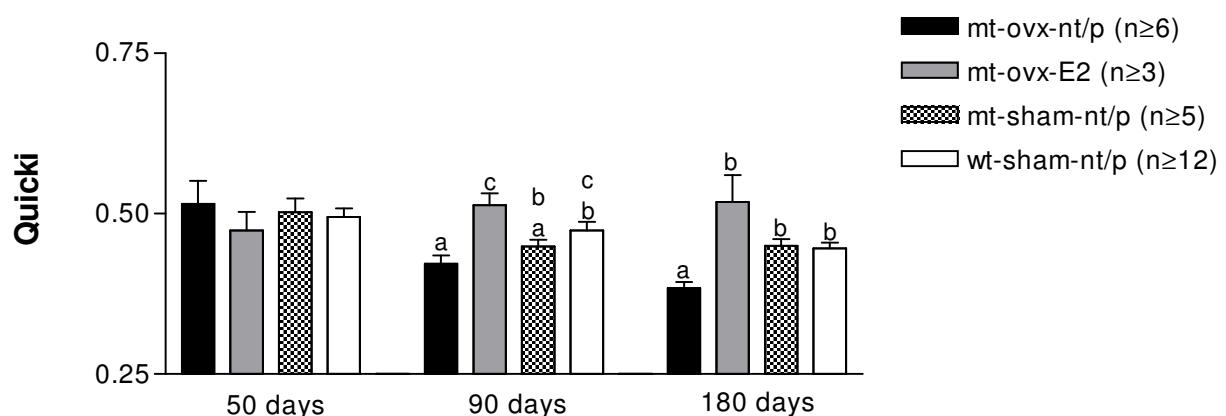


**Figure 4.11: Quantitative insulin-sensitivity check index (Quicki) of 50-, 90- and 180-day-old mice**

At an age of 90 and 180 days, non-/placebo-treated ovariectomized mutant mice (mt-ovx-nt/p) show the lowest Quicki within the four groups, whereas estradiol-treated ovariectomized mutant mice (mt-ovx-E2) exhibit the highest values.

Data are means  $\pm$  SEM; a-c: different letters show significant differences ( $p < 0.05$ ); (n): number of animals investigated

### 4.2.3 FGIR

The fasting glucose-to-insulin ratio (FGIR) demonstrated, that non-/placebo-treated ovariectomized and sham-operated mutant mice exhibited a significantly higher FGIR as compared to wild-type mice at all time points investigated (Figure 4.12). It is unlikely that this parameter, which was designed to evaluate insulin-resistance/-sensitivity in humans (FGIR<7 considered as insulin resistant, FGIR≥7 considered as insulin sensitive (Silfen *et al.* 2001)), is transferable to mice, because our results are opposite to the expected data.

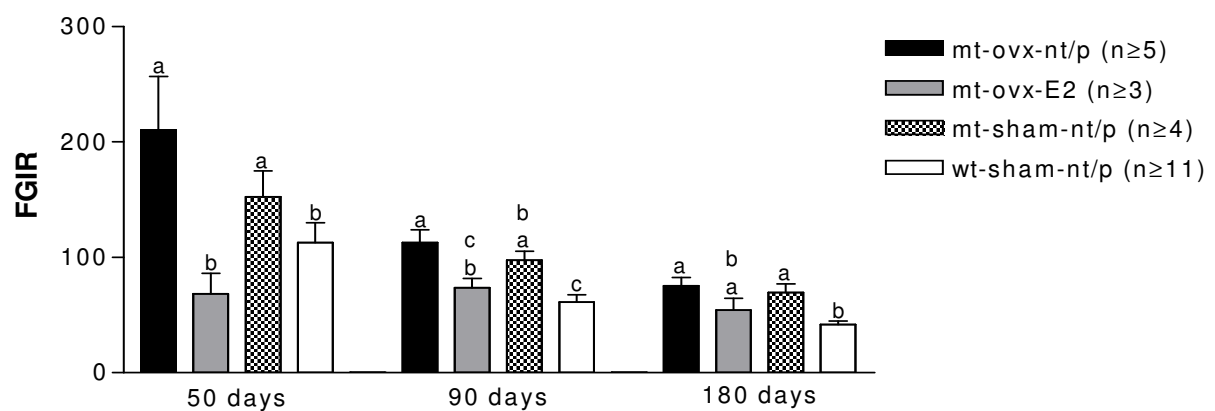


**Figure 4.12: Fasting glucose-to-insulin ratio (FGIR) of 50-, 90- and 180-day-old mice**

Data are means  $\pm$  SEM; a-d: different letters show significant differences ( $p < 0.05$ ); (n): number of animals investigated

### 4.3 Oxidative stress

Oxidative stress leads to serum lipid peroxidation which produces thiobarbituric reactive substances (TBARS). The amount of TBARS was determined in 190-day-old mice and was presented in malondialdehyde (MDA) equivalents.

Non-/placebo-treated ovariectomized mutant mice (mt-ovx-nt/p) showed a significantly higher extent of lipid peroxidation in the serum as compared to other mutant as well as to wild-type mice. The amount of MDA equivalents of mt-ovx-nt/p mice was about 2-fold higher than that of mt-sham-nt/p and wt-sham-nt/p mice and even 2.4-fold higher as compared to mt-ovx-E2 mice (Figure 4.13).

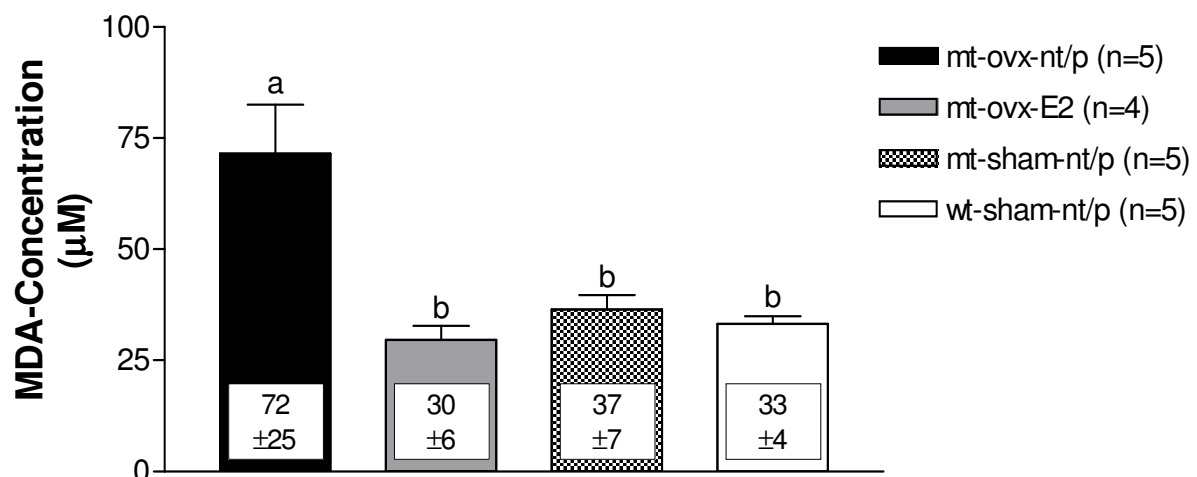


**Figure 4.13: Serum lipid peroxidation expressed in malondialdehyde (MDA) equivalents at an age of 190 days**

The serum malondialdehyde levels of non-/placebo-treated ovariectomized mutant mice (mt-ovx-nt/p) are significantly higher than those of the three other groups.

Data are means  $\pm$  SEM; a-b: different letters show significant differences ( $p < 0.05$ ); (n): number of animals investigated

Blood glucose concentrations correlated with lipid peroxidation in the serum. Mt-ovx-nt/p mice exhibited 2.8-fold higher serum blood glucose levels as compared to mt-sham-nt/p mice ( $356 \pm 193 \mu\text{M}$  vs.  $129 \pm 19 \mu\text{M}$ ) and 3-fold higher levels as compared to mt-ovx-E2 and wild-type mice ( $356 \pm 193 \mu\text{M}$  vs.  $116 \pm 38 \mu\text{M}$  vs.  $111 \pm 14 \mu\text{M}$ ) (Figure 4.14).

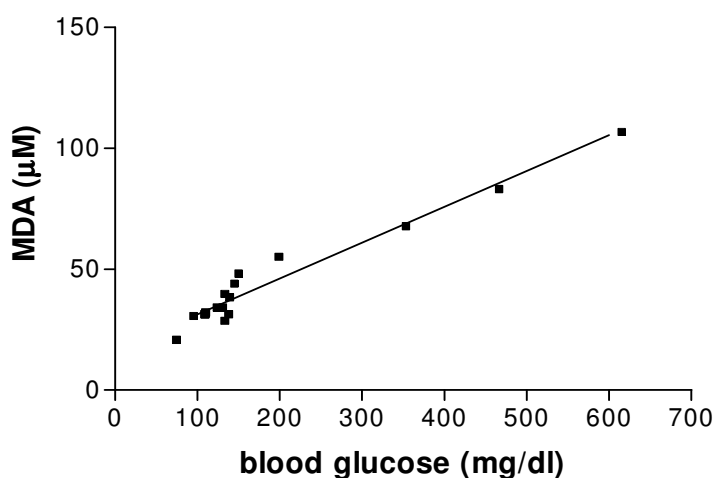


**Figure 4.14: Correlation of blood glucose concentrations and lipid peroxidation expressed in MDA equivalents at the age of 190 days**

The serum MDA equivalents and the blood glucose concentrations correlate with  $r = 0.98$  ( $p < 0.001$ )

## 4.4 Isolated pancreatic islets

Pancreatic islets of 210-day-old mice have been isolated for the determination of ER-stress, cell proliferation and apoptosis via Western blot analyses.

### 4.4.1 ER-stress

Primary antibodies against the ER-stress markers BiP, PeIF2 $\alpha$  and CHOP/GADD153 were used for the analyses. The molecular weights of the three markers were 78kDa for BiP, 40 kDa for PeIF2alpha and 25kDa for CHOP/GADD153. The optical density of the ER-stress marker bands was referred to that of  $\beta$ -actin (45kDa).

#### 4.4.1.1 BiP/ $\beta$ -actin

Mt-ovx-nt/p mice showed a significantly higher optical density of BiP/actin than mt-sham-nt/p and wild-type mice. Mt-ovx-E2 mice also demonstrated a higher optical density of BIP as compared to the two sham-operated groups, but this difference was not statistically significant (Figure 4.15).

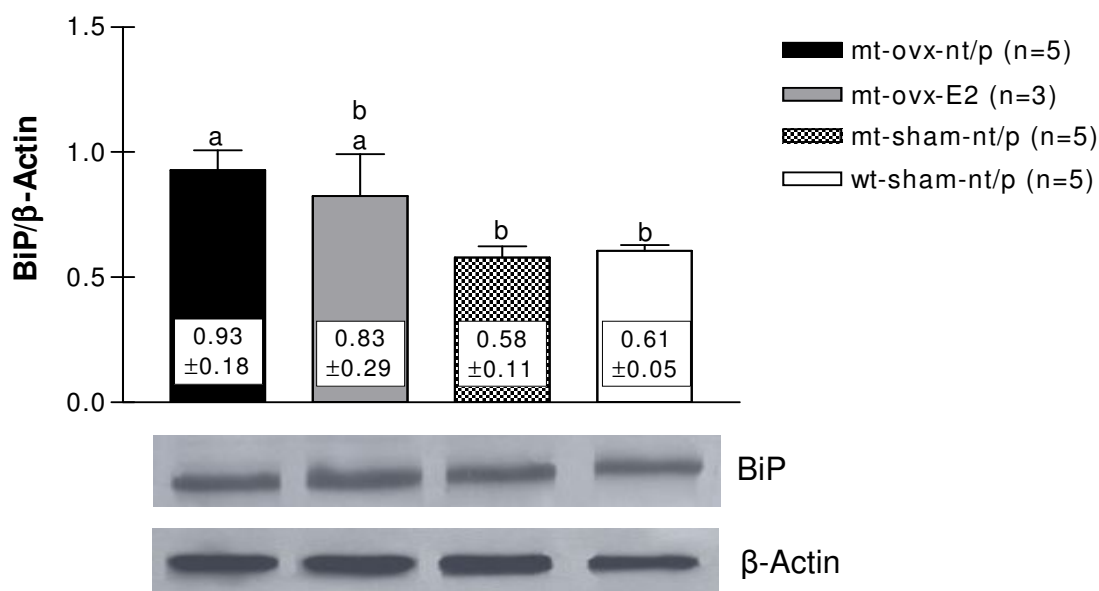


**Figure 4.15: Optical density of BiP/ $\beta$ -actin in isolated islets at the age of 190 days**

Ovariectomized non-/placebo-treated (mt-ovx-nt/p) and E2-treated (mt-ovx-E2) mutant mice showed a higher optical density of BiP/ $\beta$ -actin than sham-operated non-/placebo-treated mutant (mt-sham-nt/p) and wild-type (wt-sham-nt/p) mice.

Data are means  $\pm$  SEM; a-b: different letters show significant differences ( $p < 0.05$ ); (n): number of animals investigated

#### 4.4.1.2 PeIF2alpha/ $\beta$ -actin

The optical density of phospho-eIF2alpha/ $\beta$ -actin in the islets showed no significant difference between the four groups, although mt-ovx-nt/p and wild-type mice exhibited a marginally higher optical density than mt-ovx-E2 and mt-sham-nt/p mice (Figure 4.16).

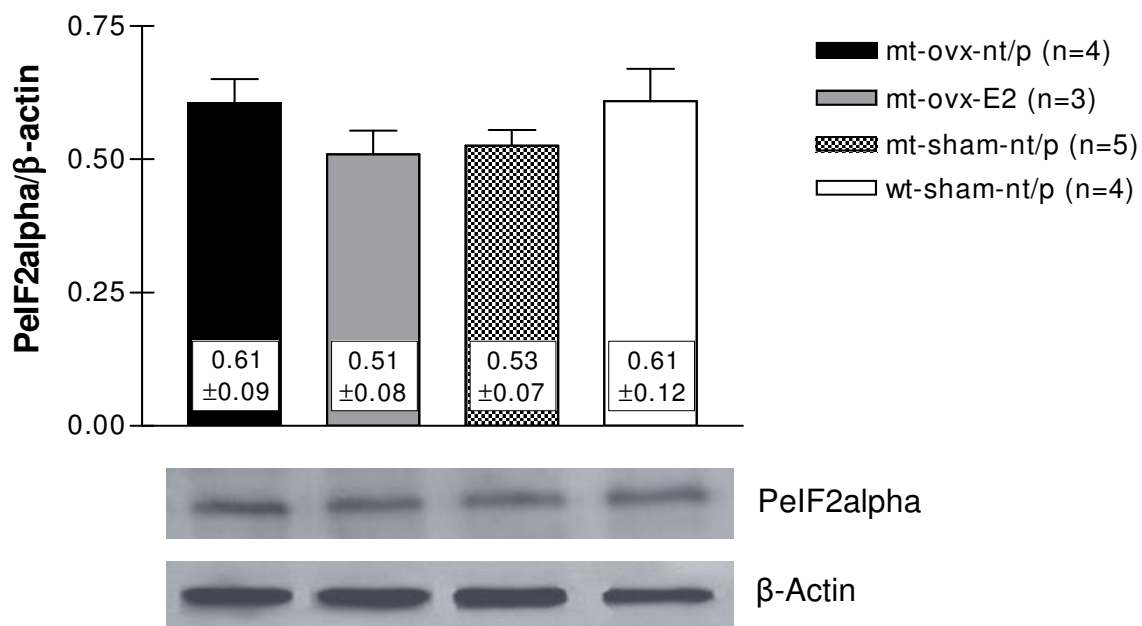


**Figure 4.16: Optical density of PeIF2alpha/ $\beta$ -actin in isolated islets at the age of 190 days**

Mt-ovx-nt/p and wild-type mice exhibit approximately the same optical density of PeIF2alpha but a higher optical density than that of mt-ovx-E2 and mt-sham-nt/p mice.

Data are means  $\pm$  SEM; (n): number of animals investigated

#### 4.4.1.3 CHOP/ $\beta$ -actin

The ER-stress marker CHOP/GADD 153 was only detectable in ovariectomized and sham-operated mutant and wild-type mice without E2- or placebo-treatment (mice of Group 1). Ovariectomized mutant mice (mt-ovx-nt) showed a significantly higher optical density of CHOP/ $\beta$ -actin than sham-operated mutant mice (mt-sham-nt). Moreover, mt-ovx-nt mice demonstrated a higher optical density of CHOP as compared to wild-type mice, although the difference was not statistically significant ( $p=0.058$ ) (Figure 4.17).

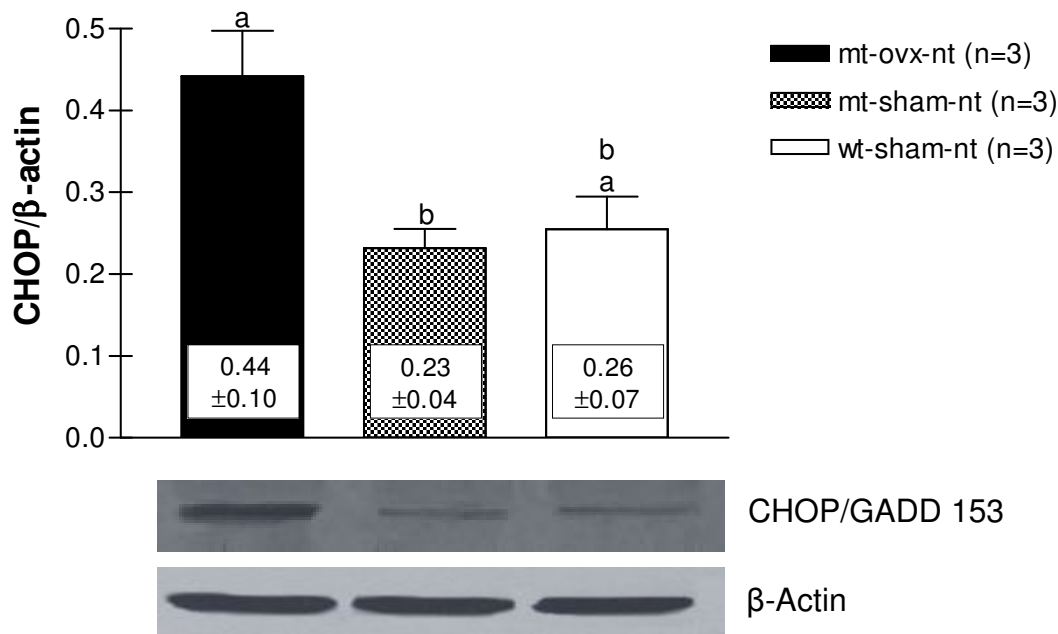


**Figure 4.17: Optical density of CHOP/β-actin in isolated islets at the age of 190 days**

Ovariectomized mutant mice (mt-ovx-nt) exhibit a higher optical density of CHOP/β-actin than sham-operated mutant mice (mt-sham-nt) and sham-operated wild-type mice (wt-sham-nt).

Data are means  $\pm$  SEM; a-b: different letters show significant differences ( $p < 0.05$ ); (n): number of animals investigated

#### 4.4.2 Apoptosis

To identify apoptotic islet-cells, a primary antibody against caspase-3 was used. Intracellular cysteine proteases (caspases), especially the effector caspase-3, are major regulators of apoptosis. In presence of cell death stimuli, inactive pro-caspase-3, which is usually expressed in mammalian cells, is activated by autoproteolytic procession from the inactive heterodimer into its active heterotetrameric form, consisting of a large (~20 kDa) and a small (~10 kDa) active subunit (Porter and Janicke 1999, Thornberry and Lazebnik 1998). The antibody used for Western blot analyses detects both, the inactive and active form of caspase-3. Lymph node homogenate was applied as positive control for the activated subunits. Pro-caspase-3 was detectable in all samples. The active large subunit of caspase-3 was only apparent in one examined sample of a placebo-treated ovariectomized mutant mouse as well as in lymph node homogenate (size ~19kDa), whereas no bands were detectable in the other islet samples examined. Only one band could be

detected for the active form of caspase-3 because the 17 and 19 kDa bands were not separated in the gel (Figure 4.18).

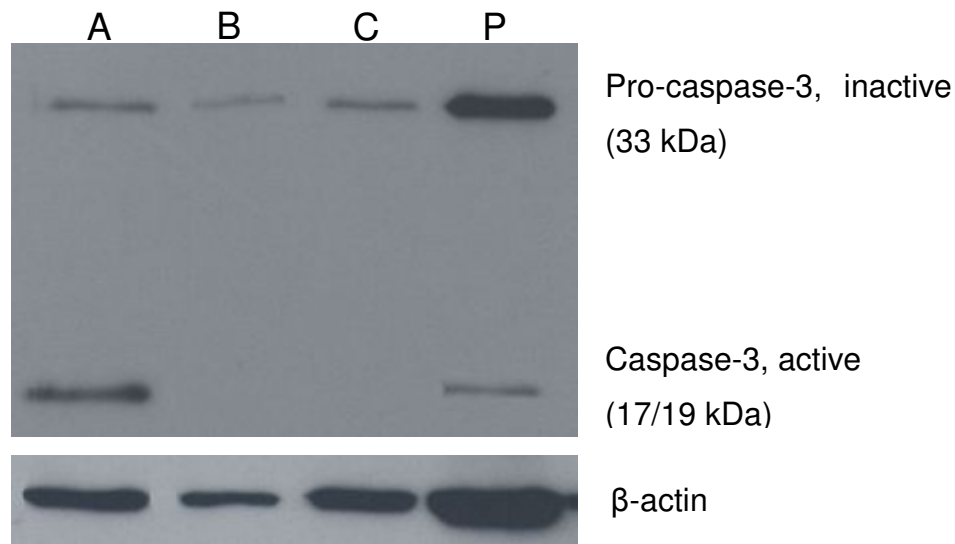


**Figure 4.18: Optical density of Caspase-3/β-actin in isolated islets at the age of 190 days**

**A:** mt-ovx-p; **B:** mt-ovx-E2; **C:** mt-sham-p; **P:** positive control (lymph node homogenate).

All examined samples show a pro-caspase band at 33kDa, whereas the active form of the enzyme (caspase-3) only appears in one sample of isolated islets from a placebo-treated ovariectomized mutant mouse (A) and the positive control (D).

#### 4.4.3 Cell proliferation

To evaluate replication of islet-cells, a primary antibody against Proliferative Cell Nuclear Antigen (PCNA) was used. PCNA is a marker for cells in early G1- and S-phase of the cell cycle. It is found in the nucleus and is a cofactor of DNA polymerase delta. PCNA acts as a homotrimer and helps to increase the processivity of leading strand synthesis during DNA replication (Majka and Burgers 2004). The molecular weight of this marker was 25kDa.

Mt-ovx-nt/p mice presented a significantly decreased optical density of PCNA/β-actin as compared to mt-sham-nt/p as well as to wild-type mice. Mt-ovx-E2 mice showed an optical density between mt-ovx-nt/p and mt-sham-nt/p mice (Figure 4.19).

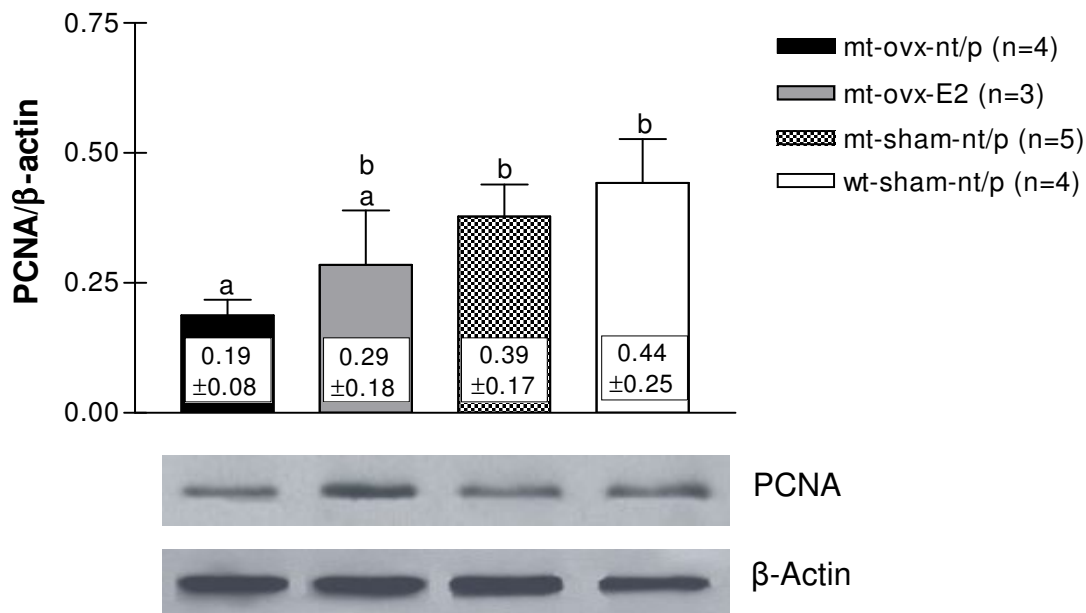


**Figure 4.19: Optical density of PCNA/β-actin in isolated islets at the age of 190 days**

Non-/placebo-treated ovariectomized mutant mice (mt-ovx-nt/p) exhibit a significantly lower optical density of PCNA/β-actin than non-/placebo-treated sham-operated mutant mice (mt-sham-nt/p) and wild-type mice (wt-sham-nt/p). The difference to estradiol-treated ovariectomized mutant mice (mt-ovx-E2) is not statistically significant.

Data are means ± SEM; a-b: different letters show significant differences ( $p < 0.05$ ); (n): number of animals investigated

## 4.5 Qualitative histological evaluations of the endocrine pancreas

Pancreata of 190-day-old mice were evaluated using qualitative histological and quantitative stereological methods (see chapter 2.6). Pancreata of non-/placebo-treated mice did not reveal any pathological changes. Two pancreata of estradiol-treated mice showed a well demarcated abscess, located in the pancreas parenchyma.

### 4.5.1 Insulin

Insulin-immunostaining was performed with pancreas sections of 16 mice belonging to Group 1 (5 mt-ovx-nt, 5 mt-sham-nt and 6 wt-sham-nt mice) and additionally with 4 estradiol-treated ovariectomized mutant mice (Group 2). Sham-operated wild-type (wt-sham-nt) mice revealed typical islet composition and distribution of insulin positive stained cells within the islets. Ovariectomized mutant mice (mt-ovx-nt)

showed less insulin positive cells than sham-operated mutants (mt-sham-nt) and wild-type mice. Sham-operated mutant mice (mt-sham-nt) and estradiol-treated ovariectomized mutant mice (mt-ovx-E2) showed almost equal amounts of insulin positive cells, lying in between the amounts of mt-ovx-nt and wild-type mice. Many of the  $\beta$ -cells in the islets of mt-ovx-nt mice demonstrated only a weak staining intensity, indicating low insulin content. Some of the insulin positive cells of mt-sham-nt mice showed almost as strong staining intensity as  $\beta$ -cells of wild-type mice, but some  $\beta$ -cells were stained as weak as those of mt-ovx-nt mice, whereas the staining intensity from mt-ovx-E2 mice was in between that of mt-ovx-nt and mt-sham-nt mice (Figure 4.20).

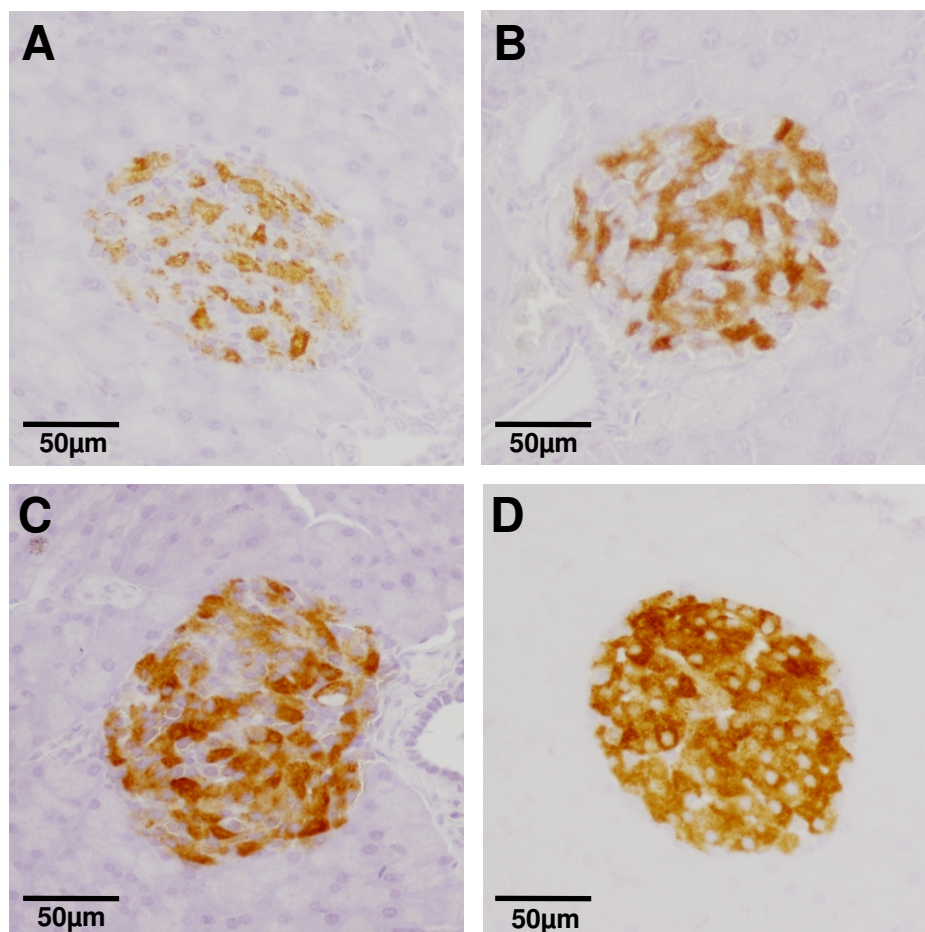


**Figure 4.20 (A-D): Pancreas sections with representative islet profiles of 190-day-old mice, immunostained for insulin**

Ovariectomized mutant mice (A) exhibit less insulin positive cells with lower staining intensity as compared to estradiol-treated ovariectomized mutant mice (B), sham-operated mutant mice (C) and wild-type mice (D). Wild-type mice show an islet profile which is predominantly composed of intensively stained  $\beta$ -cells.

#### 4.5.2 Glucagon, somatostatin and pancreatic polypeptide (PP)

Immunohistochemistry for glucagon, somatostatin and pancreatic polypeptide was accomplished with sections from 15 mice of Group 1 (5 mt-ovx-nt, 5 mt-sham-nt and 5 wt-sham-nt) and 19 mice of Group 2 (5 mt-ovx-p, 5 mt-sham-p, 4 mt-ovx-E2 and 5 wt-sham-p). Mt-ovx-nt/p and mt-ovx-E2 mice and to a lower degree also mt-sham-nt/p mice possessed more  $\alpha$ -,  $\delta$ - and PP-cells in islet cross sections than wild-type mice. The islet structure was altered in all three mutant mouse groups, with non- $\beta$ -cells being dispersed all over the islet profile whereas wild-type mice exhibited a typical murine islet composition where insulin positive  $\beta$ -cells are located in the centre of the islet and are surrounded by a ring of non- $\beta$ -cells (Figure 4.21).

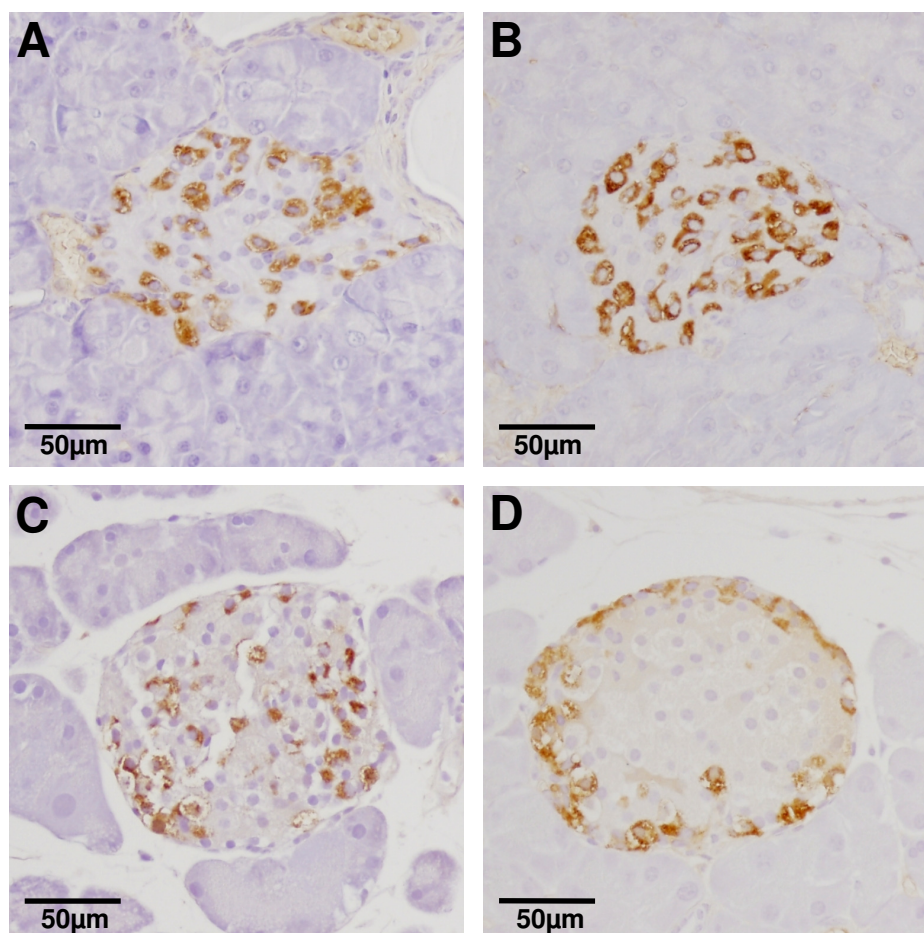


**Figure 4.21 (A-D): Pancreas sections with representative islet profiles of 190-day-old mice, simultaneously immunostained for glucagon, somatostatin and pancreatic polypeptide**

Non-/placebo-treated (A) and estradiol-treated (B) ovariectomized mutant mice exhibit an increased number of non  $\beta$ -cells which are distributed all over the islet profile. In contrast, wild-type mice (D) demonstrate a typical islet structure, characterized by a few non- $\beta$ -cells which surround a core of  $\beta$ -cells. Non-/placebo-treated sham-operated mutant mice (C) show less non- $\beta$ -cells as compared to the ovariectomized groups (A and B), but the cells are also distributed all over the islet profile.

### 4.5.3 Isolated $\beta$ -cells

Isolated  $\beta$ -cells were defined as single insulin positive cells and  $\beta$ -cell clusters of up to 4 nuclear profiles and are interpreted as a sign of islet neogenesis (Bonner-Weir *et al.* 2008, Inada *et al.* 2008). Isolated  $\beta$ -cells were found in all mice, either within the exocrine pancreas or associated to pancreatic ducts (Figure 4.22).

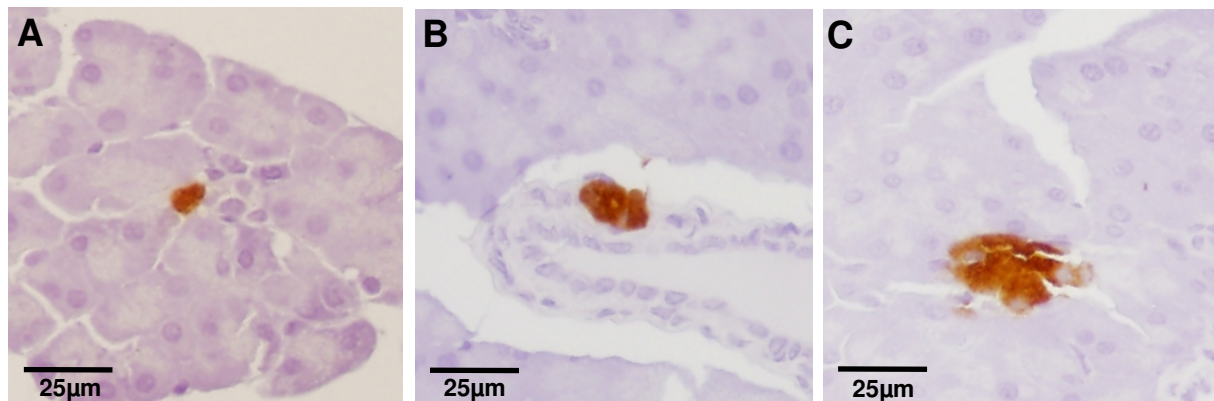


**Figure 4.22: Isolated  $\beta$ -cells in pancreas sections of 190-day-old mice, immunostained for insulin**

Isolated  $\beta$ -cells can be located as single cells within the exocrine pancreas (A), associated to pancreatic ducts (B) or as  $\beta$ -cell clusters up to four nuclear profiles (C).

## 4.6 Quantitative stereological analyses of the endocrine pancreas

### 4.6.1 Total pancreas volume

At the age of 190 days, all three placebo-treated groups showed an approximately similar total pancreas volume ( $V_{\text{pan}}$ ). Mt-ovx-E2 mice demonstrated a significantly lower total pancreas volume as compared to all the other groups (Figure 4.23).

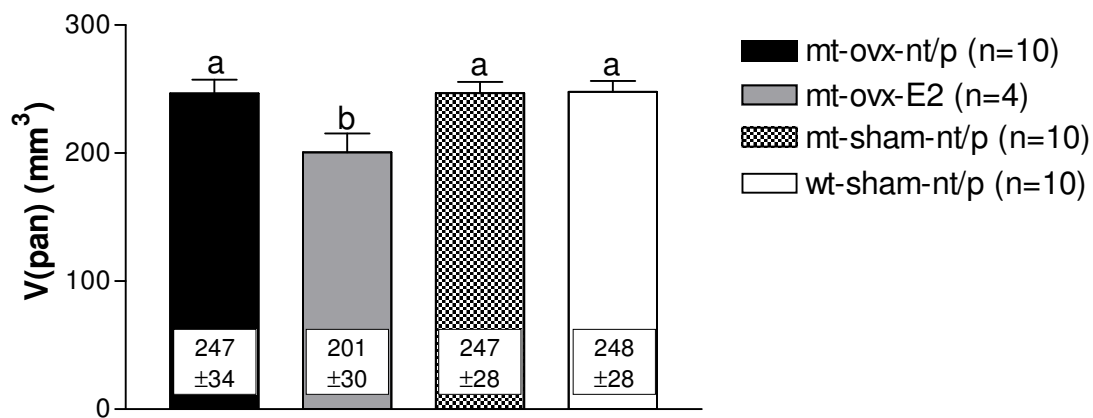


**Figure 4.23: Pancreas volume ( $V_{pan}$ ) of 190-day-old mice**

Estradiol-treated ovariectomized mutant mice (mt-ovx-E2) demonstrate a significantly lower pancreas volume as compared to the 3 other groups.

Data are means  $\pm$  SEM; a-b: different letters show significant differences ( $p < 0.05$ ); (n): number of animals investigated

#### 4.6.2 Relative pancreas weight

The relative pancreas weight (%) was almost identical between the four groups (Figure 4.24).

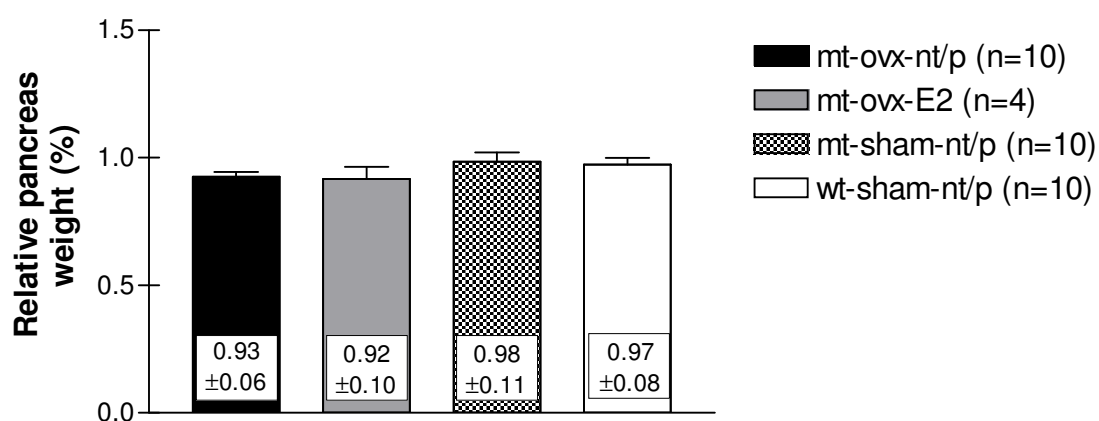


**Figure 4.24: Relative pancreas weight (%) of 190-day-old mice**

Mice of all 4 groups showed a similar relative pancreas weight. Data are means  $\pm$  SEM (n): number of animals investigated

### 4.6.3 Volume density of islets in the pancreas

The volume density of islets in the pancreas ( $Vv_{(\text{islets}/\text{pan})}$ ) of mt-ovx-E2 mice was significantly lower in comparison to mt-sham-nt/p and wild-type mice (Figure 4.25).

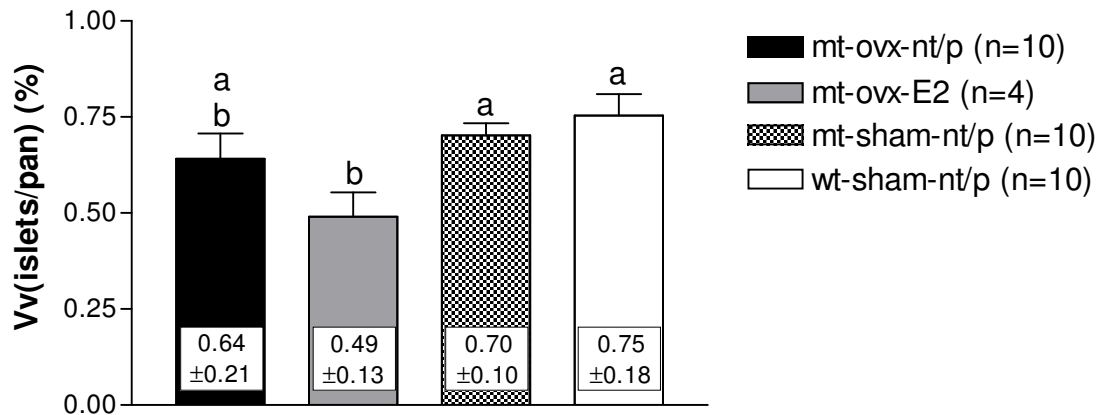


**Figure 4.25: Volume density of islets in the pancreas ( $Vv_{(\text{islets}/\text{pan})}$ ) of 190-day-old mice**

Mt-ovx-E2 mice demonstrate a significantly lower  $Vv_{(\text{islets}/\text{pan})}$  than mt-sham-nt/p and wild-type mice. Data are means  $\pm$  SEM; a-b: different letters show significant differences ( $p < 0.05$ ); (n): number of animals investigated

### 4.6.4 Total islet volume

Mt-ovx-E2 mice possessed a significantly lower total islet volume ( $V_{(\text{islets}, \text{pan})}$ ) than mice of the 3 other groups, whereas wild-type mice demonstrated the highest total islet volume within the four mice groups (Figure 4.26).

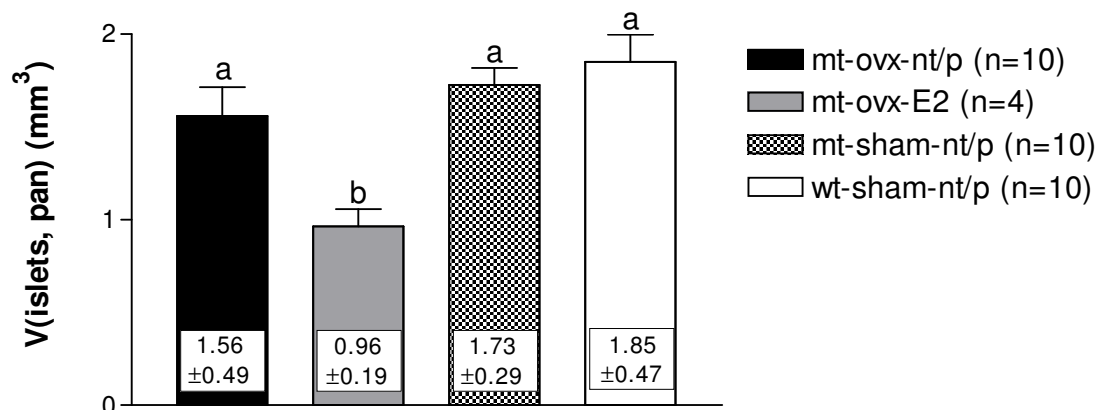


**Bild 4.26: Total islet volume in the pancreas ( $V_{(\text{islets}, \text{pan})}$ ) of 190-day-old mice**

Estradiol-treated ovariectomized mutant mice show the lowest total islet volume compared to mice of the 3 other groups.

Data are means  $\pm$  SEM; a-b: different letters show significant differences ( $p < 0.05$ ); (n): number of animals investigated

#### 4.6.5 Volume density of $\beta$ -cells in the islets

Wild-type mice exhibited a slightly but significantly higher volume density of  $\beta$ -cells in their islets ( $Vv_{(\beta\text{-cells/islet})}$ ) than mice of all the 3 other groups. Mt-sham-nt/p mice featured a slightly higher (n.s.)  $Vv_{(\beta\text{-cells/islet})}$  as compared to the two ovariectomized groups (Figure 4.27).

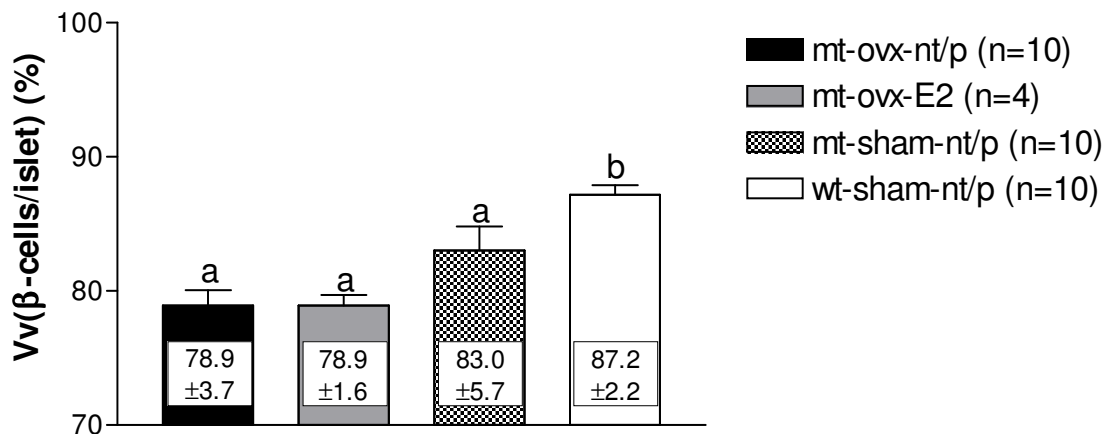


**Figure 4.27: Volume density of  $\beta$ -cells in the islets ( $Vv_{(\beta\text{-cells/islet})}$ ) of 190-day-old mice**

Wild-type mice demonstrate a significantly higher  $Vv_{(\beta\text{-cells/islet})}$  as compared to mice of all the three other groups. Data are means  $\pm$  SEM; a-b: different letters show significant differences ( $p < 0.05$ ); (n): number of animals investigated

#### 4.6.6 Total $\beta$ -cell volume

Mt-ovx-E2 mice featured a significantly lower total volume of  $\beta$ -cells in the islets ( $V_{(\beta\text{-cells, islets})}$ ) than mice of the three other groups. Mt-ovx-nt/p mice demonstrated a lower ( $p = 0.06$ )  $V_{(\beta\text{-cells, islets})}$  than mt-sham-nt/p and wild-type mice (Figure 4.28).

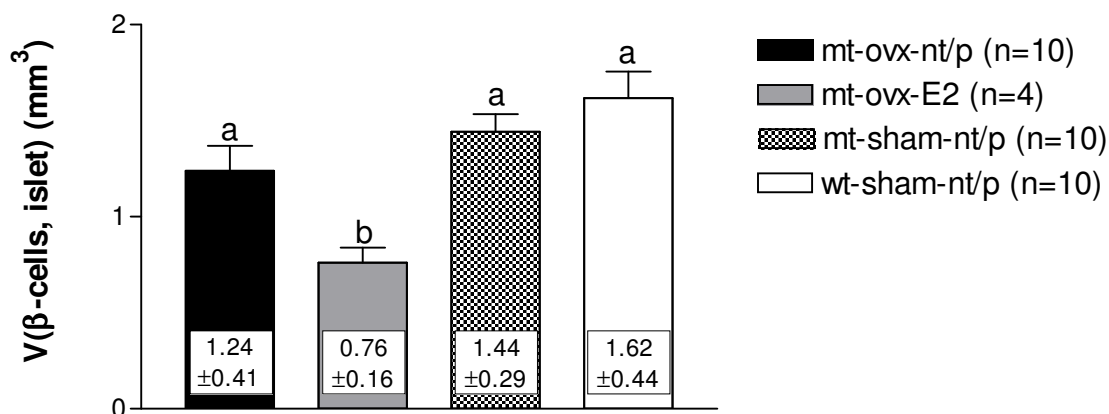


**Figure 4.28: Total volume of  $\beta$ -cells in the islets ( $V_{(\beta\text{-cells, islet})}$ ) of 190-day-old mice**

Mt-ovx-E2 mice exhibit a significantly lower total volume of  $\beta$ -cells in their islets as compared to mice of the three other groups. Data are means  $\pm$  SEM; a-b: different letters show significant differences ( $p < 0.05$ ); (n): number of animals investigated

#### 4.6.7 Volume density of non- $\beta$ -cells in the islets

All mutant mice showed a significantly higher volume density of non- $\beta$ -cells in the islets ( $V_{v(\text{non-}\beta\text{-cells/islet})}$ ) than wild-type mice. Mt-sham-nt/p mice exhibited a slightly lower (n.s.)  $V_{v(\text{non-}\beta\text{-cells/islet})}$  than the ovariectomized mutant mice (mt-ovx-nt/p and mt-ovx-E2) (Figure 4.29).

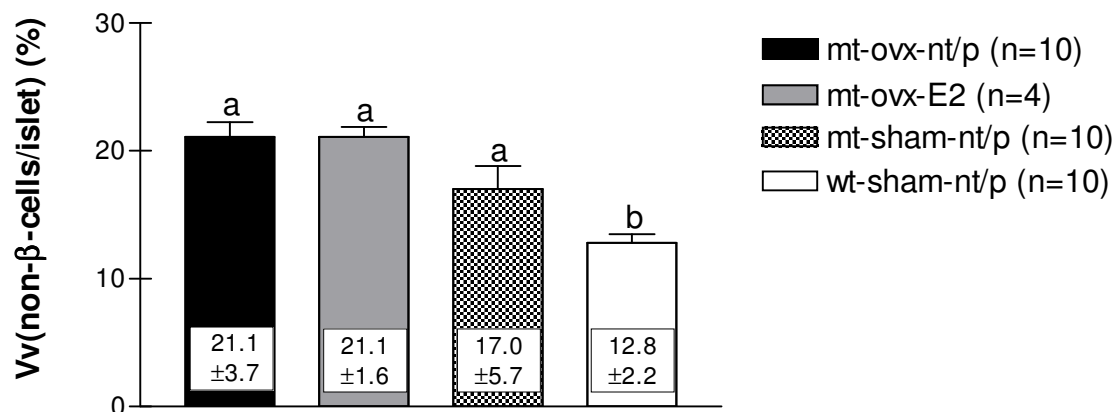


**Figure 4.29: Volume density of non- $\beta$ -cells in the islets ( $V_{v(\text{non-}\beta\text{-cells/islet})}$ ) of 190-day-old mice.**

Sham-operated mutant and wild-type mice (mt-sham-nt/p and wt-sham-nt/p) demonstrate a lower volume density of non- $\beta$ -cells in the islets than ovariectomized mutant mice (mt-ovx-nt/p and mt-ovx-E2). Data are means  $\pm$  SEM; a-b: different letters show significant differences ( $p < 0.05$ ); (n): number of animals investigated

#### 4.6.8 Total volume of non- $\beta$ -cells in the islets

Estradiol-treated ovariectomized mutant mice showed a significantly lower total volume of non- $\beta$ -cells in the islets ( $V_{(\text{non-}\beta\text{-cells, islet})}$ ) than non-/placebo-treated ovariectomized and sham-operated mutant mice. Moreover, wild-type mice exhibited a significantly lower total volume of non- $\beta$ -cells in the islets than non-/placebo-treated ovariectomized mutant mice and also a lower total volume than non-/placebo-treated sham-operated mutant mice ( $p = 0.09$ ) (Figure 4.30).

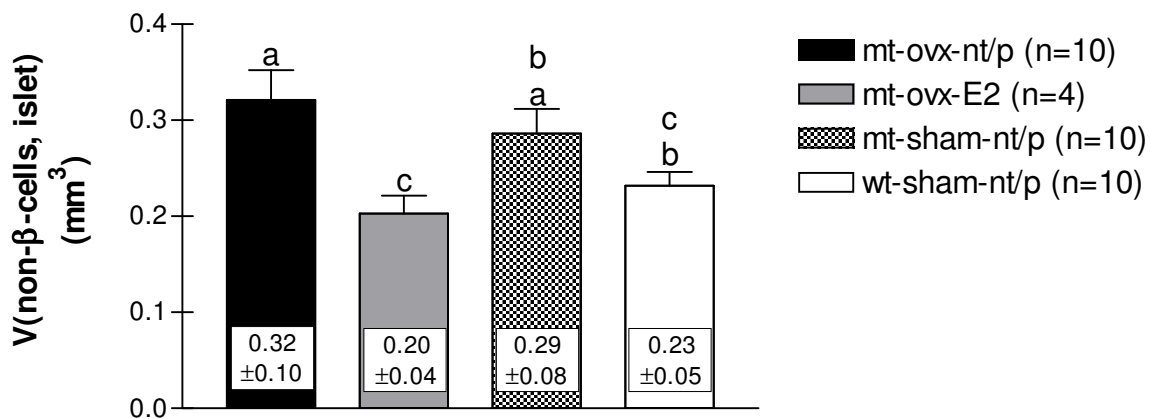


**Figure 4.30: Total volume of non- $\beta$ -cells in the islets ( $V_{(\text{non-}\beta\text{-cells, islet})}$ ) of 190-day-old mice**

Mt-ovx-E2 mice and wild-type mice demonstrate a smaller total volume of non- $\beta$ -cells in the islets, than mt-ovx-nt/p and mt-sham-nt/p mice.

Data are means  $\pm$  SEM; a-c: different letters show significant differences ( $p < 0.05$ ); (n): number of animals investigated

#### 4.6.9 B-cell to non- $\beta$ -cell ratio

Wild-type mice demonstrated the highest  $\beta$ -cell to non- $\beta$ -cell ratio, whereas non-/placebo-treated and E2-treated ovariectomized mutants showed the lowest values. Non-/placebo-treated sham-operated mutant mice offered a higher  $\beta$ -cell to non- $\beta$ -cell ratio as compared to the two other mutant groups, but the value is still lower than that of wild-type mice (Figure 4.31).

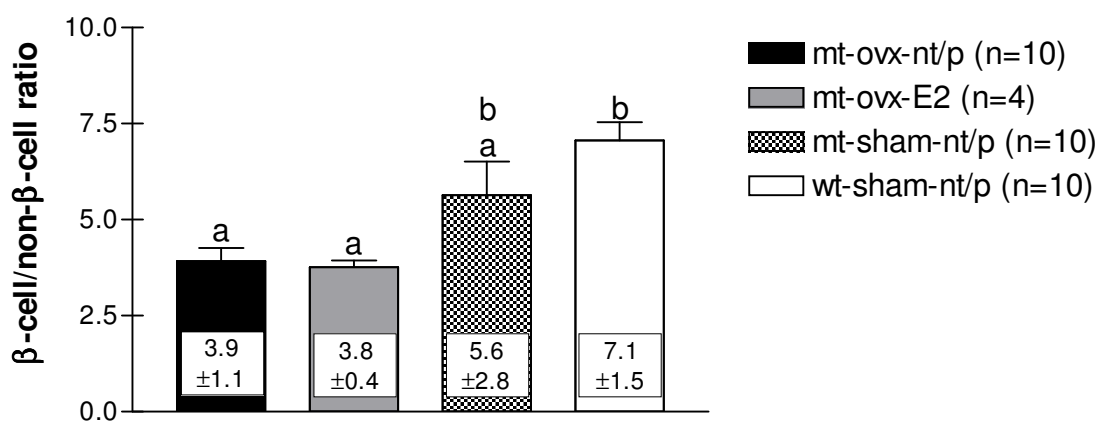


**Figure 4.31: B-cell to non- $\beta$ -cell ratio in islets of 190-day-old mice**

Non-/placebo- and E2-treated ovariectomized mutant mice demonstrated a significantly lower  $\beta$ -cell to non- $\beta$ -cell ratio as compared to wild-type mice. Non-/placebo-treated sham-operated mutant mice showed higher ratio as compared to the two ovariectomized mutant groups, but the difference is statistically not significant.

Data are means  $\pm$  SEM; a-b: different letters show significant differences ( $p < 0.05$ ); (n): number of animals investigated

#### 4.6.10 Volume density of isolated $\beta$ -cells in the pancreas

Wild-type mice showed a significantly higher volume density of isolated  $\beta$ -cells in the pancreas ( $Vv_{(isol. \beta\text{-cells}/pan)}$ ) than mice of all the three mutant groups (Figure 4.32).

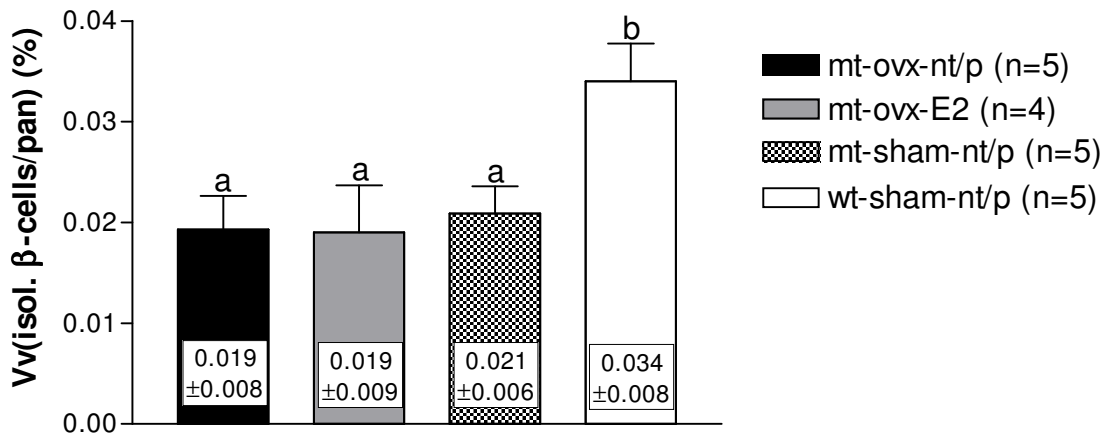


**Figure 4.32: Volume density of isolated  $\beta$ -cells in the pancreas ( $Vv_{(isol. \beta\text{-cells}/pan)}$ ) of 190-day-old mice**

Wild-type mice demonstrate a 1.6- to 1.8-fold higher volume density of isolated  $\beta$ -cells in the pancreas ( $Vv_{(isol. \beta\text{-cells}/pan)}$ ) than mutant mice. Data are means  $\pm$  SEM; a-b: different letters show significant differences ( $p < 0.05$ ); (n): number of animals investigated

#### 4.6.11 Total volume of isolated $\beta$ -cells

Wild-type mice showed a significantly higher total volume of isolated  $\beta$ -cells in the pancreas ( $V_{(isol. \beta\text{-cells}, pan)}$ ) as mice of the three mutant groups (Figure 4.33).

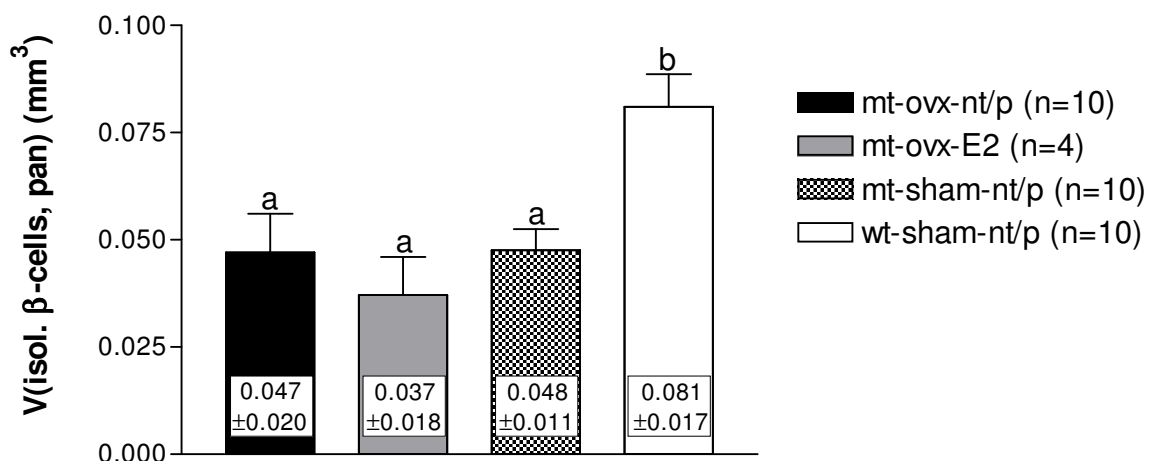


**Figure 4.33: Total volume of isolated  $\beta$ -cells in the pancreas ( $V_{(isol. \beta\text{-cells}, pan)}$ ) of 190-day-old mice**

Wild-type mice exhibit an about 1.7-fold higher total volume of isolated  $\beta$ -cells in the pancreas as compared to the two non-/placebo-treated mutant mice groups (mt-ovx-nt/p and mt-sham-nt/p) and a 2.2-fold higher  $V_{(isol. \beta\text{-cells}, pan)}$  vs. mt-ovx-E2 mice. Data are means  $\pm$  SEM; a-b: different letters show significant differences ( $p < 0.05$ ); (n): number of animals investigated

## 4.7 Transmission electron microscopy

Ultrathin pancreas sections of 190-day-old mice were examined using transmission electron microscopy. Concerning the amount and distribution of the distinct endocrine cells within the islets, electron-microscopical observations were in agreement with qualitative histological and immunohistochemical findings (4.5 Qualitative histological findings of the endocrine pancreas). Wild-type mice demonstrated a typical murine islet structure with basically  $\beta$ -cells in the centre and non- $\beta$ -cells mainly located at the border of the islet (Figure 4.34 A). In all the three mutant mouse groups, non- $\beta$ -cells were distributed all over the islet profile (Figure 4.34 B-D).

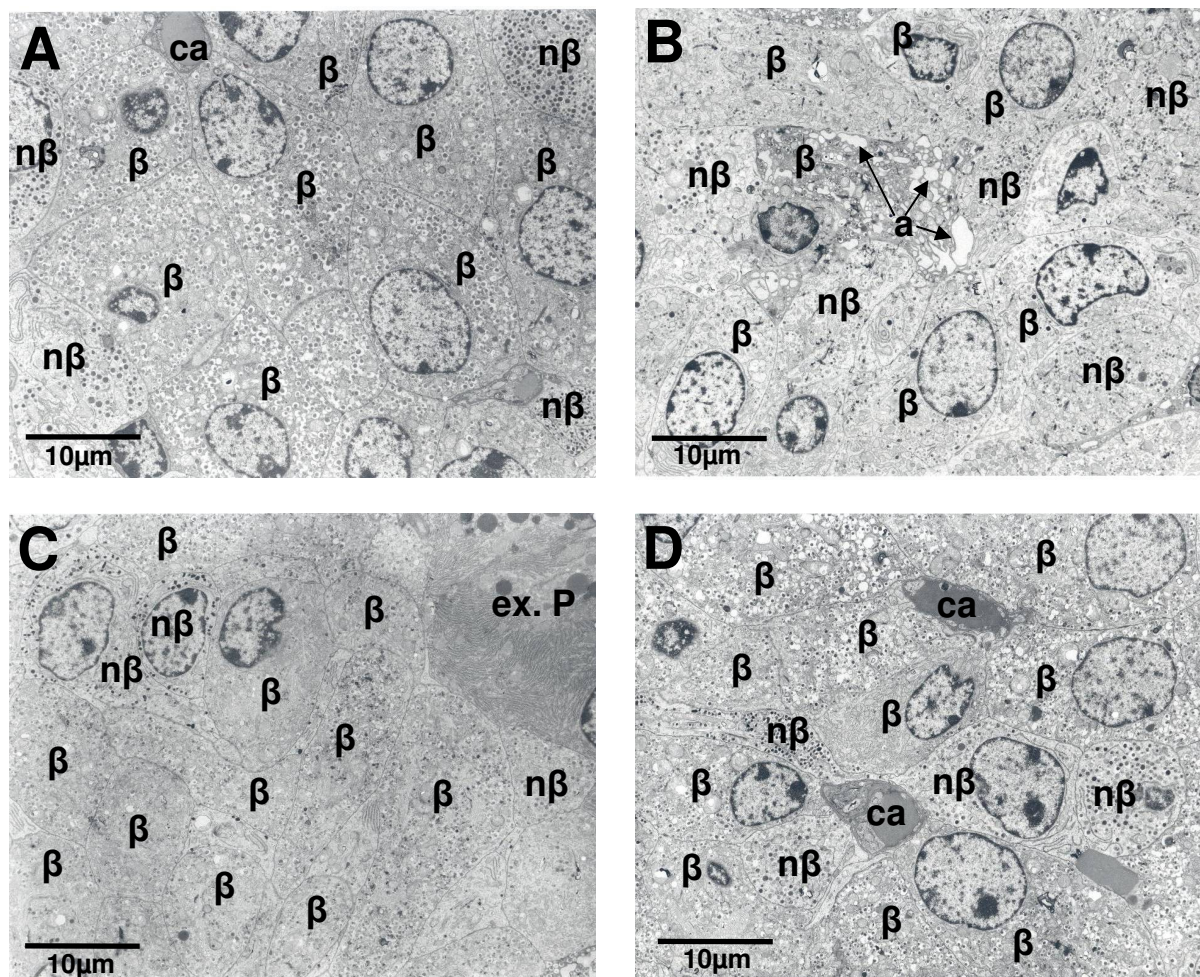


**Figure 4.34: Transmission electron microscopy (TEM) of islet-cell profiles of 190-day-old mice**

Wild-type (A) mice featured a typical murine islet structure with basically  $\beta$ -cells ( $\beta$ ) located in the centre and non- $\beta$ -cells ( $n\beta$ ) located mainly at the border of the islet. In non-/placebo-treated (B) and estradiol-treated (C) ovariectomized mutant mice as well as in non-/placebo-treated sham-operated mutant mice (D), non- $\beta$ -cells are distributed all over the islet profile. In some samples, artefacts (a), which maybe are a sign of beginning autolysis, can be found; in A, D: capillaries (ca); in C: exocrine pancreas (ex. P).

The cytoplasm of  $\beta$ -cells from wild-type mice (Figure 4.35 A) was densely packed with typical insulin secretory granules, characterised by an electron-dense core, surrounded by an electron lucent halo. In mt-ovx-nt/p mice (Figure 4.35 B), many  $\beta$ -cells exhibited very few and small secretory granules. Some of the granules presented a tiny core and a broadened halo as compared to wild-type mice. In mt-ovx-E2 mice (Figure 4.35 C) and mt-sham-nt/p mice (Figure 4.35 D),  $\beta$ -cells with a granule density comparable to wild-type mice side by side with almost granule-free cells could be found, and the size of granule-profiles seemed to be marginally smaller than those of wild-type mice, but appeared bigger than those of mt-ovx-nt/p mice (Figure 4.35). The differences in the amount and size of secretory granules are mirrored by the various immunohistochemical staining intensities of  $\beta$ -cells described above (4.5 Qualitative histological findings of the endocrine pancreas). In all mutant mice, the rough endoplasmic reticulum (rER) seemed to be dilated as compared to wild-type mice (Figure 4.36 and 4.37). A few  $\beta$ -cells of mice from all three mutant groups (Figure 4.36 B - D) contained enlarged mitochondria.

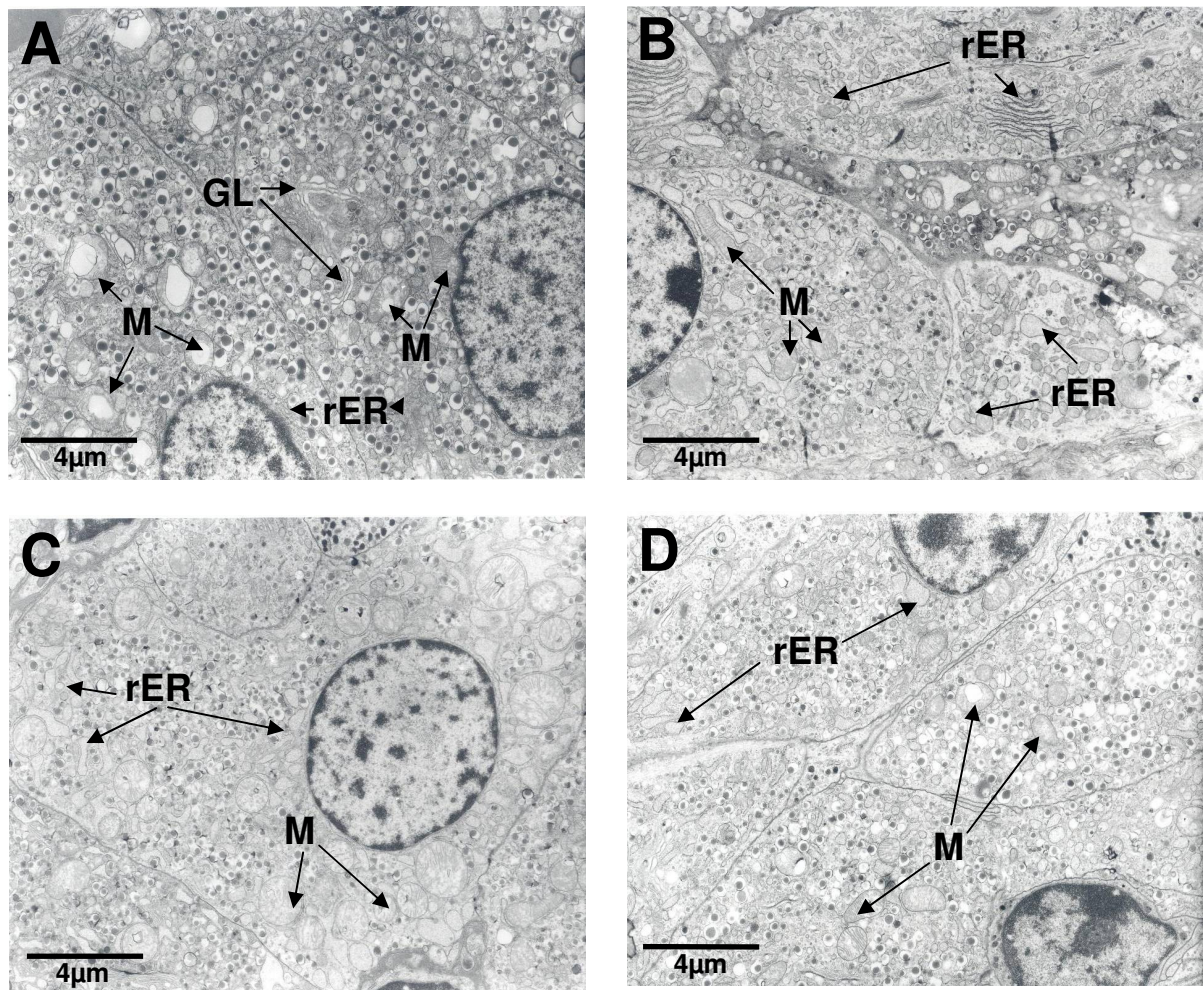


**Figure 4.35: Transmission electron microscopy (TEM) of islet-cell profiles of 190-day-old mice**

Beta-cells of wild-type mice (A) show a high density of secretory granules. The amount of secretory granules in  $\beta$ -cells of mt-ovx-nt/p (B), mt-ovx-E2 (C) and mt-sham-nt/p (D) mice varies substantially within the islet. Some  $\beta$ -cells exhibit approximately a similar granule density as wild-type mice (e.g.  $\beta$ -cell in the centre of Fig. B), but the adjacent  $\beta$ -cells are nearly devoid of insulin granules; mitochondria ( $\rightarrow$  M) (A-D); Golgi lamellae ( $\rightarrow$  GL) (A); rough endoplasmic reticulum ( $\rightarrow$  rER) (A-D).

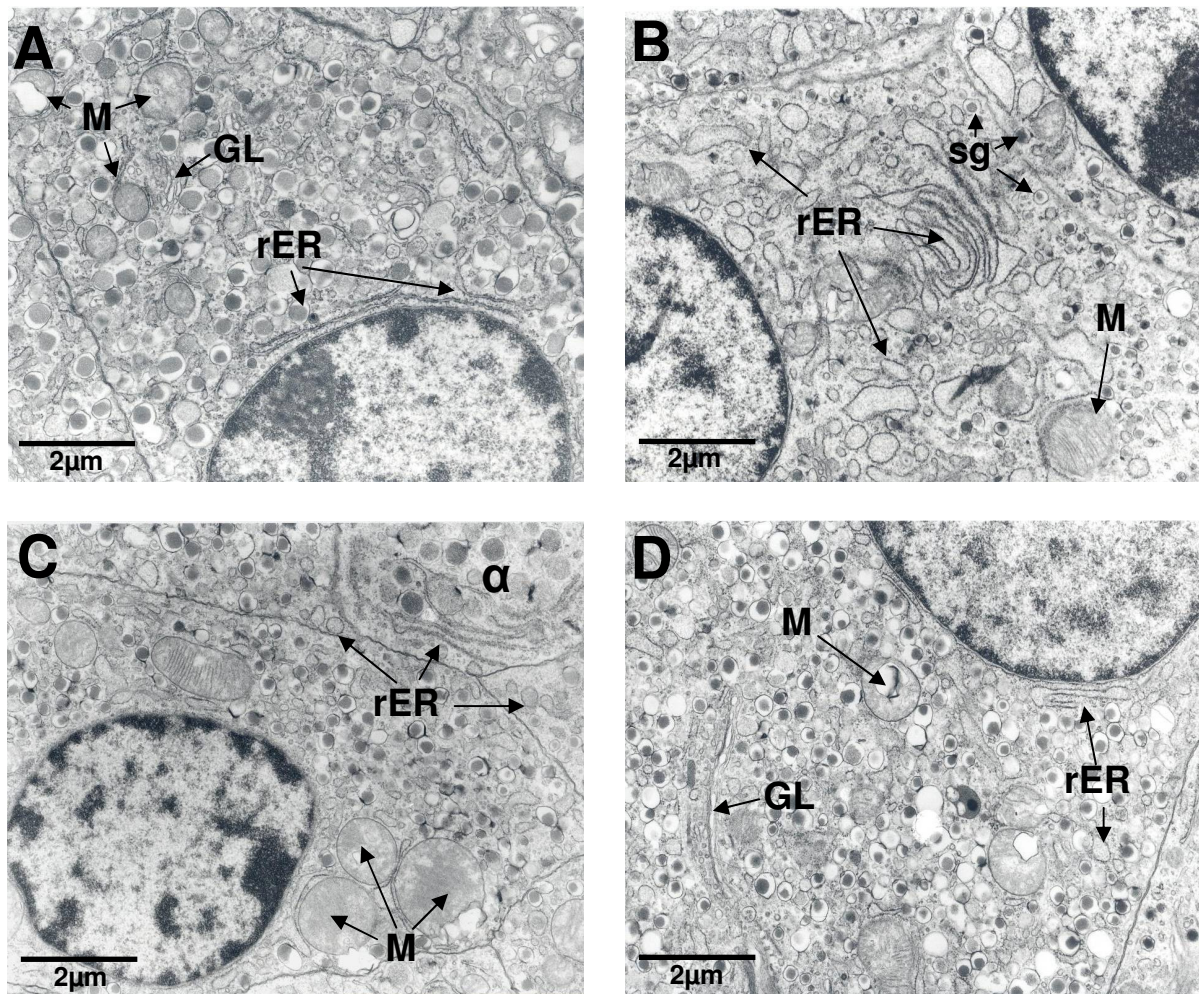


**Figure 4.36: Transmission electron microscopy (TEM) of  $\beta$ -cell profiles of 190-day-old mice**

In some  $\beta$ -cells of *mt-ovx-nt/p* mice (B), the rough endoplasmic reticulum ( $\rightarrow$  rER) appears dilated as compared to wild-type mice (A). *Mt-ovx-E2* (C) and *mt-sham-nt/p* (D) mice in the same cell demonstrate ER that is almost unaltered as well as ER that appears to be slightly dilated. *Mt-ovx-nt/p* mice exhibit only few and small secretory granules ( $\rightarrow$  sg); *mt-ovx-E2* and *mt-sham-p* mice also show slightly fewer secretory granules compared to wild-type mice, but the size seems to be a similar; mitochondria ( $\rightarrow$  M) (A-D); Golgi lamellae ( $\rightarrow$  GL) (A, D); in C:  $\alpha$ -cell ( $\alpha$ )

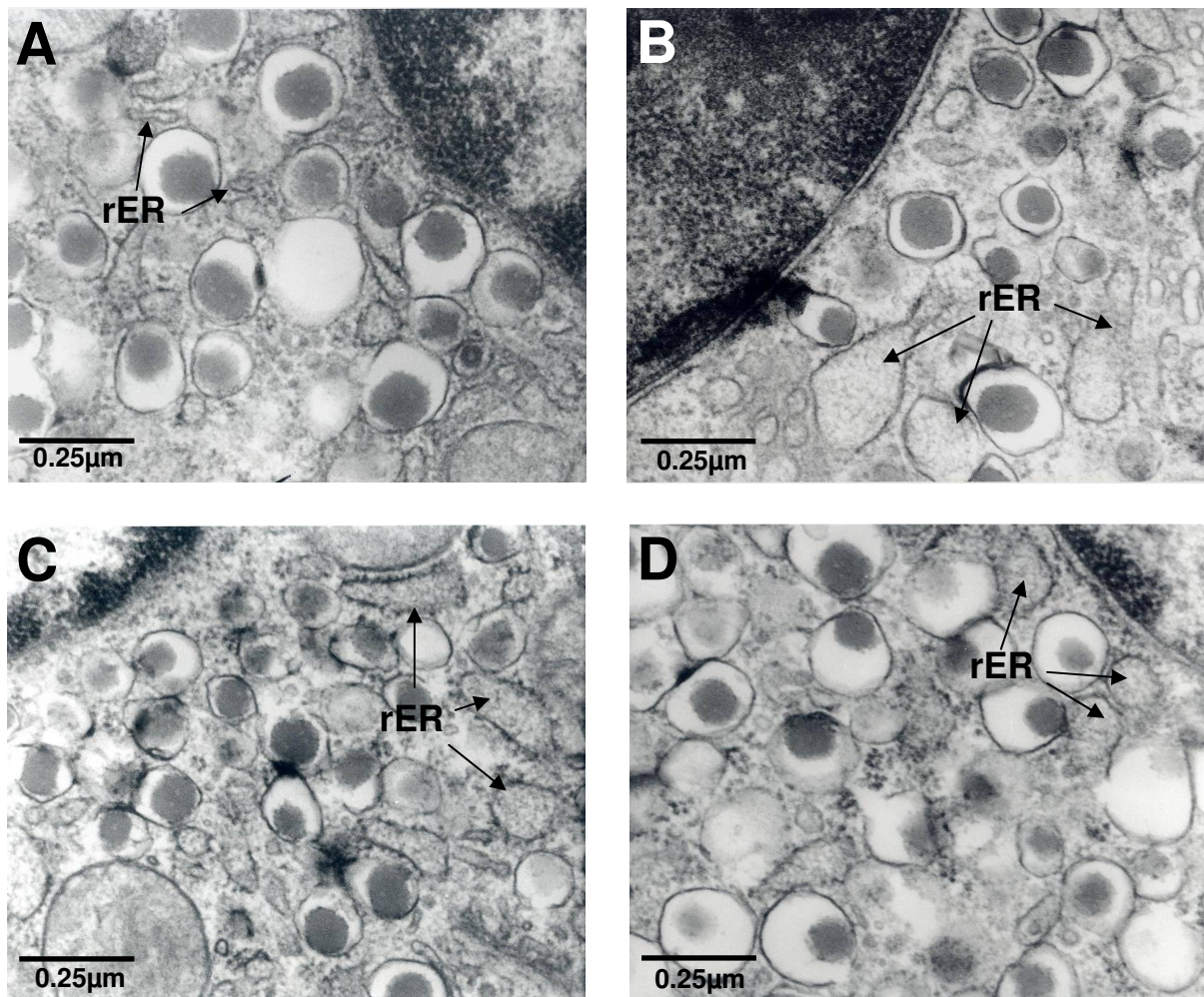


**Figure 4.37: Transmission electron microscopy (TEM) of  $\beta$ -cell profiles of 190-day-old mice**

Mt-ovx-nt/p (B), mt-ovx-E2 (C) and mt-sham-nt/p (D) mice exhibit a dilated rough endoplasmic reticulum ( $\rightarrow$  rER) as compared to wild-type mice (A).

## 5 Discussion

Heterozygous Munich *Ins2*<sup>C95S</sup> mutant mice exhibit a point mutation in the *Ins2* gene, leading to the development of diabetes mellitus. It could be shown that heterozygous male mutant mice develop a severe progressive diabetic phenotype with severe  $\beta$ -cell dysfunction and profound loss of functional  $\beta$ -cell mass, whereas female mutants show stable and much milder diabetic symptoms and  $\beta$ -cell mass was not found to be reduced (Herbach *et al.* 2007). This phenomenon is thought to result from antidiabetic actions of 17 $\beta$ Estradiol (E2) in both humans and rodents (Louet *et al.* 2004).

The present study was performed to examine the influence of 17 $\beta$ Estradiol (E2) on  $\beta$ -cell survival in the pancreas of female Munich *Ins2*<sup>C95S</sup> mutant mice as well as its impact on glucose homeostasis. For this purpose, two groups of heterozygous female mutant mice have been ovariectomized and received either a 17 $\beta$ Estradiol replacement therapy or a placebo. Non-/placebo-treated sham-operated wild-type and non-/placebo-treated sham-operated mutant mice served as controls.

### 5.1 Glucose homeostasis

#### 5.1.1 Blood glucose and insulin secretion

Mutant and wild-type mice showed almost similar randomly fed blood glucose concentrations at weaning. Five days after ovariectomy/sham-operation (at 35 days of age), ovariectomized non-/placebo-treated mutant mice already developed hyperglycaemia, and showed a progressive diabetic phenotype with raising blood glucose concentrations up to 360 mg/dl at an age of 160 days. The progressive course of disease is similar to that in male heterozygous Munich *Ins2*<sup>C95S</sup> mutant mice, but males reached even higher blood glucose levels (550 mg/dl at an age of 160 days) (Kautz 2010). Although sham-operated non-/placebo-treated mutant mice demonstrated blood glucose concentrations of almost 200 mg/dl at an age of 35 days and therefore were mildly hyperglycaemic, they showed almost constant glucose levels during their lifespan, never exceeding 200 mg/dl. Intact female heterozygous Akita mice, which also exhibit a mutation in the *Ins2* gene, demonstrated almost stable randomly fed blood glucose concentrations from an age of 4 weeks onwards

as well, never reaching 330 mg/dl. The glucose levels of female Akita mice were higher as compared to female sham-operated Munich *Ins2*<sup>C95S</sup> mutant mice, but significantly lower as compared to male Akita mice (Yoshioka *et al.* 1997).

Estradiol-treated ovariectomized Munich *Ins2*<sup>C95S</sup> mutant mice demonstrated almost similar blood glucose concentrations as wild-type mice at all time points investigated. In contrast to Munich *Ins2*<sup>C95S</sup> mutant mice and heterozygous Akita mice, single homozygous *Ins2* and *Ins1* knockout mice stay normoglycaemic, most likely due to compensation by increased *Ins1* or *Ins2* expression (Leroux *et al.* 2001, Leroux *et al.* 2003). Moreover, single heterozygous null-mutant mice with only one single *Ins2* gene (NOD<sup>Ins1<sup>-/-</sup>,Ins2<sup>+/-</sup></sup>) do not develop diabetes (Babaya *et al.* 2006), whereas double homozygous null mutant mice develop severe hyperglycaemia and die within the first 48h (Duvillie *et al.* 1997). Due to the fact that both heterozygous Munich *Ins2*<sup>C95S</sup> mutant mice as well as heterozygous Akita mice possess one intact *Ins2* allele and 2 intact *Ins1* alleles, the mutant insulin 2 seems to exert dominant negative effects on  $\beta$ -cell function and viability (Herbach *et al.* 2007, Wang *et al.* 1999). The mutant proinsulin 2 molecules aggregate more easily than wild-type proinsulin and it could be shown that such aggregates also include wild-type proinsulin due to hydrophobic interactions (Liu *et al.* 2007, Yoshinaga *et al.* 2005), leading to an aggregation as well as degradation of not only mutant, but also wild-type proinsulin and a reduced transport of both to secretory granules (Wang *et al.* 1999). Moreover, misfolded proinsulin 2 most probably causes ER-stress like it is seen in heterozygous Akita mice (Wang *et al.* 1999, Yoshinaga *et al.* 2005), leading to the induction of  $\beta$ -cell apoptosis (Oyadomari *et al.* 2002).

The progressive diabetic phenotype of non-/placebo-treated ovariectomized mutants can be explained by impaired insulin secretion, development of insulin resistance and a reduction of the total  $\beta$ -cell volume, similar to male Munich *Ins2*<sup>C95S</sup> mutant mice (Herbach *et al.* 2007). This leads to the conclusion that most likely endogenous estrogen produced in the ovaries from sham-operated non-/placebo-treated mutant mice protects them from developing a severe diabetic phenotype. Moreover, 17 $\beta$ Estradiol replacement therapy could even normalise blood glucose levels of ovariectomized mutant mice.

Fasting blood glucose concentrations of ovariectomized non-/placebo-treated mutant mice were significantly higher as compared to sham-operated non-/placebo-treated mutant mice at all time points investigated, reaching the highest level of almost 200 mg/dl at an age of 120 days. Nevertheless, the glucose levels were always lower as compared to male mutant mice with fasting blood glucose concentrations exceeding 300 mg/dl at an age of 180 days (Herbach *et al.* 2007). Estradiol-treated ovariectomized mutant mice however did not exhibit fasting hyperglycaemia and moreover demonstrated even lower fasting blood glucose concentrations as compared to wild-type mice. Sham-operated non-/placebo-treated mutant mice only showed a mild diabetic phenotype with mean fasting blood glucose levels always under 135 mg/dl.

The mechanisms that regulate the plasma glucose concentration during the post-absorptive state (fasting plasma glucose) are very different from those that regulate the plasma glucose concentration after a meal (DeFronzo 2004). Fasting plasma glucose (FPG) is primarily determined by the rate of hepatic glucose production (DeFronzo *et al.* 1989), whereas postprandial glucose concentration is determined by the rate of glucose-stimulated insulin secretion and skeletal muscle insulin sensitivity. Physiologically, pancreatic  $\alpha$ -cells release glucagon during hypoglycaemia to induce hepatic glucose output (Gromada *et al.* 2007). High blood glucose concentrations inhibit glucagon secretion via direct effects on  $\alpha$ -cells and most likely also in an indirect manner, for example via increasing insulin secretion (Dunning *et al.* 2005). Alpha-cells in chronically hyperglycaemic patients demonstrate disturbed glucose sensing resulting in hyperglucagonaemia which can further contribute to hyperglycaemia (Quesada *et al.* 2008, Unger *et al.* 1970). In male Munich *Ins2*<sup>C95S</sup> mutant mice, an increase in randomly fed glucagon levels was observed, whereas glucagon levels in female mutant and wild-type mice were almost similar (Kautz 2010). The mechanisms contributing to the  $\alpha$ -cell pathology/dysfunction are still largely unknown (Quesada *et al.* 2008). Since fasted glucagon concentrations in mutant mice of both genders were similar to those of sex-matched wild-type mice (Kautz 2010), the fasting hyperglycaemia seen in ovariectomized placebo-treated mutant mice seems not to be aroused by elevated hepatic glucose synthesis due to hyperglucagonaemia.

In oral glucose tolerance tests, all three mutant groups showed higher areas under the blood glucose curve ( $AUC_{\text{blood glucose}}$ ) as compared to wild-type mice, irrespective of age at sampling. Non-/placebo-treated ovariectomized mutant mice showed significantly higher  $AUC_{\text{blood glucose}}$  as compared to E2-treated ovariectomized and sham-operated mutants, indicating that the loss of estrogen leads to a further deterioration of glucose tolerance. Although estradiol-treated ovariectomized mutant mice demonstrated normalised fasting and randomly fed glucose levels vs. non-/placebo-treated mutant mice, the  $AUC_{\text{blood glucose}}$  during OGTT was not improved vs. sham-operated mutant mice. The improved glucose tolerance in estrogen-treated vs. non-/placebo-treated ovariectomized mice is likely due to positive effects of estrogen on glucose stimulated insulin secretion (Ropero *et al.* 1999), insulin sensitivity in peripheral tissues (Barros *et al.* 2006b, Lee *et al.* 1999), or a combination of both. In estrogen receptor  $\alpha$  knock-out mice ( $\alpha$ ERKO) an impaired glucose tolerance compared to wild-type mice was observed (Heine *et al.* 2000). These findings are consistent with data that ovariectomy in rodents impairs glucose tolerance and alters glucose-induced insulin secretion, whereas estrogen replacement partially or completely prevents this (Bailey and Ahmed-Sorour 1980). However, E2-treatment is not sufficient to restore glucose tolerance of female Munich  $Ins2^{\text{C95S}}$  mutants completely. Therefore it seems likely that the effects of the mutation have higher negative impact on glucose tolerance than the positive effects of E2 to prevent them.

The decrease of blood glucose concentrations after glucose challenge in all three mutant mice groups was delayed compared to wild-type mice and most likely due to disturbed insulin secretion 10 minutes after glucose application (Herbach *et al.* 2007). The fasted serum insulin concentrations of all mutant mice groups were almost similar to that of wild-type mice at an age of 90 days. At an age of 180 days E2-treated ovariectomized mutant mice demonstrated significantly lower fasted serum insulin levels as compared to non-/placebo-treated ovariectomized mutants and wild-type mice.

Ten minutes after oral glucose application, the insulin secretion in wild-type mice increased about 10-fold as compared to basal values, whereas non-/placebo-treated ovariectomized and sham-operated mutant mice just showed a 1.4 and 1.9-fold increase from basal insulin levels at an age of 180 days. E2-treated ovariectomized

mutant mice showed with a 2.5-fold increase the highest level within the three mutant mice groups.

The  $\beta$ -cell function indices homeostasis model assessment of baseline insulin secretion (HOMA B) and insulin resistance (HOMA IR (%)), were developed to calculate  $\beta$ -cell function and insulin resistance in human-beings (Lee *et al.* 2008, Wallace *et al.* 2004). The relationship between glucose and insulin in the basal (fasting) state reflects the balance between hepatic glucose output and insulin secretion, which is maintained by a feedback loop between the liver and  $\beta$ -cells (Turner *et al.* 1979). HOMA B, reflecting  $\beta$ -cell function, was significantly lower in both ovariectomized as well as sham-operated non-/placebo-treated mutant mice as compared to estradiol-treated ovariectomized mutant and wild-type mice.

All these results indicate that mutant mice suffer from a disturbed glucose-stimulated insulin secretion (GSIS) that is fractionally ameliorated by estradiol. Nevertheless, the GSIS seen in E2-treated ovariectomized mutants is still exceeding low as compared to wild-type mice. It could be shown, that chronic hyperglycaemia can cause alterations in mitochondrial protein expression levels like e.g. the inner mitochondrial protein uncoupling protein 2 (UCP2), which has been associated with impaired GSIS (Nyblom *et al.* 2006, Wang *et al.* 1999). This could be one reason for the disturbed GSIS of placebo-treated ovariectomized and sham-operated mutant mice, but it could not explain the impaired GSIS in estradiol-treated ovariectomized mutant mice, because they did not show chronic hyperglycaemia, indicating that high blood glucose levels cannot be the main reason for the disturbed GSIS. It also could be shown that the disturbance in GSIS of female mutant mice is equal to that of male Munich *Ins2* mutants despite a higher pancreatic insulin content of female vs. male mutants (Herbach *et al.* 2007), arguing against depletion of insulin stores as a cause of impaired GSIS. Isolated pancreatic islets of male Akita mice also demonstrated a reduced GSIS compared to wild-type mice, speaking for the point that partial misfolding of mutant proinsulin like in both the Munich *Ins2*<sup>C95S</sup> mutant mouse as well as the Akita mutant mouse, may lead to the disturbed insulin secretion (Izumi *et al.* 2003, Liu *et al.* 2005). In the Munich *Ins2*<sup>C95S</sup> mutant mouse, the A6-A11 intrachain disulfide bond is disrupted whereas the mutation existent in the Akita mutant mouse prevents formation of the A7-B7 interchain disulfide bond. In studies with HEK293 cells, expressing the mutant proinsulin from Akita mice, an increased

fraction of non-native proinsulin disulfide isomers was observed as well as a profound decrease in secretion, probably leading to intracellular degradation of non-secreted proinsulin (Colombo *et al.* 2008). Izumi *et al.* (2003) could demonstrate that the early secretory pathway in  $\beta$ -cells of Akita mice is impaired due to the intracellular accumulation of misfolded proinsulin. As a consequence, secretion of both, wild-type and mutant proinsulin is disturbed (Izumi *et al.* 2003).

Furthermore, ER-stress, caused by the misfolded proinsulin, may be involved in the disturbed GSIS. Energy consumption by chaperones participating in ER-stress mediated pathways can decrease the ATP/ADP ratio, leading to a reduced increase of this ratio after glucose uptake. Moreover,  $\text{Ca}^{2+}$  release from the ER upon ER-stress may elevate intracellular  $\text{Ca}^{2+}$  levels (Scheuner and Kaufman 2008, Xu *et al.* 2005). Likewise, chronically high glucose leads to high basal  $\text{Ca}^{2+}$  levels, reduced glucose-induced  $\text{Ca}^{2+}$  increase and is associated with disturbed insulin secretion after glucose stimulus (Bjorklund *et al.* 2000).

Since estradiol-treated ovariectomized mutant mice at an age of 180 days demonstrated the highest increase of serum insulin 10 min after glucose stimulus as compared to mice of the two other mutant groups, it seems like estradiol may slightly improve the GSIS. This may be due to the capability of estradiol to potentiate insulin secretion after glucose stimulus (Ropero *et al.* 1999) or because of its positive effects related to ER-stress (Kozlov *et al.* 2010). Although sham-operated non-/placebo-treated mutant mice showed a significantly higher GSIS as compared to ovariectomized non-/placebo-treated mutant mice, the increase of serum insulin 10 min after glucose stimulus is slightly lower than that of estradiol-treated ovariectomized mutant mice. One explanation for this could be the absence of elevated blood glucose concentrations and therefore elimination of the negative impact of chronic hyperglycaemia on GSIS in estradiol-treated mutants (see above).

Taken together, ovariectomy aggravates the diabetic phenotype of Munich *Ins2*<sup>C95S</sup> mutant mice, as evidenced by increased fasting and postprandial glucose levels vs. sham-operated mutant mice. E2-treatment rescues ovariectomized mutant females from developing diabetes and ameliorates disturbed glucose tolerance. However, disturbed GSIS is not or only slightly improved. Therefore, misfolding of mutant

proinsulin seems to play a major role in disturbed GSIS, whereas glucotoxicity plays no or only a minor role.

### 5.1.2 Insulin sensitivity

For the analysis of insulin sensitivity, intraperitoneal insulin tolerance tests (ipITT) were performed with mice that were not supplied with E2 or placebo pellets (non-treated). Ovariectomized non-treated mutant mice showed a significantly higher  $AUC_{\text{blood glucose}}$  during ITT as compared to sham-operated non-treated mutant and wild-type mice at an age of 60 and 187 days, indicating impaired insulin sensitivity in the absence of ovarian hormones. At the same time points, sham-operated non-treated mutant and wild-type mice showed almost similar areas under the blood glucose curve. In concordance to these findings, the HOMA IR, reflecting insulin resistance in both peripheral tissues and the liver, was higher in non-/placebo-treated ovariectomized mutant mice as compared to mice of all three other groups. E2-treated ovariectomized mutant mice as well as non-/placebo-treated sham-operated mutant mice showed a similar HOMA IR. These results confirm the findings of the accomplished intraperitoneal insulin tolerance tests and reveal the positive effect of estrogen on insulin sensitivity. Due to the fact that normoglycaemic insulin-treated male Munich *Ins2*<sup>C95S</sup> mutant mice showed similar insulin sensitivity compared to sex-matched wild-type mice, whereas placebo-treated hyperglycaemic male mutant mice demonstrated severely impaired insulin sensitivity (Kautz 2010), it seems like the development of insulin resistance is likely the consequence of chronically elevated blood glucose levels. It is known that long-term hyperglycaemia may lead to oxidative stress (Robertson 2004), which reduces insulin sensitivity, for example, in myocytes and adipocytes (Houstis *et al.* 2006, Maddux *et al.* 2001). Phloridizin, a substance that can be used to lower blood glucose concentration, was able to ameliorate peripheral insulin resistance in the Akita mouse (Hong *et al.* 2007). Therefore it seems likely that the impaired insulin sensitivity seen in placebo-treated ovariectomized mutant mice in part is a result of the chronic elevated blood glucose concentrations seen in these mice. On the other hand, normoglycaemic E2-treated ovariectomized mutant mice but also mildly hyperglycaemic non-/placebo-treated sham-operated mutant mice do not or only to a minor degree suffer from impaired insulin sensitivity due to chronic hyperglycaemia, what also would explain the lower HOMA IR apparent in these two groups as well as the lower  $AUC_{\text{blood glucose}}$  during

ipITT in sham-operated mutant mice as compared to non-/placebo-treated ovariectomized mutant mice.

Furthermore it could be shown that estradiol can improve glucose uptake in peripheral tissues after binding of insulin to its receptor on the target cell by inducing the expression of the downstream signalling molecules IRS-1 and IRS-2 (Lee *et al.* 1999). In addition to this, estrogen was shown to increase  $\beta$ -cell function and mass by an increase of IRS2 and PDX-1 expression in islets of ovariectomized rats that indirectly leads to an enhanced IGF-1/insulin signalling cascade and results in an enlargement of pancreatic  $\beta$ -cell mass (Choi *et al.* 2005). Therefore it is possible that endogenous estrogen of sham-operated non-/placebo-treated female Munich *Ins2*<sup>C95S</sup> mutant mice as well as exogenous estradiol in E2-treated ovariectomized mutant mice accounts for the ameliorated peripheral insulin sensitivity and leads to the significantly lower insulin resistance as compared to estrogen lacking ovariectomized non-/placebo-treated mutant mice. It also should be taken into account that obesity in humans also is known to impair insulin sensitivity (Ahren 2005) and therefore, the mildly increased body weight of non-/placebo-treated ovariectomized mutant mice in comparison to mice of the other three groups could be another promoting factor in the development of insulin resistance.

Taken together, the findings of the present study underline the assumption that most likely hyperglycaemia and additionally obesity may lead to insulin resistance that contributes to the progressive diabetic phenotype of non-/placebo-treated ovariectomized mutants. 17 $\beta$ Estradiol seems to improve insulin sensitivity by several factors such as increased glucose uptake after insulin stimulation by mainly inducing the expression of IRS-1 in peripheral tissues (Lee *et al.* 1999) and improvement of  $\beta$ -cell function and mass by inducing the expression of IRS-2 to compensate for the increased insulin requirement (Choi *et al.* 2005). Moreover estradiol is known to reduce body weight in rodents (see below) what might also have beneficial influence on insulin sensitivity.

## 5.2 Body weight

Mice of all 4 groups showed similar body weights in the time between weaning (21 days of life) and ovariectomy (30 days of life). Five days after ovariectomy/sham-operation, non-/placebo-treated ovariectomized mutant mice already demonstrated higher body weights as compared to mice of the 3 other groups, indicating that

estrogen participates in the regulation of fat mass, most likely by affecting the expression of leptin, an important feedback controller of energy balance that acts to increase metabolism and depress appetite (Ahima *et al.* 1996). It is mainly produced and secreted by adipose cells and its circulating concentration normally correlates directly with body fat content (Considine *et al.* 1996). After release of leptin into the bloodstream it influences specific regions of the brain, such as the hypothalamus, where it affects the activity of the hypothalamus-pituitary axis by modulating the expression of several neuropeptides, such as neuropeptide Y (NPY) and corticotropin-releasing hormone (CRH) (Beck 2000). Estradiol is known to enhance the expression and secretion of leptin by adipocytes, both in vitro (Kronfeld-Schor *et al.* 2000) and in vivo (Tanaka *et al.* 2001). In rats, ovariectomy diminished leptin gene expression in white adipose tissue and caused a decline in serum leptin levels while administration of E2 reversed all the effects of ovariectomy (Chu *et al.* 1999). Bilateral ovariectomy was also reported to reduce serum leptin levels in humans (Messinis *et al.* 1999). Moreover, the administration of estrogen increases hypothalamic expression of the long form of the leptin receptor in rats (Rocha *et al.* 2004). On the other hand, estrogen deficiency increases hypothalamic NPY by direct genomic modulation and causes central and/or peripheral leptin insensitivity (Ainslie *et al.* 2001). Mice lacking estrogen receptor- $\alpha$  ( $\alpha$ ERKO mice) or aromatase (ArKO mice) showed increased fat mass and hyperlipidemia (Heine *et al.* 2000, Jones *et al.* 2000).

Taken together, ovariectomy may alter body weight by reducing the amount of leptin secreted by adipose tissue, resulting in an inappropriately low satiety signal. Moreover, lack of estrogen may affect body weight regulation at a central level like increase of NPY and decrease of CRH, which both promote hyperphagia, leading to mild obesity of non-/placebo-treated ovariectomized mutant mice.

Estradiol-treated ovariectomized mutant mice demonstrated a significantly lower body weight as compared to all 3 other groups. The reason for this may be the generally known potent suppressive effect of estradiol on food intake in rodents, but the underlying mechanism of E2 action on appetite are still not fully understood (Geary 2000). Some authors suggest a taste aversive effect, but this still remains controversial (Flanagan-Cato *et al.* 2001, Ganesan 1994). Moreover, attention was focused on the hypothalamus as a possible site of E2 action. It was suggested that a

decrease in either hypothalamic NPY, or melanin-concentrating hormone (MCH) expression and levels may mediate anorexia (Bonavera *et al.* 1994, Mystkowski *et al.* 2000). In another study it could be demonstrated that administration of fatty acid synthase (FAS) inhibitors leads to decreased food intake and body weight in rodents (Loftus *et al.* 2000). The selective estrogen receptor modulator tamoxifen (TAM) can induce anorexia and thereby is associated with the accumulation of malonyl-CoA in the hypothalamus and inhibition of FAS expression (Lopez *et al.* 2006). All these findings indicate that the low body weight of estradiol-treated ovariectomized mutant mice is a result of decreased food intake aroused by the still not completely known anorectic effects of high dose 17 $\beta$ Estradiol.

### 5.3 Oxidative stress

To reveal the degree of lipid peroxidation, thiobarbituric acid reactive substances (TBARS) are often used as a marker for oxidative stress in diabetic animal models and in humans (Maritim *et al.* 2003). At an age of 190 days, non-/placebo-treated ovariectomized mutant mice demonstrated about 2-fold higher serum TBARS levels as compared to non-/placebo-treated sham-operated mutant and wild-type mice and even 2.4-fold higher levels as compared to estradiol-treated ovariectomized mutant mice. In addition, blood glucose levels of the investigated groups correlated with lipid peroxidation in the serum, indicating that severe hyperglycaemia caused oxidative stress in non-/placebo-treated ovariectomized mutant mice. Endogenous estrogens in sham-operated non-/placebo-treated mutant mice as well as E2-treatment in ovariectomized mutants seem to prevent lipid peroxidation and probably oxidative stress. Significantly higher lipid peroxidation levels, owing to elevated free radicals, were observed in humans suffering from type 1 or type 2 diabetes mellitus (Griesmacher *et al.* 1995). Several studies accomplished on rats also demonstrated higher lipid peroxidation levels, for example in the serum of streptozotocin-induced diabetic Wistar rat (Ozansoy *et al.* 2001) and the Zucker diabetic fatty rat (Coppey *et al.* 2002).

These results confirm the potential role of elevated blood glucose concentrations to increase lipid peroxidation. Moreover, it could be shown that estrogen may directly prevent oxidative stress by blocking JNK-activity (Srivastava *et al.* 1999) and it can also protect  $\beta$ -cells after streptozotocin exposure via extranuclear mechanisms through mainly ER $\alpha$  and additional in a GPER dependent manner. Furthermore,

estrogen was shown to exhibit antioxidative effects by up-regulating the expression of mitochondrial superoxide dismutase and glutathione peroxidase via binding to the estrogen receptor and activation of the MAPK pathway (Viña *et al.* 2005).

Estrogen therefore may lead to the significantly lower lipid peroxidation in sham-operated mutant and wild-type mice as well as in ovariectomized mutant mice receiving estradiol replacement therapy.

It could be shown that oxidative stress has negative impact on insulin sensitivity of adipocytes and muscle cells (Houstis *et al.* 2006, Maddux *et al.* 2001). Oxidative stress leads to the activation of multiple serine kinase cascades (Kyriakis and Avruch 1996) and potential targets of these kinases in the insulin signalling pathway include the insulin receptor (IR) and insulin receptor substrate (IRS) 1 and 2. Phosphorylation of IRS1 and IRS2 results in disturbed binding to the IR and impaired interaction with downstream target molecules with the consequence of impaired insulin action (Evans *et al.* 2002). Further, it was demonstrated in several *in vitro* and *in vivo* studies that oxidative stress reduces DNA binding activity of the transcription factors PDX-1 and MafA in  $\beta$ -cells, resulting in disturbed glucose-stimulated insulin secretion (GSIS) (Kaiser *et al.* 2003, Robertson and Harmon 2006). In addition, chronic hyperglycaemia and oxidative stress may reduce functional  $\beta$ -cell mass and lead to  $\beta$ -cell apoptosis (Kaiser *et al.* 2003).

The decreased lipid peroxidation and therefore diminished oxidative stress in non-/placebo-treated sham-operated as well as E2-treated ovariectomized mutant mice therefore may lead to an improved insulin signalling and higher insulin sensitivity in peripheral tissues as well as to an increased GSIS and reduced  $\beta$ -cell apoptosis.

## 5.4 ER-stress

### 5.4.1 Islet isolation

The isolation of pancreatic islets was accompanied by some difficulties in non-/placebo-treated ovariectomized mutant mice and some estradiol-treated ovariectomized mutant mice. Normally, islets appear brighter than exocrine tissue and are round to oval shaped, with a smooth surface. Islets of ovariectomized mutants showed almost the same colour as exocrine tissue. To improve the optical

identification of islets, mice of Group 2 were perfused with neutral red before sacrifice, thereby producing islets that are stained red. Gray *et al.* (1983) reported that intravenous given neutral red selectively stains islets in the rat, pig and dog and does not appear to affect their viability as judged by insulin secretion and transplantation (Gray *et al.* 1983). However, islets of non-/placebo-treated ovariectomized mutant mice were very fragile, leading to deformation and fragmentation. The resulting irregular shape of the fragmented islets aggravated the differentiation from exocrine pancreas clusters even more and led to a contamination of islet samples with exocrine tissue. Similar difficulties were faced during islet isolation of Akita mice, leading to a considerable contamination of islet samples with non-endocrine tissue (around 30%) (Izumi *et al.* 2003). It is documented that oxidative stress due to hyperglycaemia leads to protein oxidation in serum of type 1 diabetic patients (Ramakrishna and Jaikhanani 2007) as well as in pancreata of Cohen diabetic rats (Ryu *et al.* 2008). This suggests that the reduced stability of the islets of hyperglycaemic non-/placebo-treated ovariectomized mutant mice may be due to reactive oxygen species that interact with proteins within the peri-insular capsule.

#### **5.4.2 ER-stress markers**

Isolated islets of 210-day-old non-/placebo-treated ovariectomized mutant mice demonstrated an increased abundance of BiP and CHOP as compared to non-/placebo-treated sham-operated mutant as well as wild-type mice. Estradiol-treated ovariectomized mutant mice also exhibited a higher abundance of BiP as compared to the two sham-operated groups, but the amount was slightly less as compared to non-/placebo-treated ovariectomized mutant mice. Sham-operated non-/placebo-treated mutant and wild-type mice showed almost similar amounts of BiP and CHOP. All 4 groups demonstrated a similar abundance of p-eIF2 $\alpha$ . However, it must be taken into account that the contamination of the islet samples of ovariectomized mutant mice with exocrine pancreas tissue results in decreased islet-protein content in samples, especially of non-/placebo-treated ovariectomized mutants. This may lead to an underestimation of ER-stress associated proteins in  $\beta$ -cells of these mice and therefore Western blot analyses have to be interpreted carefully.

The three transducers of ER-stress signalling IRE1 $\alpha$ , ATF6 and PERK together emanate a transcriptional and translational program, the so called unfolded protein

response (UPR), when unfolded proteins accumulate within the ER lumen (Kaufman *et al.* 2002, Ron and Walter 2007). They are maintained in an inactivate state through interaction with the protein chaperone BiP (Bertolotti *et al.* 2000). Upon accumulation of unfolded protein, BiP is released from each sensor, leading to its activation (Scheuner and Kaufman 2008). BiP and CHOP are both induced during UPR and it could be shown that both BiP and CHOP levels were significantly elevated in islets from type 2 diabetic patients compared to non-diabetics (Laybutt *et al.* 2007). Since BiP synthesis is induced by the accumulation of mutated proteins in the ER or by a number of different stress conditions that increase aberrant protein folding (Gething and Sambrook 1992), the accumulation of misfolded proinsulin 2 in  $\beta$ -cells of Akita mice leads to the induction of BiP and other ER-stress markers. It also could be shown in islets of Akita mice that high molecular weight forms of proinsulin existed with concomitant overexpression of BiP (Wang *et al.* 1999). Therefore it was expected that Munich *Ins2*<sup>C95S</sup> mutant mice also show elevated BiP amounts in their islets because of accumulation of unfolded proinsulin 2. Due to the fact that only non-/placebo-treated and estradiol-treated ovariectomized mutant mice demonstrated a higher BiP abundance as compared to wild-type mice, it is likely that sham-operated non-/placebo-treated mutant mice were somehow protected from ER-stress. It is suggested that 17 $\beta$ Estradiol has a protective effect against ER-stress by decreasing XBP1(S) and CHOP mRNA levels (Kozlov *et al.* 2010), but the exact mechanisms are still unclear. Since estradiol-treated ovariectomized mutant mice showed only slightly less BiP abundance as compared to non-/placebo-treated ovariectomized mutant mice, it seems like other ovarian hormones or gonadal factors may have protective effects against ER-stress. The transmembrane signalling protein PERK senses the biosynthetic protein-folding load on the ER and attenuates and thereby controls the rate of mRNA translation initiation by phosphorylation of its major physiological substrate, eukaryotic initiation factor 2, on the  $\alpha$ -subunit (eIF2 $\alpha$ ) (Scheuner and Kaufman 2008). In islets of diabetic *db/db* mice, expression of various genes of the unfolded protein response (UPR) was increased including that of PeIF2 $\alpha$  compared to non-diabetic controls (Laybutt *et al.* 2007). However, the abundance of PeIF2 $\alpha$  was almost similar in all Munich *Ins2*<sup>C95S</sup> mutants and wild-type mice, speaking for the point that the mutation did not lead to a translational attenuation. These results are in accordance with the

findings in Akita mice, where mutant proinsulin does not profoundly reduce protein synthesis (Izumi *et al.* 2003).

The transcription factor CHOP (GADD153) activates downstream genes encoding proapoptotic functions (Scheuner and Kaufman 2008). In the Akita mouse, CHOP mRNA levels were much higher as compared to controls (Oyadomari *et al.* 2002). Due to the fact that non-/placebo-treated ovariectomized Munich *Ins2*<sup>C95S</sup> mutant mice showed a higher CHOP-abundance than non-/placebo-treated sham-operated mutant and wild-type mice, it appears that a substance produced from the ovaries may protect  $\beta$ -cells from ER-stress induced apoptosis mediated by CHOP (Oyadomari and Mori 2004). E2 may be such a substance, but this could not be analysed in this study because CHOP was not detectable in samples of mice from Group 2.

Taken together, the results indicate that ovariectomy enhances ER-stress in islets of Munich *Ins2*<sup>C95S</sup> mutants. However, due to the lower purity of islet extracts of mutant mice vs. wild-type mice, these data have to be interpreted carefully.

## 5.5 Qualitative and quantitative morphological investigations of the endocrine pancreas

Pancreas sections have been immunostained for insulin ( $\beta$ -cells) or simultaneously stained for glucagon, somatostatin and pancreatic polypeptide (non- $\beta$ -cells). Staining for non- $\beta$ -cells was performed due to the fact that the insulin content in islets of Munich *Ins2*<sup>C95S</sup> mutants is low and  $\beta$ -cells are severely degranulated, thereby leading to a weak staining intensity of  $\beta$ -cells for insulin (Herbach *et al.* 2007). In addition, the antibody used in studies on Akita mice only detected wild-type, but not mutant insulin (Izumi *et al.* 2003, Wang *et al.* 1999). Therefore,  $\beta$ -cells might not be identified by insulin staining, leading to an underestimation of the  $\beta$ -cell proportion in the islets of both Akita and Munich *Ins2*<sup>C95S</sup> mutant mice. Furthermore, in 4-week-old male Akita mice, the islet area stained for insulin and glucagon was documented to be less than 50% that of wild-type mice (Yoshioka *et al.* 1997). Since it is estimated that  $\delta$ - and PP-cells together account for less than about 10% of the islet area (Brissova *et al.* 2005, Herbach *et al.* 2007), it seems likely that many of the endocrine cells without detectable immunoreactivity for insulin nevertheless were  $\beta$ -cells.

### 5.5.1 Qualitative histological analyses

Pancreas sections immunostained for insulin revealed that all mutant mice demonstrated less insulin-positive cells in their islet profiles as compared to wild-type mice, with non-treated ovariectomized mutant mice featuring fewest insulin-positive cells and an all-in-all weaker staining intensity as compared to wild-type mice. Non-treated sham-operated mutant mice and E2-treated ovariectomized mutant mice seemed to possess almost similar amounts of insulin-positive cells within their islets, but exhibited more insulin positive cells than non-treated ovariectomized mutants and fewer than wild-type mice. Immunostaining for non- $\beta$ -cells demonstrated an altered islet composition in all mutant groups, especially in non-treated and estradiol-treated ovariectomized mutant mice. While wild-type mice exhibited a typical murine islet composition with a core of mainly insulin-positive cells, surrounded by a small ring of non- $\beta$ -cells, mutant mice showed an increased proportion of non- $\beta$ -cells that were dispersed all over the islet profile. Such alterations in the islet composition were also observed in other diabetic mouse models like the PERK knockout mouse (Harding *et al.* 2001) and GIPR<sup>dn</sup> transgenic mice (Herbach *et al.* 2005), irrespective of the underlying genetic manipulation. Therefore, it is considered that hyperglycaemia plays a central role in the disturbed islet composition. Nevertheless, GIPR<sup>dn</sup> transgenic mice demonstrated a disturbed islet composition already before the onset of hyperglycaemia (Herbach *et al.* 2005). Further, insulin-treated heterozygous male Munich *Ins*<sup>2C95S</sup> mutant mice, which demonstrated normalised blood glucose concentrations compared to placebo-treated heterozygous mutants, also showed an about 40% reduction of the  $\beta$ -/non- $\beta$ -cell ratio as compared to wild-type mice (Kautz 2010).

### 5.5.2 Quantitative stereological analyses

Quantitative stereological investigations were performed using state-of-the-art unbiased model-independent stereological methods (Gundersen *et al.* 1988, Wanke *et al.* 1994).

The volume density of  $\beta$ -cells in the pancreatic islets was slightly decreased in all mutant groups as compared to wild-type mice at an age of 190 days. Islets of wild-type mice comprised 87%  $\beta$ -cells, both ovariectomized non-/placebo- and estradiol-treated mutant mice exhibited 79% and sham-operated non-/placebo-treated mutants 83%  $\beta$ -cells in their islets.

The total  $\beta$ -cell volume was significantly reduced only in E2-treated mutants as compared to wild-type mice. Non-/placebo-treated ovariectomized mutants showed an about 20% and sham-operated non-/placebo-treated mutant mice an about 10% decreased total  $\beta$ -cell volume, whereas E2-treated ovariectomized mutant mice demonstrated a 53% decrease compared to wild-type mice, but this is most probably due to the significantly reduced total pancreas volume compared to all three other groups. Since the relative pancreas weight of all 4 groups was almost identical, the reduced total pancreas volume of E2-treated ovariectomized mutants most likely is a result of the reduced body weight. Remarkable is the fact that the total  $\beta$ -cell volume of 180-day-old male Munich *Ins2*<sup>C95S</sup> mutant mice was decreased by 81% compared with sex-matched wild-type mice whereas female mutants only showed a 19% decrease. This resulted in a large increase of the total volume of non- $\beta$ -cells in male mutant mice (Herbach *et al.* 2007). The differences in the total volume of  $\beta$ -cells between male and female mutant mice led to the assumption, that female mutant mice are somehow protected from changes in the islet structure and this may be due to beneficial effects of ovarian hormones or other substances produced in the ovaries. Surprisingly, ovariectomy had only a minor influence on the total volume as well as the volume density of  $\beta$ -cells in islets of Munich *Ins2*<sup>C95S</sup> mutants vs. wild-type mice and therefore it seems likely that ovarian hormones, especially 17 $\beta$ Estradiol, could not alone be responsible for the remarkable differences in the total  $\beta$ -cell volume between male and female mutants. One explanation for the only minor decrease in total  $\beta$ -cell volume in non-/placebo-treated ovariectomized mutants compared with sham-operated non-/placebo-treated mutants may be extraovarian production of ovarian hormones/substances in ovariectomized mutant mice. It is known that in women of reproductive age, estradiol formation takes place in a number of tissues such as subcutaneous fat and skin or other physiological and pathological sites, such as the hypothalamus or breast cancer cells (Hemsell *et al.* 1974). The extraovarian estradiol production therefore is more pronounced in obese women because of increased mass of adipose tissue and skin (Bulun *et al.* 1999). Thus it may be possible that non-/placebo-treated ovariectomized mutant mice profit from extraovarian estradiol production, particularly due to increased body fat, and this may account for the almost similar volume density of  $\beta$ -cells in non-/placebo- and E2-treated ovariectomized mutants. Moreover it is

known that testosterone can be converted of the precursor androstenedione in extraovarian tissues, accounting for two thirds of testosterone production in reproductive-age women (Bardin and Lipsett 1967). It could be shown that testosterone treatment was able to reduce streptozotocin induced apoptosis of pancreatic  $\beta$ -cells in castrated male Wistar rats (Morimoto *et al.* 2005). If such beneficial effects of testosterone also play a role in female animals remains unclear. Another study on partial pancreatectomized ovariectomized female OLETF rats could demonstrate that testosterone supplementation has no positive effect on pancreatic  $\beta$ -cell mass (Zhu *et al.* 1998).

The volume density of non- $\beta$ -cells in the islets was about 65% increased in non-/placebo- and E2-treated ovariectomized mutant mice and about 33% increased in non-/placebo-treated sham-operated mutant mice as compared to wild-type mice. The total volume of non- $\beta$ -cells of non-/placebo-treated ovariectomized and sham-operated mutant mice was about 50% and 35% increased as compared to wild-type mice, respectively. In contrast, E2-treated ovariectomized mutant mice demonstrated a similar total non- $\beta$ -cell volume as wild-type mice but this is most likely due to the lower pancreas volume of E2-treated ovariectomized mutant mice compared to mice of the 3 other groups (see above). In male mutant mice, the total volume of non- $\beta$ -cells was also increased, and insulin-treatment could reduce the total volume of non- $\beta$ -cells to an amount comparable with male wild-type mice (Kautz 2010), indicating that chronic hyperglycaemia may lead to an increased differentiation and development of non- $\beta$ -cells. Herbach *et al.* (2007) could show that most of the non- $\beta$ -cells of both male and female Munich *Ins2*<sup>C95S</sup> mutant mice represented  $\alpha$ -cells (Herbach *et al.* 2007). Investigations in several other diabetic animal models like in the PERK knockout mouse (Harding *et al.* 2001) or in the GIPR<sup>dn</sup> transgenic mouse (Herbach *et al.* 2005) affirm this observation by showing a disturbed islet composition, irrespective of the underlying causative mutation. Moreover, morphometric analyses in humans suffering from type 2 diabetes demonstrated an increased  $\alpha$ -cell fraction in pancreatic islets (Yoon *et al.* 2003).

Several studies could demonstrate that long-term hyperglycaemia reduces the concentration of PDX-1 mRNA as well as PDX-1 DNA binding activity in pancreatic  $\beta$ -cells, which is essential for  $\beta$ -cell development and maintenance (Melloul 2004, Robertson and Harmon 2006). Moreover, it was shown that inhibition of

*Pdx-1* expression results in increased volume density of glucagon positive cells that are homogeneously distributed all over the islet (Lottmann *et al.* 2001) in the same manner like it was seen in mutant mice in this study. It also could be shown *in vitro* that inhibition of *Pdx-1* expression in insulin expressing INSR $\beta$  cells leads to 5- to 10-fold increased levels of glucagon mRNA and largely reduced transcription of the insulin gene. The suppression of *Pdx1* converts the insulin-producing  $\beta$ -cell lineage to an  $\alpha$ -cell-dominated phenotype with over 90% glucagon positive cells in the whole cell population (Wang *et al.* 2001). In addition, the  $\beta$ -cell-specific disruption of *Pdx-1* *in vivo* shifted the  $\beta$ -/ $\alpha$ -cell ratio from physiologically 5:1 to 1:1 (Ahlgren *et al.* 1998). All these findings lead to the assumption, that chronic hyperglycaemia may restrain  $\beta$ -cell development and may increase the differentiation of glucagon expressing  $\alpha$ -cells from common progenitor cells. Moreover, it seems to be possible that  $\alpha$ -cells arise from existing  $\beta$ -cells via trans-differentiation, leading to the altered  $\beta$ - to non- $\beta$ -cell ratio as well as to the higher total volume of non- $\beta$ -cells existent in islets of Munich *Ins2*<sup>C95S</sup> mutant mice. Non-/placebo-treated as well as E2-treated ovariectomized mutant mice demonstrated a markedly decreased  $\beta$ -/non- $\beta$ -cell ratio of about 4:1 compared to sham-operated mutant mice with a ratio of about 6:1 and wild-type mice demonstrating a  $\beta$ -/non- $\beta$ -cell ratio of about 7:1. Chronic hyperglycaemia would explain the altered islet architecture in placebo-treated ovariectomized mutant mice, but it is questionable why E2-treated ovariectomized mutant mice, which did not demonstrate hyperglycaemia, showed the same decrease in the  $\beta$ -/non- $\beta$ -cell ratio as non-/placebo-treated ovariectomized mutant mice from over 40% as compared to wild-type mice. Therefore, chronically elevated blood glucose levels do not seem to be the only reason for the altered islet architecture in ovariectomized Munich *Ins2*<sup>C95S</sup> mutant mice. This assumption is in line with observations made in insulin-treated male heterozygous Munich *Ins2*<sup>C95S</sup> mutant mice and GIPR<sup>dn</sup> transgenic mice, where altered islet composition was also apparent in the absence of hyperglycaemia (Herbach *et al.* 2005; Kautz 2010). In Munich *Ins2*<sup>C95S</sup> mutant mice, long-term ER-stress, caused by unfolded proinsulin 2, may lead to reduced total  $\beta$ -cell volume in Munich *Ins2*<sup>C95S</sup> mutant mice, via programmed cell death (Herbach *et al.* 2007), thereby explaining a shift towards non- $\beta$ -cells. Taken together, the findings suggest that 17 $\beta$ Estradiol has no positive effects on islet composition of ovariectomized Munich *Ins2*<sup>C95S</sup> mutants. The ovaries produce

several steroid hormones, including pregnenolone, progesterone, 17 $\alpha$ -hydroxyprogesterone, dehydroepiandrosterone (DHEA), androstenedione, testosterone, estrone, and estradiol. Moreover a large number of peptides that can act in an intracrine, autocrine, paracrine, or endocrine fashion are produced. These include numerous growth factors (e.g., insulin-like growth factors (IGFs)) and cytokines (e.g., interleukin-1b) (Bulun and Adashi 2008).

A direct effect of progesterone on the islets of Langerhans may be possible in intact female rats, as both the pancreatic  $\alpha$ - and  $\beta$ -cells of these animals possess progesterone receptors (El Seifi *et al.* 1981). It could be shown that progesterone can increase proliferation of both  $\alpha$ - and  $\beta$ -cells within the pancreatic islets of intact male and female Wistar rats, but not the number of single insulin- or glucagon-containing cells outside the pancreatic islet, suggesting that progesterone does not stimulate differentiation of duct cells into endocrine cells. These effects were not apparent in progesterone treated gonadectomized male and female rats, suggesting that the gonads play an essential role in the genesis of the proliferative effect of progesterone (Nieuwenhuizen *et al.* 1999). An explanation for this may be the observation that ovariectomy leads to the loss of progesterone binding sites within pancreatic islets (El Seifi *et al.* 1981). Therefore it is suggested that the treatment with progesterone has an indirect effect and is mediated by (some) gonadal factor(s) (Nieuwenhuizen *et al.* 1999). Such factors may be insulin-like growth factors-1 and -2 (IGF1 and IGF2) because they are known to be capable of stimulating pancreatic islet-cell proliferation (Hill and Hogg 1991, Nieuwenhuizen *et al.* 1999).

On the other hand, Picard *et al.* (2002) reported that 12-week-old progesterone receptor knock-out mice (PR<sup>-/-</sup>) demonstrated an almost two-fold increased  $\beta$ -cell number due to a higher rate of  $\beta$ -cell proliferation (Picard *et al.* 2002). These findings about the effects of progesterone *per se* are contradictory to the effects mediated most likely through gonadal factors. Therefore it is not clear if progesterone is the causative hormone responsible for the unaltered islet architecture and  $\beta$ -cell mass observed in female mutant mice.

Today there is evidence that the endocrine pancreas represents a dynamic, in adult life slowly renewing tissue and  $\beta$ -cell mass is determined by the balance between proliferation/neogenesis and apoptosis under physiological conditions as well as in

response to varying secretory demand (Ackermann and Gannon 2007, Bonner-Weir 2001). Beta-cell mass is increased by differentiation of new  $\beta$ -cells from progenitor cells within pancreatic ducts (neogenesis), replication of  $\beta$ -cells within existing islets (proliferation) or by increase of the size of existing  $\beta$ -cells (hypertrophy), whereas decrease in  $\beta$ -cell mass arises primarily through apoptosis and  $\beta$ -cell atrophy (Ackermann and Gannon 2007, Butler *et al.* 2003).

Isolated  $\beta$ -cells in the pancreas are considered as a parameter for new islet formation and are defined as single, scattered insulin positive cells, endocrine cells budding from epithelium of pancreatic ducts and extra-islet insulin positive cell-clusters up to 4 cells (EICs) (Bonner-Weir 2001, Kauri *et al.* 2007). The volume density and total volume of isolated  $\beta$ -cells was significantly decreased in all 3 mutant mice groups as compared to wild-type mice. These data suggest that the slightly reduced  $\beta$ -cell mass in female mutants is particularly due to impaired islet neogenesis. In contrast, it could be shown that insulin treatment in male Munich *Ins2*<sup>C95S</sup> mutant mice led to a significantly higher total volume of isolated  $\beta$ -cells as compared to non-/placebo-treated mutant mice (Kautz 2010). Chronic severe hyperglycaemia can lead to reduced *Pdx1* expression, resulting in reduced differentiation of progenitor cells to  $\beta$ -cells and therefore decreased total volume of isolated  $\beta$ -cells. It was expected that sham-operated non-/placebo-treated mutant mice and E2-treated ovariectomized mutant mice, which both showed only mild or even no hyperglycaemia, would demonstrate a higher total volume and volume density of isolated  $\beta$ -cells as compared to severe hyperglycaemic non-/placebo-treated ovariectomized mutant mice, but surprisingly all three mutant groups showed similar values. Therefore, ER-stress, rather than hyperglycaemia may be responsible for altered islet neogenesis of female Munich *Ins2*<sup>C95S</sup> mutant mice.

The cell proliferation marker PCNA was used in Western blot analyses to detect  $\beta$ -cell replication. Non-/placebo-treated ovariectomized mutant mice showed a more than 50% decreased pancreatic islet abundance of PCNA as compared to wild-type mice whereas non-/placebo-treated sham-operated mutant mice demonstrated only a 12% decrease. Although E2-treatment of ovariectomized mutant mice led to a 35% higher PCNA-abundance as compared to non-/placebo-treatment, PCNA-levels were about 25% lower as compared to sham-operated mutants.

Various factors are already known to be involved in regulating  $\beta$ -cell mass (Ackermann and Gannon 2007), but since glucose and insulin are known to be potent stimulators of  $\beta$ -cell mass expansion *in vitro* (Guillen *et al.* 2008, Schuppin *et al.* 1993) as well as *in vivo* (Paris *et al.* 2003) it seems that glucose metabolism and insulin-signalling pathways play a central role in expansion of the endocrine pancreas. It could be shown that glucose infusion in mice over 4 days, leading to mild sustained increase in circulating blood glucose and insulin levels, resulted in a marked increase in  $\beta$ -cell replication as compared to mice infused with saline. The replication rate of existing  $\beta$ -cells increased in a dose dependent relationship with glucose concentration, while  $\beta$ -cell size and islet number remained unchanged and markers of neogenesis remained unaltered. It is suggested that cyclin D2 may be involved in postnatal glucose-induced compensatory  $\beta$ -cell expansion (Alonso *et al.* 2007). The mild hyperglycaemia apparent in sham-operated non-/placebo-treated mutant mice could therefore be a stimulus for  $\beta$ -cell replication and may explain the higher PCNA-abundance compared to the two other mutant mouse groups.

In addition, long-term severe hyperglycaemia can lead to  $\beta$ -cell apoptosis, resulting in a decreased total  $\beta$ -cell mass most likely due to the effect of glucotoxicity (Donath *et al.* 1999). The detection of apoptosis in pancreatic islets revealed that only placebo-treated ovariectomized mutant mice showed apoptotic events as evidenced by Western blot analysis of the inactive and active form of Caspase-3. This could be explained by the influence of severe chronic hyperglycaemia apparent in these mice. However, apoptotic events could only be demonstrated in islets from one mouse and it is known that detection and quantification of apoptosis in  $\beta$ -cells is associated with several difficulties. Although the process of  $\beta$ -cell destruction is extended over weeks or months, only very few apoptotic  $\beta$ -cells are likely to be observable even in mouse models of severe  $\beta$ -cell destruction (Augstein *et al.* 1998, O'Brien *et al.* 1996). One reason could be the short duration of apoptotic events with only few minutes elapsing from initiation to complete disintegration of the cell (Butler *et al.* 2003) as well as the rapid clearance by macrophages, which makes it difficult to quantify programmed cell death (Izumi *et al.* 2003, Weir *et al.* 2001). Moreover, only one time point to detect apoptosis in  $\beta$ -cells may not be representative for the real rate of programmed cell death in the analysed tissue

(Donath and Halban 2004, Huerta *et al.* 2007). However, since  $\beta$ -cell mass was not significantly reduced in female Munich  $Ins2^{C95S}$  mutant mice, islet-cell apoptosis may not be of great relevance in these mice.

Taken together, the results reveal that 17 $\beta$ Estradiol alone has no protective effects on  $\beta$ -cell survival of ovariectomized female Munich  $Ins2^{C95S}$  mutant mice. Rather it seems that other hormones or substances produced in the ovaries of sham-operated mutant mice may lead to the marginally increased total  $\beta$ -cell volume vs. non-/placebo- and E2-treated ovariectomized mutants. Nevertheless, ovarian substances alone could not explain the great differences concerning  $\beta$ -cell mass between male and female mutant mice.

## 5.6 Electron microscopic findings in $\beta$ -cells

Electron microscopic investigations in 190-day-old mice of all 4 groups revealed that the different staining intensities of  $\beta$ -cells observed in pancreas sections immunostained for insulin, can be attributed to a different insulin granule density within the  $\beta$ -cells. Moreover, the altered islet structure, concerning number and distribution of non- $\beta$ -cells was also in line with the immunohistochemical results.

Wild-type mice showed  $\beta$ -cells that are densely packed with typical insulin secretory granules, whereas non-/placebo-treated ovariectomized mutant mice featured many  $\beta$ -cells containing very small amounts of secretory granules. Although non-/placebo-treated sham-operated and E2-treated ovariectomized mutant mice also demonstrated several  $\beta$ -cells that were almost degranulated, they nevertheless seemed to exhibit more  $\beta$ -cells with a granule density comparable to wild-type mice. In contrast, insulin secretory granules were almost missing in male heterozygous Munich  $Ins2^{C95S}$  mutant mice and the remaining granules appeared smaller than those of male wild-type mice (Herbach *et al.* 2007; Kautz 2010).

The insulin granule density is influenced by several factors such as the rate of insulin gene transcription, insulin mRNA translation, (pro-)insulin processing as well as intracellular (pro-)insulin degradation. Moreover, discrepancy between insulin production and insulin secretion might lead to different granule density in pancreatic  $\beta$ -cells. The serum insulin levels measured 10 minutes after glucose stimulus showed that E2-treated ovariectomized mutant mice were able to release marginally more insulin into the blood stream than mice of the two other mutant groups, whereas non-/placebo-treated ovariectomized mutants demonstrated the lowest insulin

secretion. This leads to the assumption that either E2-treated mutants possess more insulin granules that can be secreted after glucose stimulus or the secretion of existing granules is more effective. The latter seems to be likely since it is known that estrogen can potentiate insulin secretion after glucose stimulus (see above). Due to the fact that non-/placebo-treated ovariectomized mutant mice demonstrated a low granule density in almost every  $\beta$ -cell and E2-treated ovariectomized mutants exhibited several  $\beta$ -cells with a high amount of secretory granules, it seems likely that E2-treated ovariectomized mutant mice also benefit from the higher amount of granules that can be secreted. Moreover, it seems likely that physiological E2 levels do not have the same effect on potentiating insulin secretion like high-dose E2-treatment, since sham-operated non-/placebo-treated mutant mice exhibited similar amounts of secretory granules in the  $\beta$ -cells as compared to E2-treated ovariectomized mutant mice but showed lower serum insulin levels after glucose stimulus.

One reason for the reduced amount of insulin granules in non-/placebo-treated ovariectomized mutant mice in comparison to the two other mutant mice groups might be the influence of chronically high blood glucose concentrations and, therefore, oxidative stress that may result in reduced *Ins* expression due to decreased insulin promoter binding activity of PDX-1 and other transcription factors, such as MafA (Andrali *et al.* 2008, Melloul 2004, Melloul *et al.* 2002). It also could be shown that insulin mRNA was reduced after long-term glucose incubation of HIT-T15 cells and this effect could be partially prevented by co-incubation with antioxidants (Tanaka *et al.* 1999). Since E2-treated ovariectomized mutant mice showed normoglycaemia and sham-operated non-/placebo-treated mutant mice showed only mild hyperglycaemia, another reason for the severe depletion of insulin granules within the  $\beta$ -cells of these two mouse groups must exist. ER-stress is known to reduce mRNA translation via phosphorylation of eIF2 $\alpha$  (Sundar Rajan *et al.* 2007). The results of Western blot analyses showed no significant difference of PeIF2 $\alpha$  abundance between the 4 groups, indicating that insulin mRNA translation is not reduced in mutant mice. In concordance with this, measurement of total insulin mRNA in isolated islets of 8- to 12-week-old Akita mice showed that mutant proinsulin 2 was transcribed to similar degree as wild-type insulin, although PeIF2 $\alpha$  was not analysed (Wang *et al.* 1999). As a response to ER-stress, the so called ER-

associated protein degradation (ERAD) eliminates misfolded protein to preserve the functionality of the endoplasmic reticulum (Scheuner and Kaufman 2008). It could be shown that HRD1, a component of the ERAD system, is upregulated in pancreatic islets of the Akita mouse and enhances intracellular degradation of misfolded and accumulated proinsulin (Allen *et al.* 2004). Therefore, it seems likely that the misfolded (pro)insulin 2, of Munich *Ins2*<sup>C95S</sup> mutants might also be degraded and leads, at least in part, to the reduced density of secretory granules.

Another indicator for existing ER-stress in  $\beta$ -cells is the presence of dilated endoplasmic reticulum. This is most clearly apparent in non-/placebo-treated ovariectomized mutant mice, where almost every  $\beta$ -cell featured dilated ER-structures. Although the dilatation of the ER was not as pronounced in E2-treated ovariectomized and sham-operated non-/placebo-treated mutant mice as compared to non-/placebo-treated ovariectomized mutants, it was nevertheless also existent in several  $\beta$ -cells. Male heterozygous Munich *Ins2*<sup>C95S</sup> mutant mice showed an even more pronounced disorganization of the rough endoplasmic reticulum, appearing as dilated cisterna, as compared to non-/placebo-treated ovariectomized female mutant mice (Herbach *et al.* 2007; Kautz 2010). Further, remarkable dilated ER was also seen in Akita mice (Wang *et al.* 1999). In general, conditions that disrupt metabolic homeostasis and protein-folding can cause distension of the ER cisternae, with the consequence that the ER is not longer able to fulfil protein-folding and -processing. Therefore, ER distension has become a hallmark for cells that exhibit defective protein-folding in the ER lumen and is observed in response to pharmacological induction of ER-stress, genetically impaired N-linked glycosylation, enhanced mRNA translation, or expression of proteins that are subject to misfolding (Scheuner and Kaufman 2008). The dilated structures that were apparent in all Munich *Ins2*<sup>C95S</sup> mutant mice mostly represent dilated rough ER that is found throughout the cytoplasm and, to a lower degree, pre-Golgi intermediates that are located in close association to the Golgi complex. Electron dense material, like it was observable in the ER lumen of male mutant mice (Kautz 2010), could also be identified to a lower degree in female mutants. It was shown in the Akita mouse that this electron dense material is composed of accumulated proinsulin (Zuber *et al.* 2004). Therefore, the observed electron dense material observed in Munich *Ins2*<sup>C95S</sup> mutant mice most likely is a result of accumulated proinsulin 2.

Taken together, the lower amount of insulin granules visible in all three mutant mouse groups, most probably results from a combination of reduced *Ins2* gene expression due to chronically elevated blood glucose levels and due to ER-stress caused by misfolded and accumulated proinsulin 2. Since in E2-treated ovariectomized and non-/placebo-treated sham-operated mutant mice hyperglycaemia is not as severe as in non-/placebo-treated ovariectomized mutant mice, ER-stress may probably be the main cause for the reduced granule density. 17 $\beta$ Estradiol seems to exert positive effects on the total amount of insulin granules through several mechanisms such as decrease of blood glucose concentrations and the assumed protective effect in the presence of ER-stress. Due to the fact that sham-operated mutant mice presented a marginally higher secretory granule density in  $\beta$ -cells than E2-treated ovariectomized mutant mice, it may be possible that other ovarian hormones or non-steroidal substances produced and secreted from the ovaries may also exert positive effects on the total amount of secretory granules.

The electron-microscopical observations also demonstrated that mice of all three mutant groups demonstrated several  $\beta$ -cells that contained enlarged mitochondria. In male heterozygous Munich *Ins2*<sup>C95S</sup> mutant mice, mitochondrial swelling was also observed, though to a much higher degree and additionally mitochondria showed largely destroyed crests and myelin figures (Herbach *et al.* 2007; Kautz 2010). It is documented that oxidative stress and also ER-stress can increase the permeability of the inner mitochondrial membrane and alter its potential (Kanwar *et al.* 2007), leading to mitochondrial swelling and release of cytochrome c and as a result to the activation of apoptotic mitochondrial pathways (Jiang *et al.* 2001, Zhang *et al.* 2008). Since all mutant mice most likely suffer from ER-stress and placebo-treated ovariectomized mutant mice also from severe chronic hyperglycaemia, it is probably that the alterations in mitochondrial appearance result from activated apoptotic mitochondrial pathways.

## 5.7 Conclusion

The findings in this study demonstrate that ovariectomy leads to severe deterioration of glucose homeostasis in Munich *Ins2*<sup>C95S</sup> mutant mice, which can be completely normalised by E2 replacement therapy. Therefore, the hypothesis of beneficial effects of E2 on insulin secretion and insulin sensitivity was proven in Munich *Ins2*<sup>C95S</sup> mutant mice, thereby explaining the different diabetic phenotypes of male

and female mutant mice. In contrast, ovariectomy did not significantly alter total islet or  $\beta$ -cell volumes but severely disturbed islet composition, which could not be prevented by E2 replacement therapy. This shows that chronic hyperglycaemia does not induce severe  $\beta$ -cell loss in ovariectomized female mutants like it was observed in male mutants, leading to the assumption that other hormones or factors produced in the ovaries and/or the whole female body, but not  $17\beta$ Estradiol, are responsible for preserved  $\beta$ -cell mass. As evidenced by electron microscopy, ovariectomy seems to lead to increased ER-stress in pancreatic  $\beta$ -cells of mutant mice vs. sham-operated mutant mice, which can be ameliorated by E2 supplementation.

In the last years, several *INS* mutations that lead to conformational changes of the insulin molecule were described in humans as a new monogenic cause of permanent neonatal diabetes. The Munich *Ins2*<sup>C95S</sup> mutant mouse therefore represents an essential tool to further investigate the influence of *INS* mutations on the development of diabetes mellitus as well as to develop new treatment strategies.

## 6 Perspective

Since  $17\beta$ Estradiol was shown to fail to protect ovariectomized Munich *Ins2*<sup>C95S</sup> mutants from ER-stress and  $\beta$ -cell loss, the influence of other hormones such as progesterone or testosterone or of other substances produced in the ovaries, e.g. growth factors such as IGF1 and IGF2, on  $\beta$ -cell survival should be examined in female Munich *Ins2*<sup>C95S</sup> mutant mice.

In order to get further insights into the role of ER-stress in the pathogenesis of diabetes mellitus and the protective effects of ovarian hormones/substances in female Munich *Ins2*<sup>C95S</sup> mutant mice, treatment of ovariectomized mutant mice with chemical chaperones, like 4-phenyl butyric acid or tauroursodeoxycholic acid, which increase ER folding capacity, would be useful.

To examine the role of estrogen and the estrogen receptors in ER-stress and  $\beta$ -cell loss it would be helpful to cross Munich *Ins2*<sup>C95S</sup> mutant mice with estrogen-receptor knock out mice ( $\alpha$ ERKO,  $\beta$ ERKO or  $\alpha\beta$ ERKO mice). Moreover it would be interesting to use selective estrogen receptor modulators (SERMs) such as propyl-pyrazole-triol (PPT) for ER $\alpha$  and diarylpropionitrile (DPN) for ER $\beta$  to examine the estrogenic effects on the appropriate receptors.

## 7 Summary

### **Impact of 17 $\beta$ Estradiol on $\beta$ -cell survival of female Munich *Ins2*<sup>C95S</sup> mutant mice**

Munich *Ins2*<sup>C95S</sup> mutant mice were generated within the Munich ENU mouse mutagenesis project and exhibit a point mutation in the insulin 2 gene. In recent years, several mutations in the INS gene were also observed in humans, leading to early onset of diabetes with severe hyperglycaemia.

It could be shown that male Munich *Ins2*<sup>C95S</sup> mutant mice develop a severe progressive diabetic phenotype with profound loss of functional  $\beta$ -cell mass, whereas female mutants only showed mild glucose intolerance throughout life and no  $\beta$ -cell loss. The aim of this study was to investigate the impact of 17 $\beta$ Estradiol (E2) on the development of diabetes mellitus and  $\beta$ -cell survival in female Munich *Ins2*<sup>C95S</sup> mutant mice. For this purpose, female mutant mice were ovariectomized and received either 17 $\beta$ Estradiol replacement therapy via subcutaneous E2 long-term pellets or non-treatment/placebo pellet. Non-/placebo-treated sham-operated mutant and wild-type mice served as controls. Clinical parameters, such as fasted and randomly fed blood glucose concentration, oral glucose tolerance, insulin sensitivity, glucose induced insulin secretion as well as fasted serum insulin concentration were determined. Moreover, serum was analysed with regard to oxidative-stress and isolated pancreatic islets were used to determine ER-stress markers. Qualitative histological and quantitative stereological analyses of the pancreas were performed, and  $\beta$ -cell apoptosis as well as  $\beta$ -cell replication were determined.

Ovariectomy without E2 supplementation led to the development of a severe and progressive diabetic phenotype. The supplementation of 17 $\beta$ Estradiol after ovariectomy normalised blood glucose concentrations of female mutant mice to the level of wild-type mice.

Both, E2-treated ovariectomized and non-/placebo-treated sham-operated mutant mice, demonstrated an improved oral glucose tolerance, preserved insulin sensitivity and higher glucose induced insulin secretion as compared to non-/placebo-treated ovariectomized mutant mice. However, mice of all three mutant groups showed a severely disturbed glucose-stimulated insulin secretion as compared to wild-type

controls, indicating that the mutation in *Ins2* and the resulting misfolding of proinsulin 2 leads to disturbed insulin secretion.

In addition, it could be shown that the normalised or only mildly increased blood glucose concentrations of E2-treated ovariectomized and non-/placebo-treated sham-operated mutant mice led to reduced oxidative stress, as evidenced by significantly reduced malondialdehyde serum levels.

Non-/placebo- and E2-treated ovariectomized mutant mice exhibited a lower total volume and volume density of  $\beta$ -cells in the islets as well as a lower  $\beta$ -cell/non- $\beta$ -cell ratio as compared to sham-operated non-/placebo-treated mutants, indicating that ovarian hormones/substances, other than 17 $\beta$ Estradiol, are responsible for the preserved  $\beta$ -cell mass of female Munich *Ins2*<sup>C95S</sup> mutants. Since the abundance of the ER-stress marker BIP was only increased in non-/placebo- and E2-treated mutant mice but not in sham-operated non-/placebo-treated mutant mice, ER-stress is likely to be responsible for reduced  $\beta$ -cell mass, and a substance produced in the ovaries other than E2 seems to protect sham-operated mutant mice from ER-stress.

Since the volume density of isolated  $\beta$ -cells in the pancreas, which indicate islet neogenesis, was decreased in an almost identical manner in all three mutant groups as compared to wild-type mice, decreased islet neogenesis may explain the reduced  $\beta$ -cell mass apparent in all mutant mice.

Ultrastructural changes in the  $\beta$ -cells were most prominent in placebo-treated ovariectomized mutant mice. Nevertheless, all mutant mice demonstrated accumulation of electron dense material in the dilated endoplasmic reticulum, suggesting that ER-stress is existent not only in ovariectomized, but also to a lower degree in sham-operated mutant mice.

In conclusion, 17 $\beta$ Estradiol could ameliorate the diabetic phenotype by improving insulin secretion and insulin sensitivity but did not prevent ER-stress or loss of functional  $\beta$ -cell mass in ovariectomized Munich *Ins2*<sup>C95S</sup> mutant mice, suggesting that ovarian hormones/substances other than E2, or other substances produced in the whole female body, prevent female Munich *Ins2*<sup>C95S</sup> mutant mice from ER-stress and  $\beta$ -cell loss.

## 8 Zusammenfassung

### **Einfluss von 17 $\beta$ Estradiol auf das Betazellüberleben von weiblichen Munich *Ins2*<sup>C95S</sup> Mausmutanten**

Munich *Ins2*<sup>C95S</sup> Mausmutanten wurden innerhalb des Münchner ENU-Maus-Mutagenese Projektes generiert und weisen eine Punktmutation im Insulin 2 Gen auf. In den letzten Jahren wurden verschiedene Insulingenmutationen beim Menschen beobachtet, welche zu einem früh einsetzenden Diabetes mellitus führen. Männliche heterozygote Munich *Ins2*<sup>C95S</sup> Mausmutanten zeigten einen hochgradigen Verlust funktioneller Betazellmasse und entwickelten einen schwerwiegenden, progressiven diabetischen Phänotyp, wohingegen weibliche Mutanten nur eine milde Glukose-Intoleranz aufwiesen und kein deutlicher Betazellverlust nachzuweisen war. In dieser Studie sollte der Einfluss von 17 $\beta$ Estradiol (E2) auf die Entwicklung von Diabetes mellitus sowie den Betazellverlust bei weiblichen Munich *Ins2*<sup>C95S</sup> Mausmutanten untersucht werden. Um die Effekte von 17 $\beta$ Estradiol zu analysieren wurden weibliche heterozygote Mutanten ovariectomiert und erhielten anschließend entweder eine 17 $\beta$ Estradiol Ersatztherapie mittels subkutaner Implantation von 17 $\beta$ Estradiol Langzeit-Pellets, ein entsprechendes Placebo oder keine Therapie. Nicht-/Placebo-behandelte schein-ovariectomierte heterozygote Mutanten sowie Wildtyptiere dienten als Kontrollen. Es wurden klinische Parameter wie Blutglukosekonzentration, Insulinsensitivität, Glukose-stimulierte Insulinsekretion, sowie Nüchtern-Seruminsulinspiegel bestimmt und orale Glukosetoleranztests durchgeführt. Des Weiteren wurde Serum zur Ermittlung von oxidativem Stress untersucht sowie an isolierten pankreatischen Inseln verschiedene Marker für endoplasmatischen Retikulum-Stress (ER-Stress) detektiert. Die Komposition des endokrinen Pankreas wurde qualitativ histologisch und mittels quantitativ stereologischer Methoden untersucht und darüber hinaus wurden Betazell-Apoptose- und -Zellproliferationsraten ermittelt.

Ovariectomie ohne E2-Supplementierung führte zur Ausbildung eines schwerwiegenden diabetischen Phänotyps, wohingegen eine 17 $\beta$ Estradiol Ersatztherapie die Blutglukosekonzentrationen auf das Niveau von Wildtyptieren senken konnte. Sowohl Schein-Ovariectomie als auch E2-Supplementierung nach

Ovariectomie führten zu einer verbesserten Glukosetoleranz, einer erhaltenen Insulinsensitivität und einer erhöhten Glukose-stimulierten Insulinsekretion im Vergleich zu Nicht-/Placebo-behandelten ovariectomierten Mutanten. Dennoch zeigten alle heterozygoten Mutanten im Vergleich zu den Wildtyptieren eine hochgradig gestörte Insulinsekretion nach Glukosestimulation.

Anhand der signifikant niedrigeren Malondialdehyd-Serumwerte konnte gezeigt werden, dass die Normalisierung der Blutglukosekonzentrationen E2-supplementierter ovariectomierter Mutanten sowie die nur leicht erhöhten Werte der schein-ovariectomierten Mutanten darüber hinaus zu einer Reduktion des oxidativen Stress im Vergleich zu Nicht-/Placebo-behandelten ovariectomierten Mutanten führten.

Nicht-/Placebo-behandelte und E2-supplementierte Mutanten wiesen beide ein niedrigeres Gesamtbetazellvolumen, eine reduzierte Volumendichte von Betazellen in den Inseln sowie ein erniedrigtes Betazell- zu Nicht-Betazell-Verhältnis im Vergleich zu schein-ovariectomierten Mutanten auf, was darauf hindeutet, dass Ovarhormone oder andere Substanzen die in den Ovarien produziert werden, nicht aber 17 $\beta$ Estradiol, zum Schutz der Betazellen bei weiblichen Munich *Ins2*<sup>C95S</sup> Mausmutanten beitragen. Da die Abundanz des ER-Stress-Markers BiP nur bei Nicht-/Placebo-behandelten und E2-supplementierten ovariectomierten, nicht aber bei schein-ovariectomierten Mutanten erhöht war, scheint es wahrscheinlich, dass ER-Stress für das reduzierte Betazellvolumen verantwortlich ist und demzufolge andere in den Ovarien produzierte Substanzen als 17 $\beta$ Estradiol schein-ovariectomierte Mutanten vor ER-Stress schützen.

Da außerdem die Volumendichte und das Gesamtvolumen isolierter Betazellen, beides Indikatoren für Inselneogenese, bei allen drei Mutantengruppen in annähernd gleicher Weise im Vergleich zu Wildtyptieren reduziert war, könnte dies als Erklärung für die reduzierte Betazellmasse von heterozygoten Munich *Ins2*<sup>C95S</sup> Mausmutanten dienen.

Ultrastrukturelle Veränderungen der Betazellen waren bei Nicht-/Placebo-behandelten ovariectomierten Mutanten am deutlichsten ausgeprägt. Trotzdem zeigten Tiere aller drei Mutantengruppen eine Anreicherung elektronendichten Materials im dilatierten endoplasmatischen Retikulum was zu der Annahme führt, dass nicht nur Nicht-/Placebo-behandelte ovariectomierte Mutanten ER-Stress

aufweisen, sondern auch E2-supplementierte ovariektomierte und schein-ovariektomierte Tiere zu einem geringeren Grad davon betroffen sind.

Zusammenfassend kann gesagt werden, dass  $17\beta$ Estradiol durch eine Steigerung der Insulinsekretion und Insulinsensitivität zwar den diabetischen Phänotyp verbessern kann, dennoch aber nicht in der Lage ist, vor ER-Stress zu schützen und den durch Ovariektomie gesteigerten Betazellverlust zu verhindern. Deshalb wird vermutet, dass Substanzen, die in den Ovarien oder eventuell auch im gesamten weiblichen Körper produziert werden, nicht aber  $17\beta$ Estradiol, weibliche Munich *Ins2*<sup>C95S</sup> Mutanten vor ER-Stress und Betazellverlust schützen.

## 9 References

- Ackermann, A. M. and Gannon, M. (2007), "Molecular Regulation of Pancreatic Beta-Cell Mass Development, Maintenance, and Expansion", *J Mol Endocrinol*, 38, 193-206.
- Ackermann, S., Hiller, S., Osswald, H., Losle, M., Grenz, A. and Hambrock, A. (2009), "17beta-Estradiol Modulates Apoptosis in Pancreatic Beta-Cells by Specific Involvement of the Sulfonylurea Receptor (Sur) Isoform Sur1", *J Biol Chem*, 284, 4905-4913.
- American Diabetes Association (ADA) (2003), "Report of the Expert Committee on the Diagnosis and Classification of Diabetes Mellitus", *Diabetes Care*, 26 Suppl 1, S5-20.
- American Diabetes Association (ADA) (2009), "Diagnosis and Classification of Diabetes Mellitus", *Diabetes Care*, 32 Suppl 1, S62-67.
- Ahima, R. S., Prabakaran, D., Mantzoros, C., Qu, D., Lowell, B., Maratos-Flier, E. and Flier, J. S. (1996), "Role of Leptin in the Neuroendocrine Response to Fasting", *Nature*, 382, 250-252.
- Ahlgren, U., Jonsson, J., Jonsson, L., Simu, K. and Edlund, H. (1998), "Beta-Cell-Specific Inactivation of the Mouse *Ipf1/Pdx1* Gene Results in Loss of the Beta-Cell Phenotype and Maturity Onset Diabetes", *Genes Dev*, 12, 1763-1768.
- Ahmed-Sorour, H. and Bailey, C. J. (1981), "Role of Ovarian Hormones in the Long-Term Control of Glucose Homeostasis, Glycogen Formation and Gluconeogenesis", *Ann Nutr Metab*, 25, 208-212.
- Ahren, B. (2005), "Type 2 Diabetes, Insulin Secretion and Beta-Cell Mass", *Curr Mol Med*, 5, 275-286.
- Aigner, B., Rathkolb, B., Herbach, N., Hrabe de Angelis, M., Wanke, R. and Wolf, E. (2008), "Diabetes Models by Screen for Hyperglycemia in Phenotype-Driven ENU Mouse Mutagenesis Projects", *Am J Physiol Endocrinol Metab*, 294, E232-240.
- Ainslie, D. A., Morris, M. J., Wittert, G., Turnbull, H., Proietto, J. and Thorburn, A. W. (2001), "Estrogen Deficiency Causes Central Leptin Insensitivity and Increased Hypothalamic Neuropeptide Y", *Int J Obes Relat Metab Disord*, 25, 1680-1688.
- Alberti, K. G. and Zimmet, P. Z. (1998), "Definition, Diagnosis and Classification of Diabetes Mellitus and Its Complications. Part 1: Diagnosis and Classification of Diabetes Mellitus Provisional Report of a Who Consultation", *Diabet Med*, 15, 539-553.

- Allen, J. R., Nguyen, L. X., Sargent, K. E., Lipson, K. L., Hackett, A. and Urano, F. (2004), "High Er Stress in Beta-Cells Stimulates Intracellular Degradation of Misfolded Insulin", *Biochem Biophys Res Commun*, 324, 166-170.
- Alonso-Magdalena, P., Morimoto, S., Ripoll, C., Fuentes, E. and Nadal, A. (2006), "The Estrogenic Effect of Bisphenol a Disrupts Pancreatic Beta-Cell Function in Vivo and Induces Insulin Resistance", *Environ Health Perspect*, 114, 106-112.
- Alonso-Magdalena, P., Ropero, A. B., Carrera, M. P., Cederroth, C. R., Baquie, M., Gauthier, B. R., Nef, S., Stefani, E. and Nadal, A. (2008), "Pancreatic Insulin Content Regulation by the Estrogen Receptor Er Alpha", *PLoS ONE*, 3, e2069.
- Alonso-Magdalena, P., Ropero, A. B., Soriano, S., Quesada, I. and Nadal, A. (2010), "Bisphenol-A: A New Diabetogenic Factor?", *Hormones (Athens)*, 9, 118-126.
- Alonso, L. C., Yokoe, T., Zhang, P., Scott, D. K., Kim, S. K., O'Donnell, C. P. and Garcia-Ocana, A. (2007), "Glucose Infusion in Mice: A New Model to Induce Beta-Cell Replication", *Diabetes*, 56, 1792-1801.
- Ammendrup, A., Maillard, A., Nielsen, K., Aabenhus Andersen, N., Serup, P., Dragsbaek Madsen, O., Mandrup-Poulsen, T. and Bonny, C. (2000), "The C-Jun Amino-Terminal Kinase Pathway Is Preferentially Activated by Interleukin-1 and Controls Apoptosis in Differentiating Pancreatic Beta-Cells", *Diabetes*, 49, 1468-1476.
- Andrali, S. S., Sampley, M. L., Vanderford, N. L. and Ozcan, S. (2008), "Glucose Regulation of Insulin Gene Expression in Pancreatic Beta-Cells", *Biochem J*, 415, 1-10.
- Araki, E., Oyadomari, S. and Mori, M. (2003), "Impact of Endoplasmic Reticulum Stress Pathway on Pancreatic Beta-Cells and Diabetes Mellitus", *Exp Biol Med (Maywood)*, 228, 1213-1217.
- Ashcroft, F. M. (2007), "The Walter B. Cannon Physiology in Perspective Lecture, 2007. Atp-Sensitive K<sup>+</sup> Channels and Disease: From Molecule to Malady", *Am J Physiol Endocrinol Metab*, 293, E880-889.
- Augstein, P., Elefanty, A. G., Allison, J. and Harrison, L. C. (1998), "Apoptosis and Beta-Cell Destruction in Pancreatic Islets of Nod Mice with Spontaneous and Cyclophosphamide-Accelerated Diabetes", *Diabetologia*, 41, 1381-1388.
- Babaya, N., Nakayama, M., Moriyama, H., Gianani, R., Still, T., Miao, D., Yu, L., Hutton, J. C. and Eisenbarth, G. S. (2006), "A New Model of Insulin-Deficient Diabetes: Male Nod Mice with a Single Copy of Ins1 and No Ins2", *Diabetologia*, 49, 1222-1228.
- Bailey, C. J. and Ahmed-Sorour, H. (1980), "Role of Ovarian Hormones in the Long-Term Control of Glucose Homeostasis. Effects of Insulin Secretion", *Diabetologia*, 19, 475-481.

- Balhuizen, A., Kumar, R., Amisten, S., Lundquist, I. and Salehi, A. (2010), "Activation of G Protein-Coupled Receptor 30 Modulates Hormone Secretion and Counteracts Cytokine-Induced Apoptosis in Pancreatic Islets of Female Mice", *Mol Cell Endocrinol*, 320, 16-24.
- Balling, R. (2001), "Enu Mutagenesis: Analyzing Gene Function in Mice", *Annu Rev Genomics Hum Genet*, 2, 463-492.
- Barbaric, I. and Dear, T. N. (2007), "Optimizing Screening and Mating Strategies for Phenotype-Driven Recessive N-Ethyl-N-Nitrosourea Screens in Mice", *J Am Assoc Lab Anim Sci*, 46, 44-49.
- Bardin, C. W. and Lipsett, M. B. (1967), "Testosterone and Androstenedione Blood Production Rates in Normal Women and Women with Idiopathic Hirsutism or Polycystic Ovaries", *J Clin Invest*, 46, 891-902.
- Barkhem, T., Carlsson, B., Nilsson, Y., Enmark, E., Gustafsson, J. and Nilsson, S. (1998), "Differential Response of Estrogen Receptor Alpha and Estrogen Receptor Beta to Partial Estrogen Agonists/Antagonists", *Mol Pharmacol*, 54, 105-112.
- Barros, R. P., Gabbi, C., Morani, A., Warner, M. and Gustafsson, J. A. (2009), "Participation of Eralpha and Erbeta in Glucose Homeostasis in Skeletal Muscle and White Adipose Tissue", *Am J Physiol Endocrinol Metab*, 297, E124-133.
- Barros, R. P., Machado, U. F. and Gustafsson, J. A. (2006a), "Estrogen Receptors: New Players in Diabetes Mellitus", *Trends Mol Med*, 12, 425-431.
- Barros, R. P., Machado, U. F., Warner, M. and Gustafsson, J. A. (2006b), "Muscle Glut4 Regulation by Estrogen Receptors Erbeta and Eralpha", *Proc Natl Acad Sci U S A*, 103, 1605-1608.
- Beato, M. (1989), "Gene Regulation by Steroid Hormones", *Cell*, 56, 335-344.
- Beato, M., Chavez, S. and Truss, M. (1996), "Transcriptional Regulation by Steroid Hormones", *Steroids*, 61, 240-251.
- Beck, B. (2000), "Neuropeptides and Obesity", *Nutrition*, 16, 916-923.
- Beier, D. R. (2000), "Sequence-Based Analysis of Mutagenized Mice", *Mamm Genome*, 11, 594-597.
- Bertolotti, A., Zhang, Y., Hendershot, L. M., Harding, H. P. and Ron, D. (2000), "Dynamic Interaction of Bip and Er Stress Transducers in the Unfolded-Protein Response", *Nat Cell Biol*, 2, 326-332.
- Bjorklund, A., Lansner, A. and Grill, V. E. (2000), "Glucose-Induced [Ca<sup>2+</sup>] Abnormalities in Human Pancreatic Islets: Important Role of Overstimulation", *Diabetes*, 49, 1840-1848.

- Bjornholm, M. and Zierath, J. R. (2005), "Insulin Signal Transduction in Human Skeletal Muscle: Identifying the Defects in Type II Diabetes", *Biochem Soc Trans*, 33, 354-357.
- Boesgaard, T. W., Pruhova, S., Andersson, E. A., Cinek, O., Obermannova, B., Lauenborg, J., Damm, P., Bergholdt, R., Pociot, F., Pisinger, C. et al. (2010), "Further Evidence That Mutations in *INS* Can Be a Rare Cause of Maturity-Onset Diabetes of the Young (MODY)", *BMC Med Genet*, 11, 42.
- Bonavera, J. J., Dube, M. G., Kalra, P. S. and Kalra, S. P. (1994), "Anorectic Effects of Estrogen May Be Mediated by Decreased Neuropeptide-Y Release in the Hypothalamic Paraventricular Nucleus", *Endocrinology*, 134, 2367-2370.
- Bonner-Weir, S. (2001), "Beta-Cell Turnover: Its Assessment and Implications", *Diabetes*, 50 Suppl 1, S20-24.
- Bonner-Weir, S., Inada, A., Yatoh, S., Li, W. C., Aye, T., Toschi, E. and Sharma, A. (2008), "Transdifferentiation of Pancreatic Ductal Cells to Endocrine Beta-Cells", *Biochem Soc Trans*, 36, 353-356.
- Brissova, M., Fowler, M. J., Nicholson, W. E., Chu, A., Hirshberg, B., Harlan, D. M. and Powers, A. C. (2005), "Assessment of Human Pancreatic Islet Architecture and Composition by Laser Scanning Confocal Microscopy", *J Histochem Cytochem*, 53, 1087-1097.
- Bryzgalova, G., Gao, H., Ahren, B., Zierath, J. R., Galuska, D., Steiler, T. L., Dahlman-Wright, K., Nilsson, S., Gustafsson, J. A., Efendic, S. et al. (2006), "Evidence That Oestrogen Receptor-Alpha Plays an Important Role in the Regulation of Glucose Homeostasis in Mice: Insulin Sensitivity in the Liver", *Diabetologia*, 49, 588-597.
- Bulun, E. and Adashi, E. Y. (2008), "The Physiology and Pathology of the Female Reproductive Axis," in *Williams Textbook of Endocrinology* (11<sup>th</sup> ed.), eds. H. M. Kronenberg, S. Melmed, K. S. Polonsky and P. R. Larsen, Philadelphia: Saunders Elsevier, Chapter 16 pp. 541-614.
- Bulun, S. E., Zeitoun, K., Sasano, H. and Simpson, E. R. (1999), "Aromatase in Aging Women", *Semin Reprod Endocrinol*, 17, 349-358.
- Butler, A. E., Janson, J., Bonner-Weir, S., Ritzel, R., Rizza, R. A. and Butler, P. C. (2003), "Beta-Cell Deficit and Increased Beta-Cell Apoptosis in Humans with Type 2 Diabetes", *Diabetes*, 52, 102-110.
- Carani, C., Qin, K., Simoni, M., Faustini-Fustini, M., Serpente, S., Boyd, J., Korach, K. S. and Simpson, E. R. (1997), "Effect of Testosterone and Estradiol in a Man with Aromatase Deficiency", *N Engl J Med*, 337, 91-95.
- Chambliss, K. L., Yuhanna, I. S., Anderson, R. G., Mendelsohn, M. E. and Shaul, P. W. (2002), "ErbB2 Has Nongenomic Action in Caveolae", *Mol Endocrinol*, 16, 938-946.

- Chiasson, J. L., Aris-Jilwan, N., Belanger, R., Bertrand, S., Beaugard, H., Ekoe, J. M., Fournier, H. and Havrankova, J. (2003), "Diagnosis and Treatment of Diabetic Ketoacidosis and the Hyperglycemic Hyperosmolar State", *CMAJ*, 168, 859-866.
- Choi, S. B., Jang, J. S. and Park, S. (2005), "Estrogen and Exercise May Enhance Beta-Cell Function and Mass Via Insulin Receptor Substrate 2 Induction in Ovariectomized Diabetic Rats", *Endocrinology*, 146, 4786-4794.
- Chu, S. C., Chou, Y. C., Liu, J. Y., Chen, C. H., Shyu, J. C. and Chou, F. P. (1999), "Fluctuation of Serum Leptin Level in Rats after Ovariectomy and the Influence of Estrogen Supplement", *Life Sci*, 64, 2299-2306.
- Clarke, C. H., Norfleet, A. M., Clarke, M. S., Watson, C. S., Cunningham, K. A. and Thomas, M. L. (2000), "Perimembrane Localization of the Estrogen Receptor Alpha Protein in Neuronal Processes of Cultured Hippocampal Neurons", *Neuroendocrinology*, 71, 34-42.
- Clee, S. M. and Attie, A. D. (2007), "The Genetic Landscape of Type 2 Diabetes in Mice", *Endocr Rev*, 28, 48-83.
- Cnop, M., Igoillo-Esteve, M., Cunha, D. A., Ladriere, L. and Eizirik, D. L. (2008), "An Update on Lipotoxic Endoplasmic Reticulum Stress in Pancreatic Beta-Cells", *Biochem Soc Trans*, 36, 909-915.
- Colombo, C., Porzio, O., Liu, M., Massa, O., Vasta, M., Salardi, S., Beccaria, L., Monciotti, C., Toni, S., Pedersen, O. et al. (2008), "Seven Mutations in the Human Insulin Gene Linked to Permanent Neonatal/Infancy-Onset Diabetes Mellitus", *J Clin Invest*, 118, 2148-2156.
- Concepcion, D., Seburn, K. L., Wen, G., Frankel, W. N. and Hamilton, B. A. (2004), "Mutation Rate and Predicted Phenotypic Target Sizes in Ethylnitrosourea-Treated Mice", *Genetics*, 168, 953-959.
- Considine, R. V., Sinha, M. K., Heiman, M. L., Kriauciunas, A., Stephens, T. W., Nyce, M. R., Ohannesian, J. P., Marco, C. C., McKee, L. J., Bauer, T. L. et al. (1996), "Serum Immunoreactive-Leptin Concentrations in Normal-Weight and Obese Humans", *N Engl J Med*, 334, 292-295.
- Coppey, L. J., Gellert, J. S., Davidson, E. P., Dunlap, J. A. and Yorek, M. A. (2002), "Changes in Endoneurial Blood Flow, Motor Nerve Conduction Velocity and Vascular Relaxation of Epineurial Arterioles of the Sciatic Nerve in Zdf-Obese Diabetic Rats", *Diabetes Metab Res Rev*, 18, 49-56.
- DeFronzo, R. A. (2004), "Pathogenesis of Type 2 Diabetes Mellitus", *Med Clin North Am*, 88, 787-835, ix.
- DeFronzo, R. A., Bonadonna, R. C. and Ferrannini, E. (1992), "Pathogenesis of Niddm. A Balanced Overview", *Diabetes Care*, 15, 318-368.

- DeFronzo, R. A., Ferrannini, E. and Simonson, D. C. (1989), "Fasting Hyperglycemia in Non-Insulin-Dependent Diabetes Mellitus: Contributions of Excessive Hepatic Glucose Production and Impaired Tissue Glucose Uptake", *Metabolism*, 38, 387-395.
- Del Prato, S., Leonetti, F., Simonson, D. C., Sheehan, P., Matsuda, M. and DeFronzo, R. A. (1994), "Effect of Sustained Physiologic Hyperinsulinaemia and Hyperglycaemia on Insulin Secretion and Insulin Sensitivity in Man", *Diabetologia*, 37, 1025-1035.
- Donath, M. Y., Gross, D. J., Cerasi, E. and Kaiser, N. (1999), "Hyperglycemia-Induced Beta-Cell Apoptosis in Pancreatic Islets of Psammomys Obesus During Development of Diabetes", *Diabetes*, 48, 738-744.
- Donath, M. Y. and Halban, P. A. (2004), "Decreased Beta-Cell Mass in Diabetes: Significance, Mechanisms and Therapeutic Implications", *Diabetologia*, 47, 581-589.
- Dunning, B. E., Foley, J. E. and Ahren, B. (2005), "Alpha Cell Function in Health and Disease: Influence of Glucagon-Like Peptide-1", *Diabetologia*, 48, 1700-1713.
- Duvillie, B., Cordonnier, N., Deltour, L., Dandoy-Dron, F., Itier, J. M., Monthieux, E., Jami, J., Joshi, R. L. and Bucchini, D. (1997), "Phenotypic Alterations in Insulin-Deficient Mutant Mice", *Proc Natl Acad Sci U S A*, 94, 5137-5140.
- Duvillie, B., Currie, C., Chrones, T., Bucchini, D., Jami, J., Joshi, R. L. and Hill, D. J. (2002), "Increased Islet Cell Proliferation, Decreased Apoptosis, and Greater Vascularization Leading to Beta-Cell Hyperplasia in Mutant Mice Lacking Insulin", *Endocrinology*, 143, 1530-1537.
- Eckhoff, D. E., Smyth, C. A., Eckstein, C., Bilbao, G., Young, C. J., Thompson, J. A. and Contreras, J. L. (2003), "Suppression of the C-Jun N-Terminal Kinase Pathway by 17beta-Estradiol Can Preserve Human Islet Functional Mass from Proinflammatory Cytokine-Induced Destruction", *Surgery*, 134, 169-179.
- Edghill, E. L., Flanagan, S. E., Patch, A. M., Boustred, C., Parrish, A., Shields, B., Shepherd, M. H., Hussain, K., Kapoor, R. R., Malecki, M. et al. (2008), "Insulin Mutation Screening in 1,044 Patients with Diabetes: Mutations in the Ins Gene Are a Common Cause of Neonatal Diabetes but a Rare Cause of Diabetes Diagnosed in Childhood or Adulthood", *Diabetes*, 57, 1034-1042.
- Egede, L. E. and Ellis, C. (2010), "Diabetes and Depression: Global Perspectives", *Diabetes Res Clin Pract*, 87, 302-312.
- Eizirik, D. L. and Mandrup-Poulsen, T. (2001), "A Choice of Death--the Signal-Transduction of Immune-Mediated Beta-Cell Apoptosis", *Diabetologia*, 44, 2115-2133.
- El Seifi, S., Green, I. C. and Perrin, D. (1981), "Insulin Release and Steroid-Hormone Binding in Isolated Islets of Langerhans in the Rat: Effects of Ovariectomy", *J Endocrinol*, 90, 59-67.

- Evans, J. L., Goldfine, I. D., Maddux, B. A. and Grodsky, G. M. (2002), "Oxidative Stress and Stress-Activated Signaling Pathways: A Unifying Hypothesis of Type 2 Diabetes", *Endocr Rev*, 23, 599-622.
- Evans, R. M. (1988), "The Steroid and Thyroid Hormone Receptor Superfamily", *Science*, 240, 889-895.
- Falkenstein, E., Tillmann, H. C., Christ, M., Feuring, M. and Wehling, M. (2000), "Multiple Actions of Steroid Hormones--a Focus on Rapid, Nongenomic Effects", *Pharmacol Rev*, 52, 513-556.
- Fenner, D., Odili, S., Takahashi, J. S., Matschinsky, F. M. and Bass, J. (2009), "Insight into Glucokinase Diabetes from ENU Mutagenesis", *Diabetes Suppl. 1*, 58, A308.
- Filardo, E., Quinn, J., Pang, Y., Graeber, C., Shaw, S., Dong, J. and Thomas, P. (2007), "Activation of the Novel Estrogen Receptor G Protein-Coupled Receptor 30 (Gpr30) at the Plasma Membrane", *Endocrinology*, 148, 3236-3245.
- Filardo, E. J. and Thomas, P. (2005), "Gpr30: A Seven-Transmembrane-Spanning Estrogen Receptor That Triggers EGF Release", *Trends Endocrinol Metab*, 16, 362-367.
- Fisher, C. R., Graves, K. H., Parlow, A. F. and Simpson, E. R. (1998), "Characterization of Mice Deficient in Aromatase (Arko) Because of Targeted Disruption of the Cyp19 Gene", *Proc Natl Acad Sci U S A*, 95, 6965-6970.
- Flanagan-Cato, L. M., Grigson, P. S. and King, J. L. (2001), "Estrogen-Induced Suppression of Intake Is Not Mediated by Taste Aversion in Female Rats", *Physiol Behav*, 72, 549-558.
- Fonseca, V., Inzucchi, S. E. and Ferrannini, E. (2009), "Redefining the Diagnosis of Diabetes Using Glycated Hemoglobin", *Diabetes Care*, 32, 1344-1345.
- Ganesan, R. (1994), "The Aversive and Hypophagic Effects of Estradiol", *Physiol Behav*, 55, 279-285.
- Geary, N. (2000), "Estradiol and Appetite", *Appetite*, 35, 273-274.
- Genuth, S., Alberti, K. G., Bennett, P., Buse, J., Defronzo, R., Kahn, R., Kitzmiller, J., Knowler, W. C., Lebovitz, H., Lernmark, A. et al. (2003), "Follow-up Report on the Diagnosis of Diabetes Mellitus", *Diabetes Care*, 26, 3160-3167.
- Geraldes, P., Sirois, M. G. and Tanguay, J. F. (2003), "Specific Contribution of Estrogen Receptors on Mitogen-Activated Protein Kinase Pathways and Vascular Cell Activation", *Circ Res*, 93, 399-405.
- Gething, M. J. and Sambrook, J. (1992), "Protein Folding in the Cell", *Nature*, 355, 33-45.

- Gillett, M. J. (2009), "International Expert Committee Report on the Role of the A1c Assay in the Diagnosis of Diabetes: *Diabetes Care* 2009; 32(7): 1327-1334", *Clin Biochem Rev*, 30, 197-200.
- Gilon, P., Shepherd, R. M. and Henquin, J. C. (1993), "Oscillations of Secretion Driven by Oscillations of Cytoplasmic Ca<sup>2+</sup> as Evidences in Single Pancreatic Islets", *J Biol Chem*, 268, 22265-22268.
- Godsland, I. F. (2005), "Oestrogens and Insulin Secretion", *Diabetologia*, 48, 2213-2220.
- Gomez, B. P., Riggins, R. B., Shajahan, A. N., Klimach, U., Wang, A., Crawford, A. C., Zhu, Y., Zwart, A., Wang, M. and Clarke, R. (2007), "Human X-Box Binding Protein-1 Confers Both Estrogen Independence and Antiestrogen Resistance in Breast Cancer Cell Lines", *FASEB J*, 21, 4013-4027.
- Gonzalez, C., Alonso, A., Grueso, N. A., Diaz, F., Esteban, M. M., Fernandez, S. and Patterson, A. M. (2001), "Effect of Treatment with Different Doses of 17-Beta-Estradiol on Insulin Receptor Substrate-1", *JOP*, 2, 140-149.
- Gould, G. W. and Holman, G. D. (1993), "The Glucose Transporter Family: Structure, Function and Tissue-Specific Expression", *Biochem J*, 295 ( Pt 2), 329-341.
- Gray, D. W., Millard, P. R., McShane, P. and Morris, P. J. (1983), "The Use of the Dye Neutral Red as a Specific, Non-Toxic, Intra-Vital Stain of Islets of Langerhans", *Br J Exp Pathol*, 64, 553-558.
- Griesmacher, A., Kindhauser, M., Andert, S. E., Schreiner, W., Toma, C., Knoebl, P., Pietschmann, P., Prager, R., Schnack, C., Schernthaner, G. et al. (1995), "Enhanced Serum Levels of Thiobarbituric-Acid-Reactive Substances in Diabetes Mellitus", *Am J Med*, 98, 469-475.
- Grodin, J. M., Siiteri, P. K. and MacDonald, P. C. (1973), "Source of Estrogen Production in Postmenopausal Women", *J Clin Endocrinol Metab*, 36, 207-214.
- Gromada, J., Franklin, I. and Wollheim, C. B. (2007), "Alpha-Cells of the Endocrine Pancreas: 35 Years of Research but the Enigma Remains", *Endocr Rev*, 28, 84-116.
- Gruber, C. J., Tschugguel, W., Schneeberger, C. and Huber, J. C. (2002), "Production and Actions of Estrogens", *N Engl J Med*, 346, 340-352.
- Guillen, C., Bartolome, A., Nevado, C. and Benito, M. (2008), "Biphasic Effect of Insulin on Beta Cell Apoptosis Depending on Glucose Deprivation", *FEBS Lett*, 582, 3855-3860.
- Gundersen, H. J., Bendtsen, T. F., Korbo, L., Marcussen, N., Moller, A., Nielsen, K., Nyengaard, J. R., Pakkenberg, B., Sorensen, F. B., Vesterby, A. et al. (1988), "Some New, Simple and Efficient Stereological Methods and Their Use in Pathological Research and Diagnosis", *APMIS*, 96, 379-394.

- Hammes, S. R. and Levin, E. R. (2007), "Extranuclear Steroid Receptors: Nature and Actions", *Endocr Rev*, 28, 726-741.
- Harding, H. P., Zeng, H., Zhang, Y., Jungries, R., Chung, P., Plesken, H., Sabatini, D. D. and Ron, D. (2001), "Diabetes Mellitus and Exocrine Pancreatic Dysfunction in Perk<sup>-/-</sup> Mice Reveals a Role for Translational Control in Secretory Cell Survival", *Mol Cell*, 7, 1153-1163.
- Hardouin, S. N. and Nagy, A. (2000), "Mouse Models for Human Disease", *Clin Genet*, 57, 237-244.
- Harris, M. I. (1988), "Classification and Diagnostic Criteria for Diabetes Mellitus and Other Categories of Glucose Intolerance", *Prim Care*, 15, 205-225.
- Heine, P. A., Taylor, J. A., Iwamoto, G. A., Lubahn, D. B. and Cooke, P. S. (2000), "Increased Adipose Tissue in Male and Female Estrogen Receptor-Alpha Knockout Mice", *Proc Natl Acad Sci U S A*, 97, 12729-12734.
- Hemsell, D. L., Grodin, J. M., Brenner, P. F., Siiteri, P. K. and MacDonald, P. C. (1974), "Plasma Precursors of Estrogen. II. Correlation of the Extent of Conversion of Plasma Androstenedione to Estrone with Age", *J Clin Endocrinol Metab*, 38, 476-479.
- Herbach, N., Goeke, B., Schneider, M., Hermanns, W., Wolf, E. and Wanke, R. (2005), "Overexpression of a Dominant Negative GIP Receptor in Transgenic Mice Results in Disturbed Postnatal Pancreatic Islet and Beta-Cell Development", *Regul Pept*, 125, 103-117.
- Herbach, N., Rathkolb, B., Kemter, E., Pichl, L., Klafien, M., de Angelis, M. H., Halban, P. A., Wolf, E., Aigner, B. and Wanke, R. (2007), "Dominant-Negative Effects of a Novel Mutated Ins2 Allele Causes Early-Onset Diabetes and Severe Beta-Cell Loss in Munich Ins2c95s Mutant Mice", *Diabetes*, 56, 1268-1276.
- Hill, D. J. and Hogg, J. (1991), "Growth Factor Control of Pancreatic B Cell Hyperplasia", *Baillieres Clin Endocrinol Metab*, 5, 689-698.
- Hillier, S. G., Whitelaw, P. F. and Smyth, C. D. (1994), "Follicular Oestrogen Synthesis: The 'Two-Cell, Two-Gonadotrophin' Model Revisited", *Mol Cell Endocrinol*, 100, 51-54.
- Hitotsumachi, S., Carpenter, D. A. and Russell, W. L. (1985), "Dose-Repetition Increases the Mutagenic Effectiveness of N-Ethyl-N-Nitrosourea in Mouse Spermatogonia", *Proc Natl Acad Sci U S A*, 82, 6619-6621.
- Hong, E. G., Jung, D. Y., Ko, H. J., Zhang, Z., Ma, Z., Jun, J. Y., Kim, J. H., Sumner, A. D., Vary, T. C., Gardner, T. W. et al. (2007), "Nonobese, Insulin-Deficient Ins2akita Mice Develop Type 2 Diabetes Phenotypes Including Insulin Resistance and Cardiac Remodeling", *Am J Physiol Endocrinol Metab*, 293, E1687-1696.
- Houstis, N., Rosen, E. D. and Lander, E. S. (2006), "Reactive Oxygen Species Have a Causal Role in Multiple Forms of Insulin Resistance", *Nature*, 440, 944-948.

Huerta, S., Goulet, E. J., Huerta-Yepez, S. and Livingston, E. H. (2007), "Screening and Detection of Apoptosis", *J Surg Res*, 139, 143-156.

International Diabetes Federation (IDF) (2009). "Diabetes Atlas". Retrieved 22.07.2010 from <http://www.diabetesatlas.org>.

Inada, A., Nienaber, C., Katsuta, H., Fujitani, Y., Levine, J., Morita, R., Sharma, A. and Bonner-Weir, S. (2008), "Carbonic Anhydrase II-Positive Pancreatic Cells Are Progenitors for Both Endocrine and Exocrine Pancreas after Birth", *Proc Natl Acad Sci U S A*, 105, 19915-19919.

Inoue, M., Sakuraba, Y., Motegi, H., Kubota, N., Toki, H., Matsui, J., Toyoda, Y., Miwa, I., Terauchi, Y., Kadowaki, T. et al. (2004), "A Series of Maturity Onset Diabetes of the Young, Type 2 (Mody2) Mouse Models Generated by a Large-Scale ENU Mutagenesis Program", *Hum Mol Genet*, 13, 1147-1157.

Izumi, T., Yokota-Hashimoto, H., Zhao, S., Wang, J., Halban, P. A. and Takeuchi, T. (2003), "Dominant Negative Pathogenesis by Mutant Proinsulin in the Akita Diabetic Mouse", *Diabetes*, 52, 409-416.

Jakacka, M., Ito, M., Martinson, F., Ishikawa, T., Lee, E. J. and Jameson, J. L. (2002), "An Estrogen Receptor (Er)Alpha Deoxyribonucleic Acid-Binding Domain Knock-in Mutation Provides Evidence for Nonclassical Er Pathway Signaling in Vivo", *Mol Endocrinol*, 16, 2188-2201.

Jensen, J., Kitlen, J. W., Briand, P., Labrie, F. and Lykkesfeldt, A. E. (2003), "Effect of Antiestrogens and Aromatase Inhibitor on Basal Growth of the Human Breast Cancer Cell Line MCF-7 in Serum-Free Medium", *J Steroid Biochem Mol Biol*, 84, 469-478.

Jhala, U. S., Canettieri, G., Srean, R. A., Kulkarni, R. N., Krajewski, S., Reed, J., Walker, J., Lin, X., White, M. and Montminy, M. (2003), "cAMP Promotes Pancreatic Beta-Cell Survival Via CREB-Mediated Induction of Irs2", *Genes Dev*, 17, 1575-1580.

Jian, B., Hsieh, C. H., Chen, J., Choudhry, M., Bland, K., Chaudry, I. and Raju, R. (2008), "Activation of Endoplasmic Reticulum Stress Response Following Trauma-Hemorrhage", *Biochim Biophys Acta*, 1782, 621-626.

Jiang, D., Sullivan, P. G., Sensi, S. L., Steward, O. and Weiss, J. H. (2001), "Zn<sup>2+</sup> Induces Permeability Transition Pore Opening and Release of Pro-Apoptotic Peptides from Neuronal Mitochondria", *J Biol Chem*, 276, 47524-47529.

Jones, M. E., Thorburn, A. W., Britt, K. L., Hewitt, K. N., Wreford, N. G., Proietto, J., Oz, O. K., Leury, B. J., Robertson, K. M., Yao, S. et al. (2000), "Aromatase-Deficient (Arko) Mice Have a Phenotype of Increased Adiposity", *Proc Natl Acad Sci U S A*, 97, 12735-12740.

Kaiser, N., Leibowitz, G. and Nesher, R. (2003), "Glucotoxicity and Beta-Cell Failure in Type 2 Diabetes Mellitus", *J Pediatr Endocrinol Metab*, 16, 5-22.

- Kaku, K., Fiedorek, F. T., Jr., Province, M. and Permutt, M. A. (1988), "Genetic Analysis of Glucose Tolerance in Inbred Mouse Strains. Evidence for Polygenic Control", *Diabetes*, 37, 707-713.
- Kanwar, M., Chan, P. S., Kern, T. S. and Kowluru, R. A. (2007), "Oxidative Damage in the Retinal Mitochondria of Diabetic Mice: Possible Protection by Superoxide Dismutase", *Invest Ophthalmol Vis Sci*, 48, 3805-3811.
- Katalinic, V., Modun, D., Music, I. and Boban, M. (2005), "Gender Differences in Antioxidant Capacity of Rat Tissues Determined by 2,2'-Azinobis (3-Ethylbenzothiazoline 6-Sulfonate; Abts) and Ferric Reducing Antioxidant Power (Frap) Assays", *Comp Biochem Physiol C Toxicol Pharmacol*, 140, 47-52.
- Kato, S., Tora, L., Yamauchi, J., Masushige, S., Bellard, M. and Chambon, P. (1992), "A Far Upstream Estrogen Response Element of the Ovalbumin Gene Contains Several Half-Palindromic 5'-Tgacc-3' Motifs Acting Synergistically", *Cell*, 68, 731-742.
- Katz, A., Nambi, S. S., Mather, K., Baron, A. D., Follmann, D. A., Sullivan, G. and Quon, M. J. (2000), "Quantitative Insulin Sensitivity Check Index: A Simple, Accurate Method for Assessing Insulin Sensitivity in Humans", *J Clin Endocrinol Metab*, 85, 2402-2410.
- Katzenellenbogen, J. A. and Katzenellenbogen, B. S. (1996), "Nuclear Hormone Receptors: Ligand-Activated Regulators of Transcription and Diverse Cell Responses", *Chem Biol*, 3, 529-536.
- Kaufman, R. J., Scheuner, D., Schroder, M., Shen, X., Lee, K., Liu, C. Y. and Arnold, S. M. (2002), "The Unfolded Protein Response in Nutrient Sensing and Differentiation", *Nat Rev Mol Cell Biol*, 3, 411-421.
- Kauri, L. M., Wang, G. S., Patrick, C., Bareggi, M., Hill, D. J. and Scott, F. W. (2007), "Increased Islet Neogenesis without Increased Islet Mass Precedes Autoimmune Attack in Diabetes-Prone Rats", *Lab Invest*, 87, 1240-1251.
- Kautz, S. M. (2010), "*Mechanisms of B-Cell Loss in Male Munich Ins2<sup>c95s</sup> Mutant Mice*" Inaugural Dissertation, Institut of Veterinary Pathology, Ludwig Maximilians Universität, Munich.
- Kayo, T. and Koizumi, A. (1998), "Mapping of Murine Diabetogenic Gene Mody on Chromosome 7 at D7mit258 and Its Involvement in Pancreatic Islet and Beta Cell Development During the Perinatal Period", *J Clin Invest*, 101, 2112-2118.
- Keays, D. A., Clark, T. G. and Flint, J. (2006), "Estimating the Number of Coding Mutations in Genotypic- and Phenotypic-Driven N-Ethyl-N-Nitrosourea (ENU) Screens", *Mamm Genome*, 17, 230-238.
- Khoo, S., Griffen, S. C., Xia, Y., Baer, R. J., German, M. S. and Cobb, M. H. (2003), "Regulation of Insulin Gene Transcription by Erk1 and Erk2 in Pancreatic Beta Cells", *J Biol Chem*, 278, 32969-32977.

- Kozlov, A. V., Duvigneau, J. C., Hyatt, T. C., Raju, R., Behling, T., Hartl, R. T., Staniek, K., Miller, I., Gregor, W., Redl, H. et al. (2010), "Effect of Estrogen on Mitochondrial Function and Intracellular Stress Markers in Rat Liver and Kidney Following Trauma-Hemorrhagic Shock and Prolonged Hypotension", *Mol Med*, 16, 254-261.
- Kronfeld-Schor, N., Zhao, J., Silvia, B. A., Bicer, E., Mathews, P. T., Urban, R., Zimmerman, S., Kunz, T. H. and Widmaier, E. P. (2000), "Steroid-Dependent up-Regulation of Adipose Leptin Secretion in Vitro During Pregnancy in Mice", *Biol Reprod*, 63, 274-280.
- Kukreja, A. and Maclaren, N. K. (1999), "Autoimmunity and Diabetes", *J Clin Endocrinol Metab*, 84, 4371-4378.
- Kyriakis, J. M. and Avruch, J. (1996), "Sounding the Alarm: Protein Kinase Cascades Activated by Stress and Inflammation", *J Biol Chem*, 271, 24313-24316.
- Lai, E., Teodoro, T. and Volchuk, A. (2007), "Endoplasmic Reticulum Stress: Signaling the Unfolded Protein Response", *Physiology (Bethesda)*, 22, 193-201.
- Lantin-Hermoso, R. L., Rosenfeld, C. R., Yuhanna, I. S., German, Z., Chen, Z. and Shaul, P. W. (1997), "Estrogen Acutely Stimulates Nitric Oxide Synthase Activity in Fetal Pulmonary Artery Endothelium", *Am J Physiol*, 273, L119-126.
- Laybutt, D. R., Preston, A. M., Akerfeldt, M. C., Kench, J. G., Busch, A. K., Biankin, A. V. and Biden, T. J. (2007), "Endoplasmic Reticulum Stress Contributes to Beta Cell Apoptosis in Type 2 Diabetes", *Diabetologia*, 50, 752-763.
- Le May, C., Chu, K., Hu, M., Ortega, C. S., Simpson, E. R., Korach, K. S., Tsai, M. J. and Mauvais-Jarvis, F. (2006), "Estrogens Protect Pancreatic Beta-Cells from Apoptosis and Prevent Insulin-Deficient Diabetes Mellitus in Mice", *Proc Natl Acad Sci U S A*, 103, 9232-9237.
- Lee, A. V., Jackson, J. G., Gooch, J. L., Hilsenbeck, S. G., Coronado-Heinsohn, E., Osborne, C. K. and Yee, D. (1999), "Enhancement of Insulin-Like Growth Factor Signaling in Human Breast Cancer: Estrogen Regulation of Insulin Receptor Substrate-1 Expression in Vitro and in Vivo", *Mol Endocrinol*, 13, 787-796.
- Lee, S., Muniyappa, R., Yan, X., Chen, H., Yue, L. Q., Hong, E. G., Kim, J. K. and Quon, M. J. (2008), "Comparison between Surrogate Indexes of Insulin Sensitivity and Resistance and Hyperinsulinemic Euglycemic Clamp Estimates in Mice", *Am J Physiol Endocrinol Metab*, 294, E261-270.
- Legro, R. S., Finegood, D. and Dunaif, A. (1998), "A Fasting Glucose to Insulin Ratio Is a Useful Measure of Insulin Sensitivity in Women with Polycystic Ovary Syndrome", *J Clin Endocrinol Metab*, 83, 2694-2698.
- Lehmann, R. and Spinass, G. (2005), "Diagnostik Und Pathogenese Des Diabetes Mellitus Typ 2", *Diabetes*, 7, 1.

- Leroux, L., Desbois, P., Lamotte, L., Duville, B., Cordonnier, N., Jackerott, M., Jami, J., Bucchini, D. and Joshi, R. L. (2001), "Compensatory Responses in Mice Carrying a Null Mutation for Ins1 or Ins2", *Diabetes*, 50 Suppl 1, S150-153.
- Leroux, L., Durel, B., Autier, V., Deltour, L., Bucchini, D., Jami, J. and Joshi, R. L. (2003), "Ins1 Gene up-Regulated in a Beta-Cell Line Derived from Ins2 Knockout Mice", *Int J Exp Diabetes Res*, 4, 7-12.
- Levin, E. R. (2005), "Integration of the Extranuclear and Nuclear Actions of Estrogen", *Mol Endocrinol*, 19, 1951-1959.
- Liu, M., Hodish, I., Rhodes, C. J. and Arvan, P. (2007), "Proinsulin Maturation, Misfolding, and Proteotoxicity", *Proc Natl Acad Sci U S A*, 104, 15841-15846.
- Liu, M., Li, Y., Cavener, D. and Arvan, P. (2005), "Proinsulin Disulfide Maturation and Misfolding in the Endoplasmic Reticulum", *J Biol Chem*, 280, 13209-13212.
- Liu, M. M., Albanese, C., Anderson, C. M., Hilty, K., Webb, P., Uht, R. M., Price, R. H., Jr., Pestell, R. G. and Kushner, P. J. (2002), "Opposing Action of Estrogen Receptors Alpha and Beta on Cyclin D1 Gene Expression", *J Biol Chem*, 277, 24353-24360.
- Liu, S., Le May, C., Wong, W. P., Ward, R. D., Clegg, D. J., Marcelli, M., Korach, K. S. and Mauvais-Jarvis, F. (2009), "Importance of Extranuclear Estrogen Receptor-Alpha and Membrane G Protein-Coupled Estrogen Receptor in Pancreatic Islet Survival", *Diabetes*, 58, 2292-2302.
- Loftus, T. M., Jaworsky, D. E., Frehywot, G. L., Townsend, C. A., Ronnett, G. V., Lane, M. D. and Kuhajda, F. P. (2000), "Reduced Food Intake and Body Weight in Mice Treated with Fatty Acid Synthase Inhibitors", *Science*, 288, 2379-2381.
- Lopez, M., Lelliott, C. J., Tovar, S., Kimber, W., Gallego, R., Virtue, S., Blount, M., Vazquez, M. J., Finer, N., Powles, T. J. et al. (2006), "Tamoxifen-Induced Anorexia Is Associated with Fatty Acid Synthase Inhibition in the Ventromedial Nucleus of the Hypothalamus and Accumulation of Malonyl-Coa", *Diabetes*, 55, 1327-1336.
- Lottmann, H., Vanselow, J., Hessabi, B. and Walther, R. (2001), "The Tet-on System in Transgenic Mice: Inhibition of the Mouse Pdx-1 Gene Activity by Antisense Rna Expression in Pancreatic Beta-Cells", *J Mol Med*, 79, 321-328.
- Louet, J. F., LeMay, C. and Mauvais-Jarvis, F. (2004), "Antidiabetic Actions of Estrogen: Insight from Human and Genetic Mouse Models", *Curr Atheroscler Rep*, 6, 180-185.
- Madak-Erdogan, Z., Kieser, K. J., Kim, S. H., Komm, B., Katzenellenbogen, J. A. and Katzenellenbogen, B. S. (2008), "Nuclear and Extranuclear Pathway Inputs in the Regulation of Global Gene Expression by Estrogen Receptors", *Mol Endocrinol*, 22, 2116-2127.

- Maddux, B. A., See, W., Lawrence, J. C., Jr., Goldfine, A. L., Goldfine, I. D. and Evans, J. L. (2001), "Protection against Oxidative Stress-Induced Insulin Resistance in Rat L6 Muscle Cells by Micromolar Concentrations of Alpha-Lipoic Acid", *Diabetes*, 50, 404-410.
- Maggiolini, M. and Picard, D. (2010), "The Unfolding Stories of Gpr30, a New Membrane-Bound Estrogen Receptor", *J Endocrinol*, 204, 105-114.
- Majka, J. and Burgers, P. M. (2004), "The PcnA-Rfc Families of DNA Clamps and Clamp Loaders", *Prog Nucleic Acid Res Mol Biol*, 78, 227-260.
- Marban, S. L., DeLoia, J. A. and Gearhart, J. D. (1989), "Hyperinsulinemia in Transgenic Mice Carrying Multiple Copies of the Human Insulin Gene", *Dev Genet*, 10, 356-364.
- Marino, M., Galluzzo, P. and Ascenzi, P. (2006), "Estrogen Signaling Multiple Pathways to Impact Gene Transcription", *Curr Genomics*, 7, 497-508.
- Maritim, A. C., Sanders, R. A. and Watkins, J. B., 3rd. (2003), "Diabetes, Oxidative Stress, and Antioxidants: A Review", *J Biochem Mol Toxicol*, 17, 24-38.
- Mathis, D., Vence, L. and Benoist, C. (2001), "Beta-Cell Death During Progression to Diabetes", *Nature*, 414, 792-798.
- Matthews, J. and Gustafsson, J. A. (2003), "Estrogen Signaling: A Subtle Balance between Er Alpha and Er Beta", *Mol Interv*, 3, 281-292.
- Melloul, D. (2004), "Transcription Factors in Islet Development and Physiology: Role of Pdx-1 in Beta-Cell Function", *Ann N Y Acad Sci*, 1014, 28-37.
- Melloul, D., Marshak, S. and Cerasi, E. (2002), "Regulation of Insulin Gene Transcription", *Diabetologia*, 45, 309-326.
- Messinis, I. E., Milingos, S. D., Alexandris, E., Kariotis, I., Kollios, G. and Seferiadis, K. (1999), "Leptin Concentrations in Normal Women Following Bilateral Ovariectomy", *Hum Reprod*, 14, 913-918.
- Metzger, B. E., Buchanan, T. A., Coustan, D. R., de Leiva, A., Dunger, D. B., Hadden, D. R., Hod, M., Kitzmiller, J. L., Kjos, S. L., Oats, J. N. et al. (2007), "Summary and Recommendations of the Fifth International Workshop-Conference on Gestational Diabetes Mellitus", *Diabetes Care*, 30 Suppl 2, S251-260.
- Meur, G., Simon, A., Harun, N., Virally, M., Dechaume, A., Bonnefond, A., Fetita, S., Tarasov, A. I., Guillausseau, P. J., Boesgaard, T. W. et al. (2010), "Insulin Gene Mutations Resulting in Early-Onset Diabetes: Marked Differences in Clinical Presentation, Metabolic Status, and Pathogenic Effect through Endoplasmic Reticulum Retention", *Diabetes*, 59, 653-661.
- Mizukami, Y. (2010), "In Vivo Functions of Gpr30/Gper-1, a Membrane Receptor for Estrogen: From Discovery to Functions in Vivo", *Endocr J*, 57, 101-107.

- Molven, A., Ringdal, M., Nordbo, A. M., Raeder, H., Stoy, J., Lipkind, G. M., Steiner, D. F., Philipson, L. H., Bergmann, I., Aarskog, D. et al. (2008), "Mutations in the Insulin Gene Can Cause Mody and Autoantibody-Negative Type 1 Diabetes", *Diabetes*, 57, 1131-1135.
- Mori, K. (2000), "Tripartite Management of Unfolded Proteins in the Endoplasmic Reticulum", *Cell*, 101, 451-454.
- Morimoto, S., Mendoza-Rodriguez, C. A., Hiriart, M., Larrieta, M. E., Vital, P. and Cerbon, M. A. (2005), "Protective Effect of Testosterone on Early Apoptotic Damage Induced by Streptozotocin in Rat Pancreas", *J Endocrinol*, 187, 217-224.
- Mucci, L. A., Lagiou, P., Tamimi, R. M., Hsieh, C. C., Adami, H. O. and Trichopoulos, D. (2003), "Pregnancy Estriol, Estradiol, Progesterone and Prolactin in Relation to Birth Weight and Other Birth Size Variables (United States)", *Cancer Causes Control*, 14, 311-318.
- Mystkowski, P., Seeley, R. J., Hahn, T. M., Baskin, D. G., Havel, P. J., Matsumoto, A. M., Wilkinson, C. W., Peacock-Kinzig, K., Blake, K. A. and Schwartz, M. W. (2000), "Hypothalamic Melanin-Concentrating Hormone and Estrogen-Induced Weight Loss", *J Neurosci*, 20, 8637-8642.
- Naaz, A., Zakroczymski, M., Heine, P., Taylor, J., Saunders, P., Lubahn, D. and Cooke, P. S. (2002), "Effect of Ovariectomy on Adipose Tissue of Mice in the Absence of Estrogen Receptor Alpha (Eralpha): A Potential Role for Estrogen Receptor Beta (Erbeta)", *Horm Metab Res*, 34, 758-763.
- Nadal, A., Alonso-Magdalena, P., Ripoll, C. and Fuentes, E. (2005), "Disentangling the Molecular Mechanisms of Action of Endogenous and Environmental Estrogens", *Pflugers Arch*, 449, 335-343.
- Nadal, A., Alonso-Magdalena, P., Soriano, S., Quesada, I. and Ropero, A. B. (2009), "The Pancreatic Beta-Cell as a Target of Estrogens and Xenoestrogens: Implications for Blood Glucose Homeostasis and Diabetes", *Mol Cell Endocrinol*, 304, 63-68.
- Nadal, A., Quesada, I. and Soria, B. (1999), "Homologous and Heterologous Asynchronicity between Identified Alpha-, Beta- and Delta-Cells within Intact Islets of Langerhans in the Mouse", *J Physiol*, 517 ( Pt 1), 85-93.
- Nadal, A., Ropero, A. B., Laribi, O., Maillet, M., Fuentes, E. and Soria, B. (2000), "Nongenomic Actions of Estrogens and Xenoestrogens by Binding at a Plasma Membrane Receptor Unrelated to Estrogen Receptor Alpha and Estrogen Receptor Beta", *Proc Natl Acad Sci U S A*, 97, 11603-11608.
- Nadal, A., Rovira, J. M., Laribi, O., Leon-quinto, T., Andreu, E., Ripoll, C. and Soria, B. (1998), "Rapid Insulinotropic Effect of 17beta-Estradiol Via a Plasma Membrane Receptor", *FASEB J*, 12, 1341-1348.

- Nanjo, K., Sanke, T., Miyano, M., Okai, K., Sowa, R., Kondo, M., Nishimura, S., Iwo, K., Miyamura, K., Given, B. D. et al. (1986), "Diabetes Due to Secretion of a Structurally Abnormal Insulin (Insulin Wakayama). Clinical and Functional Characteristics of [Leu<sup>a</sup>3] Insulin", *J Clin Invest*, 77, 514-519.
- Nathan, D. M. (2009), "International Expert Committee Report on the Role of the A1c Assay in the Diagnosis of Diabetes", *Diabetes Care*, 32, 1327-1334.
- Nathan, D. M., Turgeon, H. and Regan, S. (2007), "Relationship between Glycated Haemoglobin Levels and Mean Glucose Levels over Time", *Diabetologia*, 50, 2239-2244.
- Nelson, L. R. and Bulun, S. E. (2001), "Estrogen Production and Action", *J Am Acad Dermatol*, 45, S116-124.
- Nieuwenhuizen, A. G., Schuiling, G. A., Liem, S. M., Moes, H., Koiter, T. R. and Uilenbroek, J. T. (1999), "Progesterone Stimulates Pancreatic Cell Proliferation in Vivo", *Eur J Endocrinol*, 140, 256-263.
- Nilsson, S., Makela, S., Treuter, E., Tujague, M., Thomsen, J., Andersson, G., Enmark, E., Pettersson, K., Warner, M. and Gustafsson, J. A. (2001), "Mechanisms of Estrogen Action", *Physiol Rev*, 81, 1535-1565.
- Nolan, P. M., Hugill, A. and Cox, R. D. (2002), "Enu Mutagenesis in the Mouse: Application to Human Genetic Disease", *Brief Funct Genomic Proteomic*, 1, 278-289.
- Nozaki, J., Kubota, H., Yoshida, H., Naitoh, M., Goji, J., Yoshinaga, T., Mori, K., Koizumi, A. and Nagata, K. (2004), "The Endoplasmic Reticulum Stress Response Is Stimulated through the Continuous Activation of Transcription Factors Atf6 and Xbp1 in Ins2<sup>+</sup>/Akita Pancreatic Beta Cells", *Genes Cells*, 9, 261-270.
- Nyblom, H. K., Thorn, K., Ahmed, M. and Bergsten, P. (2006), "Mitochondrial Protein Patterns Correlating with Impaired Insulin Secretion from Ins-1e Cells Exposed to Elevated Glucose Concentrations", *Proteomics*, 6, 5193-5198.
- O'Brien, B. A., Harmon, B. V., Cameron, D. P. and Allan, D. J. (1996), "Beta-Cell Apoptosis Is Responsible for the Development of Iddm in the Multiple Low-Dose Streptozotocin Model", *J Pathol*, 178, 176-181.
- O'Lone, R., Frith, M. C., Karlsson, E. K. and Hansen, U. (2004), "Genomic Targets of Nuclear Estrogen Receptors", *Mol Endocrinol*, 18, 1859-1875.
- Osbak, K. K., Colclough, K., Saint-Martin, C., Beer, N. L., Bellanne-Chantelot, C., Ellard, S. and Gloyn, A. L. (2009), "Update on Mutations in Glucokinase (Gck), Which Cause Maturity-Onset Diabetes of the Young, Permanent Neonatal Diabetes, and Hyperinsulinemic Hypoglycemia", *Hum Mutat*, 30, 1512-1526.
- Oyadomari, S., Koizumi, A., Takeda, K., Gotoh, T., Akira, S., Araki, E. and Mori, M. (2002), "Targeted Disruption of the Chop Gene Delays Endoplasmic Reticulum Stress-Mediated Diabetes", *J Clin Invest*, 109, 525-532.

- Oyadomari, S. and Mori, M. (2004), "Roles of Chop/Gadd153 in Endoplasmic Reticulum Stress", *Cell Death Differ*, 11, 381-389.
- Ozansoy, G., Akin, B., Aktan, F. and Karasu, C. (2001), "Short-Term Gemfibrozil Treatment Reverses Lipid Profile and Peroxidation but Does Not Alter Blood Glucose and Tissue Antioxidant Enzymes in Chronically Diabetic Rats", *Mol Cell Biochem*, 216, 59-63.
- Pan, X. R., Li, G. W., Hu, Y. H., Wang, J. X., Yang, W. Y., An, Z. X., Hu, Z. X., Lin, J., Xiao, J. Z., Cao, H. B. et al. (1997), "Effects of Diet and Exercise in Preventing Niddm in People with Impaired Glucose Tolerance. The Da Qing Igt and Diabetes Study", *Diabetes Care*, 20, 537-544.
- Pappas, T. C., Gametchu, B. and Watson, C. S. (1995), "Membrane Estrogen Receptors Identified by Multiple Antibody Labeling and Impeded-Ligand Binding", *FASEB J*, 9, 404-410.
- Paris, M., Bernard-Kargar, C., Berthault, M. F., Bouwens, L. and Ktorza, A. (2003), "Specific and Combined Effects of Insulin and Glucose on Functional Pancreatic Beta-Cell Mass in Vivo in Adult Rats", *Endocrinology*, 144, 2717-2727.
- Picard, F., Wanatabe, M., Schoonjans, K., Lydon, J., O'Malley, B. W. and Auwerx, J. (2002), "Progesterone Receptor Knockout Mice Have an Improved Glucose Homeostasis Secondary to Beta -Cell Proliferation", *Proc Natl Acad Sci U S A*, 99, 15644-15648.
- Porter, A. G. and Janicke, R. U. (1999), "Emerging Roles of Caspase-3 in Apoptosis", *Cell Death Differ*, 6, 99-104.
- Prentki, M., Joly, E., El-Assaad, W. and Roduit, R. (2002), "Malonyl-Coa Signaling, Lipid Partitioning, and Glucolipotoxicity: Role in Beta-Cell Adaptation and Failure in the Etiology of Diabetes", *Diabetes*, 51 Suppl 3, S405-413.
- Quesada, I., Fuentes, E., Viso-Leon, M. C., Soria, B., Ripoll, C. and Nadal, A. (2002), "Low Doses of the Endocrine Disruptor Bisphenol-a and the Native Hormone 17beta-Estradiol Rapidly Activate Transcription Factor Creb", *FASEB J*, 16, 1671-1673.
- Quesada, I., Tuduri, E., Ripoll, C. and Nadal, A. (2008), "Physiology of the Pancreatic Alpha-Cell and Glucagon Secretion: Role in Glucose Homeostasis and Diabetes", *J Endocrinol*, 199, 5-19.
- Ramachandran, A., Snehalatha, C., Latha, E., Manoharan, M. and Vijay, V. (1999), "Impacts of Urbanisation on the Lifestyle and on the Prevalence of Diabetes in Native Asian Indian Population", *Diabetes Res Clin Pract*, 44, 207-213.
- Ramakrishna, V. and Jaikhani, R. (2007), "Evaluation of Oxidative Stress in Insulin Dependent Diabetes Mellitus (Iddm) Patients", *Diagn Pathol*, 2, 22.
- Rees, D. A. and Alcolado, J. C. (2005), "Animal Models of Diabetes Mellitus", *Diabet Med*, 22, 359-370.

- Revankar, C. M., Cimino, D. F., Sklar, L. A., Arterburn, J. B. and Prossnitz, E. R. (2005), "A Transmembrane Intracellular Estrogen Receptor Mediates Rapid Cell Signaling", *Science*, 307, 1625-1630.
- Robertson, R. P. (2004), "Chronic Oxidative Stress as a Central Mechanism for Glucose Toxicity in Pancreatic Islet Beta Cells in Diabetes", *J Biol Chem*, 279, 42351-42354.
- Robertson, R. P., Harmon, J., Tran, P. O., Tanaka, Y. and Takahashi, H. (2003), "Glucose Toxicity in Beta-Cells: Type 2 Diabetes, Good Radicals Gone Bad, and the Glutathione Connection", *Diabetes*, 52, 581-587.
- Robertson, R. P. and Harmon, J. S. (2006), "Diabetes, Glucose Toxicity, and Oxidative Stress: A Case of Double Jeopardy for the Pancreatic Islet Beta Cell", *Free Radic Biol Med*, 41, 177-184.
- Robles-Diaz, G. and Duarte-Rojo, A. (2001), "Pancreas: A Sex Steroid-Dependent Tissue", *Isr Med Assoc J*, 3, 364-368.
- Rocha, M., Bing, C., Williams, G. and Puerta, M. (2004), "Physiologic Estradiol Levels Enhance Hypothalamic Expression of the Long Form of the Leptin Receptor in Intact Rats", *J Nutr Biochem*, 15, 328-334.
- Ron, D. (2002), "Proteotoxicity in the Endoplasmic Reticulum: Lessons from the Akita Diabetic Mouse", *J Clin Invest*, 109, 443-445.
- Ron, D. and Walter, P. (2007), "Signal Integration in the Endoplasmic Reticulum Unfolded Protein Response", *Nat Rev Mol Cell Biol*, 8, 519-529.
- Ropero, A. B., Alonso-Magdalena, P., Garcia-Garcia, E., Ripoll, C., Fuentes, E. and Nadal, A. (2008a), "Bisphenol-a Disruption of the Endocrine Pancreas and Blood Glucose Homeostasis", *Int J Androl*, 31, 194-200.
- Ropero, A. B., Alonso-Magdalena, P., Quesada, I. and Nadal, A. (2008b), "The Role of Estrogen Receptors in the Control of Energy and Glucose Homeostasis", *Steroids*, 73, 874-879.
- Ropero, A. B., Alonso-Magdalena, P., Ripoll, C., Fuentes, E. and Nadal, A. (2006), "Rapid Endocrine Disruption: Environmental Estrogen Actions Triggered Outside the Nucleus", *J Steroid Biochem Mol Biol*, 102, 163-169.
- Ropero, A. B., Fuentes, E., Rovira, J. M., Ripoll, C., Soria, B. and Nadal, A. (1999), "Non-Genomic Actions of 17beta-Oestradiol in Mouse Pancreatic Beta-Cells Are Mediated by a Cgmp-Dependent Protein Kinase", *J Physiol*, 521 Pt 2, 397-407.
- Ropero, A. B., Soria, B. and Nadal, A. (2002), "A Nonclassical Estrogen Membrane Receptor Triggers Rapid Differential Actions in the Endocrine Pancreas", *Mol Endocrinol*, 16, 497-505.

- Rorsman, P., Eliasson, L., Renstrom, E., Gromada, J., Barg, S. and Gopel, S. (2000), "The Cell Physiology of Biphasic Insulin Secretion", *News Physiol Sci*, 15, 72-77.
- Russell, W. L., Kelly, E. M., Hunsicker, P. R., Bangham, J. W., Maddux, S. C. and Phipps, E. L. (1979), "Specific-Locus Test Shows Ethylnitrosourea to Be the Most Potent Mutagen in the Mouse", *Proc Natl Acad Sci U S A*, 76, 5818-5819.
- Ryu, S., Ornoy, A., Samuni, A., Zangen, S. and Kohen, R. (2008), "Oxidative Stress in Cohen Diabetic Rat Model by High-Sucrose, Low-Copper Diet: Inducing Pancreatic Damage and Diabetes", *Metabolism*, 57, 1253-1261.
- Sakuraba, Y., Sezutsu, H., Takahasi, K. R., Tsuchihashi, K., Ichikawa, R., Fujimoto, N., Kaneko, S., Nakai, Y., Uchiyama, M., Goda, N. et al. (2005), "Molecular Characterization of Enu Mouse Mutagenesis and Archives", *Biochem Biophys Res Commun*, 336, 609-616.
- Scheuner, D. and Kaufman, R. J. (2008), "The Unfolded Protein Response: A Pathway That Links Insulin Demand with Beta-Cell Failure and Diabetes", *Endocr Rev*, 29, 317-333.
- Schuppin, G. T., Bonner-Weir, S., Montana, E., Kaiser, N. and Weir, G. C. (1993), "Replication of Adult Pancreatic-Beta Cells Cultured on Bovine Corneal Endothelial Cell Extracellular Matrix", *In Vitro Cell Dev Biol Anim*, 29A, 339-344.
- Shaw, J. E., Sicree, R. A. and Zimmet, P. Z. (2010), "Global Estimates of the Prevalence of Diabetes for 2010 and 2030", *Diabetes Res Clin Pract*, 87, 4-14.
- Shupnik, M. A., Pitt, L. K., Soh, A. Y., Anderson, A., Lopes, M. B. and Laws, E. R., Jr. (1998), "Selective Expression of Estrogen Receptor Alpha and Beta Isoforms in Human Pituitary Tumors", *J Clin Endocrinol Metab*, 83, 3965-3972.
- Silfen, M. E., Manibo, A. M., McMahon, D. J., Levine, L. S., Murphy, A. R. and Oberfield, S. E. (2001), "Comparison of Simple Measures of Insulin Sensitivity in Young Girls with Premature Adrenarche: The Fasting Glucose to Insulin Ratio May Be a Simple and Useful Measure", *J Clin Endocrinol Metab*, 86, 2863-2868.
- Silver, L. (1995), *Mouse Genetics: Concepts and Applications*, Oxford University Press, USA.
- Simpson, E. R., Mahendroo, M. S., Means, G. D., Kilgore, M. W., Hinshelwood, M. M., Graham-Lorence, S., Amarneh, B., Ito, Y., Fisher, C. R., Michael, M. D. et al. (1994), "Aromatase Cytochrome P450, the Enzyme Responsible for Estrogen Biosynthesis", *Endocr Rev*, 15, 342-355.
- Soewarto, D., Fella, C., Teubner, A., Rathkolb, B., Pargent, W., Heffner, S., Marschall, S., Wolf, E., Balling, R. and Hrabe de Angelis, M. (2000), "The Large-Scale Munich Enu-Mouse-Mutagenesis Screen", *Mamm Genome*, 11, 507-510.
- Srinivasan, K. and Ramarao, P. (2007), "Animal Models in Type 2 Diabetes Research: An Overview", *Indian J Med Res*, 125, 451-472.

- Srivastava, S., Weitzmann, M. N., Cenci, S., Ross, F. P., Adler, S. and Pacifici, R. (1999), "Estrogen Decreases Tnf Gene Expression by Blocking Jnk Activity and the Resulting Production of C-Jun and JunD", *J Clin Invest*, 104, 503-513.
- Støy, J., Edghill, E. L., Flanagan, S. E., Ye, H., Paz, V. P., Pluzhnikov, A., Below, J. E., Hayes, M. G., Cox, N. J., Lipkind, G. M. et al. (2007), "Insulin Gene Mutations as a Cause of Permanent Neonatal Diabetes", *Proc Natl Acad Sci U S A*, 104, 15040-15044.
- Sun, X. J., Miralpeix, M., Myers, M. G., Jr., Glasheen, E. M., Backer, J. M., Kahn, C. R. and White, M. F. (1992), "Expression and Function of Irs-1 in Insulin Signal Transmission", *J Biol Chem*, 267, 22662-22672.
- Sundar Rajan, S., Srinivasan, V., Balasubramanyam, M. and Tatu, U. (2007), "Endoplasmic Reticulum (Er) Stress & Diabetes", *Indian J Med Res*, 125, 411-424.
- Takeda, K., Toda, K., Saibara, T., Nakagawa, M., Saika, K., Onishi, T., Sugiura, T. and Shizuta, Y. (2003), "Progressive Development of Insulin Resistance Phenotype in Male Mice with Complete Aromatase (Cyp19) Deficiency", *J Endocrinol*, 176, 237-246.
- Tanaka, M., Nakaya, S., Kumai, T., Watanabe, M., Tateishi, T., Shimizu, H. and Kobayashi, S. (2001), "Effects of Estrogen on Serum Leptin Levels and Leptin Mrna Expression in Adipose Tissue in Rats", *Horm Res*, 56, 98-104.
- Tanaka, Y., Gleason, C. E., Tran, P. O., Harmon, J. S. and Robertson, R. P. (1999), "Prevention of Glucose Toxicity in Hit-T15 Cells and Zucker Diabetic Fatty Rats by Antioxidants", *Proc Natl Acad Sci U S A*, 96, 10857-10862.
- Thomas, P., Pang, Y., Filardo, E. J. and Dong, J. (2005), "Identity of an Estrogen Membrane Receptor Coupled to a G Protein in Human Breast Cancer Cells", *Endocrinology*, 146, 624-632.
- Thornberry, N. A. and Lazebnik, Y. (1998), "Caspases: Enemies Within", *Science*, 281, 1312-1316.
- Toye, A. A., Moir, L., Hugill, A., Bentley, L., Quarterman, J., Mijat, V., Hough, T., Goldsworthy, M., Haynes, A., Hunter, A. J. et al. (2004), "A New Mouse Model of Type 2 Diabetes, Produced by N-Ethyl-Nitrosourea Mutagenesis, Is the Result of a Missense Mutation in the Glucokinase Gene", *Diabetes*, 53, 1577-1583.
- Turner, R. C., Holman, R. R., Matthews, D., Hockaday, T. D. and Peto, J. (1979), "Insulin Deficiency and Insulin Resistance Interaction in Diabetes: Estimation of Their Relative Contribution by Feedback Analysis from Basal Plasma Insulin and Glucose Concentrations", *Metabolism*, 28, 1086-1096.
- Unger, R. H., Aguilar-Parada, E., Muller, W. A. and Eisentraut, A. M. (1970), "Studies of Pancreatic Alpha Cell Function in Normal and Diabetic Subjects", *J Clin Invest*, 49, 837-848.

- Valdeolmillos, M., Nadal, A., Contreras, D. and Soria, B. (1992), "The Relationship between Glucose-Induced K<sup>+</sup>Atp Channel Closure and the Rise in [Ca<sup>2+</sup>]<sub>i</sub> in Single Mouse Pancreatic Beta-Cells", *J Physiol*, 455, 173-186.
- van Burck, L., Blutke, A., Kautz, S., Rathkolb, B., Klaften, M., Wagner, S., Kemter, E., Hrabe de Angelis, M., Wolf, E., Aigner, B. et al. (2010), "Phenotypic and Pathomorphological Characteristics of a Novel Mutant Mouse Model for Maturity-Onset Diabetes of the Young Type 2 (Mody 2)", *Am J Physiol Endocrinol Metab*, 298, E512-523.
- Viña, J., Borrás, C., Gambini, J., Sastre, J. and Pallardo, F. V. (2005), "Why Females Live Longer Than Males? Importance of the Upregulation of Longevity-Associated Genes by Oestrogenic Compounds", *FEBS Lett*, 579, 2541-2545.
- Wallace, T. M., Levy, J. C. and Matthews, D. R. (2004), "Use and Abuse of Homa Modeling", *Diabetes Care*, 27, 1487-1495.
- Wang, H., Maechler, P., Ritz-Laser, B., Hagenfeldt, K. A., Ishihara, H., Philippe, J. and Wollheim, C. B. (2001), "Pdx1 Level Defines Pancreatic Gene Expression Pattern and Cell Lineage Differentiation", *J Biol Chem*, 276, 25279-25286.
- Wang, J., Takeuchi, T., Tanaka, S., Kubo, S. K., Kayo, T., Lu, D., Takata, K., Koizumi, A. and Izumi, T. (1999), "A Mutation in the Insulin 2 Gene Induces Diabetes with Severe Pancreatic Beta-Cell Dysfunction in the Mody Mouse", *J Clin Invest*, 103, 27-37.
- Wanke, R., Weis, S., Kluge, D., Kahnt, E., Schenck, E., Brem, G. and Hermanns, W. (1994), "Morphometric Evaluation of the Pancreas of Growth Hormone-Transgenic Mice", *ACTA STEREOLOGICA*, 13, 3-3.
- Waterston, R. H., Lindblad-Toh, K., Birney, E., Rogers, J. and Lander, E. S. (2002), "Initial Sequencing and Comparative Analysis of the Mouse Genome", *Nature*, 420, 520-562.
- Weigel, N. L. and Zhang, Y. (1998), "Ligand-Independent Activation of Steroid Hormone Receptors", *J Mol Med*, 76, 469-479.
- Weir, G. C., Laybutt, D. R., Kaneto, H., Bonner-Weir, S. and Sharma, A. (2001), "Beta-Cell Adaptation and Decompensation During the Progression of Diabetes", *Diabetes*, 50 Suppl 1, S154-159.
- Weiss, M. A. (2009), "Proinsulin and the Genetics of Diabetes Mellitus", *J Biol Chem*, 284, 19159-19163.
- White, M. F. and Kahn, C. R. (1994), "The Insulin Signaling System", *J Biol Chem*, 269, 1-4.
- Withers, D. J., Gutierrez, J. S., Towery, H., Burks, D. J., Ren, J. M., Previs, S., Zhang, Y., Bernal, D., Pons, S., Shulman, G. I. et al. (1998), "Disruption of Irs-2 Causes Type 2 Diabetes in Mice", *Nature*, 391, 900-904.

- Wong, W. P., Tiano, J. P., Liu, S., Hewitt, S. C., Le May, C., Dalle, S., Katzenellenbogen, J. A., Katzenellenbogen, B. S., Korach, K. S. and Mauvais-Jarvis, F. (2010), "Extranuclear Estrogen Receptor-Alpha Stimulates Neurod1 Binding to the Insulin Promoter and Favors Insulin Synthesis", *Proc Natl Acad Sci U S A*, 107, 13057-13062.
- Wood, I. S. and Trayhurn, P. (2003), "Glucose Transporters (Glut and Sglt): Expanded Families of Sugar Transport Proteins", *Br J Nutr*, 89, 3-9.
- Xing, C., Schumacher, F. R., Xing, G., Lu, Q., Wang, T. and Elston, R. C. (2005), "Comparison of Microsatellites, Single-Nucleotide Polymorphisms (Snps) and Composite Markers Derived from Snps in Linkage Analysis", *BMC Genet*, 6 Suppl 1, S29.
- Xu, C., Bailly-Maitre, B. and Reed, J. C. (2005), "Endoplasmic Reticulum Stress: Cell Life and Death Decisions", *J Clin Invest*, 115, 2656-2664.
- Yoon, K. H., Ko, S. H., Cho, J. H., Lee, J. M., Ahn, Y. B., Song, K. H., Yoo, S. J., Kang, M. I., Cha, B. Y., Lee, K. W. et al. (2003), "Selective Beta-Cell Loss and Alpha-Cell Expansion in Patients with Type 2 Diabetes Mellitus in Korea", *J Clin Endocrinol Metab*, 88, 2300-2308.
- Yoshida, H., Matsui, T., Yamamoto, A., Okada, T. and Mori, K. (2001), "Xbp1 Mrna Is Induced by Atf6 and Spliced by Ire1 in Response to Er Stress to Produce a Highly Active Transcription Factor", *Cell*, 107, 881-891.
- Yoshinaga, T., Nakatome, K., Nozaki, J., Naitoh, M., Hoseki, J., Kubota, H., Nagata, K. and Koizumi, A. (2005), "Proinsulin Lacking the A7-B7 Disulfide Bond, Ins2akita, Tends to Aggregate Due to the Exposed Hydrophobic Surface", *Biol Chem*, 386, 1077-1085.
- Yoshioka, M., Kayo, T., Ikeda, T. and Koizumi, A. (1997), "A Novel Locus, Mody4, Distal to D7mit189 on Chromosome 7 Determines Early-Onset Niddm in Nonobese C57bl/6 (Akita) Mutant Mice", *Diabetes*, 46, 887-894.
- Zhang, D., Lu, C., Whiteman, M., Chance, B. and Armstrong, J. S. (2008), "The Mitochondrial Permeability Transition Regulates Cytochrome C Release for Apoptosis During Endoplasmic Reticulum Stress by Remodeling the Cristae Junction", *J Biol Chem*, 283, 3476-3486.
- Zhang, K. and Kaufman, R. J. (2006), "The Unfolded Protein Response: A Stress Signaling Pathway Critical for Health and Disease", *Neurology*, 66, S102-109.
- Zhao, C., Dahlman-Wright, K. and Gustafsson, J. A. (2008), "Estrogen Receptor Beta: An Overview and Update", *Nucl Recept Signal*, 6, e003.
- Zhu, M., Mizuno, A., Kuwajima, M., Ogino, T., Murakami, T., Noma, Y., Sano, T. and Shima, K. (1998), "Ovarian Hormone-Induced Beta-Cell Hypertrophy Contributes to the Homeostatic Control of Beta-Cell Mass in Oletf Female Rat, a Model of Type II Diabetes", *Diabetologia*, 41, 799-805.

---

Zirilli, L., Rochira, V., Diazzi, C., Caffagni, G. and Carani, C. (2008), "Human Models of Aromatase Deficiency", *J Steroid Biochem Mol Biol*, 109, 212-218.

Zuber, C., Fan, J. Y., Guhl, B. and Roth, J. (2004), "Misfolded Proinsulin Accumulates in Expanded Pre-Golgi Intermediates and Endoplasmic Reticulum Subdomains in Pancreatic Beta Cells of Akita Mice", *FASEB J*, 18, 917-919.

## 10 Acknowledgements

I would like to thank Prof. Dr. R. Wanke for giving me the opportunity to do this dissertation. I am grateful for his support and advice, in particular for the time he spent in discussing this doctorate, especially the quantitative stereological investigations.

Special thanks go to Dr. Nadja Herbach for her endless support and the many hours she spent in discussing all the different features of this doctorate and always giving good advice for several problems.

Moreover I would like to thank Prof. Dr. W. Hermanns for his immense support.

Further acknowledgements go to all employees at the Institute of Veterinary Pathology for their help, especially Mrs. Lisa Pichl for the introduction in several laboratory practices and methods as well as for her help in many experiments, Mrs. Elisabeth Kemper for her supporting knowledge in various immunohistochemical methods, Mrs. Angela Siebert for the precise accomplishment of electron microscopic work and Mrs. Sabine Zwirz for her passionate animal care and her help in the procedures of weaning.

I am very grateful for the generous and never ending support from my colleagues Sabine Kautz and Lelia van Bürck, who always had an open ear, not only in questions concerning this doctorate. Also very thanks to my roommate Pierre Börrjes for his psychological support and to Johanna Leitenbacher, who always encouraged me during the time of writing. Moreover, I want to thank Dr. Andreas Blutke for his brilliant ideas in generating special not available technical equipment and in resolving different problems.

I also want to thank the Gene Center of the LMU Munich to provide the laboratories to analyse various radioimmunoassays.

Many thanks to the Institute of Physiology of the LMU Munich for giving me the possibility to perform several ELISAs.

This study was implemented within the framework of the graduate college “Functional genomics in veterinary medicine” (GRK 1029), supported by the “Deutsche Forschungsgemeinschaft” (DFG). Many thanks for the temporarily sponsoring of this doctorate.

The last acknowledgement is dedicated to my flatmate, who shared the sometimes difficult times with me, to my endearing friend Veronika Nowitzky and to my family and friends for their endless human support.